Universidade de São Paulo
Instituto de Física

Aspectos da dualidade holográfica fora do equilíbrio

Giancarlo Thales Camilo da Silva

Orientador: Prof. Dr. Elcio Abdalla
Co-orientadora: Profa. Dra. Bertha Cuadros-Melgar

Tese apresentada ao Instituto de Física como requisito para a obtenção do título de Doutor em Ciências

Comissão examinadora:

Prof. Dr. Elcio Abdalla – IFUSP (orientador)
Prof. Dr. Diego Trancanelli – IFUSP
Prof. Dr. Fernando Tadeu Caldeira Brandt – IFUSP
Prof. Dr. Horatiu Stefan Nastase – IFT/UNESP
Prof. Dr. Vilson Tonin Zanchin - UFABC

São Paulo
2017

FICHA CATALOGRÁFICA
Preparada pelo Serviço de Biblioteca e Informação do Instituto de Física da Universidade de São Paulo

Silva, Giancarlo Thales Camilo da

Aspectos da dualidade holográfica fora do equilíbrio.
São Paulo, 2017.

Tese (Doutorado) – Universidade de São Paulo. Instituto de Física. Depto. de Física Matemática

Orientador: Prof. Dr. Elcio Abdalla

Área de Concentração: Física Teórica

Unitermos: 1. Física teórica; 2. Relatividade (Física); 3. Teoria de campos e ondas.

USP/IF/SBI-016/2017

Universidade de São Paulo
Instituto de Física

Non-equilibrium aspects of the holographic duality

Giancarlo Thales Camilo da Silva

Supervisor: Prof. Dr. Elcio Abdalla
Co-supervisor: Prof. Dr. Bertha Cuadros-Melgar

Thesis presented to the Institute of Physics as a requisite for obtaining the title of Doctor of Sciences

Examining committee:

Prof. Dr. Elcio Abdalla – IFUSP (supervisor)
Prof. Dr. Diego Trancanelli – IFUSP
Prof. Dr. Fernando Tadeu Caldeira Brandt – IFUSP
Prof. Dr. Horatiu Stefan Nastase – IFT/UNESP
Prof. Dr. Vilson Tonin Zanchin - UFABC

São Paulo
2017

Acknowledgements

First of all, I would like to express my gratitude to professor Elcio Abdalla for giving me the opportunity to work under his supervision as well as the freedom to follow any research direction I wished. I am equally grateful to Bertha Cuadros-Melgar for her constant support over all these years, the fruitful collaborations, and for each of her countless objections on the random use of commas in my english writing. I am grateful also to Jorge Noronha for nice discussions, Fernando Brandt for valuable comments on the text, and in particular Diego Trancanelli for comments, discussions and his tremendous support in my struggle to find a postdoc position.

I also want to thank everyone at USP that contributed to make this 4-year journey so enjoyable. Specially Marcela Muniz and Lucas Müssnich (honorable mention here to Ana Luiza for her nice occasional stays), with whom sharing the 337 office has always been a privilege – and that's not because of the espresso machine or the sofa. Also Ricardo Landim, Marcos Brum, Alan Maciel, Daniel Guariento, Gustavo Soares, Riis Bachega, Daniel Teixeira, Leonardo Werneck, Maria Fernanda, Raju Roychowdhury, Ricardo Medina, and others for each (physics-related or not) conversation, coffee, and daily meal at bandejão; and the DFMA secretaries Amelia, Cecília, and Simone for being so nice and competent in helping us with the daily bureaucracy.

I owe very special thanks to my family as well. Specially my brother Giulio, who also decided to become a physicist (poor kid) and with whom I had the pleasure to share the last couple of years both as students at IFUSP; to my parents Maristela and Carlos for their constant love and support ever since I decided to pursue such an arduous and unconventional career; and to my parents-in-law Bete and Eugênio for their fondness during all those years.

Last but not least, I have not enough words to express how lucky and grateful I am to have the love of my life, Marina, by my side during this whole time. Thank you very much for every little thing, I would never be able to make it without your help. Te amo!

This work was financially supported by CNPq.

Abstract

This thesis is devoted to study far-from-equilibrium aspects of quantum systems at strong coupling using the holographic duality as a tool. The duality, originated from string theory and further generalized to broader scenarios, relates certain strongly coupled gauge theories to classical gravity theories in higher dimensions. Over the last years, it has proved itself useful as a calculational tool to map difficult questions of interest in the gauge theory into a "dual" (i.e., equivalent) problem in a higher-dimensional gravity language where the solution may become feasible. The interest in strongly coupled quantum field theories, in particular non-Abelian gauge theories, is motivated by a number of nuclear and condensed matter physics phenomena which are known to take place at a non-perturbative regime, such as the quark-gluon plasma phase of quantum chromodynamics or high-T_c superconducting materials. While dealing with strong coupling is typically a very hard task even at equilibrium, the situation becomes yet more dramatic when non-equilibrium setups are concerned since the main non-perturbative tool available nowadays – lattice field theory – suffers from serious problems when it comes to real-time dynamics. This is the reason why unconventional techniques such as the ones provided by holography are welcome. Of particular interest here are the problems of thermalization of strongly coupled plasmas as well as the quench dynamics of quantum systems, both of which admit a dual gravitational description involving time-dependent solutions to the corresponding classical equations of motion in the bulk of Anti de Sitter (AdS) spacetimes, such as collapsing solutions describing AdS black hole formation. Specifically, and always from a holographic point of view, in this thesis we deal with three classes of problems: the thermalization properties of a charged non-Abelian plasma after a sudden injection of energy (such as a heavy ion collision); the dynamics of a symmetry breaking quench process from a relativistic to a non-relativistic setup of the Lifshitz type with dynamical exponent z; and, finally, a new analytical approach to the non-equilibrium properties of conformal field theory plasmas placed in an expanding background. Apart from the specific problems, we also provide a self-contained but concise introduction to the holographic duality with a view towards newcomers with an elementary general relativity and quantum field theory background.

Keywords:
holography, non-equilibrium dynamics, thermalization, quenches, strongly coupled plasmas

Resumo

Esta tese designa-se ao estudo de sistemas quânticos fortemente acoplados e fora do equilíbrio utilizando como ferramenta a dualidade holográfica. A dualidade, originária da teoria de cordas e posteriormente generalizada a cenários mais abrangentes, relaciona certas teorias de calibre fortemente acopladas e teorias de gravidade clássica em dimensões mais altas. Nos últimos anos, ela tem se mostrado útil como uma ferramenta de cálculo para mapear questões complicadas na teoria de gauge em um problema "dual" (isto é, equivalente) formulado na linguagem completamente diferente de gravidade em dimensões extras, onde obter uma solução pode ser viável. O interesse em teorias quânticas de campo fortemente acopladas, em particular teorias de calibre não-Abelianas, motiva-se por uma variedade de fenômenos das físicas nuclear e da matéria condensada que, reconhecidamente, ocorrem em um regime não-perturbativo, tais como o plasma de quarks e glúons da cromodinâmica quântica ou certos materiais supercondutores com temperatura crítica alta. Em geral, lidar com acoplamentos fortes é uma tarefa bastante complicada mesmo em configurações de equilíbrio, mas a situação se torna ainda mais dramática quando configurações longe do equilíbrio são tratadas, visto que a principal ferramenta não-perturbativa disponível atualmente (teoria de campos na rede) enfrenta sérios problemas em situações dinâmicas. Esta é a principal razão pela qual técnicas alternativas tais como as fornecidas pela dualidade holográfica são bem vindas. De particular interesse aqui são os problemas da termalização de plasmas fortemente acoplados bem como a dinâmica pós-*quench* de sistemas quânticos, ambos os quais admitem uma descrição gravitacional dual envolvendo soluções dependentes do tempo às correspondentes equações gravitacionais em espaços-tempo de Anti de Sitter (AdS), tais como soluções de colapso descrevendo a formação de buracos negros assintoticamente AdS. Especificamente, e sempre sob um ponto de vista holográfico, nesta tese lidamos com três tipos diferentes de problemas: a termalização de um plasma não-Abeliano carregado como resultado de uma injeção repentina de energia (tal como uma colisão de íons pesados); a dinâmica durante um processo de quebra da simetria relativística para uma simetria não-relativística do tipo Lifshitz com expoente dinâmico z; e, finalmente, uma nova abordagem analítica para tratar propriedades fora do equílibrio de plasmas conformes colocados em um fundo que se expande. Além de tais problemas específicos, este texto fornece também uma introdução sucinta e auto-contida à dualidade holográfica direcionada a um leitor com conhecimento elementar de relatividade geral e teoria quântica de campos.

Palavras-chave:
holografia, dinâmica fora do equilíbrio, termalização, *quenches*, plasmas fortemente acoplados

Contents

Introduction

The Anti de Sitter/Conformal Field Theory (AdS/CFT) correspondence (or duality) is one of the most remarkable discoveries in modern theoretical physics over the last two decades. Conjectured by Maldacena in 1997 [1], it became popular a few months later after the works by Witten [2] and Gubser, Polyakov, and Klebanov [3]. In its original version it posits the rather surprising equivalence between a specific 4-dimensional quantum field theory with conformal symmetry and no gravity at all (a "CFT") in flat spacetime and a string theory (a theory that contains gravity) living in a higher dimensional Anti-de Sitter spacetime. The CFT lives in the conformal boundary of the AdS spacetime, a 4-dimensional timelike slice of this spacetime with very peculiar properties. Remarkably, the correspondence is of the strong/weak type, meaning that in the particular limit where the CFT is strongly coupled (in other words, hard to solve) the stringy dual becomes weakly coupled, i.e., essentially classical gravity coupled to extra fields, where the corresponding calculations become tractable.

The existence of mathematical dualities between different quantum field theories is an old fact and does not sound surprising nowadays, even though their physical content may be quite striking. A classical example from 2-dimensional quantum field theory is the so-called bosonization, namely the exact equivalence between a massive Dirac fermion system with a quartic self-interaction (the massive Thirring model) and a bosonic scalar field with a cosine interaction (the sine-Gordon model) discovered by Coleman back in the 70's [4] (see also [5] for a nice survey of dualities in field and string theories). What does sound surprising about AdS/CFT, however, is the fact that one of the two dual theories contains gravity while the other does not. It is a widely spread fact that gravity and the principles of quantum mechanics cannot be easily reconciled, so how can it be that a theory of gravity is equivalent to a quantum field theory involving no gravity at all? This has no previously known analog and opens up a whole new window of possibilities to be explored.

In fact, AdS/CFT can be viewed as an explicit realization of the *holographic principle* proposed by 't Hooft [6] (see also [7]), according to which any consistent theory of quantum gravity must be holographic in the sense that the number of microscopic degrees of freedom contained inside a given volume V must scale as the surface area ∂V of that volume (instead of V itself, as typical in non-gravitational theories).

Although Maldacena's original construction involves a specific pair of theories with very special properties such as conformal symmetry and supersymmetry, there are compelling evidences that the AdS/CFT correspondence is just a representative example of a class of more fundamental relations between quantum field theories and gravity theories in higher dimensions. The generalized version of the correspondence relating "non-AdS" spacetimes and "non-CFTs" is sometimes referred to as *gauge/gravity duality* or, still, the one we choose to adopt in this thesis, ***holographic duality***.

The mere existence of such a duality is exciting for at least two immediate reasons, depending on which direction we choose to explore it, namely,

1. "AdS $\rightarrow$ CFT": the possibility to use it as a tool to approach difficult problems in quantum field theory by mapping them into equivalent problems in the gravitational counterpart, where they might be solvable. Examples include applications to QCD and quark-gluon plasma physics, as well as to condensed matter systems;

2. "AdS ← CFT": the possibility of approaching the longstanding problem of finding a theory of quantum gravity in the language of an equivalent lower-dimensional quantum field theory without gravity. In fact, since the present understanding of string theory (a candidate quantum gravity theory) is only at the perturbative quantum level, AdS/CFT can be used to shed light into the non-perturbative behavior of strings by using their dual CFT as a guide.

The first direction is the one taken in this thesis (and in the vast majority of works in the literature).

The present thesis is devoted to the use of the holographic duality as a tool to study a variety of time-dependent problems in strongly coupled quantum field theories. Such phenomena are ubiquitous in nature, as it becomes obvious when we think about microscopic degrees of freedom – afterall, strictly speaking every macroscopic state (equilibrium ones included) is governed by a complicated dynamics at the microscopic level – or about cosmological scenarios, since our universe *per se* is explicitly expanding in time. Understanding the non-equilibrium properties of quantum systems at strong coupling thus becomes mandatory for an adequate comprehension of the world. This is certainly not an easy task, since the standard treatment of strongly coupled quantum systems is complicated enough even at equilibrium and the main non-perturbative tool currently available, lattice field theory, fails to work when real-time dynamics is concerned as a Wick rotation to Euclidean time is involved. That is the main reason why we need to resort to alternative techniques such as a holographic approach. Rather remarkably, this sort of problem has only started to receive a significant amount of attention over the last years: while most of the success obtained from applications of the duality involve equilibrium or near-equilibrium situations, such as the calculation of transport coefficients using linear response theory, treating the full real-time dynamics of systems away from equilibrium has attracted much less attention.

Typical non-equilibrium problems on the "CFT side" of the duality involve the dynamics of quantum field theories following a sudden injection of energy of some kind (such as a particle collision) or an abrupt change in one of the control parameters of the system, such as the temperature or the charge density. The former is important, for instance, to describe the thermalization process of the quark-gluon plasma formed after heavy ion collisions, which is an important open problem in QCD and is likely to have played an essential role in the primordial universe shortly after the big bang. The latter, on the other hand, corresponds to the problem of so-called quantum quenches, which is of special interest in condensed matter experiments. In both cases, from the point of view of the gravity dual in the "AdS side" of the duality the problem can be boiled down to finding dynamical solutions to the Einstein-plus-matter equations of motion. Namely, the problem of thermalization can be mapped to a black hole formation process in the bulk, while the problem of quantum quenches maps to solving field equations in the bulk with prescribed time-dependent boundary conditions as dictated by the holographic dictionary, as we shall see later.

Outline of the thesis

In Chapter **1** we introduce all the essential ingredients necessary for a satisfactory comprehension of the holographic duality. This is a review Chapter intended to establish a ground to guide newcomers into the subject, since it requires a combination of nontrivial ideas from different research areas such as general relativity, quantum field theory, and string theory. The idea is to provide the necessary background on Anti de Sitter spacetimes, conformal field theories, non-Abelian gauge theories, and string theory in a practical way. Of particular importance is to understand the large N_c behavior of $SU(N_c)$ gauge theories and its similarity to the perturbative expansion in string theory, which is one of the main motivations that lead Maldacena to discover the AdS/CFT correspondence.

Chapter **2** then introduces the main features of the holographic duality and its applications. Again this an introductory Chapter, designed with a view towards someone starting to learn the topic. The intention here is to give a self-contained introduction to the subject by defining all the necessary ingredients, motivating with heuristic pictures, and presenting the important pieces of the argument

to construct the duality. We also discuss its main properties such as the strong/weak nature, as well as the possible "bottom-up" or "top-down" extensions to more general setups, and take an effort to describe their utility for gaining insight into real-world strongly coupled systems.

Chapters **3**, **4**, and **5** in the sequence contain the original results obtained during this PhD research project, each of them corresponding to a different non-equilibrium problem approached from a dual gravity point of view.

In Chapter **3** we study the problem of holographic thermalization. After briefly introducing the problem and the previous approaches in the literature, we present our contribution including all the technical details. Namely, we consider α'-like corrections of the Born-Infeld (BI) type to the holographic thermalization of a conformal field theory (CFT) plasma having a non-vanishing chemical potential. By using a Vaidya thin shell model for the black hole collapse on the gravity side, we analyze the effect of the BI nonlinear corrections on the thermalization time of different nonlocal observables with a gravity dual description.

In Chapter **4** we move to the problem of quantum *quenches* of strongly coupled systems. After a brief review of the subject and a description of how to holographically approach this problem we present our original contribution to the subject. Namely, in order to understand the real-time dynamics during a symmetry breaking process, we study a particular class of quenches that break the relativistic invariance of a zero-temperature CFT towards a non-relativistic scaling symmetry of the Lifshitz type with dynamical exponent z (very close to unity) and probe the dynamical process using different observables.

Finally, Chapter **5** presents a new and very simple analytical approach to study strongly coupled CFT plasmas away from equilibrium. The idea is to consider, as a toy model for non-equilibrium physics, a 4-dimensional plasma defined in a dynamical background of the Friedmann-Lemaître-Robertson-Walker (FLRW) type. Although the plasma is locally at rest, globally it expands as a result of the expansion of the background itself. In order to holographically model this situation we introduce a new slicing of 5-dimensional Anti de Sitter black holes in such a way that the conformal boundary of AdS (where the dual CFT lives) becomes the desired FLRW spacetime. After discussing the main features of the new slicing, we use it as a prototype to analytically study the nonequilibrium dynamics of CFT plasmas by calculating the stress-energy tensor of three illustrative examples of expanding plasmas.

Chapter **6** wraps up the thesis with some closing remarks on the application of the holographic duality to study quantum systems away from equilibrium.

Chapter 1

Essential ingredients

This chapter reviews the essential ingredients necessary to understand the holographic duality (to be introduced in Chapter **2**) as well as its applications to be explored in the subsequent chapters. It is designed to be didatic with a view towards newcomers interested in learning the subject. The idea is to define the main features in a concise way, hence providing a practical route to understand the remaining chapters. This by no means implies that the discussion is either detailed or rigorous, what would drive us far away from the scope of the thesis. Nevertheless, some effort is made to point the reader to the specific literature whenever needed.

The reader is only assumed to be familiar with the very basics of general relativity and quantum field theory (see for instance [8, 9] and [10, 11] for standard introductory textbooks on general relativity and quantum field theory, respectively). The chapter is organized as follows: in Section 1.1 we define and discuss the main features of Anti de Sitter spacetimes, including various coordinate systems, black holes and their thermodynamical properties; Section 1.2 introduces conformal symmetry and conformal field theories; Section 1.3 reviews non-Abelian gauge theories and their large N_c expansion and introduces, in particular, the so called $\mathcal{N} = 4$ SYM theory that will appear later in the original version of the AdS/CFT correspondence; finally, Section 1.4 gives a practical review of the main features of string theory.

1.1 Anti de Sitter spacetimes

Anti-de Sitter (AdS) spacetime is a maximally symmetric spacetime with negative curvature and Lorentzian signature. A good starting point is, therefore, clarifying what exactly this means. As the name suggests, a spacetime is maximally symmetric if it admits the maximum number of spacetime symmetries available. In general relativity language this means the maximum number of independent Killing vectors, which are vector fields $\xi_a(x)$ satisfying the Killing equation

$$\nabla_a \xi_b + \nabla_b \xi_a = 0 \tag{1.1}$$

(here ∇_a is the covariant derivative associated with a given metric tensor $g_{ab}(x)$). In D spacetime dimensions this maximum number of symmetries happens to be $\frac{1}{2}D(D+1)$. This nontrivial fact follows from the following identity involving the second covariant derivative of a Killing vector [12]

$$\nabla_c \nabla_a \xi_b = R^d{}_{cab} \xi_d \ ,$$

where $R^d{}_{cab} = g^{de} R_{ecab}$ is the Riemann tensor. Namely, it determines the second derivative of ξ (and, therefore, all the higher derivatives) in terms of the components of ξ itself, implying that the Killing field is completely and uniquely determined everywhere by the values of $\xi_a(x)$ and $\nabla_b \xi_a(x)$ at a particular point x_0. Since in a D-dimensional spacetime there can be at most D linearly independent

vectors $\xi_a(x_0)$ and $\frac{1}{2}D(D-1)$ independent antisymmetric tensors $\nabla_b\xi_a(x_0)$ at a given point x_0, we get at most $D+\frac{1}{2}D(D-1)=\frac{1}{2}D(D+1)$ Killing vectors.

The Riemann tensor of maximally symmetric spacetimes is related to the metric components in the simple, algebraic form (see, for instance, [8])

$$R_{abcd}=\frac{R}{D(D-1)}(g_{ac}g_{bd}-g_{ad}g_{bc})\ , \tag{1.2}$$

where R is the Ricci scalar curvature. It can be shown that this fact, together with the Bianchi identities, implies that R is a constant, and we see that maximally symmetric spacetimes can be classified according to the sign of R. For the case of Lorentzian signature in which we are interested these are flat Minkowski space ($R=0$), de Sitter space ($R>0$), and AdS space ($R<0$); in the case of Euclidean signature they correspond to flat Euclidean space, the sphere, and hyperbolic (or Lobachevsky) space, respectively.

It is also easy to check from (1.2) that the Ricci tensor is simply $R_{ab}=\frac{R}{D}g_{ab}$ and hence all the maximally symmetric spacetimes discussed above satisfy the vacuum Einstein equations with a cosmological constant Λ,

$$R_{ab}-\frac{1}{2}Rg_{ab}+\Lambda g_{ab}=0, \tag{1.3}$$

where

$$\Lambda=\frac{D-2}{2D}R\ . \tag{1.4}$$

Since we are interested in $D>2$, we see that the sign of R is essentially determined by Λ and, therefore, we conclude that the cosmological constant must be positive, negative, or zero in order to have de Sitter, AdS, or Minkowski space, respectively.

For future notational consistency we shall discuss here the AdS space in $D=d+1$ dimensions, or simply AdS_{d+1}. As typical for spaces with constant curvature, the best way to construct it is by embedding into a higher dimensional space (just like the sphere $\mathbb{S}^2$ can be constructed as a surface embedded into $\mathbb{R}^3$). Namely, AdS_{d+1} is the $(d+1)$-dimensional surface

$$-X_0^2-X_{d+1}^2+\sum_{i=1}^{d}X_i^2=-L^2 \tag{1.5}$$

embedded into a $d+2$ dimensional flat Minkowski space with two time directions ($\mathbb{R}^{2,d}$)

$$ds^2=-dX_0^2-dX_{d+1}^2+\sum_{i=1}^{d}dX_i^2\ . \tag{1.6}$$

The constant L has length dimensions and is called the AdS curvature radius. One of the advantages of this construction by embedding is that the isometry group of AdS_{d+1} follows trivially: it is the group $SO(2,d)$ of transformations $X^\mu\to\Lambda^\mu_{\ \nu}X^\nu$ that leave (1.5) invariant, which turns out to be the same as the conformal group of d-dimensional Minkowski space ($d>2$), as we will see in Section **1.2**. Such a coincidence is our first hint that AdS spaces and theories with conformal symmetry in one dimension less have something in common, and we will come back to this point later when discussing the AdS/CFT correspondence.

Let us solve the constraint (1.5) in order to show explicit forms for the AdS_{d+1} metric in a few coordinate systems. The coordinates (ρ,τ,Ω_i) defined by

$$\begin{aligned} X^0 &= L\cosh\rho\cos\tau \\ X^{d+1} &= L\cosh\rho\sin\tau \\ X^i &= L\sinh\rho\ \Omega_i \qquad (i=1,\ldots,d) \end{aligned} \tag{1.7}$$

automatically solve the embedding equation and are referred to as *global coordinates*. Here Ω_i are angular coordinates parametrizing a $(d-1)$-dimensional unit sphere $\mathbb{S}^{d-1}$ (i.e., they satisfy $\sum_i \Omega_i^2 = 1$), and the remaining coordinates take values $0 \leq \rho < \infty$ and $0 \leq \tau < 2\pi$. By plugging (1.7) in (1.6) yields the following metric for AdS_{d+1} in global coordinates

$$ds^2_{\mathrm{AdS}_{\mathrm{global}}} = L^2 \left(-\cosh^2\rho \; d\tau^2 + d\rho^2 + \sinh^2\rho \; d\Omega^2_{d-1}\right) \; . \tag{1.8}$$

Notice that in this parametrization only the subgroup $SO(2) \times SO(d)$ of the isometry group $SO(2,d)$ is manifest (respectively, rotations in the $X^0 X^{d+1}$ plane, here hidden in the form of τ-translations, and the rotations that preserve the sphere in the Ω_{d-1} directions). There is a subtlety here that the timelike coordinate τ is periodic and hence the metric (1.8) has closed timelike curves. By unwrapping the timelike circle (i.e., taking $\tau \in \mathbb{R}$ without identifying points) avoids physical inconsistencies by providing a causal spacetime and the resulting metric is called the *universal covering of AdS*. Although seldom mentioned, this is what is usually referred to as Anti de Sitter space for all practical purposes and we will follow the same convention.

By introducing the coordinate θ according to $\tan\theta = \sinh\rho$ the metric (1.8) becomes

$$\begin{aligned} ds^2_{\mathrm{AdS}_{\mathrm{conformal}}} &= \frac{L^2}{\cos^2\theta}\left(-d\tau^2 + d\theta^2 + \sin^2\theta \; d\Omega^2_{d-1}\right) \\ &= \frac{L^2}{\cos^2\theta}\left(-d\tau^2 + d\Omega^2_d\right) \; , \end{aligned} \tag{1.9}$$

with θ taking values in the range $0 \leq \theta < \frac{\pi}{2}$. These are called *conformal coordinates* and they tell us that AdS_{d+1} space is conformally equivalent to the upper half of the Einstein static universe $\mathbb{R} \times \mathbb{S}^d$ (which has θ in the full range $0 \leq \theta \leq \pi$). Scaling away the conformal factor and, then, adding the point $\theta = \frac{\pi}{2}$ (corresponding to spatial infinity $\rho = \infty$) defines a compact space called the *conformal compactification of AdS_{d+1}*[1], which is simply

$$\widetilde{ds}^2_{\mathrm{c.c.}} = -d\tau^2 + d\theta^2 + \sin^2\theta \; d\Omega^2_{d-1} \; , \qquad 0 \leq \theta \leq \frac{\pi}{2} \; , \qquad -\infty < \tau < \infty \; . \tag{1.10}$$

It can be used to give a precise definition of *asymptotically AdS* (aAdS) spacetimes, namely, any spacetime that can be conformally compactified into a region with the same structure as (1.10).

The d-dimensional surface $\theta = \frac{\pi}{2}$ (the boundary of the compact space (1.10)) is called the *conformal boundary* of AdS_{d+1}, which we denote by $\partial\mathrm{AdS}_{d+1}$,

$$ds^2_{\partial\mathrm{AdS}_{d+1}} = -d\tau^2 + d\Omega^2_{d-1} \; . \tag{1.11}$$

Since this is a timelike boundary, i.e., orthogonal to the spacelike direction θ (or ρ), specifying initial data for fields on a given time slice is not enough to determine the future field configuration. One needs, in addition, to specify boundary conditions at ∂AdS in order to have a well-defined time evolution problem in AdS space [13].[2] It is important to see from expression (1.10) that $\partial\mathrm{AdS}_{d+1}$ is the cylinder $\mathbb{R} \times \mathbb{S}^{d-1}$, which is conformally equivalent to d-dimensional Minkowski space. Hence, we can think of d-dimensional Minkowski (or in fact any member of its conformal class) as living at the conformal boundary of AdS_{d+1}. As we shall see later in this chapter, the two facts above are at the heart of the AdS/CFT correspondence. Namely, the need to specify boundary conditions at ∂AdS will be the key ingredient to construct the dictionary relating the two dual theories, while the conformal equivalence with Minkowski will naturally lead us to view the CFT as living on the boundary of AdS.

[1] The procedure of conformal compactification can a priori be carried out for any non-compact manifold $\mathcal{M}$. The idea is to map $\mathcal{M}$ to the interior of a compact manifold $\tilde{\mathcal{M}}$ possessing a boundary $\partial\tilde{\mathcal{M}}$, in which case one can think of $\partial\tilde{\mathcal{M}}$ as a conformal boundary of $\mathcal{M}$.

[2] In technical terms AdS space is not *globally hyperbolic*, meaning that it has no Cauchy surfaces in which to define a well-posed initial value problem.

It would be interesting to write the AdS metric in such a way as to make its d-dimensional Poincaré symmetry manifest. This can be done by introducing the so called *Poincaré coordinates* $(z > 0, t, x^i)$ defined by

$$\begin{aligned} X^0 &= \frac{1}{2z}\left(z^2 + L^2 - t^2 + \mathbf{x}^2\right) \\ X^{d+1} &= \frac{1}{2z}\left(z^2 - L^2 - t^2 + \mathbf{x}^2\right) \\ X^i &= \frac{L}{z}x^i \qquad (i = 1, \ldots, d), \end{aligned} \tag{1.12}$$

where we have defined $\mathbf{x}^2 \equiv \sum_i x_i^2$. The AdS_{d+1} metric in Poincaré coordinates then reads

$$ds^2_{\mathrm{AdS}_{\mathrm{Poincaré}}} = \frac{L^2}{z^2}\left(-dt^2 + d\mathbf{x}^2 + dz^2\right). \tag{1.13}$$

It is clear from (1.13) that the conformal boundary, now located at $z = 0$, in this case is just the d-dimensional flat Minkowski spacetime $\mathbb{R}^{1,d-1}$ with metric $ds^2 = -dt^2 + d\mathbf{x}^2$. The subgroups of $SO(2,d)$ isometries that are manifest in this patch are $ISO(1,d-1)$ (the Poincaré transformations on t, x^i) as well as $SO(1,1)$ (the dilation transformation $(t, x^i, z) \to (\lambda t, \lambda x^i, \lambda z)$). The Poincaré form of the AdS metric is the most useful for holographic applications and we shall make extensive use of it in what follows.

However, it is important to stress that the Poincaré coordinates only cover a local patch of the AdS space, not the whole space. This can be seen from the fact that z is related to the old coordinates X^0, X^{d+1} as

$$z = \frac{L^2}{X^0 - X^{d+1}}$$

and, therefore, due to the restriction $z > 0$ we cover only the half $X^0 > X^{d+1}$ of the full AdS space[3]. The Poincaré patch of AdS_{d+1} can be viewed as ordinary flat spacetime (with coordinates t, x^i) extended in an extra curved direction parametrized by z, since at each slice $z = const$ the induced metric is d-dimensional Minkowski spacetime up to a constant factor. This is illustrated in Figure **1**.

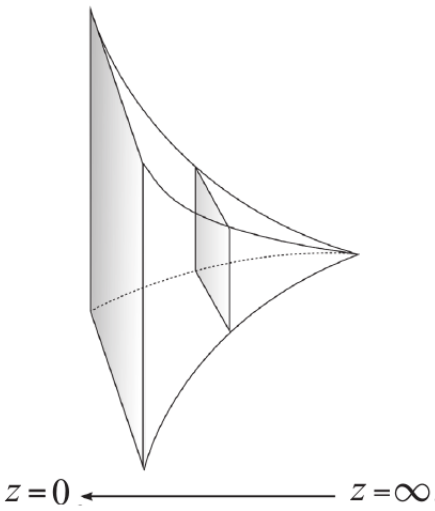

Figure 1: A cartoon of the Poincaré patch (1.13) of AdS_{d+1}. Each slice can be viewed as d-dimensional flat space. Figure adapted from [14].

[3]Of course we could equally well define another similar patch with $z < 0$ and cover the other half, but there is no way to cover both halves (and get a conformally flat metric) using the same chart.

Another useful coordinate system (specially when dealing with black holes) is the so called *static coordinates* $(\tilde{r}, \tilde{\tau}, \Omega_i)$ defined from the global ones by $\tilde{r} = L \sinh \rho, \tilde{\tau} = L\tau$. The metric, then, reads

$$ds^2_{\mathrm{AdS}_{\mathrm{static}}} = -\left(\frac{\tilde{r}^2}{L^2} + 1\right) d\tilde{\tau}^2 + \left(\frac{\tilde{r}^2}{L^2} + 1\right)^{-1} d\tilde{r}^2 + \tilde{r}^2 d\Omega^2_{d-1}. \tag{1.14}$$

As mentioned above, the AdS_{d+1} spacetime solves the Einstein equations (1.3) with a negative cosmological constant

$$\Lambda = -\frac{d(d-1)}{2L^2} \ , \tag{1.15}$$

which can be easily checked using any of the forms presented above for the metric. The corresponding Ricci scalar is $R = -\frac{d(d+1)}{L^2}$, showing that the AdS radius L indeed provides a curvature scale for the geometry. The limit $L \to \infty$, in principle, recovers flat space, but taking it formally (specially on metric coefficients) requires some care such as rescaling quantities by appropriate factors before sending L to infinity.

A very important property of AdS is that, due to its conformal boundary, it behaves like a box. This is most easily seen using the metric in conformal coordinates (1.9). Let us examine the motion of radial outgoing light rays in this metric. By setting $d\Omega^2_{d-1} = 0$ and $ds^2 = 0$ we see that such light rays obey (we take the plus sign since we want outgoing rays)

$$\frac{d\theta}{d\tau} = 1 \qquad \text{or} \qquad \tau(\theta) - \tau(\theta_0) = \theta - \theta_0 \ . \tag{1.16}$$

Now suppose we send one such light ray from deep inside AdS space at $\theta = 0$ ($\rho = 0$ in global coordinates) towards the conformal boundary at $\theta = \frac{\pi}{2}$ ($\rho = \infty$). It follows from (1.16) that the light ray reaches the AdS boundary in a finite coordinate time $\delta\tau = \frac{\pi}{2}$. This is rather counterintuitive, implying that a boundary condition is needed at the AdS boundary to determine how the light ray behaves when it gets there. In particular, if we impose reflecting boundary conditions this means that the light ray above will travel from $\theta = 0$ to the boundary of AdS and back to $\theta = 0$ in the finite coordinate time interval $2\delta\tau = \pi$. A similar calculation can be done for massive particles, and the result is that again they travel towards the boundary and back inside AdS in a finite time as seen by an internal observer, although in this case they do not even really reach the boundary (see, e.g., Section 6.2 of [15]). This fact is one of the reasons why AdS black holes can coexist in thermal equilibrium with their Hawking radiation (since all the radiation emitted outwards bounces at the boundary and eventually goes back inside the space), as we will discuss below.

Euclidean AdS

It will be useful when we formulate the AdS/CFT correspondence to define an Euclidean signature version of AdS_{d+1}, also known as Lobachevsky space, which we denote as EAdS_{d+1}. It is important to emphasize that, in general, Euclidean versions of Lorentzian metrics only make sense when understood inside path integrals, as the result of a Wick rotation to Euclidean time (this will be our case with EAdS). EAdS_{d+1} can be defined by embedding just as we did for the AdS case by merely changing the sign in front of X_0^2 and dX_0^2 in equations (1.5) and (1.6) or, equivalently, by simply Wick rotating the time coordinate of the AdS spacetime. For example, the Poincaré form (1.13) of EAdS_{d+1} reads

$$ds^2_{\mathrm{EAdS}_{\mathrm{Poincaré}}} = \frac{L^2}{z^2}\left(dt_E^2 + d\mathbf{x}^2 + dz^2\right) \ , \tag{1.17}$$

where $t_E = it$ is the Euclidean time. Notice that the isometry group of EAdS_{d+1} is not the conformal group $SO(2,d)$ anymore, but instead its Euclidean version $SO(1,d+1)$.

AdS black holes

Just like the usual Schwarzschild black hole solution is a static, spherically symmetric solution to the vacuum Einstein equations (1.3) with $\Lambda = 0$ [4], there is also an equivalent black hole solution for the case with $\Lambda < 0$. This is the *Schwarzschild-AdS* solution (or simply SAdS). In $d+1$ dimensions, with $\Lambda = -d(d-1)/2L^2$, the SAdS solution is given in static coordinates[5] in the usual black hole form

$$ds^2_{\rm BH} = -f(r)dt^2 + f(r)^{-1}dr^2 + r^2 d\Omega^2_{d-1} \ , \tag{1.18}$$

where $f(r)$ is the function

$$f(r) = 1 - \frac{2m}{r^{d-2}} + \frac{r^2}{L^2} \ . \tag{1.19}$$

The parameter m is related to the black hole mass M by means of

$$m = \frac{8\pi G_N M}{(d-1){\rm Vol}(\mathbb{S}^{d-1})} \ ,$$

where ${\rm Vol}(\mathbb{S}^{d-1}) = \frac{2\pi^{d/2}}{\Gamma(d/2)}$ is the volume of the $(d-1)$-sphere. For example, for $d = 3$ this gives $m = G_N M$. Notice that

i) near $r \to \infty$ the metric reduces to (1.14), that is, SAdS is an asymptotically AdS spacetime;

ii) near $r = 0$ the spacetime approaches the usual asymptotically flat Schwarzschild solution with $f \sim 1 - 2m/r^{d-2}$ (alternatively, by taking $L \to \infty$, which makes $\Lambda = 0$, gives exactly the Schwarzschild solution);

iii) there is an event horizon at $r = r_h$ defined by the largest solution of $f(r_h) = 0$. Sometimes it is convenient to use this equation to eliminate m in favor of r_h as $2m = r_h^{d-2}(1 + r_h^2/L^2)$, in which case the black hole warp function (1.19) can be rewritten as

$$f(r) = 1 + \frac{r^2}{L^2} - \frac{r_h^{d-2}}{r^{d-2}}\left(1 + \frac{r_h^2}{L^2}\right) \ . \tag{1.20}$$

Quantum mechanically any black hole emits thermal radiation with a temperature T_H (the Hawking temperature). This temperature depends on the mass M or, equivalently, on the location of the event horizon r_h, and there are several ways to compute it. The original computation done by Hawking is quite general but complicated, since it involves quantizing matter fields in the curved black hole background. Here we will adopt an easier, heuristic method (based on a trick borrowed from quantum field theory at finite temperature) that lacks some of the rigor of Hawking's calculation but turns out to give the right result.

The starting point is the Euclidean version of the generic black hole solution (1.18) obtained by Wick rotating $t \to -it_E$, namely,

$$ds^2 = f(r)dt_E^2 + f(r)^{-1}dr^2 + r^2 d\Omega^2_{d-1} \ . \tag{1.21}$$

Since the Lorentzian black hole does not have any curvature singularity at the event horizon r_h, the same must happen to its Euclidean version. In order to check that this is the case one should analyze the near horizon region $r \approx r_h$ of (1.21). Assuming that the function $f(r)$ has a simple zero at r_h (i.e., $f(r_h) = 0$ but $f'(r_h) \neq 0$), near the horizon it can be approximated by $f(r) \approx f'(r_h)(r - r_h)$ and the metric to leading order reads

$$\begin{aligned} ds^2 &\approx f'(r_h)(r-r_h)dt_E^2 + \frac{dr^2}{f'(r_h)(r-r_h)} + r_h^2 d\Omega^2_{d-1} \\ &= d\rho^2 + \rho^2 d\varphi^2 + r_h^2 d\Omega^2_{d-1} \ , \end{aligned} \tag{1.22}$$

[4] In fact it is **the only one**, as guaranteed by Birkhoff's theorem [16].

[5] We omit the tildes for static coordinates $\tilde{r}, \tilde{t}$ from now on.

where in the second line we have defined the coordinates ρ and φ by the relations

$$\rho = \sqrt{\frac{4(r-r_h)}{f'(r_h)}} \ , \qquad \varphi = \frac{1}{2}\sqrt{f'(r_h)^2}t_E = \frac{1}{2}|f'(r_h)|t_E \ . \tag{1.23}$$

Notice that the (ρ, φ) part of the metric looks just like the plane $\mathbb{R}^2$ written in polar coordinates, but if φ does not have periodicity 2π the metric will have a conical singularity at $\rho = 0$ (which corresponds to $r = r_h$). But, as argued above, the Euclidean black hole must be smooth at r_h, meaning that φ must have periodicity 2π, i.e., $\varphi \equiv \varphi + 2\pi$. From the definition of φ this in turn implies that t_E is periodically identified with period $\beta = 4\pi/|f'(r_h)|$, i.e., $t_E \equiv t_E + \beta$. Now if we recall that a periodic Euclidean time with periodicity β (to be understood inside the path integral) is precisely the standard prescription used in quantum field theory to put the theory at a finite temperature $T = 1/\beta$, [6] we are lead to conclude that the Hawking temperature associated with the black hole (1.18) is given by

$$T_H = \frac{|f'(r_h)|}{4\pi} \ . \tag{1.24}$$

Strictly speaking this is the result for black holes with a simple zero at $r = r_h$. If $f(r)$ has higher order zeroes the answer will be different, but the argument leading to it is essentially the same.

Let us apply this result to the Schwarzschild-AdS black hole. This is trivially done using the form (1.20) for the function $f(r)$, resulting in

$$T(r_h) = \frac{d\, r_h^2 + (d-2)L^2}{4\pi L^2 r_h} \ . \tag{1.25}$$

Two interesting limits that follow immediately are those of "small" and "large" SAdS black holes (with respect to the AdS radius L), namely

$$T(r_h \ll L) \approx \frac{d-2}{4\pi r_h} \qquad \text{and} \qquad T(r_h \gg L) \approx \frac{d\, r_h}{4\pi L^2} \ . \tag{1.26}$$

Since the temperature decreases with $1/r_h$ for small r_h and grows linearly for large r_h, there must be a minimum temperature $T_{\min}$ in between. Indeed it is easily found to be

$$T_{\min} = \frac{\sqrt{d(d-2)}}{2\pi L} \ , \tag{1.27}$$

happening for $r_{h_{\min}} = \sqrt{\frac{d-2}{d}}L$.

One can associate a heat capacity to the black hole according to

$$C \sim \frac{\partial M}{\partial T} = \frac{\partial M}{\partial r_h}\left(\frac{\partial T}{\partial r_h}\right)^{-1} . \tag{1.28}$$

Since $\frac{\partial M}{\partial r_h} > 0$ (remember that $M \sim r_h^{d-2}(1 + r_h^2/L^2)$), the sign of C is determined essentially by $\frac{\partial T}{\partial r_h}$. As shown in (1.26), for "small" SAdS black holes the temperature decreases with $1/r_h$ just like in asymptotically flat Schwarzschild black holes (in fact, $T = \frac{d-2}{4\pi r_h}$ is exactly the Hawking temperature of Schwarzschild black holes, as can be easily seen taking the limit $L \to \infty$ ($\Lambda \to 0$) in (1.25)). The heat capacity in this case is negative, signaling that they are thermodynamically unstable just like their flat space cousins. In other words, small AdS black holes evaporate as they radiate.

"Large" SAdS black holes, on the other hand, have a temperature that grows linearly with the radius r_h and hence their heat capacity is positive. Even though $C > 0$ alone does not necessarily

[6] Namely, the Euclidean partition function $Z_E[\beta]$ of the QFT, obtained in the usual way as a path integral over periodic trajectories with period β, i.e., $Z_E[\beta] = \int_{\phi(t_E,\mathbf{x})=\phi(t_E+\beta,\mathbf{x})} \mathcal{D}\phi e^{-S_E[\phi]}$, becomes the partition function of a thermal statistical ensemble with temperature $T = 1/\beta$, i.e., $Z_E[\beta] = \mathrm{Tr}\left[e^{-\beta\hat{H}}\right]$. See, e.g., [17] for details.

imply stability, this means that there is a chance that large SAdS black holes are thermodynamically stable, i.e., that they can be in thermal equilibrium with their own Hawking radiation. A detailed stability analysis requires calculating the free energy F and showing that it is minimized by the black hole solution, a calculation that is somewhat tedious to be presented here.[7] It suffices to say that there is a critical temperature

$$T_c = \frac{d-1}{2\pi L} \tag{1.29}$$

above which the SAdS black hole is thermodynamically stable. This unique property of AdS black holes is a consequence from the fact previously discussed in this section that AdS space looks like a box, in the sense that the radiation emitted by the black hole will be reflected at the boundary and reabsorbed by the black hole (note the importance of $C > 0$!) in a finite coordinate time. Below this critical temperature the "thermal AdS spacetime" (global AdS with periodic Euclidean time) is thermodynamically preferred. At $T = T_c$ there is a first order phase transition between the two solutions called the *Hawking-Page transition*. The situation is illustrated in Figure **2**.

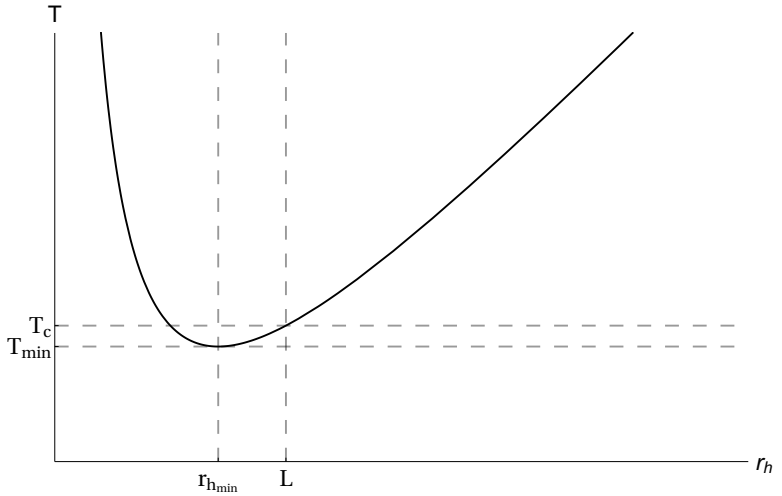

Figure 2: Thermodynamics of the SAdS black hole. No black hole can exist with $T < T_{\min}$ and thermal AdS is the only possible solution in this region. Above $T_{\min}$ a black hole can exist but whether or not it is stable depends on its size: "small" black holes ($r_h < L$) are unstable and thermal AdS is thermodynamically preferred in this region, while black holes with $r_h > L$ become the favored solution, i.e., they can coexist in thermal equilibrium with their Hawking radiation. At $r_h = L$ (corresponding to a critical temperature T_c) there is the Hawking-Page transition between the two situations.

We close this part by mentioning that many other AdS black holes can be constructed by coupling different matter fields to the Einstein-Hilbert action. For example, by introducing a nontrivial $U(1)$ gauge field $A_a(x)$ with action

$$S_m = \int d^{d+1}x\sqrt{-g}\left[-\frac{1}{4e^2}F_{ab}F^{ab}\right]$$

we can get a charged black hole solution which we would name the *Reissner-Nordström-AdS*, since it is the $\Lambda < 0$ analog of the Reissner-Nordström solution in the asymptotically flat case. However, we choose to postpone this kind of discussion at this introductory level, leaving it for the latter chapters of this thesis that are devoted to more specific topics.

[7] It can be found, e.g., in Section 14.2.2 of [15].

1.2 Conformal symmetry and conformal field theories

Here we briefly review some essential features about conformal symmetry and conformal field theories that will be necessary in order to introduce the AdS/CFT correspondence in the sequence. Anticipating the notation which will be used in that opportunity, we shall define and analyze conformal field theories in d flat spacetime dimensions (i.e., $d-1$ spacelike and 1 timelike directions) with coordinates x^μ ($\mu = 0, 1, \ldots, d-1$). The discussion here is inspired by references [18, 14, 19].

Remember that fields are objects that permeate the spacetime in a continuous way, i.e., they are defined at each point. They can be classical or quantum, depending on whether their dynamics is governed by the rules of classical or quantum mechanics. We will be mainly interested in quantum field theories (QFTs), whose quanta of excitation give rise to all the elementary particles of particle physics (see [10] for details).

1.2.1 The conformal group

Most of the QFTs of interest are relativistic, meaning by definition that they are invariant under the *Poincaré symmetry group*. The Poincaré transformations consist of constant spacetime translations a^μ and Lorentz rotations/boosts $\Lambda^\mu{}_\nu$, namely

$$\begin{aligned} x^\mu &\to x^\mu + a^\mu \\ x^\mu &\to \Lambda^\mu{}_\nu x^\nu \ . \end{aligned} \tag{1.30}$$

These transformations are generated by the momentum operator $P_\mu = -i\partial_\mu$ and angular momentum $J_{\mu\nu} = -i(x_\mu\partial_\nu - x_\nu\partial_\mu)$, respectively. It is straightforward to show that they satisfy the following algebra (the Poincaré algebra)

$$\begin{aligned} [J_{\mu\nu}, J_{\rho\sigma}] &= i(\eta_{\mu\rho}J_{\nu\sigma} + \eta_{\nu\sigma}J_{\mu\rho} - \eta_{\nu\rho}J_{\mu\sigma} - \eta_{\mu\sigma}J_{\nu\rho}) \\ [J_{\mu\nu}, P_\rho] &= i(\eta_{\mu\rho}P_\nu - \eta_{\nu\rho}P_\mu) \\ [P_\mu, P_\nu] &= 0. \end{aligned} \tag{1.31}$$

In particular, the second equation above shows that P_ρ transforms as a vector under Lorentz transformations.

The Poincaré group can be enlarged to another symmetry group of spacetime transformations called the *conformal group*. The elements of this group, called conformal transformations, can be defined as the set of all (invertible) coordinate transformations which leave the spacetime metric $g_{\mu\nu}(x)$ invariant up to an arbitrary positive x-dependent scale factor, i.e.,

$$x^\mu \to x'^\mu(x) \qquad \text{such that} \qquad g_{\mu\nu}(x) \to g'_{\mu\nu}(x') = \Omega(x)^2 g_{\mu\nu}(x) \ . \tag{1.32}$$

We will be mainly interested in conformal transformations of flat spacetime metrics, $g_{\mu\nu}(x) = \eta_{\mu\nu}$. From the definition above one can already see that the Poincaré group corresponds to the subset of transformations for which $\Omega(x) = 1$, i.e., those which leave the metric invariant. The name *conformal* is due to the fact that the length of infinitesimal spacetime intervals is changed by an overall local factor ($ds^2 \to \Omega(x)^2 ds^2$) but angles at any point are left invariant, see Figure **3**. In particular, conformal transformations preserve the causal structure of the spacetime[8].

Under an infinitesimal diffeomorphism $x'^\mu = x^\mu + \varepsilon^\mu(x)$ the metric transforms generically to

$$g'_{\mu\nu}(x') = \frac{\partial x^\alpha}{\partial x'^\mu}\frac{\partial x^\beta}{\partial x'^\nu} g_{\alpha\beta}(x) = \eta_{\mu\nu} - (\partial_\mu\varepsilon_\nu + \partial_\nu\varepsilon_\mu) \ .$$

[8]Notice here the importance of positivity of the overall factor: allowing for negative scale factors would destroy causality since timelike (spacelike) intervals would become spacelike (timelike) as a result of the transformation.

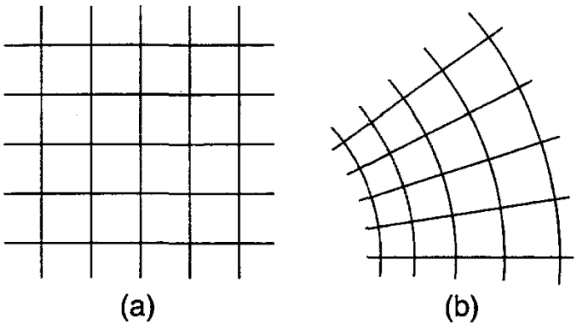

Figure 3: An illustration of a conformal mapping (b) of a given two-dimensional region (a). Angles are preserved by the transformation while distances are not. Figure adapted from [20].

By plugging this into the definition (1.32) implies that, in order to represent a conformal transformation, $\varepsilon^\mu(x)$ must satisfy the *conformal Killing equation*

$$\partial_\mu \varepsilon_\nu + \partial_\nu \varepsilon_\mu = \frac{2}{d}(\partial \cdot \varepsilon)\eta_{\mu\nu} \ , \tag{1.33}$$

where the function $f(x) = \frac{2}{d}(\partial \cdot \varepsilon) \equiv \frac{2}{d}\partial_\mu \varepsilon^\mu$ appearing in the righthand side is the first order contribution to the scale factor $\Omega(x)^2$ in (1.32), i.e., $\Omega(x)^2 = 1 - f(x) + \cdots$.

The general solution to this equation differs drastically for $d = 2$ and $d > 2$ spacetime dimensions. In $d > 2$ dimensions it reads (see [18] for the derivation)

$$\varepsilon^\mu(x) = a^\mu + \omega^\mu{}_\nu x^\nu + \lambda x^\mu + b x^2 - 2(b \cdot x)x^\mu \ , \tag{1.34}$$

where $(b \cdot x) \equiv b_\nu x^\nu$ and $x^2 \equiv x_\nu x^\nu$. It contains a finite number of infinitesimal parameters $\lambda, a^\mu, b^\mu, \omega_{\mu\nu} = -\omega_{\nu\mu}$, in fact $\frac{1}{2}(d+2)(d+1)$ in total[9], showing that the conformal group in $d > 2$ is finite dimensional. One can easily work out the finite version of each of the infinitesimal transformations (1.34) by composing many infinitesimal ones according to the group structure. For the ones associated with a^μ and $\omega_{\mu\nu}$ we get precisely the Poincaré transformations (1.30) (as anticipated above) with the same generators P_μ and $J_{\mu\nu}$ as before. The extra transformations associated with the parameters λ and b^μ are the *dilation* and *special conformal transformation* defined by

$$x'^\mu = \lambda x^\mu \qquad \text{and} \qquad x'^\mu = \frac{x^\mu - b^\mu x^2}{1 - 2(b \cdot x) + b^2 x^2} \ , \tag{1.35}$$

which correspond to the scale factors $\Omega(x) = \lambda^{-1}$ and $\Omega(x) = 1 - 2(b \cdot x) + b^2 x^2$ as defined by equation (1.32). Their generators are $D = -ix^\mu \partial_\mu$ and $K_\mu = -i(2x_\mu x^\nu \partial_\nu - x^2 \partial_\mu)$, respectively. While the former transformation has a clear physical interpretation (stretching out all the coordinates by the same constant factor), the latter may seem obscure at first sight. However, if we rewrite the special conformal transformation in the form

$$\frac{x'^\mu}{x'^2} = \frac{x^\mu}{x^2} - b^\mu$$

it becomes clear that it can be understood as the result of the following sequence of transformations: inversion, translation by $-b^\mu$, and another inversion. Also notice that

$$x'^2 = \frac{x^2}{1 - 2(b \cdot x) + b^2 x^2} \ ,$$

so that points on the surface $1 - 2(b \cdot x) + b^2 x^2 \equiv 1$ have their distance to the origin preserved while points in the interior (exterior) are mapped to the exterior (interior) of that surface.

[9] 1 scalar λ, d components for each vector a^μ and b^μ and $d(d-1)/2$ for the antisymmetric matrix $\omega_{\mu\nu}$. This matches the number of generators of the group $SO(2,d)$, which is not a coincidence as we shall see.

By brute force, using the definitions above, it is then straightforward to show that the full conformal algebra satisfied by the generators $P_\mu, J_{\mu\nu}, D, K_\mu$ consists of the old commutations relations (1.31) of the Poincaré algebra supplemented by the new ones

$$[J_{\mu\nu}, K_\rho] = i(\eta_{\mu\rho}K_\nu - \eta_{\nu\rho}K_\mu) \tag{1.36a}$$
$$[D, P_\mu] = -iP_\mu \tag{1.36b}$$
$$[D, K_\mu] = iK_\mu \tag{1.36c}$$
$$[D, J_{\mu\nu}] = 0 \tag{1.36d}$$
$$[K_\mu, K_\nu] = 0 \tag{1.36e}$$
$$[K_\mu, P_\nu] = -2i(\eta_{\mu\nu}D - J_{\mu\nu}) \ . \tag{1.36f}$$

Equations (1.36a) and (1.36d) tell, in particular, that K_μ transforms as a vector and D as a scalar under Lorentz transformations.

Interestingly, the generators above can all be packaged into a single set of $(d+2)$-dimensional generators $\bar{J}_{AB} = -\bar{J}_{BA}$ (here $A, B = 0, 1, \ldots, d+1$ while $\mu, \nu = 0, 1, \ldots d-1$) defined by

$$\begin{aligned} \bar{J}_{\mu\nu} &= J_{\mu\nu} \\ \bar{J}_{\mu d} &= \frac{1}{2}(K_\mu - P_\mu) \\ \bar{J}_{\mu(d+1)} &= \frac{1}{2}(K_\mu + P_\mu) \\ \bar{J}_{d(d+1)} &= -D \end{aligned} \tag{1.37}$$

which are easily checked to satisfy the algebra

$$[\bar{J}_{AB}, \bar{J}_{A'B'}] = i(\bar{\eta}_{AA'}\bar{J}_{BB'} + \bar{\eta}_{BB'}\bar{J}_{AA'} - \bar{\eta}_{BA'}\bar{J}_{AB'} - \bar{\eta}_{AB'}\bar{J}_{BA'}) \tag{1.38}$$

with $\bar{\eta}_{AB} = \mathrm{diag}(-1, 1, \ldots, 1, -1)$ (note the two minuses!). But this is nothing but the Lie algebra of the group $SO(2, d)$, and therefore we reach the important conclusion that *the conformal group in $d > 2$ dimensions is isomorphic to $SO(2, d)$.*[10] Remember from the previous section that $SO(2, d)$ is also the group of isometries of the AdS_{d+1} spacetime, so we shall start at this point to take more seriously the possibility that conformal theories in d dimensions and AdS_{d+1} gravity may be related. Sometimes it is useful to study the conformal group in Euclidean space – the construction is pretty much the same as done here with $\delta_{\mu\nu}$'s instead of $\eta_{\mu\nu}$'s –, in which case one shows that it is isomorphic to $SO(1, d+1)$.

So far we have discussed conformal symmetry in $d > 2$ spacetime dimensions. The story in the special case of $d = 2$ is much more interesting and rich, but here we shall quickly mention its main features without going through the details since they will not be needed in this thesis. Remarkably, in $d = 2$ there is an infinite number of solutions to the conformal Killing equation (1.33), which implies that the conformal group in $d = 2$ is infinite dimensional. In fact, if we introduce the complex coordinates $z = x^0 + ix^1$ and $\bar{z} = x^0 - ix^1$ the conformal transformations in $d = 2$ can be shown to be equivalent to the infinite set of holomorphic $z' = f(z)$ and anti-holomorphic $\bar{z}' = \bar{f}(\bar{z})$ transformations with arbitrary analytic functions $f, \bar{f}$. The conformal algebra in this case is infinite dimensional, the so called *Virasoro algebra*

$$\begin{aligned} [L_n, L_m] &= (n-m)L_{m+n} + \frac{c}{12}n(n^2-1)\delta_{m,-n} \\ [\tilde{L}_n, \tilde{L}_m] &= (n-m)\tilde{L}_{m+n} + \frac{\tilde{c}}{12}n(n^2-1)\delta_{m,-n} \\ [L_n, \tilde{L}_m] &= 0 \ , \end{aligned}$$

[10] Actually there is a small caveat in the argument here: strictly speaking the group $SO(2, d)$ only contains elements that are continuously connected to the identity, while the conformal group also contains the inversions $x'^\mu = \frac{x^\mu}{x^2}$. Thus, a more precise statement would be that the conformal group is isomorphic to $SO(2, d)$ plus inversions.

where m, n are integer indices, $L_m, \tilde{L}_m$ are the infinite set of Virasoro generators (namely, L_m generates the holomorphic transformations $\delta z = z^{m+1}$ and $\tilde{L}_m$ the anti-holomorphic ones $\delta\bar{z} = \bar{z}^{m+1}$), and $c, \tilde{c}$ are the central charges. The closed finite subalgebra defined by $\{L_{-1}, L_0, L_1, \tilde{L}_{-1}, \tilde{L}_0, \tilde{L}_1\}$ is the equivalent of the $SO(2,2)$ that appear in higher dimensions. In general, 2-dimensional theories exhibiting conformal invariance enjoy many special properties and can be exactly solved only on symmetry grounds due to their high (infinite!) degree of symmetry, and for that reason they have been the topic of a huge amount of research, specially by string theorists since the 2-dimensional worldsheet theory describing the embedding of strings into spacetime is conformally invariant (see Section **1.4** for more). For a detailed exposition of conformal theories in $2d$ we refer the reader to [18, 19], as well as [20] for a more string-oriented view.

1.2.2 Conformal field theories

Conformal field theories (CFTs, for short) are theories invariant under the conformal symmetry group defined above. Notice that this includes invariance under scale transformations, meaning that a CFT cannot have any preferred length scale and, in particular, contains only massless excitations. Even though CFTs are just a subset of relativistic quantum field theories, the tools necessary to describe them are slightly different[11]. Typical questions, then, are not those involving particles and S-matrices (even the notion of asymptotic states needed to define an S-matrix is missing due to the absence of a scale), but instead they involve correlation functions and the behaviour of different local operators under conformal transformations.

Field representations

The operators (fields) in a CFT must fall into irreducible representations of the conformal algebra. Therefore, given an infinitesimal conformal transformation parametrized by ω, $\Lambda(\omega)^\mu_{\ \nu} = (\mathbb{I} + i\omega T)^\mu_{\ \nu}$ (here T denotes one of the conformal generators $P_\mu, J_{\mu\nu}, D, K_\mu$), the task is to find a matrix representation $\mathcal{T}$ of the conformal algebra such that a given field $\Phi(x)$ transforms as

$$\Phi'(x') = (\mathbb{I} + i\omega\mathcal{T})\Phi(x). \tag{1.39}$$

We refer the interested reader to references [18] or [14] for the detailed derivation and simply claim here that the transformation rules for a generic field $\Phi(x)$ under each of the conformal generators are given by

$$\mathcal{P}_\mu\Phi(x) = -i\partial_\mu\Phi(x) \tag{1.40a}$$
$$\mathcal{J}_{\mu\nu}\Phi(x) = i(x_\mu\partial_\nu - x_\nu\partial_\mu)\Phi(x) + \mathcal{S}_{\mu\nu}\Phi(x) \tag{1.40b}$$
$$\mathcal{D}\Phi(x) = -i(x^\mu\partial_\mu + \Delta)\Phi(x) \tag{1.40c}$$
$$\mathcal{K}_\mu\Phi(x) = (-2i\Delta x_\mu - x^\nu\mathcal{S}_{\mu\nu} - 2ix_\mu x^\nu\partial_\nu + ix^2\partial_\mu)\Phi(x)\ , \tag{1.40d}$$

which are fully characterized by the antisymmetric matrix $\mathcal{S}_{\mu\nu}$ and the number Δ. Their interpretation becomes clear when we particularize to $x = 0$, i.e., to the subgroup of conformal transformations (namely all but translations) which leave invariant the origin $x = 0$,

$$\mathcal{J}_{\mu\nu}\Phi(0) = \mathcal{S}_{\mu\nu}\Phi(0) \tag{1.41a}$$
$$\mathcal{D}\Phi(0) = -i\Delta\Phi(0) \tag{1.41b}$$
$$\mathcal{K}_\mu\Phi(0) = 0\ . \tag{1.41c}$$

[11] Unfortunately, so it is also the jargon: while in standard relativistic QFTs the dynamical variables are usually called *fields*, in CFTs they are referred to in general as *operators*. To add to the confusion, the CFT operators are divided in two special classes called *primaries* and *descendants*, depending on their transformation rules under conformal transformations. We shall discuss them below.

That is, the matrix $\mathcal{S}_{\mu\nu}$ is the spin operator associated with the field Φ, while $-i\Delta$ is its eigenvalue under the dilation operator D (at $x = 0$). The number Δ is called the *scaling dimension* of Φ due to the fact that under dilations $x^\mu \to \lambda x^\mu$ it transforms as

$$\Phi(x) \longrightarrow \Phi'(\lambda x) = \lambda^{-\Delta}\Phi(x) \ . \tag{1.42}$$

It follows from the algebra (1.36) that Δ is increased by one when acting with P_μ and decreased by one when acting with K_μ (just like the energy level of a quantum oscillator is raised/lowered by acting with creation/annihilation operators $a^\dagger, a$), namely

$$[D, P_\mu] = -iP_\mu \quad \Longrightarrow \quad D(P_\mu\Phi) = P_\mu(D\Phi) - iP_\mu\Phi = -i(\Delta+1)P_\mu\Phi \tag{1.43a}$$
$$[D, K_\mu] = iK_\mu \quad \Longrightarrow \quad D(K_\mu\Phi) = K_\mu(D\Phi) + iK_\mu\Phi = -i(\Delta-1)K_\mu\Phi \ . \tag{1.43b}$$

This suggests that successive application of K_μ may reduce the scaling dimension indefinitely. However, it turns out that the requirement of unitarity of the theory (i.e., that all physical states have positive norm) implies that there must be a lower bound on the scaling dimension of operators (see [14] for more details on unitarity bounds). For instance, unitarity demands $\Delta \geq (d-2)/2$ for scalar operators in d dimensions. The operators $\mathcal{O}(0)$ having this lowest possible scaling dimension must then be annihilated by K_μ (at $x = 0$), i.e.,

$$K_\mu\mathcal{O}(0) = 0 \ , \tag{1.44}$$

and are called *primary operators*. We have been implicitly talking about primaries since equation (1.40). Given a primary we can construct *descendant* operators with higher scaling dimension simply by acting with momentum generators as explained above[12],

$$\begin{aligned} \mathcal{O}(0) &\to P_{\mu_1}\cdots P_{\mu_n}\mathcal{O}(0) \\ \Delta &\to \Delta + n \ . \end{aligned}$$

Roughly speaking descendants are just operators that can be written as (linear combinations of) derivatives of others, while primaries are the ones which cannot. The properties of descendants follow immediately from those of the corresponding primaries using conformal symmetry. A given primary operator $\mathcal{O}(0)$ and the set of all its descendants – a *conformal family* – form an irreducible unitary representation of the conformal algebra. Hence, we see that the study of any CFT can be boiled down essentially to the construction of its spectrum of primaries, the crucial objects. In fact, as we shall see in a moment, a CFT is completely solved only on symmetry grounds provided that the full set of primary operator dimensions $\{\Delta_i\}$ and OPE coefficients $\{f_{ijk}\}$ (together they are sometimes referred to as the "CFT data") is specified.[13]

Another important property of CFTs is the so called *state-operator correspondence*, namely, the fact that any quantum state $|\mathcal{O}\rangle$ in a CFT is in one-to-one correspondence with a local operator $\mathcal{O}(x)$ of the theory (at $x = 0$),

$$\mathcal{O}(0) \quad \longleftrightarrow \quad \mathcal{O}(0)|\text{vacuum}\rangle \equiv |\mathcal{O}\rangle \ . \tag{1.45}$$

In other words, every state in the theory can be obtained by acting with the corresponding local operator on the vacuum (for example, the vacuum itself trivially corresponds to the identity operator).

[12] Let us explicitly confirm that the condition (1.44) is only satisfied by primary operators. To do that let us show that the first descendant of a primary $\mathcal{O}(0)$ (with dimension Δ and spin $\mathcal{S}_{\mu\nu}$), the operator $\Phi_\nu(0) \equiv P_\nu\mathcal{O}(0)$, is **not** annihilated by K_μ. This follows trivially from the conformal algebra:

$$K_\mu\Phi_\nu(0) = K_\mu\big(P_\nu\mathcal{O}(0)\big) = [K_\mu, P_\nu]\mathcal{O}(0) = -2i(\eta_{\mu\nu}D - J_{\mu\nu})\mathcal{O}(0) = -2i(-i\Delta\eta_{\mu\nu} - \mathcal{S}_{\mu\nu})\mathcal{O}(0) \neq 0 \ .$$

Of course the same argument applies for all the higher order descendants.

[13] This is the philosophy of the *conformal bootstrap* method, a very active topic of recent research in conformal field theories. Namely, the idea is to do a first principles construction of all physically consistent CFTs by determining all the possible sets of CFT data $\{\Delta_i, f_{ijk}\}$ compatible with reasonable physical assumptions such as unitarity and crossing symmetry. A good introduction to the conformal bootstrap is [21].

An important consequence of the state-operator correspondence is that knowledge of the full spectrum of primary operators in a CFT (and consequently all their descendants) is equivalent to knowing the full Hilbert space of the theory.

To summarize this section, representations of the conformal algebra for a given CFT of interest are constructed from its primary operators. These are annihilated by K_μ at the origin and can be chosen to be eigenfunctions of the Lorentz generators $J_{\mu\nu}$ and of the dilation operator D at $x = 0$, meaning that they are completely classified by their spin quantum number (characterizing Lorentz scalars, fermions, vectors, etc.) and scaling dimension Δ (determining the behavior under scaling transformations). In addition, knowledge of the full spectrum of primaries determines the full Hilbert space of states of the theory via the state-operator map.

Correlation functions

Conformal symmetry also significantly constrains the possible form of quantum field theory correlation functions of local operators in a CFT. In particular, it completely determines the spacetime dependence of both 2- and 3-point functions. For example, the two-point function of any two primary scalar fields $\mathcal{O}_i(x), \mathcal{O}_j(y)$ of scaling dimensions Δ_i, Δ_j in a CFT is given by

$$\langle \mathcal{O}_i(x)\mathcal{O}_j(y)\rangle = \delta_{ij}\frac{C_\mathcal{O}}{|x-y|^{2\Delta_i}} \ , \tag{1.46}$$

i.e., it vanishes if the two operators are different and is fully specified (up to a normalization constant $C_\mathcal{O}$, which can be set to 1 after a field redefinition) by the scaling dimension $\Delta_i = \Delta_j \equiv \Delta$ when they are equal. The same happens for the two-point correlator of conserved currents $J_\mu(x)$ (which have $\Delta = d-1$ as a consequence of $\partial_\mu J^\mu = 0$), for which conformal invariance gives

$$\langle J_\mu(x)J_\nu(y)\rangle = C_J\frac{I_{\mu\nu}(x-y)}{|x-y|^{2(d-1)}} \ , \tag{1.47}$$

with $I_{\mu\nu}(x-y) = \delta_{\mu\nu} - 2x_\mu x_\nu/x^2$. For the case of the energy-momentum tensor $T_{\mu\nu}(x)$ (which has $\Delta = d$ due to $\partial_\mu T^{\mu\nu} = 0$) one has

$$\langle T_{\mu\nu}(x)T_{\rho\sigma}(y)\rangle = C_T\frac{\mathcal{I}_{\mu\nu\rho\sigma}(x-y)}{|x-y|^{2d}} \ , \tag{1.48}$$

where $\mathcal{I}_{\mu\nu\rho\sigma}(x-y) \equiv I_{\mu\alpha}(x-y)I_{\nu\beta}(x-y)P^{\alpha\beta}_{\rho\sigma}$ and $P^{\rho\sigma}_{\mu\nu} \equiv \frac{1}{2}(\delta^\rho_\mu\delta^\sigma_\nu + \delta^\sigma_\mu\delta^\rho_\nu) - \frac{1}{d}\eta_{\mu\nu}\eta^{\rho\sigma}$. The normalization constants C_J and C_T in general cannot be set to unity by a proper redefinition of the fields as before since J_μ and $T_{\mu\nu}$ already have a natural normalization fixed by demanding the appropriate Ward identities to be satisfied.

Similarly, the 3-point functions of primary operators in any CFT is completely fixed only on symmetry grounds. For instance, for scalar operators $\mathcal{O}_i$ with dimensions Δ_i they are given by

$$\langle \mathcal{O}_i(x)\mathcal{O}_j(y)\mathcal{O}_k(z)\rangle = \frac{f_{ijk}}{|x-y|^{\Delta_i+\Delta_j-\Delta_k}|y-z|^{\Delta_j+\Delta_k-\Delta_i}|z-x|^{\Delta_k+\Delta_i-\Delta_j}} \tag{1.49}$$

(there are analogous expressions for the 3-point functions of J_μ's and $T_{\mu\nu}$'s, but they are too cumbersome to be presented here, see e.g. [14]). In other words, they are determined up to the overall constants f_{ijk}. Notice that f_{ijk} now cannot be set to unity by field redefinitions, since the normalization of the operators has already been fixed by the 2-point functions. In fact, f_{ijk} are physical parameters depending on the operator content of the CFT and, in a sense, together with the spectrum $\{\Delta_i\}$ of primaries they *define* the particular CFT in question (go back to footnote [13] for more details).

It is tempting to keep going and try to determine higher-point correlators only by evoking conformal symmetry, but unfortunately the impressive performance above stops at three points. With

four points $x_1, \ldots, x_4$ (and similarly with more) it is possible to construct two conformally invariant combinations or *cross-ratios* (here $x_{ij} \equiv x_i - x_j$)

$$u = \frac{x_{12}^2 x_{34}^2}{x_{13}^2 x_{24}^2} , \qquad v = \frac{x_{23}^2 x_{14}^2}{x_{13}^2 x_{24}^2} \tag{1.50}$$

on which four-point functions can depend nontrivially. For example, in the case of a scalar operator $\mathcal{O}$ with dimension Δ, all one can say based on conformal symmetry is that

$$\langle \mathcal{O}(x_1)\mathcal{O}(x_2)\mathcal{O}(x_3)\mathcal{O}(x_4)\rangle = \frac{g(u,v)}{x_{12}^{2\Delta} x_{34}^{2\Delta}} \tag{1.51}$$

but the function $g(u, v)$ of the conformal cross-ratios is left arbitrary[14] and depends on the particular CFT.

However, the calculation of higher-point functions can be simplified using the *operator product expansion (OPE)*, where each product of two primary operators is written as a combination of single primary operators,

$$\phi_1(x_1)\phi_2(x_2) = \sum_{\text{primaries } \mathcal{O}} f_{12\mathcal{O}} C_{\mathcal{O}}(x_{12}, \partial_{x_2})\mathcal{O}(x_2) \tag{1.52}$$

(to be understood inside correlation functions), where $f_{12\mathcal{O}}$ are the 3-point function coefficients mentioned above and the differential operators $C_{\mathcal{O}}(x_{12}, \partial_{x_2})$ are all determined by conformal symmetry once we specify which are the operators ϕ_1, ϕ_2 whose OPE we are interested. The existence of the OPE is a well known fact for any quantum field theory (see e.g. Chapter 18 in [10]), but for generic QFTs the OPE is just as an approximation for x_1 very close x_2 and should actually be written using a $\approx$ instead of an equal sign (it amounts to the intuitive statement that two operator insertions at points close enough to each other can be well approximated by a sum of local operators defined at one of the points). In a CFT, on the other hand, thanks to conformal symmetry the OPE is an exact and convergent expansion even at finite separations. To be more precise, the radius of convergence of the OPE above is given by any x_1, x_2 provided that there are no further operator insertions in between them, i.e., for a correlator of the form $\langle \phi_1(x_1)\phi_2(x_2)\psi(y)\rangle$ the result (1.52) holds exactly provided that

$$|x_1 - x_2| < |y - x_2| . \tag{1.53}$$

By recursive application of the OPE, any n-point function of a CFT can be reduced to a (often huge) combination of 3-point functions, each of which is readily given by formulas such as (1.49) thanks to conformal symmetry. This explains the previously mentioned fact that knowledge of the "CFT data" $\{\Delta_i, f_{ijk}\}$ is equivalent to completely solving the CFT, since any correlator of the theory can be calculated in terms of the dimensions Δ_i and the 3-point coefficients f_{ijk} via recursive application of the OPE.

Energy-momentum tensor

Last, we shall discuss the energy momentum-tensor of CFTs. We have already mentioned it above when discussing the 2-point functions, but its most important property has not yet been presented. It turns out that in any CFT, as a result of conformal invariance, the energy-momentum tensor must be traceless at the classical level. To see this, we just need to recall (see, e.g., [9]) that $T_{\mu\nu}$ in any field theory described by an action S can be obtained using the following trick. We first consider the

[14] Actually not completely arbitrary: since the left-hand side of (1.51) is manifestly invariant under permutations of the x_i, this leads to the following consistency conditions on $g(u, v)$:

$$g(u,v) = g(\tfrac{u}{v}, \tfrac{1}{v}) \text{ (from } 1 \leftrightarrow 2 \text{ or } 3 \leftrightarrow 4) \qquad \text{and} \qquad g(u,v) = \left(\frac{u}{v}\right)^{\Delta} g(v,u) \text{ (from } 1 \leftrightarrow 3 \text{ or } 2 \leftrightarrow 4) .$$

This *crossing symmetry* is one of the pillars of the conformal bootstrap program mentioned in footnote [13].

theory in a curved spacetime metric $g_{\mu\nu}$; then, by considering a transformation which modifies the metric as $g_{\mu\nu} \to g_{\mu\nu} + \delta g_{\mu\nu}$, the energy-momentum tensor is the coefficient multiplying $\delta g_{\mu\nu}$ in the corresponding change of the action, i.e,

$$\delta S = -\frac{1}{2}\int d^d x\sqrt{-g}\; T^{\mu\nu}\delta g_{\mu\nu} \qquad \text{or} \qquad T^{\mu\nu} = -\frac{2}{\sqrt{-g}}\frac{\delta S}{\delta g_{\mu\nu}} \ . \tag{1.54}$$

This means essentially that the energy-momentum tensor sources the metric. The factors of -2 are just conventional and this expression works equally well for the case of field theory in flat space (the one we are interested in) provided we set $g_{\mu\nu} = \eta_{\mu\nu}$ at the end. In the case where the transformation mentioned above is a conformal transformation $x^\mu \to x^\mu + \varepsilon^\mu(x)$, we have already determined in equation (1.33) that the corresponding change in the metric is

$$\delta g_{\mu\nu} = -(\nabla_\mu \varepsilon_\nu + \nabla_\nu \varepsilon_\mu) = -\frac{2}{d}(\nabla\cdot\varepsilon) g_{\mu\nu} \ . \tag{1.55}$$

The variation of the action then reads

$$\delta S = \frac{1}{d}\int d^d x\sqrt{-g}\; g_{\mu\nu}T^{\mu\nu}(\nabla\cdot\varepsilon) \ , \tag{1.56}$$

which must be zero since conformal transformations are assumed to be a symmetry. Hence, the fact that $\varepsilon(x)$ is an arbitrary parameter implies that

$$T^\mu_{\ \mu} \equiv g_{\mu\nu}T^{\mu\nu} = 0 \ , \tag{1.57}$$

i.e., the classical energy-momentum tensor of any CFT has zero trace. At the quantum level this may not be the case – the conformal symmetry may be broken by quantum effects and, as a result, the stress-tensor operator may acquire a nonvanishing trace. This is the so called Weyl anomaly (see [20] for details).

1.3 Gauge theories

In quantum field theory the procedure of turning a global symmetry into a local one is known as *gauging* and the resulting theories are referred to as *gauge theories*. They are some of the building blocks for the description of all the four fundamental forces in nature, since the standard model of elementary particles (describing the strong, weak, and electromagnetic forces) is formulated in terms of gauge theories and even gravity can be understood as a gauge theory. Here we introduce the essential features of gauge theories that will be needed in this thesis, with special emphasis on non-Abelian ones (Yang-Mills theories). Then we discuss a specific supersymmetric generalization that is in the core of the original AdS/CFT correspondence, as we shall see in Section 2.2. Again, this is not at all intended to be a rigorous analysis of gauge theories, for which we refer the interested reader e.g. to [10, 11] (for a general particle physics view) or [14, 22] (for a holography-oriented view).

1.3.1 Abelian gauge theories

The simplest example of a gauge symmetry to start with is that of the Abelian gauge symmetry of electromagnetism. Namely, the well known Maxwell vector field $A_\mu(x)$ is described by the action

$$S_{\text{Maxwell}} = -\frac{1}{4}\int d^d x F_{\mu\nu}F^{\mu\nu} \ , \tag{1.58}$$

where

$$F_{\mu\nu} = \partial_\mu A_\nu - \partial_\nu A_\mu \tag{1.59}$$

is the electromagnetic field strength tensor. The action is clearly invariant under the $U(1)$ gauge transformation

$$A_\mu(x) \to A_\mu(x) - \partial_\mu \alpha(x) \tag{1.60}$$

for any smooth function $\alpha(x)$, since $F_{\mu\nu}$ itself is not changed.[15]

A beautiful way in which the Maxwell action above can be introduced (and which will set the ground for the discussion of non-Abelian theories in the sequence) is as follows. Suppose we have a free field theory action with a *global* $U(1)$ symmetry, which for simplicity we take to be a Dirac fermion field $\Psi(x)$ of mass m. Namely, its action

$$S_\Psi = \int d^d x \bar{\Psi}(i\gamma^\mu \partial_\mu - m)\Psi \tag{1.61}$$

is obviously invariant under the global $U(1)$ transformation

$$\Psi(x) \to \Psi'(x) = e^{iq\alpha}\Psi(x) \tag{1.62}$$

with real and constant parameter α (here $q \in \mathbb{R}$ is the $U(1)$ charge of Ψ), since $\bar{\Psi}(x) \to \bar{\Psi}'(x) = e^{-iq\alpha}\bar{\Psi}(x)$ and the bilinears $\bar{\Psi}\Psi, \bar{\Psi}\gamma^\mu\partial_\mu\Psi$ remain unchanged. However, the action is **not** invariant under the *local* $U(1)$ transformation with $\alpha \equiv \alpha(x)$ due to the failure of the derivative $\partial_\mu\Psi$ to transform as Ψ (namely, $\partial_\mu\Psi'(x) \neq e^{iq\alpha(x)}\partial_\mu\Psi(x)$ due to the extra contribution $+iq\partial_\mu\alpha(x)$ coming from the chain rule). If one insists in constructing an action for our Dirac fermion exhibiting such a local symmetry, i.e., we try to gauge this $U(1)$ symmetry, we are forced to replace the usual derivative ∂_μ by a gauge covariant derivative

$$D_\mu = \partial_\mu + iqA_\mu(x) \tag{1.63}$$

in such a way that $D_\mu\Psi$ now transforms in the same way as Ψ, that is $D_\mu\Psi(x) \to e^{iq\alpha(x)}D_\mu\Psi(x)$. The action then remains invariant provided that A_μ introduced in (1.63) transforms simultaneously under the $U(1)$ local transformation as in (1.60) (notice the minus sign!) in order to cancel the extra $+iq\partial_\mu\alpha(x)$ mentioned above. In other words, we must couple a Maxwell field to our fermion Ψ if we want a theory with $U(1)$ gauge symmetry. The resulting action for the fermion and the Maxwell field enjoying this symmetry,

$$S_{\text{QED}} = \int d^d x \left[-\frac{1}{4}F_{\mu\nu}F^{\mu\nu} + \bar{\Psi}(i\gamma^\mu D_\mu - m)\Psi\right] , \tag{1.64}$$

is the famous quantum electrodynamics (QED) action describing the interaction between photons (particle excitations of A_μ) and, e.g., electrons (particle excitations of Ψ). Notice that the "kinetic" term for the fermion, $\bar{\Psi}i\gamma^\mu D_\mu\Psi$, is the one responsible for coupling A_μ to Ψ via the cubic vertex $-q\bar{\Psi}\gamma^\mu\Psi A_\mu$. The strength of the interaction is set by the electric charge q, meaning that electrically neutral fermions (such as neutrinos) are unable to interact with photons.

1.3.2 Non-Abelian gauge theories

The generalization of the procedure above for the case of non-Abelian symmetry groups $\mathbf{G}$ leads to the so called non-Abelian gauge theories or *Yang-Mills theories*. We will be mostly interested here in the gauge group $SU(N_c)$ (the group of $N_c \times N_c$ unitary matrices with unit determinant), with Lie algebra

$$[T^a, T^b] = if^{abc}T^c , \tag{1.65}$$

where T^a are the generators, the totally antisymmetric symbols f^{abc} are the structure constants characterizing the group[16], and the indices a, b, c run from 1 to $N_c^2 - 1$ (the dimension, or total

[15] Strictly speaking, any other Lagrangian of the form $\mathcal{L}(F_{\mu\nu}F^{\mu\nu})$ would leave the arguments in this section unchanged, since this is also trivially gauge invariant. We focus here on the linear Maxwell Lagrangian $\sim F_{\mu\nu}F^{\mu\nu}$ both for simplicity and to obtain standard Quantum Electrodynamics at the end of the gauging procedure.

[16] For example, for $SU(2)$ they are $f^{abc} = \epsilon^{abc}$ (the Levi-Civita symbol).

number of generators of $SU(N_c)$). The integer number N_c is called by physicists the number of *colors*, borrowing terminology from the theory of quantum chromodynamics (QCD) that corresponds to $N_c = 3$ (more on that below)[17].

There are many irreducible representations $\mathcal{R}$ of the $SU(N_c)$ algebra, but the most common ones in physics are

- the *fundamental representation*, consisting of traceless Hermitian $N_c \times N_c$ matrices (with dimension $\dim(\mathcal{R}_{\text{fund}}) = N_c$);
- the *adjoint representation*, consisting of the $(N_c^2-1)\times(N_c^2-1)$ matrices T^a defined by the structure constants themselves according to $(T^a)^{bc} = f^{abc}$ (with dimension $\dim(\mathcal{R}_{\text{adj}}) = N_c^2 - 1$, the same as the number of generators).

An illustration for the simplest case of $SU(2)$ may be helpful here. The fundamental in this case is given by the 2×2 Pauli matrices σ^a (divided by 2), namely

$$T^1_{\text{fund}} = \frac{\sigma_x}{2} = \begin{pmatrix} 0 & 1/2 \\ 1/2 & 0 \end{pmatrix}, \quad T^2_{\text{fund}} = \frac{\sigma_y}{2} = \begin{pmatrix} 0 & -i/2 \\ i/2 & 0 \end{pmatrix}, \quad T^3_{\text{fund}} = \frac{\sigma_z}{2} = \begin{pmatrix} 1/2 & 0 \\ 0 & -1/2 \end{pmatrix},$$

while the adjoint corresponds to the 3×3 matrices T^a_{adj} defined by $(T^a_{\text{adj}})^{bc} = \epsilon^{abc}$,

$$T^1_{\text{adj}} = \begin{pmatrix} 0 & 0 & 0 \\ 0 & 0 & 1 \\ 0 & -1 & 0 \end{pmatrix}, \quad T^2_{\text{adj}} = \begin{pmatrix} 0 & 0 & -1 \\ 0 & 0 & 0 \\ 1 & 0 & 0 \end{pmatrix}, \quad T^3_{\text{adj}} = \begin{pmatrix} 0 & 1 & 0 \\ -1 & 0 & 0 \\ 0 & 0 & 0 \end{pmatrix}.$$

It is straightforward to check that both representations indeed satisfy the algebra (1.65).

The procedure of gauging a non-Abelian symmetry is, then, analogous to the Abelian case discussed above (with just a fancier notation). One starts with a field $\Psi(x)$, which again we take to be a Dirac fermion for simplicity, transforming in a given representation $\mathcal{R}$ of $SU(N_c)$. In other words, $\Psi(x)$ is a multicomponent field with components $\Psi^I(x)$, $I = 1, \ldots, \dim(\mathcal{R})$, where $\dim(\mathcal{R}) = N_c$ or $N_c^2 - 1$ for the fundamental or the adjoint representations, respectively. The action for such fields takes the same form as (1.61) (now understood as a shorthand matrix notation for the sum over all the internal Ψ_I's) and is invariant under the global $SU(N_c)$ transformations

$$\Psi(x) \to U_{\mathcal{R}}\Psi(x) \qquad \text{with} \qquad U_{\mathcal{R}} = e^{ig\alpha^a T^a_{\mathcal{R}}} \tag{1.66}$$

with constant parameters $\alpha^a \in \mathbb{R}$ (we have factorized a constant g just as we did for the electric charge in the Abelian case; the meaning of g will become clear soon). However, it is **not** invariant under the local $SU(N_c)$ transformations $U_{\mathcal{R}}(x)$ with $\alpha^a \equiv \alpha^a(x)$ due to the failure of the derivative $\partial_\mu\Psi$ to transform in the same way as Ψ. Once again, if we insist in having such a local invariance we are forced to introduce gauge fields and a gauge covariant derivative D_μ just as in (1.63), but now things look a bit fancier since there may be $N_c^2 - 1$ gauge fields $A^a_\mu(x)$ (one for each generator) and both $A_\mu(x)$ and the covariant derivative are $SU(N_c)$ matrices depending on the representation $\mathcal{R}$, with matrix components

$$(A_\mu)^{IJ} = A^a_\mu (T^a_{\mathcal{R}})^{IJ} \tag{1.67a}$$

$$(D_\mu)^{IJ} = \delta^{IJ}\partial_\mu - igA^a_\mu (T^a_{\mathcal{R}})^{IJ} \ . \tag{1.67b}$$

The fermion action with ∂_μ replaced by D_μ is then gauge invariant provided that $A_\mu(x)$ also transforms as

$$A_\mu \to U A_\mu U^\dagger - \frac{i}{g}(\partial_\mu U)U^\dagger \tag{1.68}$$

[17] In addition to $N_c = 3$ appearing in QCD, the $SU(N_c)$ gauge group with $N_c = 2$ appears in the electroweak sector of the Standard Model, while $N_c = 5$ appears as one of the possible Grand Unification Theories (GUTs) that contain the Standard Model. As we shall see in Chapter 2, a gauge theory with $N_c \to \infty$ appears in the original version of the AdS/CFT correspondence.

in order to compensate for the extra term coming from the derivative of Ψ.

The last step is to give the fields A_μ^a some dynamics. This can be done by defining the field strength

$$\begin{aligned} F_{\mu\nu} \equiv \frac{i}{g}[D_\mu, D_\nu] &= \partial_\mu A_\nu - \partial_\nu A_\mu - ig[A_\mu, A_\nu] \\ &\equiv F^a_{\mu\nu} T^a_{\mathcal{R}} \ , \end{aligned} \tag{1.69}$$

with

$$F^a_{\mu\nu} = \partial_\mu A^a_\nu - \partial_\nu A^a_\mu + f^{abc} A^b_\mu A^c_\nu \ , \tag{1.70}$$

where in (1.69) we have introduced the matrix representation (1.67a) for A_μ and used the Lie algebra (1.65) to arrive at (1.70). Naively, one would take $F_{\mu\nu}F^{\mu\nu}$ to get a Maxwell-like action describing our non-Abelian gauge fields. However, as follows directly from the transformation rule (1.68) for A_μ, this object is not gauge invariant since $F_{\mu\nu}$ itself is not gauge invariant, transforming as

$$F_{\mu\nu} \to U F_{\mu\nu} U^\dagger \ . \tag{1.71}$$

But clearly if we take the trace with respect to the representation $\mathcal{R}$ then it follows from the cyclic property of the trace (and $UU^\dagger = \mathbb{I}$) that the following *Yang-Mills* action is gauge invariant[18]

$$S_{\rm YM} = -\frac{1}{2}\int d^d x \, {\rm Tr}(F_{\mu\nu}F^{\mu\nu}) = -\frac{1}{4}\int d^d x \ F^a_{\mu\nu}F^{a\mu\nu} \ , \tag{1.72}$$

where in the last step we have taken the trace explicitly in the fundamental of $SU(N_c)$.[19]

The full fermion-Yang-Mills action enjoying our desired $SU(N_c)$ gauge invariance then is

$$S_{\rm QCD} = \int d^d x \left[-\frac{1}{4}\,{\rm Tr}(F_{\mu\nu}F^{\mu\nu}) + \bar\Psi(i\gamma^\mu D_\mu - m)\Psi \right] \ . \tag{1.73}$$

We have labeled this action $S_{\rm QCD}$ in an abuse of language since the particular case of $N_c = 3$ (i.e., $SU(3)$ gauge group) and $N_f = 6$ fermions just like Ψ above (each with a different mass) all transforming in the fundamental representation corresponds to the theory of quantum chromodynamics (QCD) that describes the strong nuclear force. Namely, each of the 6 fermions Ψ is a quark field (they are denoted as up, down, charm, strange, top, and bottom) and the property distinguising them is called *flavor*; the 8 Yang-Mills fields A^a_μ are the gluons; and $N_c = 3$ corresponds to the number of "colors" that can be carried by each quark.

It is important to note that $F_{\mu\nu}F^{\mu\nu}$ for a non-Abelian field is not just a kinetic term as in the Abelian case. As can be seen from the definition (1.70), besides the standard kinetic term $\sim (\partial A)^2$ it contains two self-interaction terms $\sim g(\partial A)A^2$ and $\sim g^2 A^4$ between the gluons. That is, contrary to the electromagnetic case (where photons do not couple to each other) the gluons interact amongst themselves by means of cubic and quartic vertices proportional to g and g^2, respectively. This is a general feature of non-Abelian gauge theories. The constant g (sometimes denoted by $g_{\rm YM}$) is the fundamental Yang-Mills coupling, which is dimensionless in $d = 4$ spacetime dimensions.

1.3.3 $\mathcal{N} = 4$ SYM theory

There is a specific generalization of the Yang-Mills theories defined above in $d = 4$ spacetime dimensions, the so called $\mathcal{N} = 4$ *supersymmetric* $SU(N_c)$ *Yang-Mills theory* or simply $\mathcal{N} = 4$ SYM, which appears on the CFT side of the original AdS/CFT duality, and our goal here is to briefly discuss its main features.

[18] Again this is not the only possible gauge invariant action that can be constructed from $F_{\mu\nu}$, but we focus for simplicity in this simple form in order to obtain the standard Quantum Chromodynamics action below.

[19] In general, one has to use the fact that ${\rm Tr}(T^a T^b) = C(\mathcal{R})\delta^{ab}$, where $C(\mathcal{R})$ is a real number that depends on the representation. For the fundamental, which is our case, we have $C(\mathcal{R}) = 1/2$.

Let us begin by presenting the $\mathcal{N}=4$ SYM action to, then, discuss its main features. It is given by[20]

$$\begin{aligned} S_{\mathcal{N}=4\text{ SYM}} &= -\frac{1}{g_{\text{YM}}^2}\int d^4x\ \text{Tr}\left\{\frac{1}{2}F_{\mu\nu}F^{\mu\nu}+i\bar{\lambda}^I\gamma^\mu D_\mu\lambda^I+D_\mu X^i D^\mu X^i\right. \\ &\left.+\bar{\lambda}^I\Gamma^i_{IJ}[X^i,\lambda^J]-\sum_{i<j}[X^i,X^j]^2\right\}. \end{aligned} \tag{1.74}$$

First of all, this action enjoys $SU(N_c)$ gauge invariance with all the fields transforming in the adjoint representation of the gauge group (see previous subsection for details), so the trace is taken in the adjoint of $SU(N_c)$. The three terms in the first line are "kinetic terms" for the set of fields (A^a_μ,λ^I,X^i) that constitute the theory, namely 4 Weyl spinors (4 real components each) λ^I and 6 real scalars X^i all minimally coupled to the N_c^2-1 gauge fields A^a_μ via the gauge covariant derivative D_μ (see (1.63)) as required for gauge invariance. The second line contains interactions between the fermions and the scalars, that is, a quartic interaction $\sim[X,X]^2$ between the scalars and a Yukawa-like interaction $\sim\bar{\lambda}[X,\lambda]$ between the fermions and the scalars (the Γ^i_{IJ} are gamma matrices for $SO(6)$, whose meaning will become clear soon).[21]

Besides the $SU(N_c)$ gauge symmetry, $\mathcal{N}=4$ SYM has many more symmetries. Namely, it is invariant under four supersymmetry transformations (the reason why it has $\mathcal{N}=4$ in the name) of the type

$$\begin{aligned} \delta_A(\text{boson}) &= \text{fermion} \\ \delta_A(\text{fermion}) &= \text{boson} \end{aligned}$$

$(A=1,\ldots,4)$ which mix the gauge field, the fermions, and the scalars. We shall not show the transformations explicitly here since they are too complicated (they can be found e.g. in Section 3.3.6 of [14]). The corresponding (fermionic) generators are called Q^A. It can be shown that this is the maximal number of supersymmetries in $d=4$ dimensions, so $\mathcal{N}=4$ SYM is, in fact, the maximally supersymmetric theory in 4 dimensions. All the relative interactions between the fields are completely fixed by supersymmetry, the only overall tunable parameter of the theory being the gauge coupling g_{YM}. Also, due to the extended $\mathcal{N}=4$ supersymmetry there is an extra $SU(4)\equiv SO(6)$ bosonic symmetry called *R-symmetry* which have the effect of rotating the 4 supersymmetry generators Q^A amongst themselves.

In addition, it can be proven that, rather remarkably, $\mathcal{N}=4$ SYM is invariant both at the classical and quantum levels under the full conformal symmetry group $SO(2,4)$, so it is truly a CFT of the type discussed before in Section 1.2. Just to give a flavor, the beta function (which encodes how the coupling varies as we change the energy scale of the theory) of a $SU(N_c)$ gauge theory having N_f Weyl fermions and N_s scalars all transforming in the adjoint is given at 1-loop by[22]

$$\beta_{\text{1-loop}}(g_{\text{YM}})=-\frac{g_{\text{YM}}^3}{48\pi^2}N_c\left(11-2N_f-\frac{1}{2}N_s\right)+\mathcal{O}(g_{\text{YM}}^5)\ , \tag{1.75}$$

[20] There may be also a so called theta-angle term $\frac{\theta_{\text{YM}}}{8\pi^2}F_{\mu\nu}{}^*F^{\mu\nu}$, but this is a topological term which does not affect the equations of motion and in most applications one can set $\theta_{\text{YM}}=0$ (which will be the case here).

[21] The $\mathcal{N}=4$ SYM action (1.74) is complicated and seems quite hard to construct from scratch. A nice way to get this 4-dimensional action (which, by the way, was used in the original work [23]) is by starting with the 10-dimensional $\mathcal{N}=1$ SYM action, which is the only supersymmetric action in $d=10$,

$$S_{d=10,\ \mathcal{N}=1\text{ SYM}}=\int d^{10}x\ \text{Tr}\left[-\frac{1}{2}F_{mn}F^{mn}+\frac{i}{2}\bar{\Psi}\Gamma^m D_m\Psi\right]$$

(Γ^m are the 10-dimensional Dirac matrices), and then dimensionally reducing à la Kaluza-Klein (see [22] for a good introduction to KK reduction) on the torus $\mathbb{T}^6$, i.e., restrict to field configurations which have no momentum along the torus. We shall not do the explicit calculation here (the interested reader is referred to Section 3.3.6 of [14] for details).

[22] This is a quite lengthy but canonical textbook calculation in QFT, see e.g. Chapter 16 of [10] for details.

which magically vanishes for the case of $\mathcal{N}=4$ SYM (i.e., $N_f=4$ and $N_s=6$). In fact, the β function of $\mathcal{N}=4$ SYM has been shown to vanish to all orders in perturbation theory [24], telling us that the theory is truly scale-invariant (which for practical purposes means conformal-invariant) also at the quantum level. Even more than that, as a bonus, there is an extra symmetry transformation called *superconformal transformation* generated by another fermionic generator S in such a way that Q^A, S and the generators $J_{\mu\nu}, P_\mu, K_\mu, D$ of the conformal group combine (together with the R-symmetry generators) into the *supergroup* called $PSU(2,2|4)$, which is the full symmetry group of $\mathcal{N}=4$ SYM. Roughly speaking, we can use this superconformal symmetry to classify the spectrum of all states/operators of $\mathcal{N}=4$ SYM in a very similar way as we did for CFTs (i.e., we can define superconformal primaries, descendants, etc.).

The discussion can be summarized as follows. $\mathcal{N}=4$ SYM is a superconformal field theory (SCFT) with $SU(N_c)$ gauge symmetry and a global $SO(6)$ R-symmetry. It is probably the most symmetric relativistic field theory that can be constructed in $d=4$ dimensions.

As we shall see below when we present the AdS/CFT correspondence, the holographic dual to $\mathcal{N}=4$ SYM involves a supergravity theory in the 10-dimensional $\mathrm{AdS}_5\times S^5$ spacetime. As bizarre as this might sound for now, at this point one is already in a position to check that such a duality makes a minimal amount of sense from the point of view of bosonic symmetries, since the isometry group of $\mathrm{AdS}_5\times S^5$ spacetime, $SO(2,4)\times SO(6)$ (the conformal group in $d=4$ and rotations on the 5-sphere), perfectly matches the (global) bosonic symmetries of $\mathcal{N}=4$ SYM.[23]

1.3.4 't Hooft large N_c expansion

Non-Abelian gauge theories with a large number of colors ($N_c\to\infty$) have many remarkable properties (see [25] for a review). This nontrivial limit was first pointed out by 't Hooft in 1974 in the celebrated work [26]. Besides of considerably simplifying the treatment, the limit also provides a very important clue on the connection between gauge theories and string theory that two decades later turned out to play a fundamental role in the discovery of the AdS/CFT duality, as we shall see in the next chapter. Hence, we now review this very important aspect of non-Abelian gauge theories.

A good starting point is to look at the 1-loop beta function of pure $SU(N_c)$ Yang-Mills theory. This is given by (1.75) with $N_f=0, N_s=0$, namely

$$\mu\frac{dg_{\mathrm{YM}}}{d\mu}=-\frac{11N_c}{48\pi^2}g_{\mathrm{YM}}^3+\mathcal{O}(g_{\mathrm{YM}}^5)\ , \tag{1.76}$$

where we have written explicitly the definition of the beta function. By looking at this expression, at first sight the limit $N_c\to\infty$ seems to be ill-defined. However, if we define the *'t Hooft coupling* $\lambda\equiv g_{\mathrm{YM}}^2N_c$ and declare that we want to study the limit of large N_c with λ kept fixed then one can in principle make sense of it. This is the so called *'t Hooft limit*:

$$N_c\to\infty\quad\text{with}\quad\lambda\equiv g_{\mathrm{YM}}^2N_c\quad\text{kept fixed}\ . \tag{1.77}$$

The fact that it is a nontrivial limit can be seen by writing (1.76) in terms of λ,

$$\mu\frac{d\lambda}{d\mu}=-\frac{11}{24\pi^2}\lambda^2+\mathcal{O}(\lambda^3)\ . \tag{1.78}$$

This does not even depend on N_c, therefore having a well-defined $N_c\to\infty$ limit, and the resulting field theory is nontrivial (i.e., interacting) since the beta function for the coupling λ written above does not vanish.

[23] The $SU(N_c)$ gauge symmetry, as any other gauge symmetry, is not a fundamental symmetry (it is just an artifact of having an over-complete description of a given physical system). It just tells us that we have redundant degrees of freedom. That is why there is no counterpart on the gravity side of the correspondence for it as there is for the global symmetries.

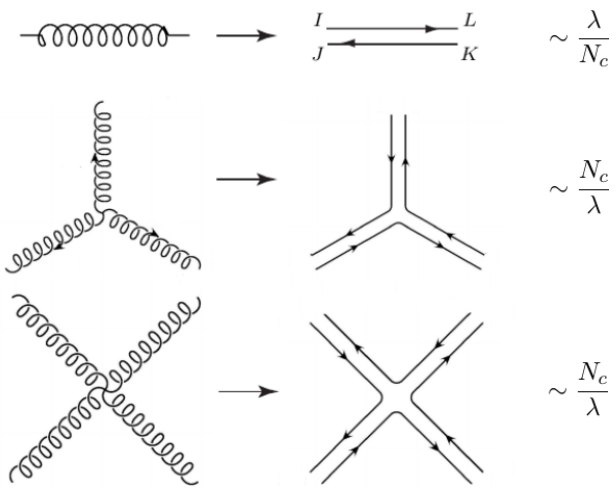

Figure 4: Gluon propagator (top) and the two self-interaction vertices in double-line notation with their corresponding N_c scaling. Remember that λ is to be thought as fixed while N_c we will take to be large.

The Lagrangian for pure $SU(N_c)$ gauge theory (see equations (1.72) and (1.69)) can be written schematically as

$$\mathcal{L} = \frac{N_c}{\lambda}\left[(\partial A)^2 + A^2(\partial A) + A^4\right], \tag{1.79}$$

where we have redefined the field A_μ by absorbing the coupling $g_{\rm YM}$ as $A_\mu \to \frac{1}{g_{\rm YM}} A_\mu$ so as to get a global $\frac{1}{g^2_{\rm YM}}$ factor which we then conveniently expressed in terms of the 't Hooft coupling $\lambda = g^2_{\rm YM} N_c$. From this it is straightforward to derive the Feynman rules for the gluon propagator and the two interaction vertices. In particular, for the point we aim to make here we do not need to worry about the explicit expressions with all the momentum, Lorentz, and color index dependence. We just want to determine how Feynman diagrams scale with N_c, so all we need to read from the Lagrangian above is that

- each gluon propagator ("inverse" of the kinetic term) contributes a factor of $\frac{\lambda}{N_c}$;
- each interaction vertex in the diagram (cubic or quartic) contributes a factor of $\frac{N_c}{\lambda}$;
- each gluon index loop contributes an extra factor of N_c since it implies summation over N_c colors.

Since the gluon field transforms in the adjoint of $SU(N_c)$, i.e., it is a $(N_c^2-1)\times(N_c^2-1)$ matrix $(A_\mu)^{IJ} = A^a_\mu (t^a)^{IJ}$, it is convenient to follow 't Hooft and use the double-line notation illustrated in Figure **4** for gluon vertices and propagators. This was designed to explicitly keep track of all color indices (rows and columns of the matrix), contrary to the standard spiral line notation for gluons (also shown in the Figure) widely used in particle physics calculations, and will play a crucial role in the sequence. For instance, the gluon propagator with double lines and pointing arrows shown in the Figure is a shorthand notation for (in position space)[24]

$$\left\langle \big(A_\mu(x)\big)^I{}_J \big(A_\nu(x')\big)^K{}_L \right\rangle = \delta^I{}_L \delta^K{}_J \frac{\lambda}{N_c} \frac{\eta_{\mu\nu}}{4\pi^2 (x-x')^2}\ , \tag{1.80}$$

with similar expressions for the vertices which will not be needed here. All we need to care about in the following is the $\frac{\lambda}{N_c}$ prefactor.

[24]There is a subtlety here. Strictly speaking, (1.80) is the propagator of a $U(N_c)$ (not $SU(N_c)$) Yang-Mills field. In fact, this was the case studied by 't Hooft in the original work. For the case of $SU(N_c)$ the color factor $\delta^I{}_L \delta^K{}_J$ in (1.80) is changed to $\delta^I{}_L \delta^K{}_J - \frac{1}{N_c}\delta^I{}_J \delta^K{}_L$. However, in the large N_c limit we are interested in here they become the same, so we shall ignore this subtlety and refer always to $SU(N_c)$ which is our case of interest.

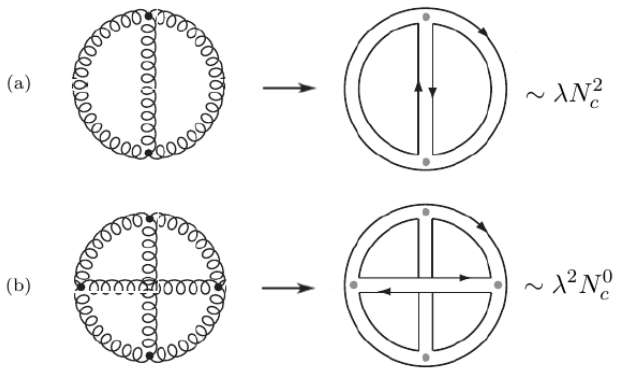

Figure 5: Two examples of Feynman diagrams in double-line notation. (a) is a planar diagram since it can be drawn on the plane without crossing legs, while (b) is not (only on top of a torus we can draw it properly, i.e., without crossing extra legs).

At this point we are ready to start analyzing Feynman diagrams and determining how they scale with N_c. In Figure **5** we show two examples. The first one (a) has 3 propagators, 2 vertices, and 3 index loops and hence according to the Feynman rules above it is proportional to λN_c^2. The second one (b) contains two extra vertices, 3 more propagators and one less index loop as it becomes clear from the double line notation and, therefore, goes like $\lambda^2 N_c^0$. Note that at large N_c the diagram (b) is subleading compared to (a). Visually, what distinguishes them is the fact that (a) can be drawn on a plane (it is a *planar* diagram) while (b) cannot. In fact, whether diagrams dominate or not at large N_c depends on whether one is or not able to draw it on a plane, as we shall now try to make more precise.

In general, a diagram having V vertices, E propagators (edges), and F index loops (faces) scales as

$$\sim \left(\frac{N_c}{\lambda}\right)^V \left(\frac{\lambda}{N_c}\right)^E {N_c}^F = \lambda^{E-V} N_c^{V-E+F} \equiv \lambda^{E-V} N_c^{\chi} \ . \tag{1.81}$$

The power of N_c appearing above is precisely (and rather amazingly) the *Euler characteristic*

$$\chi = V - E + F \tag{1.82}$$

of the two-dimensional surface defined by the double-line diagram by "filling the loops with faces". This number is well known by mathematicians to be a topological invariant, meaning that it is the same for all surfaces which are topologically equivalent (such as a sphere and a plane, or a donut and a coffee mug). In fact, it can be written in terms of the *genus* h of the surface (the number of handles or "holes" in the surface) as

$$\chi = 2 - 2h \ . \tag{1.83}$$

For instance, a sphere has no holes ($h = 0$) so $\chi = 2$, a torus has $h = 1$ hole and thus $\chi = 0$, a two-torus has $h = 2, \chi = -2$, and so on. In Figure **6** we try to illustrate the situation.

Since every Feynman diagram in the theory has a particular dependence on N_c fixed by its genus h, this means that any physical quantity of the theory that can be constructed from Feynman diagrams may as well be written as an expansion in N_c and h. For instance, the partition function Z (given by the sum of all Feynman diagrams with amputated external legs such as the ones shown in Figure **5**) read

$$\log Z = \sum_{h=0}^{\infty} N_c^{2-2h} f_h(\lambda) \ , \tag{1.84}$$

where $f_h(\lambda) = \sum_i c_{h,i} \lambda^i$ is some polynomial in the 't Hooft parameter λ.[25] Although here we are

[25]This polynomial nature should be clear from our two examples above, where each diagram contributes with a different power of λ. To be precise, the sum over i here is over all the diagrams with a given topology h and the coefficients $c_{h,i}$ carry all the information regarding the internal structure of a particular diagram.

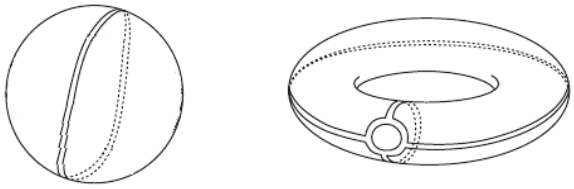

Figure 6: A double-line diagram defines a two-dimensional surface by "filling loops with faces" in such a way that they become faces of the resulting surface. Here we show the surfaces defined by the illustrating diagrams of Figure **5**. The planar diagram (a) defines a genus-0 surface while (b) defines one of genus-1. The details of the surface are of course different (and hard to draw) for different diagrams, but remarkably the large N_c counting ignores that fact completely and only cares about topology. Figure adapted from [27].

focusing on pure $SU(N_c)$ Yang-Mills theory for simplicity, it is important to stress that the same conclusion can be reached if fermions are present (such as in QCD or even in the $\mathcal{N} = 4$ SYM theory).

It follows from the discussion above, or equivalently from expression (1.84), that in the strict limit $N_c \to \infty$ all the diagrams containing holes ($h > 0$) can be neglected since they are suppressed by $1/N_c^2$ factors. In this limit, for any physical process of interest one just needs to take into account the contribution of planar diagrams, which simplifies a lot the treatment since loop diagrams simply do not appear. This is referred to as the *planar limit* of the theory.

To summarize, the important lesson to take from here is the following:

- the large N_c expansion organizes Feynman diagrams in decreasing powers of N_c according to their topology: genus-0 diagrams are proportional to N_c^2, genus-1 to N_c^0, genus-2 to N_c^{-2}, etc.;
- in the $N_c \to \infty$ limit the theory simplifies considerably since only planar diagrams survive.

1.4 String theory in a nutshell

The last ingredient necessary in order to introduce the AdS/CFT correspondence is string theory. Of course this is a vast topic and an appropriate presentation containing all the details is way beyond the scope of this thesis (we refer the reader, for example, to the canonical textbook [20, 28]). The goal here is just to review in a concise way the core concepts of string theory – specially the role of D-branes – that are essential to understand the conjecture in its original form and its motivation.

String theory, as the name suggests, is a theory of one-dimensional extended (rather than pointlike) objects, or *strings*. They have a natural length scale set by the string length l_s (sometimes $\alpha' \equiv l_s^2$ is more appropriate) and can be open or closed depending on whether they have endpoints or not.

When a string moves in spacetime, it sweeps out a 2-dimensional worldsheet rather than a worldline, as illustrated in Figure **7**. The worldsheet description of strings is governed by the *Polyakov*

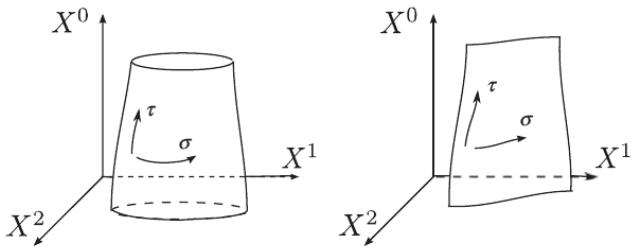

Figure 7: Embedding of closed (left) and open (right) strings into spacetime. The worldsheet is parametrized by (τ, σ), where τ is the proper time (similar to the point particle case) and σ is a parameter along the spatial extent of the string. For closed strings the worldsheet looks like a cylinder, while for open strings it is a strip. Figure taken from [14].

action

$$S_{\text{Polyakov}} = -\frac{1}{4\pi\alpha'}\int d\tau d\sigma\ \sqrt{-g}g^{\alpha\beta}\partial_\alpha X^\mu \partial_\beta X_\mu\ , \tag{1.85}$$

where $g_{\alpha\beta}$ is the metric on the worldsheet and $X^\mu(\tau,\sigma)$ describes its embedding into spacetime. This is nothing but the area of the worldsheet (just as the point particle action is given by the length of its worldline) written in a different form with the help of an auxiliary field $g_{\alpha\beta}$. In fact, this statement can be made clear by simply eliminating $g_{\alpha\beta}$ using its equations of motion to show that we are left with the so called Nambu-Goto action $S_{\text{NG}} = \frac{1}{2\pi\alpha'}\int d^2\sigma\sqrt{-\gamma}$, where $\gamma_{\alpha\beta} \equiv \frac{\partial X^\mu}{\partial\sigma^\alpha}\frac{\partial X^\nu}{\partial\sigma^\beta}\eta_{\mu\nu}$ is the induced metric on the worldsheet. However, the Polyakov form of the action is much more convenient for quantization since it involves no square root of the quantum operators and also enjoys nice symmetries such as worldsheet diffeomorphisms and the very important Weyl invariance

$$g_{\alpha\beta}(\tau,\sigma) \to \Omega(\tau,\sigma)^2 g_{\alpha\beta}(\tau,\sigma)\ . \tag{1.86}$$

These can be used to fix a gauge where $g_{\alpha\beta}(\tau,\sigma) = \eta_{\alpha\beta}$ (flat worldsheet metric) and we are still left with the remnant Weyl symmetry $\eta_{\alpha\beta} \to \Omega(\tau,\sigma)^2\eta_{\alpha\beta}$ which we immediately recognize as 2d conformal symmetry! In other words, string theory can be described as a 2-dimensional CFT on a flat worldsheet, which makes it very powerful for calculations since (as we have seen in Section 1.2) 2d CFTs have an infinite amount of conserved charges that tipically allows them to be exactly solved only on symmetry grounds.

Strings can be quantized in a similar way as we do for pointlike particles, i.e., either from a canonical or from a path integral perspective. An unusual feature is that mathematical consistency of the quantum theory (for instance, to keep Lorentz invariance at the quantum level) requires a number of extra dimensions. Namely, a total of $d = 26$ spacetime dimensions are required for the purely bosonic version of string theory, while for the supersymmetric version (the *superstring* theory) $d = 10$ dimensions are needed. In the present thesis we will only deal with the superstring, although we shall ignore the prefix and keep refering to it simply as string theory. The superstring action is given by a generalization of the Polyakov action (1.85) to include worldsheet fermions. After quantization, the full spectrum of particle states can be constructed by acting with creation operators in the vacuum state in the very same way as done in standard QFT.[26] As a result, it follows that the closed string spectrum contains gravity among its massless excitations, while massless open string excitations include gauge fields. There appears in addition an infinite tower of both open and closed massive excitations with masses proportional to $1/\sqrt{\alpha'}$.

The quantum strings can interact with each other. The interaction strength (so called *string coupling*) is set by the closed string, $g_s \equiv g_{\text{closed}}$. There could be in principle also an open string coupling g_{open}, but it turns out that this is simply related to the closed string coupling as $g_s \sim g_{\text{open}}^2$, since two open strings can join their endpoints to form (or arise from the splitting of) a closed string. One can then talk about Feynman diagrams and scattering amplitudes for strings just as we do for pointlike particles – see Figure **8** for an example. It is interesting to note that the coupling g_s is not a free parameter of string theory, being instead set dynamically by the vacuum expectation value of one of the fields of the theory (a massless scalar ϕ in the closed string spectrum called the *dilaton*), namely $g_s = \langle e^\phi\rangle$. Indeed, there is only one fundamental tunable parameter in string theory, the string length l_s (or α'), which is one of the nice features in favor of string theory as a possible unifying theory. That in turn does not mean the theory is free of problems. There is a huge number ($\sim 10^{500}$!) of available vacua in which to take the expectation value above and nobody knows which is the right one.

In the path integral formulation of strings we must integrate over all possible 2-dimensional worldsheets in spacetime. By taking into account the string interactions mentioned above, this means

[26] For the bosonic string the vacuum has the unfortunate feature of being a *tachyon*, i.e., it has a negative mass-squared. This signals a bad (unstable) vacuum and at present it is unclear whether there is another alternative vacuum to which this one could decay in order to bosonic strings make better sense. Anyway, the tachyon is eliminated once we deal with the superstring, which is our case of interest, so we will ignore this problem.

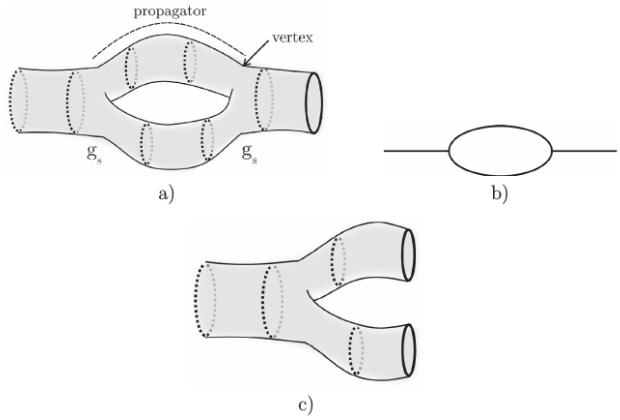

Figure 8: a) An example of a 1-loop diagram involving two external closed strings. This is the stringy analog of the well known cubic interaction b) for point particles. c) The basic interaction vertex ("pair of pants") of closed strings. Figure taken from [22].

we must use more involved worldsheet topologies than the ones shown in Figure **7**. For instance, the worldsheet of interacting closed strings can have handles (or "holes") coming from the splitting and joining of the strings via the "pair of pants" interaction vertex of Figure **8**. The resulting path integral is given by a weighted sum over all different worldsheet topologies connecting initial and final string configurations, the weight being a power of g_s^2 for each hole in the worldsheet (as should be clear from Figure **8**). That is,

$$\log Z_{\text{string}} = \sum_{h=0}^{\infty} g_s^{2h-2} Z_h(\alpha') \ , \tag{1.87}$$

where Z_h is the path integral over the particular worldsheets with fixed genus h, which has the standard exponential-of-the-action form

$$Z_h(\alpha') = \int_{\Sigma_h} \mathcal{D}X^\mu \mathcal{D}g_{\alpha\beta}\ e^{-S_{\text{Polyakov}}} \ . \tag{1.88}$$

This is illustrated in Figure **9** below. In practice, performing this path integral explicitly for arbitrary genus surfaces is very difficult. However, understanding the formal structure in terms of a topological expansion as explained above is of fundamental importance, specially if we recall from the previous section that an identical formal structure appears in the large N_c expansion of gauge theories with $g_s \sim 1/N_c$ (see equation (1.84)). We will come back to this point in the next chapter, since it is in the core of the AdS/CFT correspondence.

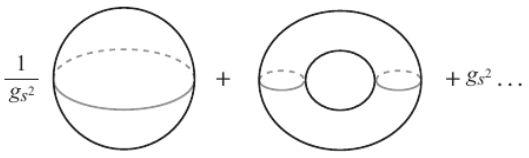

Figure 9: The perturbative string genus expansion (1.87). Figure taken from [15].

Apart from the strings, string theory also contains other fundamental objects called *D-branes*[27]. These are extended objects on which the open string endpoints are stuck to, and a D-brane with p spatial dimensions – so called *Dp-brane* – sweeps a $(p+1)$-dimensional worldvolume as it moves in spacetime. The dynamics of open string endpoints is then equivalent to the dynamics of the D-branes

[27]The D here is for Dirichlet, refering to the fact that the open string endpoints have Dirichlet boundary conditions on these D-branes.

themselves, which are truly dynamical objects in their own right. Namely, excitations of the open string endpoints that are transverse to the brane can be understood as fluctuations of the brane itself in spacetime, while excitations parallel to the brane give rise to gauge fields living on the world-volume of the brane. In general, which gauge field appears in a particular D-brane construction depends on the type and the number of D-branes considered. In particular, non-Abelian gauge fields appear when multiple D-branes are put on top of each other. For example, for a number N_c of coincident D3-branes, the relevant worldvolume gauge theory happens to be 4-dimensional $\mathcal{N} = 4$ SYM with $SU(N_c)$ gauge symmetry. A last comment about gauge fields and D-branes is that, since the gauge field appears from open string dynamics and we have argued above that $g_s \sim g_{\text{open}}^2$, it should not be surprising at this point that the gauge field coupling constant $g_{\text{YM}} \sim g_{\text{open}}$ must be related to the (closed) string coupling constant as $g_s \sim g_{\text{YM}}^2$.

There are five different versions of (super)string theory, but all of them are equivalent in the sense that they are connected to each other by a set (or "web") of dualities as shown in the seminal work by Witten [29]. The two versions we are interested in here are the maximally supersymmetric type IIA and type IIB string theories. Both contain open and closed strings as well as D-branes of different dimensions, but one of the differences is that type IIA contains only Dp-branes with p even while type IIB contains only odd p. The particular one among the "web" of dualities mentioned above relating type IIA and type IIB string theories is called *T-duality*, meaning essentially that type IIA compactified on a spatial direction with radius R is equivalent to type IIB compactified on a spatial direction with inverse radius α'/R.

Treating string theory in its full generality is quite hard, and often a low-energy limit is used to simplify things. In the low-energy limit of string theory we keep only the massless states of the spectrum. We have mentioned above that the massive states have masses $\sim 1/\sqrt{\alpha'}$, so the low-energy limit $E \ll 1/\sqrt{\alpha'}$ can be thought of as the limit $\alpha' \to 0$ [28]. Notice that there is another independent limit, $g_s \to 0$, that can be taken to simplify the treatment. This corresponds to the classical limit of string theory, since the strings only interact at tree level. By combining these two limits, the resulting effective theory (low-energy, tree level) of the closed string sector of type IIA/B string theory is described by type IIA/B *supergravity*, a supersymmetric gravitational theory which is basically a generalization of Einstein gravity in $d = 10$ dimensions coupled to a number of extra fields.[29] In summary,

$\alpha' \to 0$	low-energy limit; still quantum!
$g_s \to 0$	classical (tree level) limit; still stringy!
$\alpha' \to 0, g_s \to 0$	classical supergravity limit

In particular, in this low-energy supergravity description, we can construct and study static solutions such as black holes just as we do in general relativity. An important example is the seminal work by Polchinski [30] showing that the Dp-branes (understood at that time only as the "walls" where open strings are attached) are actually the same as extremal (mass = charge) p-brane solutions of supergravity, which are black-hole-like objects extended in p spatial dimensions.[30] This means that the seemingly harmless Dp-branes of string theory actually curve the spacetime. In fact, this is an important piece of the argument to establish the AdS/CFT conjecture, as we will see later in Section 2.2.

[28] To be more precise, since α' is dimensionful, one should actually say $\alpha'/L^2 \to 0$, with L an appropriate length scale.

[29] Expressions for the type IIA/B supergravity actions can be found e.g. in Section 4.2.3 of [14]. We shall not reproduce them here in our qualitative discussion since they will not be needed.

[30] Indeed, it was this work (together with [29] by Witten, quoted above) that triggered what string theorists refer to as the "second superstring revolution", since after that nonperturbative calculations involving D-branes became possible.

Chapter 2

The holographic duality

This Chapter introduces the holographic duality (or *AdS/CFT correspondence*) and its most important features. We do so by establishing the original $\mathrm{AdS}_5/\mathrm{CFT}_4$ correspondence as introduced by Maldacena in the celebrated work [1] (and soon after, in 1998, refined by Gubser, Klebanov and Polyakov [3] and Witten [2], or simply GKPW) as well as commenting on subsequent generalizations of interest for the present thesis. The idea is to build on the ingredients introduced in the previous Chapter to give an intuitive picture of why the existence of such a highly nontrivial duality is reasonable and deserves the special attention it got over the years.

The Chapter is organized as follows. We start in Section 2.1 by motivating the duality with a sequence of nonrigorous arguments for plausibility followed by the famous decoupling argument due to Maldacena involving a specific D-brane construction, which points towards the equivalence between two very different theories – 4-dimensional $SU(N_c)$ $\mathcal{N}=4$ SYM theory and type IIB supergravity in $\mathrm{AdS}_5 \times S^5$. Inspired by this construction, in Section 2.2 we give a precise statement of three different versions of the $\mathrm{AdS}_5/\mathrm{CFT}_4$ conjecture (which we call weak, strong, and the strongest) depending on how much we extrapolate in parameter space the clues unraveled by the decoupling argument. Section 2.3 then shows how the duality works in practice as a powerful calculation tool to deal with $\mathcal{N}=4$ SYM at strong coupling, the so called GKPW prescription for correlation functions. Section 2.4 gives the first and most important generalization of the conjecture, namely, to finite temperatures T, while Section 2.5 summarizes a number of further extensions of special interest for us.

2.1 Hand-waving arguments

2.1.1 The holographic principle

The AdS/CFT correspondence can be viewed as an explicit realization of the *holographic principle* proposed by t'Hooft [6] and elaborated later on by Susskind [7] in the early 1990's. This principle states that any consistent theory of quantum gravity, unlike all the other known physical theories, must be holographic in the sense that the number of microscopic degrees of freedom needed to describe a given region of spacetime is proportional to the area of that region rather than the volume.

The holographic principle has its roots in 1970's black hole physics, namely the seminal works of Bardeen, Carter, Hawking, and Bekenstein [31, 32, 33]. At that time it was realized that the macroscopic properties of black holes resemble the usual laws of thermodynamics. In particular, there is a first law of black hole thermodynamics (here we are using natural units $\hbar = c = k_B = 1$),

$$dM = \frac{\kappa}{8\pi G_N} dA + \cdots \tag{2.1}$$

where G_N is the Newton constant, κ is the surface gravity at the black hole horizon, A is the area of the horizon (a strictly increasing quantity) and the $\cdots$ include other terms such as ΩdJ for a rotating black hole (Ω is the angular velocity and J is the angular momentum) or ΦdQ for a charged one (Φ is

the electric potential at infinity and Q is the charge). Later it was shown that, quantum mechanically, black holes are not black at all – they emit thermal radiation at a *Hawking temperature* $T_H = \kappa/2\pi$ proportional do their surface gravity and, therefore, are truly thermodynamical objects. By taking this thermodynamical analogy seriously one is lead to conclude from (2.1) that the entropy of black holes is given by the celebrated Bekenstein-Hawking entropy formula[1]

$$S_{\rm BH} = \frac{A}{4G_N} \ . \tag{2.2}$$

The fact that the black hole entropy is proportional to the area of the event horizon is quite striking. It means that the black hole entropy is not an extensive quantity. Even more, it says that the number of possible microstates of a black hole is not proportional to its volume like in conventional statistical systems, but to its area instead. The formula suggests that a theory of quantum gravity has to be fundamentally different from all the other known physical theories. The event horizon must act as some sort of hologram in the sense that all the information contained inside can be projected on it. If we think of areas as volumes in one less dimension, the Bekenstein-Hawking formula seems to suggest that the degrees of freedom of gravity in $d+1$ dimensions might be the same as those of a non-gravitational system living in some d-dimensional slice. In fact, the AdS/CFT correspondence realizes this expectation explicitly by relating a specific quantum theory of gravity to a conformal field theory living in one less dimension, as we shall see.

2.1.2 Large N_c gauge theories and perturbative strings

We have already faced before the observation by 't Hooft in 1974 (two decades before the advent of AdS/CFT!) that non-Abelian gauge theories with a large number of degrees of freedom and perturbative string theories have much in common. Historically, this was one of the crucial clues that lead to the development of the AdS/CFT correspondence, which we shall now briefly recap to set the ground for the sequence (see Section 1.3 for details).

Namely, by rephrasing the usual Feynman rules in terms of a double-line notation, 't Hooft has shown that all the Feynman diagrams in a $U(N_c)$ or $SU(N_c)$ gauge theory with $N_c \gg 1$ can be organized according to their topology. In particular, the partition function of the theory becomes an expansion in topologies of the form (1.84),

$$\log Z_{\rm gauge} = \sum_{h=0}^{\infty} N_c^{2-2h} f_h(\lambda) \ , \tag{2.3}$$

where $f_h(\lambda)$ is the sum of all amputated Feynman diagrams that can be drawn in a surface of genus h and λ is the 't Hooft parameter. In the strict limit $N_c \to \infty$ the theory simplifies considerably since all the diagrams containing holes ($h > 0$) can be neglected (they are suppressed by $1/N_c^2$ factors) and we only need to take into account the contribution of planar diagrams.

On the other hand, we have also seen in Section 1.4 that the perturbative series in string theory is a topological expansion of the same type,

$$\log Z_{\rm string} = \sum_{h=0}^{\infty} g_s^{2h-2} Z_h(\alpha') \ , \tag{2.4}$$

where $Z_h(\alpha')$ denotes the path integral on worldsheet surfaces of genus h. The two expansions above are formally the same with the string coupling and the number of colors being inversely related,

$$g_s \sim \frac{1}{N_c} \ . \tag{2.5}$$

[1]The subscript in $S_{\rm BH}$ here stands either for Bekenstein-Hawking or Black Hole.

In particular, the simplifying planar limit $N_c \to \infty$ corresponds to the classical (tree-level) limit $g_s \to 0$ of string theory, while successive $1/N_c$ corrections from the gauge theory perspective correspond to successive loop quantum corrections in string theory.

Such an intriguing connection suggests that the two theories may actually be equivalent, i.e.,

$$Z_{\text{gauge}} \stackrel{?}{=} Z_{\text{string}} \tag{2.6}$$

with $N_c \sim g_s^{-1}$. Of course 't Hooft coupling λ and $\alpha' = l_s^2$ must also be somehow related ($\lambda \leftrightarrow \alpha'$) if we are to take this equality seriously, but at this point there is no way to determine how. In fact, at this level of speculation there is no way either to tell specifically which gauge theory and which perturbative string theory construction should be used in order to match this expectation in a precise way. This will be provided by the AdS/CFT correspondence, which states that $SU(N_c)$ $\mathcal{N} = 4$ SYM theory and type IIB superstring theory in an Anti de Sitter background are actually the same thing – both describe the same physics using two different languages – and gives the precise dictionary $N_c \leftrightarrow g_s, \lambda \leftrightarrow \alpha'$ relating the parameters on the two sides.

2.1.3 Why AdS?

Having in mind the speculation raised by the large N_c counting together with the holographic principle, let us now try to argue that Anti de Sitter spacetime may be a natural setup in which to define the string theory appearing on the righthand side of (2.6) in order to give a precise meaning to the equality. We have seen in Section 1.1 that AdS_{d+1} spacetimes naturally have a well-defined codimension-1 surface (the conformal boundary) in which the holographic principle can be applied. Besides, we have also seen that light rays in AdS reach the boundary in a finite time, meaning that such a boundary is in causal contact with the interior and, therefore, there seems to be a real chance for it to be holographic.

The argument consists in counting the total number of degrees of freedom in a d-dimensional $SU(N_c)$ gauge theory (with $N_c \gg 1$) and showing that it is compatible with that of a $(d+1)$-dimensional gravity theory in AdS spacetime. Of course they are both infinity, so we better use regulators to keep track of the relevant cutoff dependences.

We start with the gauge theory in d dimensions. To regulate the theory at the IR we put the system in a spatial box of size R, while UV divergences can be regulated by introducing a small lattice spacing δ. The system thus has $(R/\delta)^{d-1}$ cells. At each cell we have $\sim N_c^2$ degrees of freedom (the number of generators of $SU(N_c)$ at large N_c), so the total number of degrees of freedom is

$$N_{\text{d.o.f., gauge}} \sim \left(\frac{R}{\delta}\right)^{d-1} N_c^2 \ . \tag{2.7}$$

Now let us move to gravity in AdS_{d+1}. It will be convenient to work in the Poincaré system (1.13), namely,

$$ds^2 = \frac{L^2}{z^2}\Big(-dt^2 + \sum_{i=1}^{d-1} dx_i^2 + dz^2 \Big). \tag{2.8}$$

By taking into account the holographic principle mentioned above as well as the Bekenstein-Hawking formula (2.2), the number of gravitational degrees of freedom must be

$$N_{\text{d.o.f., gravity}} = \frac{A_\partial}{4G_N} \ , \tag{2.9}$$

where A_∂ is the spatial area of the AdS boundary located at $z = 0$. This can be regulated by putting the boundary at $z = \delta \to 0$, in which case we get

$$A_\partial = \int_{z=\delta} d^{d-1}x \ \sqrt{-\gamma} = \left(\frac{L}{\delta}\right)^{d-1} \int d^{d-1}x = \left(\frac{LR}{\delta}\right)^{d-1} \ ,$$

where again we have introduced an IR regulator $R \equiv \int dx$ (size of the box). Hence, we find that the number of degrees of freedom of the gravity theory is

$$N_{\text{d.o.f., gravity}} = \frac{1}{4G_N}\left(\frac{LR}{\delta}\right)^{d-1} , \tag{2.10}$$

which has the same parametric dependence on the UV and IR cutoffs as expression (2.7) for the gauge theory provided that we identify

$$N_c^2 \sim \frac{L^{d-1}}{G_N} . \tag{2.11}$$

An identification of this sort arises quite naturally in the original $\text{AdS}_5/\text{CFT}_4$ construction, namely $N_c^2 = \frac{\pi L^3}{2G_N}$ (see Section 2.2).

The fact that the lower dimension gauge theory dual to AdS must actually be a CFT may be motivated at this point as follows. The most general metric ansatz in $d+1$ dimensions compatible with relativistic invariance in d dimensions can be written as

$$ds^2 = \Omega(z)^2\Big(-dt^2 + \sum_{i=1}^{d-1} dx_i^2 + dz^2\Big), \tag{2.12}$$

where the warp factor $\Omega(z)$ depends only on the extra direction z in order to preserve the Poincaré symmetry in the (t, x^i) directions. Not much can be said about the specific form of $\Omega(z)$ for a generic QFT. However, if we restrict our attention to CFTs, the requirement of d-dimensional scaling invariance $(t, \mathbf{x}) \to \lambda(t, \mathbf{x})$ of the above metric fixes it to be the AdS metric (2.8). Namely, the only chance to get this symmetry is by also transforming the extra coordinate z as $z \to \lambda z$ while at the same time scaling the warp factor as $\Omega(z) \to \lambda^{-1}\Omega(z)$ in order to cancel the global λ^2 factor, which uniquely determines

$$\Omega(z) = \frac{L}{z} . \tag{2.13}$$

As a matter of fact, this should not sound surprising at all if we recall from the previous Chapter that the group of isometries of the AdS_{d+1} metric, $SO(2, d)$, is the same as the conformal group in d dimensions.

2.1.4 The extra dimension as the energy scale in the QFT

It is well known since the pioneering works by Kadanoff [34] and Wilson [35] in the 1960's (see [36] for a modern view) that QFTs can be organized in energy (or length) scales. If we wish to understand properties of a QFT system at a length scale $z \gg \epsilon$, where ϵ is some characteristic scale of the system, instead of using the bare theory defined at scale ϵ it is more convenient to "integrate out" short distance degrees of freedom (i.e., to get rid of them by path integrating over their modes) and obtain an effective action valid at the desired length scale z. Of course we can do the same and also get rid of these modes if the interest lies in physics at an even larger scale $z' \gg z$, and so on. The procedure of successively integrating out short-distance degrees of freedom hence defines a flow – the *renormalization group (RG) flow* – describing how the theory changes as a result of this "zooming out" procedure.

If we picture a generic d-dimensional QFT evaluated at continuously increasing length scales z and put them in a sequence labeled by z, we can think of the resulting continuous family of effective theories as a $(d+1)$-dimensional spacetime (see Figure **1**). The extra direction z parametrizes the RG flow, and each particular effective theory corresponds to a constant-z slice, i.e., a point in the RG trajectory. Anti de Sitter space naturally provides such a geometrical picture and it is said to "geometrize the RG flow". In fact, by recalling the AdS metric (in Poincaré coordinates) (2.8) and specially its scaling symmetry

$$(t, x^i, z) \longrightarrow \lambda(t, x^i, z), \tag{2.14}$$

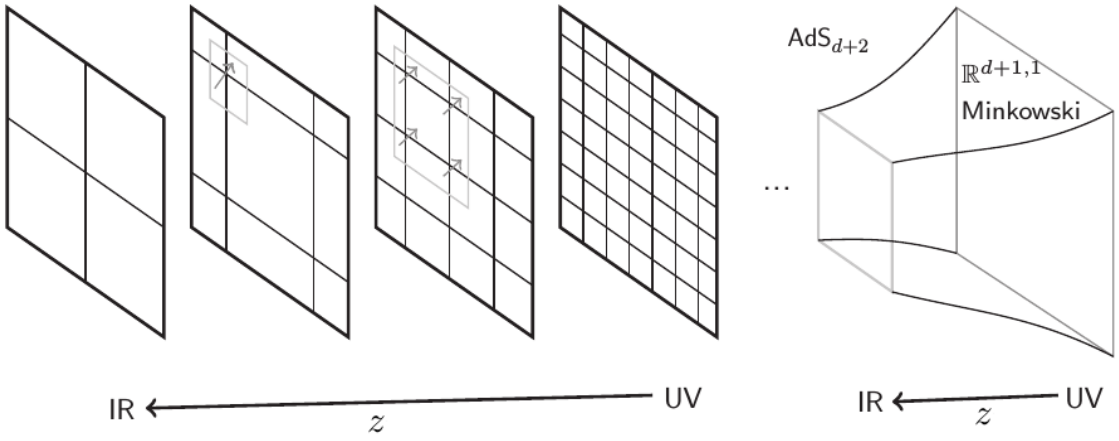

Figure 1: Geometrization of the RG flow by AdS gravity. Figure adapted from [38].

this sounds plausible since the zooming out procedure mentioned above, $(t, x^i) \to \lambda(t, x^i)$, can be understood as moving along the z direction in AdS by the same factor λ. In other words, the extra direction z in AdS space can be thought of as the energy scale in the dual QFT viewed *à la* Wilson. The AdS boundary $z = 0$ (think of a $\lambda \to 0$ transformation) corresponds to the short distance (high energy) or *ultraviolet (UV)* region in the dual QFT, while the deep bulk interior $z = \infty$ (think of $\lambda \to \infty$) corresponds to large distances (small energies) or the *infrared (IR)* region. For further details and a less sketchy argument the reader is referred to Section 4.1 of Ref. [37].

2.1.5 D-branes and the decoupling argument

We have already seen in Chapter **1** that superstring theory contains, besides strings, other fundamental objects called D-branes. These are extended objects having p spatial dimensions (Dp-branes) which can be interpreted in two different ways. First, as fixed "walls" on which open string endpoints are attached with Dirichlet boundary conditions – the so-called *open string perspective*. In this case, the brane dynamics can be described perturbatively in terms of excitations of the open strings themselves. And second, D-branes can be seen as truly gravitating objects on their own, i.e., as black hole-like solutions of supergravity (the low energy limit of superstring theory) – this is the *closed string perspective*. Which view is more appropriate depends on the value of the string coupling constant, namely small g_s for the former and large g_s for the latter. This should become clear in a second when we start writing explicit formulas.

Having this in mind is enough to finally show how the original version of AdS/CFT emerges from a particular D-brane construction in string theory. Namely, one must consider a system of type IIB (super)strings in the presence of a stack of N_c coincident D3-branes (i.e., all on top of each other) in 10-dimensional flat spacetime, as illustrated in Figure **2**. After analyzing this system in the low-energy limit $E \ll 1/\sqrt{\alpha'}$ from the two different perspectives described above and taking some clever "decoupling" limit the AdS/CFT conjecture arises quite naturally as the claim that both pictures are equivalent, as we now show.

The open string picture

Let us start with the open string view. There are two kinds of perturbative string excitations in this system: open strings beginning and ending on the branes, whose vibrations can be seen as excitations of the branes themselves, and the closed strings which are excitations of the background spacetime. Of course they are in general coupled, since open and closed strings can interact with each other by splitting and joining (see Section 1.4). For simplicity, we are interested in the low energy limit $E \ll 1/\sqrt{\alpha'}$ of the system, where only the massless excitations need to be taken into account.

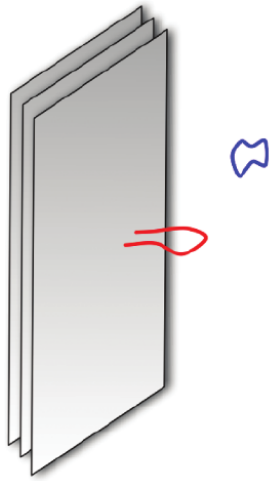

Figure 2: Open and closed string excitations in a system of N_c ($N_c = 3$ here) coincident D3-branes in type IIB string theory. Figure taken from [39].

The effective action for the system has, then, three contributions

$$S = S_{\text{open}} + S_{\text{closed}} + S_{\text{int}} \ , \tag{2.15}$$

with $S_{\text{open,closed,int}}$ denoting the respective open, closed, or open-closed interaction string actions.

The most important piece for our argument here is S_{open}. As we have discussed before, a striking feature of Dp-branes is that they naturally give rise to gauge fields living on their worldvolume, i.e., quantum open strings ending on a Dp-brane have an Abelian gauge field A_μ ($\mu = 0, 1, \ldots, p$) among their massless modes. When a stack of N_c coincident Dp-branes is used instead of a single one the resulting gauge theory becomes non-Abelian, acquiring an $SU(N_c)$ gauge symmetry associated with the freedom of attaching the string endpoints to any of the equivalent N_c branes. Namely, the gauge field becomes a matrix $(A_\mu)^a{}_b$, where the upper (lower) index labels the brane on which the string starts (ends), which is nothing but the adjoint representation of the $SU(N_c)$ gauge group. Besides the gauge field, there are also $9 - p$ excitations transverse to the branes which are nothing but massless scalar[2] modes ϕ_i ($i = p + 1, \ldots, 9$), and the fermionic superpartners which appear due to supersymmetry, all of them also transforming in the adjoint representation since they all have the same stringy origin. For our particular case of interest, a stack of N_c D3-branes, the resulting 4-dimensional $SU(N_c)$ gauge theory has 6 scalars and 4 Weyl fermions and turns out to be precisely the $\mathcal{N} = 4$ SYM theory studied in Section 1.3 (plus α' corrections), i.e.,

$$S_{\text{open}} = S_{\{\mathcal{N}=4 \text{ SYM in } \mathbb{R}^{1,3}\}} + \mathcal{O}(\alpha'), \tag{2.16}$$

with the action $S_{\{\mathcal{N}=4 \text{ SYM}\}}$ given in (1.74). The Yang-Mills coupling g_{YM} appearing in front of the

[2] "Scalar" here means with respect to $SO(1, p)$ representations on the worldvolume of the Dp-brane. The ϕ_i are all scalars since they do not even depend on the coordinates $(x^0, \ldots, x^p)$ along the brane.

action is related to the string coupling by[3]

$$g_{\rm YM}^2 = 2\pi g_s. \tag{2.17}$$

The remaining pieces correspond to closed string modes emitted and absorbed by the branes ($S_{\rm int}$), as well as the self-interaction between the closed strings themselves ($S_{\rm closed}$). Although the explicit expressions can be worked out, for our purposes this will not be necessary (see, e.g., Section 5.2 of [14] for details). It suffices to say that, since gravity modes (low energy closed strings) are involved, both actions have their strength controlled by the 10-dimensional gravitational constant $G_N^{(10)} \sim \alpha'^4$, i.e.,

$$S_{\rm closed} = S_{\{\text{free gravity in } \mathbb{R}^{1,9}\}} + \mathcal{O}(\alpha'^4) \qquad \text{and} \qquad S_{\rm int} = \mathcal{O}(\alpha'^4), \tag{2.18}$$

where $S_{\{\text{free gravity in } \mathbb{R}^{1,9}\}}$ corresponds to free Einstein gravity in 10-dimensional Minkowski space $\mathbb{R}^{1,9}$ (the $\alpha' = 0$ contribution). Therefore, it is clear from equations (2.16),(2.18) that if we take the limit $\alpha' \to 0$ the action for our stack of D3-branes becomes simply

$$S = S_{\{\mathcal{N}=4 \text{ SYM in } \mathbb{R}^{1,3}\}} + S_{\{\text{free gravity in } \mathbb{R}^{1,9}\}} \ , \tag{2.19}$$

i.e., the open strings completely decouple from the closed strings. This is the so called *decoupling limit*. It is important to stress that the result above is reliable only in the regime $g_s N_c \ll 1$ (perturbative strings). Now let us analyze the same system from a different perspective.

The closed string picture

We know that D-branes can, alternatively, also be viewed as gravitating objects that curve the spacetime around them. In this description there are no open strings at all, only closed strings propagating in a curved geometry. In particular, the spacetime metric sourced by our system of N_c coincident D3-branes can be found by explicitly solving the type IIB supergravity equations of motion. Without delving into the details (see also Section 4.4.2 of [14] for a detailed derivation), it is enough to state that the solution for the metric reads [40]

$$ds^2 = H(r)^{-1/2}\big[-dt^2 + dx_1^2 + dx_2^2 + dx_3^2\big] + H(r)^{1/2}\big[dr^2 + r^2 d\Omega_5^2\big], \tag{2.20}$$

where r denotes the transverse distance from the stack of branes and

$$H(r) = 1 + \frac{L^4}{r^4} \qquad \text{and} \qquad L^4 \equiv 4\pi g_s N_c \alpha'^2 \ . \tag{2.21}$$

This metric is supported by a constant dilaton field and a self-dual 5-form configuration $F_{(5)}(r)$ whose expressions will not be needed for our purposes. Notice that the form of the metric above preserves a subgroup $SO(1,3) \times SO(6)$ (Lorentz symmetry on the worldvolume of the branes and rotations in the 6 transverse directions) of the Lorentz symmetry $SO(1,9)$ of 10-dimensional Minkowski space.

[3] We are trying to be economic here by hiding unnecessary calculations, but let us at least give a flavor of why $g_{\rm YM}^2 = 2\pi g_s$, since this relation will turn out to be part of the holographic dictionary relating the parameters on the two sides of AdS/CFT. This comes from the Dirac-Born-Infeld (DBI) action that describes a single Dp-brane excitation (the same reasoning apply to multiple branes),

$$S_{\rm DBI} = -T_p \int d^{p+1}x \sqrt{-\det\big(g_{\mu\nu} + 2\pi\alpha' F_{\mu\nu} + 2\pi\alpha'(\text{scalars})\big)},$$

where $T_p = (2\pi)^{-p} g_s^{-1} \alpha'^{-\frac{p+1}{2}}$ is the tension on the brane and F is the field strength. In our case of interest, $p = 3$, expanding to leading order in α' yields precisely the Yang-Mills action $S_{\rm YM} = -\frac{1}{g_{\rm YM}^2}\int d^4x \left(\frac{1}{4} F^a_{\mu\nu} F^{\mu\nu a}\right)$ with $g_{\rm YM}^2 \equiv 2\pi g_s$ (plus a bunch of extra terms).

The important thing to note is that this background consists of two completely different regions for small and large r. For $r \gg L$ we have $H(r) \approx 1$ and the metric above reduces simply to flat spacetime in 10 dimensions, while for $r \ll L$ we get $H(r) \approx L^4/r^4$ and the metric reads

$$\begin{aligned} ds^2 &= \frac{r^2}{L^2}\big[-dt^2 + dx_1^2 + dx_2^2 + dx_3^2\big] + \frac{L^2}{r^2}dr^2 + L^2 d\Omega_5^2 \\ &= \frac{L^2}{z^2}\big[\eta_{\mu\nu}dx^\mu dx^\nu + dz^2\big] + L^2 d\Omega_5^2 \ . \end{aligned} \tag{2.22}$$

In the last step above we have introduced a new radial coordinate $z \equiv \frac{L^2}{r}$ and used the 4-dimensional Minkowski metric $\eta_{\mu\nu}$ to put the metric in a more compact form. The first piece is just the AdS_5 metric in Poincaré coordinates (see (1.13)) with AdS radius L while the last piece is a 5-sphere having the same radius L, so the geometry at large r is factorized into $\mathrm{AdS}_5 \times S^5$. The parameter $L = \left(4\pi g_s N_c \alpha'^2\right)^{1/4}$ can thus be thought of as a characteristic length scale for the gravitational effects of the D3-branes, i.e., these effects are weak for $r \gg L$ (spacetime there is nearly flat) but become strong for $r \ll L$, where the spacetime develops sort of a "throat" geometry. A cartoon of the resulting 10-dimensional spacetime is shown in Figure **3**.

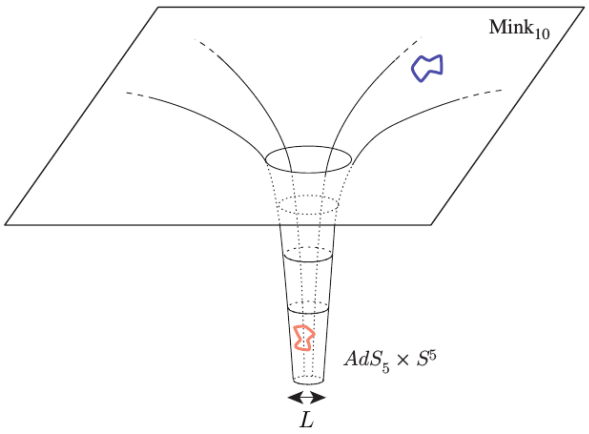

Figure 3: A cartoon of the low-energy excitations of a system of N_c coincident D3-branes according to the closed string perspective. Near the branes the geometry develops a "throat" whose width is determined by $L = \left(4\pi g_s N_c \alpha'^2\right)^{1/4}$. Inside the throat we have interacting closed strings in $\mathrm{AdS}_5 \times S^5$, while far away from it we get free strings in flat spacetime. Figure adapted from [39].

At this point we have free closed string modes in the flat region outside the throat and interacting closed strings in $\mathrm{AdS}_5 \times S^5$ inside the throat. The question now is: how to decouple them? That is, what is the analog here of the decoupling limit in the open string analysis? This is the so called *Maldacena limit* (or near-horizon limit). The idea is again to send $\alpha' \to 0$, but we need to be careful here since this implies $L \to 0$ (see (2.21)). The Maldacena limit corresponds to taking $\alpha' \to 0$ while, at the same time, sending $r \to 0$ so as to keep the ratio $u \equiv \frac{r}{\alpha'}$ fixed and, hence, ensure that we remain deep inside the throat. In this limit the modes inside the throat are completely ignored to an observer at $r \to \infty$ (outside the throat), which can be easily seen as follows. A string excitation at radius r with a fixed energy E_r is measured by an observer at infinity with a redshift factor, i.e.,

$$E_\infty = \sqrt{-g_{00}}E_r = H(r)^{-1/4}E_r = \left(1 + \frac{4\pi g_s N_c}{\alpha'^2 u^4}\right)^{-1/4} E_r \ , \tag{2.23}$$

where we have introduced $u = \frac{r}{\alpha'}$. In the Maldacena limit $\alpha' \to 0$ with $u =$ fixed this gives simply $E_\infty = 0$, which means that the strings inside the throat do not have enough energy to climb out of the throat, so they decouple from the ones outside. Therefore, the closed string picture of the system

of N_c D3-branes in the $\alpha' \to 0$ limit corresponds to the effective action

$$S = S_{\{\text{IIB Sugra in } \text{AdS}_5 \times S^5\}} + S_{\{\text{free gravity in } \mathbb{R}^{1,9}\}} \ , \tag{2.24}$$

It is important to stress that this view is valid as far as we remain in the supergravity approximation $L/\sqrt{\alpha'} \gg 1$, which is equivalent to $g_s N_c \gg 1$ since $L = (4\pi g_s N_c \alpha'^2)^{1/4}$.

Combining the two views

Let us summarize the two different descriptions of the system of N_c D3-branes in the low energy limit discussed above.

- **Open view:** a hyperplane defect in flat spacetime where open strings are attached. The low energy effective action is given by (2.19), namely free gravity modes in $\mathbb{R}^{1,9}$ and $SU(N_c)$ $\mathcal{N} = 4$ SYM theory on the worldvolume of the branes, all decoupled from each other. The description is appropriate when $g_s N_c \ll 1$.
- **Closed view:** the curved spacetime geometry (2.20) where only closed strings can propagate. The low energy effective action corresponds to (2.24), namely free gravity modes in $\mathbb{R}^{1,9}$ and type IIB supergravity modes propagating inside the $\text{AdS}_5 \times S^5$ throat. The description is appropriate when $g_s N_c \gg 1$.

Inspired by the seminal 1995 work by Polchinski [30], which showed (by calculating the tensions and charges of the D-branes from both the string theory and the supergravity perspective and showing that they match) that the two views of D-branes are actually the same, it is natural to claim that the results from the two views above must be the same. In other words, equations (2.19) and (2.24) must be equal. By canceling the common factors $S_{\text{free gravity in } \mathbb{R}^{1,9}}$ on the two sides we are lead to conjecture that

$$S_{\{\text{IIB Sugra in } \text{AdS}_5 \times S^5\}} = S_{\{\mathcal{N}=4 \text{ SYM in } \mathbb{R}^{1,3}\}}. \tag{2.25}$$

The parameters on the two sides are translated into each other by equations (2.17) and (2.21), that is,

$$g^2_{\text{YM}} = 2\pi g_s \qquad \text{and} \qquad L^4 = 4\pi g_s N_c \alpha'^2 = 2 g^2_{\text{YM}} N_c \alpha'^2 \ . \tag{2.26}$$

Notice the natural appearance of the gauge theory 't Hooft coupling $\lambda = g^2_{\text{YM}} N_c$. In particular, the criterion mentioned above to decide which representation of the low energy D-brane system is more appropriate – whether $g_s N_c$ is large or small – translates in the question of whether λ is large or small in the dual $\mathcal{N} = 4$ SYM theory (i.e., whether the theory is strongly or weakly coupled). For instance, if the conjecture turns out to be correct and we wish to use the type IIB supergravity description ($g_s N_c \gg 1$) this means that the $\mathcal{N} = 4$ SYM must be at strong coupling $\lambda \gg 1$.

The intuitive argument above for the equivalence between $\mathcal{N} = 4$ SYM and type IIB supergravity in $\text{AdS}_5 \times S^5$ based on properties of D-branes has been constructed by resorting to the low energy limit. A tempting speculation would be to relax this low energy approximation to obtain an equivalence between $\mathcal{N} = 4$ SYM and the *full type IIB string theory* on $\text{AdS}_5 \times S^5$. Depending on the degree of speculation we get different versions of the AdS/CFT conjecture (the more we extrapolate on parameter space, the harder to prove or "stronger" the conjecture is). Let us finally define and analyze carefully the different versions of AdS/CFT in the next Section including some validity checks.

2.2 AdS/CFT: precise statement

The precise statement of the AdS/CFT conjecture in its **strongest form** is the following

AdS/CFT: strongest version

$\mathcal{N}=4$ SYM theory with gauge group $SU(N_c)$ and coupling $g_{\rm YM}$

=

Type IIB string theory on $\mathrm{AdS}_5\times S^5$ with radius of curvature L and arbitrary α', g_s

The free parameters $(N_c, g_{\rm YM})$ and $(L/\sqrt{\alpha'}, g_s)$ on each side are mapped into each other by

$$g^2_{\rm YM}=2\pi g_s \qquad \text{and} \qquad g^2_{\rm YM}N_c=\frac{L^4}{2\alpha'^2} \tag{2.27}$$

The "CFT side" of the correspondence is a supersymmetric non-Abelian gauge theory introduced in the previous chapter (see Section 1.3), namely the $\mathcal{N}=4$ SYM field theory living in 4-dimensional flat spacetime. It has two dimensionless free parameters, the gauge coupling $g_{\rm YM}$ and the rank N_c of the gauge group (or equivalently N_c and the 't Hooft coupling $\lambda\equiv g^2_{\rm YM}N_c$). The "AdS side" consists of Type IIB string theory (see Section 1.4) defined on the 10-dimensional product spacetime $\mathrm{AdS}_5\times S^5$, where both AdS_5 and S^5 have the same curvature radius L. It also contains two dimensionless free parameters, the string coupling g_s and $L/\sqrt{\alpha'}$ (the curvature radius L measured in units of the string length $l_s=\sqrt{\alpha'}$). The parameters on the two sides are identified as indicated in (2.27),[4] and we refer to this as the strongest version of the conjecture in the sense that no restrictions or particular limits are imposed to any of these parameters – they are left completely arbitrary. Weaker versions of the proposal will be presented below in which particular limits are taken in the parameter space and the claimed correspondence becomes easier to check.

The metric for the $\mathrm{AdS}_5\times S^5$ spacetime where the string theory is defined is given in Poincaré coordinates (see equation (1.13)) by

$$ds^2_{\mathrm{AdS}_5\times S^5}=\frac{L^2}{z^2}\left(-dt^2+d\mathbf{x}^2+dz^2\right)+L^2d\Omega_5^2\,, \tag{2.28}$$

where Ω_5 are coordinates on the sphere S^5. Remember that this spacetime has a conformal boundary, defined in the present coordinate system by $z=0$, which is just the 4-dimensional Minkowski spacetime $ds^2_{\rm bdry}=-dt^2+d\mathbf{x}^2$ where the CFT lives (notice that the 5-sphere is suppressed at $z=0$, so the boundary is effectively four dimensional). Hence, it is often said that the $\mathcal{N}=4$ SYM theory lives on the conformal boundary of the bulk spacetime $\mathrm{AdS}_5\times S^5$. This is sometimes referred to as $\mathrm{AdS}_5/\mathrm{CFT}_4$ correspondence, since a generalization is expected to hold for arbitrary dimensions of the form $\mathrm{AdS}_{d+1}/\mathrm{CFT}_d$.

Before proceeding, we must discuss what is meant by the "=" sign between the two theories in the statement of the conjecture. It really means that the two theories are dynamically equivalent, i.e., they describe the same physics using two (very) different languages. All the physical content of one description – states, observables, etc. – is supposed to be in one-to-one correspondence with objects on the other side[5], and calculations in one theory should in principle give the same result as the corresponding calculations in the other. On the one hand, this means that one can check the validity of the conjecture by calculating equivalent objects on both sides, which is in general very hard but possible in a few cases. On the other hand, this is the reason why the correspondence has attracted so much attention: if the conjecture is correct, then it is possible to learn about any one

[4] We are following here the conventions of [14]. It differs from [22] by a factor of 2 in the definition of $g_{\rm YM}$.

[5] A nice discussion on the conceptual aspects of the AdS/CFT duality can be found in [41].

of the two theories by studying its dual counterpart, which can be a lot easier in special limits to be discussed below.

An immediate sanity check of the duality would be to compare the global symmetries of the two theories[6]. As we have seen before, the global symmetries of $\mathcal{N}=4$ SYM are all packed into the supergroup $PSU(2,2|4)$. In particular, the bosonic sector of this supergroup consists of the conformal symmetry group $SO(2,4)$ and the $SO(6)$ R-symmetry that rotates the 6 scalars. This trivially matches the bosonic symmetries of the type IIB string theory on $\mathrm{AdS}_5 \times S^5$, as can be easily seen at the level of geometry since the AdS_5 spacetime has $SO(2,4)$ as isometry group while the sphere S^5 is invariant under $SO(6)$ rotations.

The strongest form of the AdS/CFT correspondence as stated above is certainly suggestive, but not quite useful for applications since neither string theory is understood beyond perturbation theory (small coupling g_s) nor $\mathcal{N}=4$ SYM is solved for arbitrary values of N_c, g_{YM}. Aiming at more tractable forms for explicit calculations, it is necessary to lessen the strength of the conjecture by taking certain convenient limits on both sides. A natural limit is the one where the string theory side is best understood: $g_s \to 0$ with $L/\sqrt{\alpha'}$ kept constant. The AdS side treated to leading order in g_s then reduces to classical (tree-level) string theory (beware: classical, but still stringy!). According to the relations (2.27), on the CFT side this implies that $g_{\mathrm{YM}} \to 0$ and $N_c \to \infty$ with $\lambda \equiv g^2_{\mathrm{YM}} N_c$ (the 't Hooft coupling) kept constant – this is known as the *'t Hooft limit*. The AdS/CFT conjecture at this restricted level is referred to as the *strong form* of the correspondence, namely,

AdS/CFT: strong version

$\mathcal{N}=4$ SYM theory with gauge group $SU(N_c)$ and coupling g_{YM}
in the *planar limit* (large N_c and fixed $\lambda \equiv g^2_{\mathrm{YM}} N_c$)
=
Type IIB string theory on $\mathrm{AdS}_5 \times S^5$
in the classical limit ($g_s \to 0$) and with arbitrary radius of curvature L and α'

The free parameters λ and $L/\sqrt{\alpha'}$ on each side are mapped into each other by

$$\lambda = \frac{L^4}{2\alpha'^2} \tag{2.29}$$

As we have seen in Section 1.3, in this limit the $\mathcal{N}=4$ SYM theory simplifies considerably since only so-called planar Feynman diagrams contribute to physical processes. Non-planar diagrams are all of subleading order in N_c, being supressed by factors of $1/N_c^2$. In particular, notice from (2.27) that $1/N_c$ corrections on the field theory side correspond to quantum (g_s) loop corrections to string theory, since $1/N_c \sim g_s$ for fixed λ.

There is an even more interesting simplifying limit to be taken which is, in fact, the one that makes the duality really powerful for applications. Notice that after taking the 't Hooft limit above, we are left with a single free parameter on each side, namely λ on the field theory side and $L/\sqrt{\alpha'}$ on the AdS side, and the relation between them is given by (2.29). If, in addition, one takes $\lambda \to \infty$ (strong 't Hooft coupling limit), it follows immediately that $\sqrt{\alpha'}/L \to 0$, i.e., the string length $\sqrt{\alpha'}$ must be much smaller than the AdS radius L. But we have seen before (see Section 1.4) that this is nothing but the pointlike limit of type IIB string theory, which is given by type IIB supergravity. This leads to the following *weak form* of the duality:

[6]Local symmetries such as the $SU(N_c)$ gauge invariance of $\mathcal{N}=4$ SYM, on the other hand, are not expected to match since they are just redundancies in the choice of dynamical variables, hence are not physical.

AdS/CFT: weak version

$\mathcal{N} = 4$ SYM theory with gauge group $SU(N_c)$ and coupling $g_{\rm YM}$
in the *planar limit* (large N_c and fixed $\lambda \equiv g^2_{\rm YM} N_c$) at strong 't Hooft coupling $\lambda \to \infty$
=
(Classical) type IIB supergravity on $\mathrm{AdS}_5 \times S^5$ with radius of curvature $L \gg \sqrt{\alpha'}$

In other words, the highly quantum, infinitely strong coupling limit of (large N_c) $\mathcal{N} = 4$ SYM is mapped to classical type IIB supergravity on the weakly curved $\mathrm{AdS}_5 \times S^5$ space. This is a quite remarkable fact. Strongly coupled QFTs are very difficult to treat using conventional methods, since perturbation theory is obviously not allowed and no other widely applicable technique is known. Classical supergravity, on the other hand, is just general relativity coupled to a bunch of extra fields (see Section 1.4), so the complicated strong coupling limit on the field theory side corresponds to a simple (i.e., tractable) limit in the language of the holographic gravity dual. This is a manifestation of the strong/weak nature of the duality expressed in equation (2.29), meaning that we can in principle obtain new insights into the non-perturbative behaviour of one theory from the computable weak coupling perturbative behaviour of the other. Since there are plenty of strongly coupled quantum systems in nuclear and condensed matter physics lacking proper understanding from the point of view of conventional methods, it is perhaps not a surprise that the weak version of AdS/CFT shown above has gained so much attention over the last decade.

It is instructive to express the "dictionary" above between the parameters on both sides in terms of the gravitational constant G_N that appears in the type IIB supergravity limit. The 10-dimensional Newton constant, defined such that the corresponding supergravity action has the standard $\frac{1}{16\pi G_N^{(10)}}$ prefactor, i.e., $S_{\rm IIB} = \frac{1}{16\pi G_N^{(10)}} \int d^{10}x(\cdots)$, in terms of the string parameters reads

$$16\pi G_N^{(10)} = (2\pi)^7 \alpha'^4 g_s^2, \tag{2.30}$$

which can be expressed using the relations (2.27) as

$$G_N^{(10)} = \frac{\pi^4 L^8}{2N_c^2} \ . \tag{2.31}$$

The 5-dimensional Newton constant, defined using the similar criterion that the 5-dimensional gravitational action (obtained by dimensionally reducing the supergravity action on the S^5) comes with the standard prefactor $\frac{1}{16\pi G_N^{(5)}}$, is related to $G_N^{(10)}$ by a volume factor, namely

$$G_N^{(5)} = \frac{G_N^{(10)}}{\mathrm{vol}(S^5)} = \frac{\pi L^3}{2N_c^2}. \tag{2.32}$$

Note that this has precisely the right form required in order to have a matching on the number of degrees of freedom between AdS_5 gravity and CFT_4, as estimated in (2.11).

The complementarity of the strong/weak regimes mentioned above makes AdS/CFT an extremely powerful tool to learn about physics at strong coupling. At the same time, unfortunately, it is also what makes the correspondence difficult to be mathematically proven, since this would require performing calculations in both descriptions at a fixed coupling and comparing them. On the one hand, this is hard on the field theory side because of the well known complications of dealing with interacting quantum field theories beyond the perturbative regime. On the other hand, on the string theory side this would require a full nonperturbative understanding of string theory in a curved spacetime background which does not even exist nowadays.

Let us finish by quickly mentioning checks of the duality. Despite the lack of mathematical proof, there are a number of very nontrivial tests of the conjectured duality. They all involve the calculation of specific observables on both sides of the duality looking for agreement. Actually we need to calculate quantities that are independent of the coupling λ ("protected" quantities with respect to quantum corrections), such as correlation functions, the conformal anomaly, or Wilson loop operators, whose existence here is guaranteed thanks to some nice features provided by supersymmetry. The idea is very simple: if a quantity in $\mathcal{N} = 4$ SYM can be shown to be independent of the coupling λ (using, e.g., so-called *non-renormalization theorems*), we can calculate it at weak coupling $\lambda \ll 1$ using standard perturbative methods and at strong coupling $\lambda \gg 1$ using the dual gravity description and they should give the same result if AdS/CFT is right. In fact, perfect agreement has been found so far in many such calculations, what supports both the weak form and the strong form of the correspondence as defined above (note that both require the $N_c \to \infty$ limit on the field theory side, in such a way that the dual gravity calculation is always classical). The strongest form, however, remains elusive since the string theory side in this case is not even understood in a satisfactory way. The interested reader is referred to Chapters **6** and **7** of reference [14] for nontrivial tests of the correspondence.

2.3 The duality at work

The precise way in which the two theories are equivalent was proposed independently by Witten [2] and Gubser, Klebanov, Polyakov [3] (we will refer to this as the GKPW prescription), which is now understood as part of the AdS/CFT conjecture itself. In order to motivate this prescription, we shall pause for a moment to study the behaviour of supergravity fields near the conformal boundary of AdS.

2.3.1 A short digression: fields in AdS

For simplicity it is sufficient to focus on the simplest case of a massive scalar field ϕ (the dilaton of type IIB supergravity) in AdS spacetime. For future convenience we shall show the calculation in an arbitrary number of dimensions, i.e., we consider AdS_{d+1} spacetime ($d = 4$ being the case of interest for now). In the so called Einstein frame, the dilaton action is just the standard scalar field action

$$S = \frac{1}{2}\int d^{d+1}x\ \sqrt{-g}\left(g^{ab}\partial_a\phi\partial_b\phi + m^2\phi^2\right)\ , \tag{2.33}$$

where g_{ab} is the AdS_{d+1} metric in Poincaré coordinates, equation (1.13), and the bulk coordinates are $x^a = (z, x^\mu)$ with $x^\mu = (x^0, \ldots, x^{d-1})$ denoting the ones transverse to z (these will turn out to be the coordinates for the CFT_d living on the boundary of AdS space).

The Klein-Gordon equation for ϕ, $(\Box_g - m^2)\phi = 0$, can be written explicitly as

$$\frac{1}{L^2}\left[z^2\partial_z^2 - (d-1)z\partial_z + z^2\eta^{\mu\nu}\partial_\mu\partial_\nu - m^2L^2\right]\phi(z, x^\mu) = 0\ , \tag{2.34}$$

where $\mu, \nu = 0, 1, \ldots, d-1$ and we have used the d-dimensional Minkowski metric $\eta_{\mu\nu}$ to put ∂_t and ∂_{x^i} derivatives in a compact form. By Fourier transforming on the x^μ coordinates (but not z!) under the assumption of translation invariance on the x^μ directions, i.e.,

$$\phi(z, x^\mu) = \int \frac{d^dk}{(2\pi)^d}\ e^{ik_\mu x^\mu}\phi_k(z)\ , \tag{2.35}$$

the Klein-Gordon equation for the modes $\phi_k(z)$ becomes

$$\left[z^2\partial_z^2 - (d-1)z\partial_z - (m^2L^2 + z^2k^2)\right]\phi_k(z) = 0 \tag{2.36}$$

(here $k^2 \equiv \eta^{\mu\nu} k_\mu k_\nu$). An exact solution to this equation can be found in terms of Bessel functions[7], but since we are interested only in the asymptotic behavior of ϕ_k near the conformal boundary of AdS ($z = 0$), the exact solution is not even needed. Instead, one can just notice that the equation (2.36) near $z = 0$ simplifies since the term $z^2 k^2$ can be neglected in comparison with $m^2 L^2$, and hence a power law ansatz $\phi_k(z) \sim c_k z^\Delta$ gives

$$m^2 L^2 = \Delta(\Delta - d) \ . \tag{2.37}$$

This equation has two solutions for Δ, namely

$$\Delta_\pm = \frac{d}{2} \pm \sqrt{\frac{d^2}{4} + m^2 L^2} \ . \tag{2.38}$$

Notice that reality of $\Delta_\pm$ demands that

$$m^2 L^2 \geq -\frac{d^2}{4} \ , \tag{2.39}$$

which is known as the Breitenlohner-Freedman (BF) bound [42]. The BF bound was originally obtained as a stability bound for scalar fields in AdS in the sense that, as long as it is satisfied, the AdS space itself is stable even in the presence of a negative mass-squared scalar. This is in sharp contrast with the story in flat spacetime, where a $m^2 < 0$ scalar (a "tachion") is always unstable. Roughly speaking, the reason for that is because the gravitational effects of AdS space contribute a factor $d^2/4L^2$ to the effective scalar field mass-squared, i.e., $m^2_{\text{eff}} = m^2 + \frac{d^2}{4L^2}$, and this effective mass is the one that must be positive for the same reason as in flat space. The instability resulting from violating the BF bound is essentially the mechanism behind the holographic superconductor models, that is, the gravitational way to simulate the superconducting phase transition in the dual CFT (see [43] for an introduction).

As trivial as it might sound at this point, let us collect for future reference a list of consequences of the BF bound on the values allowed for $\Delta_\pm$ following from (2.37), namely

1. $\Delta_+ + \Delta_- = d$;
2. $\Delta_+ > \Delta_-$, meaning that the solution $\sim z^{\Delta_-}$ is always the leading one near $z \to 0$;
3. for $m^2 L^2 > 0$, Δ_+ is positive (in fact $\Delta_+ > d$) while Δ_- is negative;
4. for $m^2 L^2 = 0$, $\Delta_+ = d$ and $\Delta_- = 0$;
5. for $-\frac{d^2}{4} < m^2 L^2 < 0$, both $\Delta_\pm$ are positive, with $0 < \Delta_- < \frac{d}{2} < \Delta_+ < d$. In the special window $-\frac{d^2}{4} < m^2 L^2 < -\frac{d^2}{4} + 1$ we get $\frac{d-2}{2} < \Delta_- < \frac{d}{2} < \Delta_+ < \frac{d+2}{2}$ (this will be important later);
6. for $m^2 L^2 = -\frac{d^2}{4}$ (saturating the BF bound), the two solutions coincide, $\Delta_+ = \Delta_- = \frac{d}{2}$. In this case we need a second independent asymptotic solution (it can be found including a $\log z$ term, although we shall not worry about that).

By going back to position space, the near boundary asymptotics of the scalar field ϕ can be written as

$$\phi(z \to 0, x^\mu) = \phi_0(x^\mu) z^{\Delta_-} + \phi_1(x^\mu) z^{\Delta_+} + \cdots \ , \tag{2.40}$$

[7] Namely,

$$\phi_k(z) = (kz)^{d/2} \left[a_k K_\nu(kz) + b_k I_\nu(kz) \right] \ ,$$

where $k \equiv \sqrt{k^2}$, $\nu \equiv \sqrt{\frac{d^2}{4} + m^2 L^2}$ and K_ν, I_ν are the modified Bessel functions of the first and second kind, respectively. The coefficient b_k must actually be set to zero since the function $I_\nu(kz)$ diverges for $kz \to \infty$ (deep inside the AdS spacetime).

where $\cdots$ denote subleading terms in the small z expansion. The z^{Δ_-} mode is said to be *non-normalizable* while z^{Δ_+} is a *normalizable* mode, (non-)normalizability here meaning that the action evaluated on this particular solution is (in)finite. In fact, the explicit form of the action (2.33) after plugging the metric is

$$S = \frac{L^{d-1}}{2}\int dz d^d x \, \frac{1}{z^{d+1}}\left(z^2\partial_z\phi\partial_z\phi + m^2L^2\phi^2\right) \tag{2.41}$$

which for an asymptotic solution of the form $\sim z^\Delta$ as above gives

$$S \sim \int dz \, \frac{z^{2\Delta}}{z^{d+1}} \, .$$

Clearly the contribution near the boundary $z \to 0$ is finite provided that $\Delta > \frac{d}{2}$, which is the case for the z^{Δ_+} solution, while it diverges for the z^{Δ_-} solution.

Now let us focus for the sake of argument on the case $m^2L^2 > 0$ which, as we have seen above, corresponds to positive Δ_+ and negative Δ_- [8]. In other words, this means that the z^{Δ_+} solution in (2.40) approaches zero as $z \to 0$ while the z^{Δ_-} one does not (it blows up) and, in particular, the function $\phi_0(x^\mu)$ is left completely arbitrary by the equation of motion. This is nothing but a manifestation of the fact mentioned in Section 1.1 that, in order to have a well-posed initial value problem on AdS space, one needs to specify a boundary condition at the conformal boundary $z = 0$. Equivalently, one can reverse the argument and state that the bulk scalar field $\phi(z, x^\mu)$ naturally defines a function $\phi_0(x^\mu)$ of the boundary coordinates only according to

$$\phi_0(x) \equiv \lim_{z\to 0} z^{-\Delta_-}\phi(z, x) \, . \tag{2.42}$$

This function has a very special transformation rule under the scaling $x^\mu \to \lambda x^\mu$, namely

$$\begin{aligned}\phi_0(\lambda x) &= \lim_{z\to 0} z^{-\Delta_-}\phi(z, \lambda x) \\ &= \lambda^{-\Delta_-}\lim_{z'\to 0} z'^{-\Delta_-}\phi(\lambda z', \lambda x) \\ &= \lambda^{-\Delta_-}\phi_0(x) \, ,\end{aligned} \tag{2.43}$$

where in the first step we have defined $z' \equiv \lambda^{-1}z$ and in the last step we have used the fact that $\phi(\lambda z', \lambda x) = \phi(z', x)$ (the definition of a bulk scalar field) to identify the limit as $\phi_0(x)$ itself. That is, $\phi_0(x)$ is a field that lives on the boundary of AdS space and has scaling dimension Δ_- (recall equation (1.42) for the definition of scaling dimension), so it is a good candidate to represent a physical quantity on the CFT dual. However, when we recall that $\Delta_- < 0$, everything immediately seems to fall apart since this cannot represent any operator on the spectrum of the dual CFT – scaling dimensions in CFTs must be positive! Even worse, we saw that there is a unitarity bound for the dimension of scalar operators, $\Delta \geq (d-2)/2$.

But fortunately there is a nice way out. If, instead, the function $\phi_0(x)$ is the *source* for a CFT scalar operator $\mathcal{O}(x)$ with scaling dimension $\Delta \equiv \Delta_+$, i.e., if the CFT action contains a coupling of the form

$$\int d^d x \; \phi_0(x)\mathcal{O}(x) \, ,$$

then this term is scaling ($\sim$ conformally) invariant due to the fact that $\Delta_+ + \Delta_- = d$! Namely, under the dilation $x^\mu \to \lambda x^\mu$ we have

$$\begin{aligned} d^d x \; \phi_0(x)\mathcal{O}(x) \quad \longrightarrow \quad [\lambda^d d^d x][\lambda^{-\Delta_-}\phi_0(x)][\lambda^{-\Delta_+}\mathcal{O}(x)] &= \lambda^{-(\Delta_+ + \Delta_- - d)} d^d x \; \phi_0(x)\mathcal{O}(x) \\ &= d^d x \; \phi_0(x)\mathcal{O}(x). \end{aligned}$$

[8] The conclusions apply equally well for the cases with $-\frac{d^2}{4} \leq m^2L^2 \leq 0$, although some of the intuition is lost in these cases since both solutions vanish at $z \to 0$.

In other words, we have found the first entry of the "holographic dictionary" that links observables on the two sides of the duality. Namely, the non-normalizable mode $\phi_0(x)$ for the bulk scalar field $\phi(z,x)$ is the source for a scalar operator $\mathcal{O}(x)$ of $\mathcal{N}=4$ SYM. The dimension Δ of this CFT operator is determined by the mass of ϕ according to relation (2.37) (the largest solution, Δ_+).

There is a small caveat in the argument, however, for masses taking values in the specific range $-\frac{d^2}{4} < m^2L^2 < -\frac{d^2}{4}+1$ (close to saturating the BF bound), corresponding to $\frac{d-2}{2} < \Delta_- < \frac{d}{2} < \Delta_+ < \frac{d+2}{2}$ as discussed above. As shown by Breitenlohner and Freedman themselves [42], in this mass range there are two possible consistent boundary conditions (or "alternative quantizations") that can be applied to the scalar field: one can prescribe either $\phi_0(x)$ or $\phi_1(x)$ appearing in equation (2.40) at the AdS boundary, as opposed to the cases $m^2L^2 > -\frac{d^2}{4}+1$ where $\phi_0(x)$ is the only consistent choice (the "standard quantization"). Apart from that, it has been shown in [44] that the holographic dictionary applies in quite the same way for each of the two different boundary conditions, namely, $\phi_0(x)$ is the source for a CFT operator with dimension $\Delta \equiv \Delta_+$ as before while $\phi_1(x)$ is the source for another operator with dimension $\Delta \equiv \Delta_-$. From a purely CFT point of view the existence of such an alternative quantization is also physically reasonable if one recalls (see Section 1.2) the unitarity bound for scalar operators in d-dimensional CFT, namely $\Delta \geq \frac{d-2}{2}$. If Δ_+ were the only possible scaling dimensions of our holographic CFT operators, we would be in trouble with the unitarity bound since, as seen above, $\Delta_+ \geq \frac{d}{2}$ (so the part of the spectrum $\frac{d-2}{2} \leq \Delta < \frac{d}{2}$ would be missing). However, thanks to this subtlety allowing for an alternative quantization we can use Δ_- as the scaling dimension to cover the missing part of the spectrum.[9]

2.3.2 GKPW prescription for correlators

The conclusion from the heuristic argument above is exactly the content of the GKPW prescription (named after Gubser, Klebanov and Polyakov [3] and Witten [2] which arrived at it independently a few months after Maldacena's paper) for the precise mapping between the two sides of the AdS/CFT correspondence, which we now state in details. One just needs to remember (see e.g. the textbook [10]) that the description of any quantum field theory in the path integral formulation is by means of the *generating functional* (also known as the *partition function*) $Z[J]$,

$$Z[J] = \int \mathcal{D}[\text{fields}]\; e^{-S[\text{fields}]+\int d^dx J(x)\mathcal{O}(x)} = \left\langle e^{\int d^dx J(x)\mathcal{O}(x)} \right\rangle \,, \tag{2.44}$$

in the sense that all the connected n-point correlators for the operator $\mathcal{O}(x)$ can be derived from it by taking functional derivatives with respect to J, namely

$$\langle \mathcal{O}(x_1)\dots\mathcal{O}(x_n)\rangle = \left.\frac{\delta^n \ln Z[J]}{\delta J(x_1)\dots\delta J(x_n)}\right|_{J=0}. \tag{2.45}$$

The GKPW prescription for the AdS/CFT duality, which is the mathematically precise way to say that the two theories are equivalent, is then just the statement that the generating functionals for the two theories are the same. Namely, for the strongest version of the correspondence the prescription is

AdS/CFT: strongest version

$$Z_{\mathcal{N}=4\ SYM}[\phi_0] = Z_{\text{IIB String on AdS}_5\times S^5}\left[\phi \to \phi_0\right] \tag{2.46}$$

The only subtlety (which should be clear from the motivation in the previous section) is that on the string theory partition function one must path integrate only over field configurations $\phi(z,x)$ that

[9] The alternative quantization is not a mere formality, being of physical interest, for instance, for the holographic superconductor models where the scalar field mass falls precisely in the present window and there are two possible operators that can form a condensate [43].

approach the desired non-normalizable mode $\phi_0(x)$ at the AdS boundary. The core concept of the GKPW is therefore very simple,

$$\{\text{non-normalizable mode } \phi_0 \text{ of bulk field}\} = \{\text{source } J \text{ on the CFT side}\}.$$

The GKPW prescription also gives a nice illustration of the philosophy of a *duality* between two theories: the knowledge of the partition function of either one of the two theories (since they are equal) is enough to compute the partition function – and hence all the observables – on the dual theory.

A similar statement can be made for the strong form of the conjecture by taking the 't Hooft limit on each side ($N_c \to \infty$, fixed λ on the CFT side; $g_s \to 0$, fixed $L/\sqrt{\alpha'}$ on the AdS side), but in order to avoid unnecessary repetition we do not write it here explicitly since it will not be needed.

As beautiful as the equality (2.46) may look, the truth is that neither one of the two generating functions above is known in their full form. $\mathcal{N} = 4$ SYM theory has a very complicated field content (see the action (1.74)) while string theory is only well understood in the perturbative regime $g_s \to 0$. In the weak version of the duality, however, the situation is changed. Remember that this version involves the classical supergravity limit ($g_s \to 0, \sqrt{\alpha'}/L \to 0$) on the AdS side, meaning that the path integral defining the string partition function on the righthand side of (2.46) can be approximated by the classical (or "saddle point") contribution $e^{-S^{(\text{on-shell})}_{\text{IIB sugra}}}$, i.e.,

AdS/CFT: weak version

$$Z_{\mathcal{N}=4 \text{ SYM, large } N_c \text{ and large } \lambda}[\phi_0] \approx e^{-S^{(\text{on-shell})}_{\text{IIB sugra}}\left[\phi \to \phi_0\right]} \tag{2.47}$$

As pedantic as it might sound, it is important to emphasize how non-trivial is the statement above. The logarithm of the $\mathcal{N} = 4$ SYM generating functional (at strong coupling and large N_c) is identified with the classical type IIB supergravity action on AdS space evaluated on the solution $\phi(z, x)$ that satisfies the asymptotics (2.40) with the desired non-normalizable mode $\phi_0(x)$. Such an on-shell action is in principle easy to calculate, one just needs to solve the classical equations of motion and plug the resulting solution back into the action. Once this is done, all the connected correlators on the CFT side can be straightforwardly calculated as

$$\langle \mathcal{O}(x_1) \dots \mathcal{O}(x_n) \rangle = \frac{\delta^n \ln Z[\phi_0]}{\delta\phi_0(x_1) \dots \delta\phi_0(x_n)}\bigg|_{\phi_0=0} = -\frac{\delta^n S^{(\text{on-shell})}_{\text{IIB sugra}}\left[\phi \to \phi_0\right]}{\delta\phi_0(x_1) \dots \delta\phi_0(x_n)}\bigg|_{\phi_0=0} .$$

In particular, the one-point function $\langle \mathcal{O}(x) \rangle$ can be shown to be proportional to the normalizable mode $\phi_1(x)$ appearing in (2.40), namely

$$\langle \mathcal{O}(x) \rangle = \frac{2\Delta - d}{L} \phi_1(x) \ . \tag{2.48}$$

There is a subtlety, however, that we have ignored above. In general, the on-shell gravity action is divergent due to the infinite contribution coming from the near-boundary region. This is the same type of UV divergences inherent to quantum field theories, indicating that the conformal boundary of AdS is related to the UV regime of the dual field theory. In analogy with the renormalization process in standard QFT, one can also define the so called *holographic renormalization* procedure [45, 46] that regularizes and renormalizes the on-shell gravity action and leads to finite correlation functions. This procedure leads also to a formal way of understanding the duality as a "geometrization" of the renormalization group [47], but a detailed discussion of this is not in the scope of this thesis.

The results obtained above using the simplest bulk field content, namely a massive scalar field ϕ (dual to a scalar operator $\mathcal{O}$ in the CFT) can be extended to any other matter field appearing in the supergravity action. The dual CFT operator would then have a similar Lorentz structure (for

instance, a gauge field in the bulk corresponds to a vector current in the CFT, the metric tensor in the bulk to the energy-momentum tensor in the CFT, etc. – see [14] for more details). The only difference would be the relation (2.37) between the mass m and the scaling dimension Δ of the dual operator. In Table 1 we summarize the results for a variety of supergravity fields.

Type of field	**Relation between m and Δ**
scalar, massive spin-2	$m^2L^2 = \Delta(\Delta - d)$
massless spin-2	$m^2L^2 = 0, \Delta = d$
p-form	$m^2L^2 = (\Delta - p)(\Delta + p - d)$
spin-1/2, spin-3/2	$\|m\|L = \Delta - d/2$
rank s symmetric traceless tensor	$m^2L^2 = (\Delta + s - 2)(\Delta - s + 2 - d)$

Table 1: Relations between the mass of different bulk fields and the corresponding scaling dimension of the dual CFT operator.

It is instructive to close by relating the results here to the standard renormalization group jargon of relevant, irrelevant, and marginal operators. Namely, generic operators $\mathcal{O}_\Delta$ with dimension Δ appear in the CFT Lagrangian as

$$\sim \int d^dx (\text{mass scale})^{d-\Delta} \mathcal{O}_\Delta \ .$$

If $\Delta > d$ the operator is called *irrelevant* (with respect to IR physics) since it is suppressed by a negative power of the mass scale and, therefore, plays no role in the low energy (IR) limit of the theory. Conversely, the operator is said to be *relevant* if $\Delta < d$ since it becomes important in the IR. The limiting case of $\Delta = d$ is called a *marginal* operator, which can become either relevant or irrelevant depending on quantum interactions. We now know that CFT operators are mapped to bulk fields according to the GKPW prescription, so it would be interesting to translate how does the concept of relevance of operators translate in the bulk language. For scalar operators this is clear from our analysis above (see the list below equation (2.39)), namely

Irrelevant operators ($\Delta > d$) $\longrightarrow$ massive bulk fields with $m^2L^2 > 0$;

Relevant operators ($\Delta < d$) $\longrightarrow$ massive bulk fields with $-\frac{d^2}{4} < m^2L^2 < 0$;

Marginal operators ($\Delta = d$) $\longrightarrow$ massless bulk fields.

For non-scalar operators one can easily work out the equivalent relations from Table 1.

2.4 Finite temperature: black holes and the $\mathcal{N} = 4$ SYM plasma

So far we have focused only on the AdS/CFT duality at zero temperature. Since most of our interest in this thesis involves quantum field theories at finite temperature, we now discuss how to extend the duality to include a finite temperature T. This was originally done by Witten in [48].

We first need to recall that the standard prescription to put any quantum field theory, $\mathcal{N} = 4$ SYM included, at a finite temperature T is to Wick-rotate the time coordinate to Euclidean time t_E ($t = -it_E$) and, then, compactify t_E on a circle with period[10] $\beta = 1/T$ (the reader is referred to the textbook [17] for details). As a result, the Euclidean partition function of the QFT, which is obtained in the usual way as a path integral over the periodic trajectories with period β,

$$Z_E[\beta] = \int_{\phi(t_E,\mathbf{x})=\phi(t_E+\beta,\mathbf{x})} \mathcal{D}\phi \ e^{-S_E[\phi]} \ ,$$

[10] We set the Boltzmann constant $k_B \equiv 1$ for simplicity.

becomes the partition function of a thermal statistical ensemble with temperature $T=1/\beta$, namely, $Z_E[\beta]=\mathrm{Tr}[e^{-\beta\hat{H}}]$ ($\hat{H}$ is the Hamiltonian of the theory).

Now, how does this translate on the gravity side? A natural candidate is the Schwarzschild-AdS black hole solution discussed in **1.1**, which in the 5-dimensional case of interest and Euclidean signature (SAdS_5) reads

$$\begin{aligned} ds^2 &= f(r)dt_E^2+f(r)^{-1}dr^2+r^2d\Omega_3^2 \\ f(r) &= 1+\frac{r^2}{L^2}-\frac{2m}{r^2}=1+\frac{r^2}{L^2}-\frac{r_h^2}{r^2}\left(1+\frac{r_h^2}{L^2}\right) . \end{aligned} \tag{2.49}$$

The reason is that black holes have intrinsic thermal properties, namely they radiate and are, therefore, associated with a temperature – the Hawking temperature – given by (1.25)

$$T=\frac{2r_h^2+L^2}{2\pi L^2 r_h} . \tag{2.50}$$

In fact, it can be shown that the thermal analogy goes far beyond that, and black holes admit a full thermodynamical interpretation[11].

However, as shown in **1.1**, SAdS black holes are thermodynamically stable only if their horizon radius r_h is greater than the AdS radius L, $r_h>L$ (otherwise there is the Hawking-Page phase transition and the thermal AdS space becomes the preferred solution). This means that "large" SAdS black holes do not evaporate, meaning that they can coexist in thermal equilibrium with their own Hawking radiation. As a consequence, the whole spacetime can be thought of as being in thermal equilibrium at temperature T — in particular, this includes the $\mathcal{N}=4$ SYM theory living at the conformal boundary! This unique property of AdS black holes follows from the previously discussed property that AdS space looks like a box in the sense that radiation emitted outwards by the black hole will be reflected at the boundary, radiated back inwards, and reabsorbed by the black hole in a finite coordinate time.

But the argument above is not yet complete, there is still a subtle point left. The behavior of the metric (2.49) near the conformal boundary $r=\infty$ (which is where the $\mathcal{N}=4$ SYM theory at finite T is supposed to live) is given by

$$ds^2\big|_{r\to\infty}=\frac{r^2}{L^2}dt_E^2+\frac{L^2}{r^2}dr^2+r^2d\Omega_3^2 ,$$

which clearly has the topology of $\mathbb{S}^1\times\mathbb{S}^3$, with the radius of the $\mathbb{S}^1$ (the timelike circle) being $\frac{r}{LT}$ while the $\mathbb{S}^3$ has radius r. This poses a problem, since we want our $\mathcal{N}=4$ SYM to live in flat space instead of the sphere, i.e., we want the conformal boundary to have the form $\mathbb{S}^1\times\mathbb{R}^3$ [12]. So how can one transform the $\mathbb{S}^3$ factor into a $\mathbb{R}^3$? All we need to do is blow up the radius of $\mathbb{S}^3$ with respect to the $\mathbb{S}^1$ (the so called *infinite volume limit*), i.e.,

$$\frac{r}{r/LT}=LT\to\infty ,$$

which means (since L is fixed) that we must take $T\to\infty$. According to (2.50), this implies $r_h\to\infty$[13] or, in terms of m, $m\to\infty$. But how to make sense of the metric in such a limit? We need to rescale the coordinates by appropriate factors of m in order to obtain finite quantities. The right factors can be guessed from the limit $r\to\infty, m\to\infty$ of the warp function $f(r)$,

$$f(r)\Big|_{\text{large } r,m}=r^2\left(\frac{1}{L^2}-\frac{2m}{r^4}\right) .$$

[11] See, e.g., reference [12] (Section 12.5) for black hole thermodynamics.

[12] The $\mathbb{S}^1$ must be kept since we want to put the theory at finite temperature.

[13] Remember that $r_h\to 0$, which would be the other option, is not a thermodynamically stable solution.

Namely, we want the term inside the bracket to be finite, so r must scale as $r \sim m^{1/4}$. Then, due to the isometry of the AdS space $(r, t, \Omega_i) \to (\lambda r, \lambda^{-1} t, \lambda^{-1}\Omega_i)$ the time and angular coordinates must scale with the opposite power of m, $t \sim m^{-1/4}, \Omega_i \sim m^{-1/4}$. Including the correct factors of L to adjust the dimensions, a rescaling of coordinates that reduces the metric (2.49) to a solution with the desired boundary $\mathbb{S}^1 \times \mathbb{R}^3$ may be made as follows,

$$r \to \left(\frac{2m}{L^2}\right)^{\frac{1}{4}} \rho \ , \qquad t_E \to \left(\frac{2m}{L^2}\right)^{-\frac{1}{4}} \tau_E \ , \qquad d\Omega_i \to \left(\frac{2m}{L^2}\right)^{-\frac{1}{4}} dx_i \ . \tag{2.51}$$

With m kept fixed, this simple change of coordinates leads to

$$ds^2 = \left[\left(\frac{2m}{L^2}\right)^{-\frac{1}{2}} + \frac{\rho^2}{L^2} - \frac{L^2}{\rho^2}\right] d\tau_E^2 + \left[\left(\frac{2m}{L^2}\right)^{-\frac{1}{2}} + \frac{\rho^2}{L^2} - \frac{L^2}{\rho^2}\right]^{-1} d\rho^2 + \rho^2 dx_i dx^i$$

Then, taking $m \to \infty$ as argued above the metric becomes

$$ds^2 = \left(\frac{\rho^2}{L^2} - \frac{L^2}{\rho^2}\right) d\tau_E^2 + \left(\frac{\rho^2}{L^2} - \frac{L^2}{\rho^2}\right)^{-1} d\rho^2 + \rho^2 d\mathbf{x}^2 \tag{2.52}$$

Notice that $x_i \sim m^{1/4}\Omega_i$ with $m \to \infty$, meaning that the sphere has become flat as desired. The solution above is called a Schwarzschild-AdS *black brane* since now the horizon has planar topology. The fact that it is still an asymptotically AdS solution to Einstein equations with a negative cosmological constant is guaranteed by the fact the rescaling (2.51) is an isometry of pure AdS spacetimes.

Also, since $t_E \to (\frac{2m}{L^2})^{-1/4}\tau_E$ the Hawking temperature (2.50) must be scaled by the same factor $T \to (\frac{2m}{L^2})^{-1/4} T = (\frac{L}{r_h})T$ (with $m \to \infty$ or $r_h \to \infty$), yielding the following Hawking temperature for the black brane [14]

$$T = \frac{1}{\pi L} \ . \tag{2.53}$$

This is the temperature of the $\mathcal{N} = 4$ SYM theory living on the conformal boundary.

To summarize, the gravity dual of $\mathcal{N} = 4$ SYM at finite T in flat spacetime is obtained by considering type IIB superstring/supergravity theory in the 5-dimensional asymptotically Anti-de Sitter black brane spacetime (2.52) (times the usual 5-sphere $\mathbb{S}^5$). The Hawking temperature (2.53) of this black brane is the temperature T on the field theory side. Then, the conjecture and the GKPW prescription for correlation functions go like the zero temperature case.

2.4.1 $\mathcal{N} = 4$ SYM plasma and the quark-gluon plasma

The finite T version of the $\mathcal{N} = 4$ SYM theory discussed above is referred to as the $\mathcal{N} = 4$ *SYM plasma*. We close this section with brief comments on the similarities between the $\mathcal{N} = 4$ SYM plasma and the quark-gluon plasma (QGP) of QCD.

At zero temperature, $\mathcal{N} = 4$ SYM theory and QCD are two completely different beasts (see section **1.3**). Despite of sharing the same kind of $SU(N_c)$ gauge symmetry, the former is a supersymmetric and conformally invariant theory while the latter is not. QCD is strongly coupled at low energies but asymptotically free in the UV, while the strongly coupled $\mathcal{N} = 4$ SYM is strongly coupled at all scales since its beta function vanishes. QCD is a confining theory, while $\mathcal{N} = 4$ SYM has no confinement mechanism. The fermions and scalars of $\mathcal{N} = 4$ SYM transform in the adjoint representation of the gauge group, while the quarks of QCD transform all in the fundamental one (and other differences...).

By introducing a finite T, however, many of these differences are alleviated. Namely, the conformal symmetry of $\mathcal{N} = 4$ SYM is trivially broken by the nonvanishing T, which sets a preferred mass scale

[14] Alternatively, it could also be obtained from the metric (2.52) using the usual method of avoiding conical singularities at the horizon, see section **1.1**.

for the theory. In addition, it can be shown that the finite temperature breaks also the supersymmetry, since the fermions acquire mass while not all bosons do (see Section 15.3 of [22]). The field content of the $\mathcal{N} = 4$ SYM plasma is given by massless gauge bosons plus massive fermions and scalars in the adjoint of $SU(N_c)$, which is not so different from the field content of the QCD plasma (ignoring the fact that the massive fermions of QCD are in the fundamental representation, not the adjoint; or even worse, that $N_c = 3$ for QCD while $N_c \to \infty$ for the tractable limit of $\mathcal{N} = 4$ SYM).

Specifically, for temperatures near (but above) the confinement-deconfinement transition temperature T_c of QCD, both theories are in a deconfined but still strongly coupled phase with no conformal symmetry or supersymmetry. This means that the strongly coupled $\mathcal{N} = 4$ SYM plasma can be used as a toy model to describe the real-world quark-gluon plasma of QCD at $T \gtrsim T_c$. The hope is that understanding the strong coupling limit of this toy model using AdS/CFT might shed some light into the strong coupling phenomena of QCD (either by considering deformations of this $\mathcal{N} = 4$ SYM plasma towards the more realistic QCD plasmas, or by looking for universal signatures of this large N_c SYM plasma that might be shared by the QCD plasma). This is the main motivation for using the correspondence as a tool to understand QCD physics at strong coupling which, in fact, have culminated in a very active research area that people usually refer to as "AdS/QCD".

2.5 Generalizations and applications

Apart from the specific D3-brane construction, which makes explicit mention to a 4-dimensional worldvolume, the heuristic arguments given in Section 2.1 as a motivation for the original version of AdS/CFT correspondence clearly extend to higher dimensions, suggesting that there might be generalizations of the correspondence to an arbitrary number of dimensions d. In particular, the exact matching between the symmetry group of d-dimensional CFTs, $SO(2, d)$, and the isometry group of AdS_{d+1} spacetime provides strong evidence in favor of more general "$\mathrm{AdS}_{d+1}/\mathrm{CFT}_d$" correspondences between conformal field theories and higher dimensional AdS gravity from which the original conjecture by Maldacena would be just a particular example with $d = 4$. These new dualities are likely to involve again gauge theories with a large number of colors N_c. This is because the large N_c counting argument makes no reference to the spatial dimensionality d and, in addition, the relation (2.11) required for matching the number of degrees of freedom on both sides demands $N_c \to \infty$ if we are to have a classical gravity dual ($G_N \to 0$).

In fact, there are some known examples of AdS/CFT dualities in different dimensions. For instance, a correspondence is known between a specific superconformal Chern-Simons theory in $d = 2{+}1$ dimensions (thus a CFT_3) called *ABJM theory* and M-theory in a background with an AdS_4 factor times a compact space. Similarly, a conformal field theory known as the $\mathcal{N} = (2, 0)$ *theory* in six dimensions (a CFT_6) is known to be dual to another M-theory construction in a background with an AdS_7 factor (see Chapter 8 in [14] or Chapter 19 in [22] for further details).

Set aside these formal developments, the vast majority of generalizations of AdS/CFT is shaped by possible applications to the phenomenology of strongly coupled physical systems of interest. The two main research fronts here correspond to nuclear and condensed matter physical systems, specifically applications to QCD and the quark gluon plasma, high-T_c superconductors, Fermi liquids, strange metals, among others. The process of building a dual gravity model to approach some of these problems can be of two types, "top-down" or "bottom-up", as we now discuss in detail.

2.5.1 Bottom-up versus top-down models

We have seen before that the AdS/CFT duality provides an interesting geometric picture of quantum field theory effects such as the renormalization group flow. Hence, even when we are not able to construct the precise gravity dual of a given QFT of interest, experience has proven to be still very useful to *assume* the existence of one and to try gain intuition on the real system at hand by studying properties of would-be gravitational toy models capable of reproducing its main features.

This is the philosophy behind the so-called *bottom-up* models, namely, one simply introduces in the bulk the ingredients needed to simulate the relevant phenomenon in the dual field theory even though an exact duality is not established. The alternative is provided by *top-down* models (from which the original Maldacena's construction or the above mentioned ABJM/M-theory duality are examples). The idea is to start from the top, i.e., from the well-established mathematical setup of string theory and, via some sort of brane construction, to derive the precise field content of the two dual theories.

Top-down models are certainly more rigorous and well-motivated but also technically more involved, which makes them very hard to construct and manipulate. A typical top-down construction is in general not easy to handle, since a large number of bulk fields is involved (a remnant of the extra dimensions of string theory). Most of the models in the literature are, therefore, of the bottom-up type. The reason why they are still useful in spite of the lack of rigor is because they are usually very simple, having a minimal set of bulk ingredients to mimic the important properties of the desired system. In any case, holographic models of either bottom-up or top-down type provide a different and practical angle from which to look at quantum systems of interest – importantly, one way that is naturally suited to deal with strong coupling, in contrast to the standard weak coupling approaches resorting to the notion of quasi-particles.

Maybe the most prominent class of bottom-up holographic models is that of holographic superconductors. In such models, originally introduced by Hartnoll, Herzog, and Horowitz [49], the idea is to add only the minimal ingredients in the bulk theory necessary in order to obtain a superconducting phase transition in the dual field theory. Besides AdS gravity, we need a $U(1)$ bulk gauge field (to have a $U(1)$ conserved current on the boundary) and a charged bulk scalar field (the order parameter) that can condensate in the superconducting phase. Remarkably, this is enough to simulate the essential features of superconductors. At high temperatures the dominant phase (the one that minimizes the free energy) corresponds to a charged black hole (the AdS-Reissner-Nördstrom black hole) with no scalar "hair", i.e., with the charged scalar field vanishing everywhere. This is dual to the normal (non-superconducting) phase in the field theory, since there is no scalar condensate. At a critical temperature T_c, however, there is a second order phase transition below which the favored bulk solution now becomes a charged "hairy" black hole, referring to the fact that the bulk scalar field acquires a non-trivial profile. As a consequence, the normalizable mode of the scalar field at the AdS boundary becomes non-zero which, according to the GKPW rule, signals a non-vanishing vacuum expectation value for a scalar operator in the dual field theory. This is nothing but the spontaneous breaking of the $U(1)$ symmetry that is associated with the superconducting phase transition, the charged scalar condensate appearing as the order parameter for the superconducting phase. Many observables can then be calculated using the holographic dictionary, such as the electrical conductivity, and they all match (qualitatively) the expected behavior in a real superconductor. For a good survey of further bottom-up holographic models designed for condensed matter physics (superconductors included) we refer the reader to the book [38].

Let us exemplify some bottom-up approaches to QCD as well (AdS/QCD models). In order to build a holographic model that truly resembles QCD, it is mandatory to introduce the breaking of conformal invariance and supersymmetry, as well as a confinement mechanism and fermions in the fundamental representation (quarks). One of the simplest mechanisms to break conformal symmetry in the bulk and introduce a confining scale is to abruptly cut off AdS space in the IR region (deep inside the bulk) by putting a rigid "wall" at some fixed $z = z_0$ (in Poincaré coordinates) where the bulk fields are required to vanish. This is the so-called *hard-wall* model, which gives rise to an AdS-soliton solution as the gravity dual of the confining phase. There is also a modification called the *soft-wall* model, in which the AdS geometry is smoothly capped off due to the presence of a scalar field (the dilaton) that acts like a smooth IR cutoff. Using these simple models, fits with good concordance can be found, for instance, for the glueball spectrum of QCD. In addition, there are also more elaborated holographic QCD models such as the ones in [50, 51, 52], where an Einstein-scalar system is used in the bulk with a scalar field potential that is carefully tuned in order to reproduce certain aspects of the QCD phenomenology.

From the top-down perspective of AdS/QCD, one of the most famous models is the one introduced by Sakai and Sugimoto [53] of a holographic theory involving a large N_c strongly-coupled gauge theory where flavor degrees of freedom (quarks) are inserted. Further examples of top-down holographic models are the D3-D7 brane system introduced by Karch and Katz [54], the Klebanov/Strassler cascading $\mathcal{N} = 1$ SYM [55], among others (see [56] for an overview).

Chapter 3

Gravitational collapse and holographic Thermalization

In this Chapter we present a first application of holography to nonequilibrium situations, namely to describe the dynamical process of approaching thermal equilibrium in a quantum system as the result of some external perturbation – the so-called *thermalization* process. This problem has a broad range of applications, but it acquires special interest when non-Abelian plasmas are concerned, since this might be helpful to understand how the quark-gluon plasma (QGP) is formed in heavy ion collision experiments taking place in the Relativistic Heavy Ion Collider (RHIC) and the Large Hadron Collider (LHC). We begin by introducing the problem and how to approach it holographically by studying gravitational collapse in Anti de Sitter spaces. Then, we describe the simplified analytical approach using a Vaidya thin shell model for the gravitational collapse in the bulk and what can be learned from it by probing the thermalization process using non-local observables. Finally, we introduce our original contribution to the subject, namely the study of holographic thermalization of a plasma with non-vanishing chemical potential including α'-like stringy corrections of the Born-Infeld type for the bulk gauge field dynamics.

The results shown in this Chapter have been published as [57]

Holographic thermalization with a chemical potential from Born-Infeld electrodynamics, G. Camilo, B. Cuadros-Melgar, and E. Abdalla, JHEP **02** (2015) 103

and the exposition below makes substantial use of the published text, including literal transcriptions.

3.1 Introduction

We have seen in Chapter **2** that non-Abelian gauge theories seem to admit a dual gravitational description involving asymptotically Anti de Sitter spacetimes in one higher dimension. In particular, for $SU(N_c)$ gauge theories with large N_c and at very strong coupling the gravity dual involves essentially general relativity coupled to different matter fields. If the strongly coupled gauge theory is at zero temperature, the dual gravity description involves a pure AdS spacetime of the type (1.13), while a finite temperature field theory requires the presence of an asymptotically AdS black brane (the Hawking temperature T_H of the black hole corresponding to the temperature T of the thermal ensemble). Note that both cases correspond to equilibrium situations.

An immediate extension of the equilibrium holographic dictionary above is to consider a process of black hole formation in AdS space as the analog of thermalization of the corresponding non-Abelian plasma, i.e., the nonequilibrium dynamical process leading to a thermal equilibrium state

(for instance, as a result of some sort of external perturbation). It is important to stress that if the holographic duality is correct *à la* GKPW (see Section 2.3), i.e., if the two theories are equivalent at the level of partition functions, then this extension follows as a trivial consequence of adopting the bulk point of view. For the record, one can thus define a new entry of the holographic dictionary,

AdS black brane formation $\longleftrightarrow$ **Thermalization of the dual CFT plasma**

Due to the plethora of existing models and methods in the literature to study gravitational collapse and black hole formation (either in general relativity or in extended gravity theories, with or without AdS asymptotics), the possibility to use them to learn about the nonequilibrium physics of strongly coupled quantum field theories began to attract over the last years a considerable amount of attention from both general relativists and field theorists.

One of the most interesting scenarios where these ideas have been applied is to describe properties of the quark-gluon plasma (QGP) formed in ultra-relativistic heavy ion collisions at RHIC [58] and at LHC [59]. The QGP is a new plasma phase of QCD in which the quarks and gluons are deconfined but **not** weakly-interacting (see e.g. [60] for an introduction), which means that perturbation theory is not appropriate to describe it. In fact, the experimental data agree with predictions based on ideal hydrodynamics, an effective theory based on the *strong* nature of the interactions, and recent results suggest that the QGP behaves as an *ideal fluid* with a very small shear viscosity over entropy density ratio (η/s) [61]. The important thing for our purposes here is that the QGP phase takes place at a strong coupling regime (precisely the regime where the holographic approach becomes useful) and, therefore, it might benefit from a dual gravity treatment. Of course QCD is not a large N_c gauge theory (it has $N_c = 3$), so expecting quantitative results would not be quite reasonable, but it might be that a holographic approach may offer important insights into QGP physics. Indeed, holographic calculations using the prototypical $\mathcal{N} = 4$ $SU(N_c)$ supersymmetric Yang-Mills (SYM) theory at finite T and its string theoretical AdS gravity dual show that there seems to be a small and universal lower limit for the ratio η/s for all theories with gravity duals [62, 63], namely (see also [15] for comments on universality)

$$\frac{\eta}{s} \geq \frac{1}{4\pi} \,. \tag{3.1}$$

Remarkably, this lower bound obtained using holographic toy models is very close to the value measured for the QGP [61], which is one of the most prominent predictions of AdS/CFT at the moment. However, while the near-equilibrium properties (such as transport coefficients) of the QGP are well known, the far-from-equilibrium process of formation of QGP after a heavy ion collision, often referred to as thermalization, is not well understood. The thermalization time scale observed at RHIC ($\sim 10^{-24} s$) is considerably shorter than expected according to perturbative techniques [64], which reinforces the need of a strong coupling description of the thermalization process. But this is a very hard problem from the point of view of conventional gauge theory methods since the main tool available nowadays to explore nonperturbative aspects of generic quantum field theories (QFTs), lattice field theory, fails to work in truly time-dependent situations since a Wick rotation to Euclidean time is explicitly involved.

Some attempts were made in the literature to address this problem from a holographic point of view as a dual process of gravitational collapse in AdS space, most of them numerically (see [65, 66, 67, 68, 69, 70, 71, 72, 73] for an incomplete list). A slightly different and simpler model for holographic thermalization was introduced by Balasubramanian et al. in [74, 75] which, despite its simplicity, captures many important features of the thermalization process. It consists in the collapse of a thin shell of matter described by a Vaidya-type metric that interpolates between pure AdS space at early times and Schwarzschild-AdS black hole at late times. Namely, in the $(d+1)$-dimensional case the metric expressed in so-called ingoing Eddington-Finkelstein (EF) coordinates (v, z) is given by (with unit AdS radius)

$$ds^2 = \frac{1}{z^2}\big[-\big(1 - m(v) z^d\big) dv^2 - 2 dv dz + d\mathbf{x}^2 \big] \qquad \text{with} \qquad m(v) = \frac{M}{2}\Big(1 + \tanh\frac{v}{v_0}\Big) \,. \tag{3.2}$$

For $v \to -\infty$ the metric is just pure AdS space (in EF coordinates), while at late times $v \to +\infty$ it is essentially the Schwarzschild-AdS black hole with mass M that we have seen before in (1.18)-(1.19). The metric is, therefore, a toy model for the gravitational collapse and formation of a SAdS black hole, describing the collapse of a spherical shell of null matter with width v_0 (see [76] for more details on Vaidya collapse models). The authors used the dynamical background (3.2) to study the time evolution of nonlocal thermalization probes of the dual CFT having a well known dual gravity description in terms of geometric quantities (more on that below), from where they concluded that the thermalization is a top-down process (i.e., UV modes thermalize first while IR modes thermalize later), in contrast to the predictions of bottom-up thermalization from perturbative approaches [77]. This has a clear and intuitive interpretation from the AdS/CFT perspective: UV modes correspond to small distance scales in the boundary of AdS space and, therefore, they do not capture much of the details of the collapse process happening deep into the bulk. IR modes, on the other hand, penetrate deeper into the bulk and for that reason are naturally more sensible to details of the bulk dynamics, therefore they should thermalize later. In addition, the authors found that the thermalization time scales typically as $t_{\text{therm}} \sim \ell/2$, where ℓ is the characteristic length of the probe.

3.2 Holographic thermalization with a chemical potential: including Born-Infeld corrections

A natural extension of the abovementioned Vaidya model for holographic thermalization would be to include the effect of a non-vanishing chemical potential μ, which is usually the case in real heavy ion collision processes. One just needs to recall that the chemical potential in generic QFTs appears in the action coupled to (the time component of) a conserved vector current, i.e.,

$$S_{\text{QFT}} \sim \int d^d x \; \mu J^0(x) \tag{3.3}$$

Hence, it follows from the GKPW prescription for AdS/CFT studied in Chapter **2** that in the holographic description this amounts to include a gauge field in the bulk, which can in principle be done by coupling a Maxwell action to the bulk geometry. However, if we recall the Dirac-Born-Infeld (DBI) action describing the dynamics of abelian gauge fields living on the worldvolume of D-branes in string theory, namely[1]

$$S_{\text{DBI}} = -T_p \int d^{p+1}x \sqrt{-\det\big(g_{\mu\nu} + 2\pi\alpha' F_{\mu\nu}\big)} \; , \tag{3.4}$$

we see that from a stringy point of view it is more natural to consider nonlinear electrodynamical models. With this motivation we propose to model the presence of a chemical potential on the boundary CFT by using Einstein gravity coupled to Born-Infeld (BI) nonlinear electrodynamics in the bulk, namely using the $(d+1)$-dimensional action

$$S = \frac{1}{16\pi G} \int d^{d+1}x \sqrt{-g}\big[R - 2\Lambda + L_{BI}(F)\big] \; , \tag{3.5}$$

where the negative cosmological constant is $\Lambda = -d(d-1)/2l^2$ (being l the AdS curvature radius) and $L_{BI}(F)$ is given by

$$L_{BI}(F) = 4\beta^2 \left(1 - \sqrt{1 + \frac{F_{\mu\nu}F^{\mu\nu}}{2\beta^2}}\right) \; . \tag{3.6}$$

The constant β is the BI parameter, which in the context of string theory appears as $\beta = 1/2\pi\alpha'$ but here we shall treat as an independent parameter. It is defined in such a way that the limit $\beta \to \infty$ corresponds to the standard Maxwell Lagrangian $L_{\text{Maxwell}} = -F_{\mu\nu}F^{\mu\nu}$. We choose units in which $16\pi G = 1$, G being the Newton's constant in $(d+1)$ dimensions.

[1] For simplicity we ignore the presence of extra scalar fields.

This generalizes the discussion initiated in [78] (see also [79]), since the extra parameter β accomodates more elaborated dynamics for the gauge field including (all order) higher-derivatives of A_μ and, therefore, it may give rise to interesting effects on the chemical potential of the dual boundary theory that are not captured by the Maxwell description. Although BI electrodynamics has its origin a long time ago [80] as an attempt to obtain a finite self-energy of point-like charged particles, currently a renewed interest has been raised due to recent developments in superstring theory. BI electrodynamics provides a promising scenario to explore deviations from Maxwell electrodynamics, specially from the point of view of AdS/CFT calculations where string theory plays a prominent role (see [81, 82, 83, 84, 85, 86, 87, 88, 89, 90] for an incomplete list of previous works in this direction).

3.2.1 AdS black hole solutions in Einstein-Born-Infeld theory

The starting point is the Einstein-Born-Infeld theory (EBI) action (3.5). A charged black hole solution to the corresponding equations of motion has been obtained in [91] (see also [92]), namely

$$ds^2 = -V(r)dt^2 + \frac{dr^2}{V(r)} + r^2 d\Omega_{d-1}^2 \ , \tag{3.7}$$

where $d\Omega_{d-1}^2$ denotes the metric on the unit sphere $\mathbb{S}^{d-1}$ and

$$\begin{aligned} V(r) &= 1 - \frac{M}{r^{d-2}} + \left[\frac{4\beta^2}{d(d-1)} + \frac{1}{l^2}\right] r^2 - \frac{2\sqrt{2}\beta}{d(d-1)r^{d-3}}\sqrt{2\beta^2 r^{2d-2} + (d-1)(d-2)Q^2} \\ &\quad + \frac{2(d-1)Q^2}{dr^{2d-4}}\ {}_2F_1\left[\frac{d-2}{2d-2}, \frac{1}{2}; \frac{3d-4}{2d-2}; -\frac{(d-1)(d-2)Q^2}{2\beta^2 r^{2d-2}}\right] . \end{aligned} \tag{3.8}$$

In the above equation ${}_2F_1(a,b;c;x)$ is the hypergeometric function and M, Q are integration constants related to the ADM mass $\tilde{M}$ and charge $\tilde{Q}$ of the black hole via [2]

$$\begin{aligned} \tilde{M} &= (d-1)\omega_{d-1} M \ , \\ \tilde{Q} &= 2\sqrt{2(d-1)(d-2)}\omega_{d-1} Q \ , \end{aligned}$$

ω_{d-1} being the volume of the $\mathbb{S}^{d-1}$. There is also a purely electric gauge field given by

$$A = \left(-\sqrt{\frac{d-1}{2(d-2)}} \frac{Q}{r^{d-2}}\ {}_2F_1\left[\frac{d-2}{2d-2}, \frac{1}{2}; \frac{3d-4}{2d-2}; -\frac{(d-1)(d-2)Q^2}{2\beta^2 r^{2d-2}}\right] + \Phi \right) dt \ , \tag{3.9}$$

where Φ is a constant corresponding to the electrostatic potential at $r \to \infty$, which will be related to the chemical potential in the dual gauge theory according to the AdS/CFT correspondence. It is defined such that the gauge field vanishes at the horizon, i.e.,

$$\Phi = \sqrt{\frac{d-1}{2(d-2)}} \frac{Q}{r_h^{d-2}}\ {}_2F_1\left[\frac{d-2}{2d-2}, \frac{1}{2}; \frac{3d-4}{2d-2}; -\frac{(d-1)(d-2)Q^2}{2\beta^2 r_h^{2d-2}}\right] \ . \tag{3.10}$$

The electric field associated to (3.9) is finite at the origin $r = 0$, which is a key feature of BI theories. The black hole function (3.8), on the other hand, is in general singular at the origin. Such a singularity is hidden behind an event horizon provided the free parameters are chosen so that the equation $V(r_h) = 0$ admits a real positive solution. We should also mention that taking the limit $\beta \to \infty$ in (3.8) gives the well known Reissner-Nordström-AdS black hole studied in [93].

The solution (3.7) has the topology of $\mathbb{R} \times \mathbb{S}^{d-1}$ at the AdS boundary $r \to \infty$. In the context of the AdS/CFT correspondence it is interesting to consider the limit where the AdS boundary is $\mathbb{R}^{1,d-1}$

[2] For simplicity, we will keep referring to M and Q hereinafter simply as "mass" and "charge" parameters of the black hole without any risk of confusion.

instead, since one is often interested in dual gauge theories living on flat space. This procedure is known in the literature as the "infinite volume limit", and we have already faced it before in Chapter **2** when discussing the finite temperature version of AdS/CFT (see Section 2.4). The idea is to introduce a dimensionless parameter λ (which will soon be set to ∞) and rescale all dimensionful quantities as

$$r \to \lambda^{1/d} r, \quad t \to \lambda^{-1/d} t, \quad M \to \lambda M, \quad Q \to \lambda^{(d-1)/d} Q, \quad \beta \to \beta, \quad l \to l$$

while at the same time blowing up the sphere $\mathbb{S}^{d-1}$ as $l^2 d\Omega_{d-1}^2 \to \lambda^{-2/d} \sum_{i=1}^{d-1} dx_i^2$. This leaves the (t, r) block of the metric almost invariant (except for the contribution of the constant term in (3.8)). Finally, taking $\lambda \to \infty$ yields

$$ds^2 = -U(r)dt^2 + \frac{dr^2}{U(r)} + \frac{r^2}{l^2} \sum_{i=1}^{d-1} dx_i^2 \ , \tag{3.11}$$

where

$$U(r) \equiv V(r) - 1 \tag{3.12}$$

Notice that now the horizon, defined by $U(r_h) = 0$, is planar instead of spherical, so we should refer to (3.11) as a black brane instead of a black hole. In order to avoid the coordinate singularity at $r = r_h$ it will be interesting to express the metric in Eddington-Finkelstein coordinates by introducing a new time coordinate v defined by $dv = dt + dr/U(r)$, and also it will be convenient to work with an inverse radial coordinate $z = l^2/r$ such that the AdS boundary stays at $z = 0$ while the singularity $r = 0$ sits at infinity. The resulting metric is

$$ds^2 = \frac{l^2}{z^2} \left[-f(z)dv^2 - 2dvdz + \sum_{i=1}^{d-1} dx_i^2 \right] \ , \tag{3.13}$$

where we have defined

$$f(z) = \frac{z^2}{l^2} \left[V\left(\frac{l^2}{z}\right) - 1 \right] \ . \tag{3.14}$$

Notice that $f(z) \to 1$ near the AdS boundary $z = 0$.

The Hawking temperature of a black hole in the context of AdS/CFT can be viewed as the equilibrium temperature of the dual field theory living on the boundary. It is obtained as usual by continuing the black hole metric to its Euclidean version via $t = -it_E$ and demanding the absence of conical singularities at the horizon. This results in a periodic Euclidean time t_E whose period is identified with the inverse Hawking temperature. For the AdS Einstein-Born-Infeld black brane (3.11) this calculation gives

$$T = \frac{1}{4\pi r_h} \left[\left(\frac{4\beta^2}{d-1} + \frac{d}{l^2} \right) r_h^2 - \frac{2\sqrt{2}\beta}{(d-1) r_h^{d-3}} \sqrt{2\beta^2 r_h^{2d-2} + (d-1)(d-2)Q^2} \right] \ . \tag{3.15}$$

This expression reduces to the Hawking temperature of the Reissner-Nordström-AdS black hole in the Maxwell limit $\beta \to \infty$ [78]. When $T = 0$, the black brane is called extremal. If we think of all the parameters but the charge as fixed, then we can characterize the extremal black brane solution by a maximal value of charge Q_{ext} given by

$$Q_{ext}^2 = \frac{d}{(d-2)l^2} \left[1 + \frac{d(d-1)}{8l^2\beta^2} \right] r_h^{2d-2} \ . \tag{3.16}$$

According to the AdS/CFT dictionary, the asymptotic value of the time component $A_t(r)$ of the gauge field at the AdS boundary $r \to \infty$ (namely, the constant Φ in equation (3.9)) corresponds to the chemical potential μ in the dual quantum field theory, $\mu \sim \lim_{r\to\infty} A_t(r)$. Actually, the precise relation should include some scale ξ with length units since the chemical potential must have energy

units (or [length]$^{-1}$) while A_μ as defined by the action (3.5) is dimensionless. Hence, the chemical potential per temperature ratio of the boundary field theory is given by

$$\frac{\mu}{T} = \frac{1}{T}\lim_{r\to\infty}\frac{A_t(r)}{\xi} = \frac{\Phi}{\xi T}\,, \tag{3.17}$$

with Φ and T given by expressions (3.10) and (3.15), respectively. A remarkable feature is that if the horizon radius r_h and the BI parameter β are kept fixed, then by varying the charge from $Q=0$ (vanishing Φ) to $Q=Q_{ext}$ (vanishing T) it is possible to explore the whole range of values of the ratio μ/T in the dual field theory, i.e., from $\mu/T=0$ to ∞.

3.2.2 Vaidya thin shell model for AdS EBI black hole collapse

A Vaidya-like extension of the BI AdS black brane metric can be constructed by promoting the constant mass M and charge Q appearing inside $V(r)$ (see equation (3.8)) to arbitrary functions $M(v)$ and $Q(v)$ of the advanced Eddington-Finkelstein time v. The resulting dynamical metric has the same form as in (3.13) but now with $f(v,z)$ instead of $f(z)$ due to the time dependence introduced on the mass and charge. The same also holds for the gauge field (3.9), which now becomes $A_\mu(v,z)$. There is no need to write all the equations again – they are really the same as before with $M=M(v)$ and $Q=Q(v)$. Such a spacetime describes the collapse of a thin-shell of charged dust from the boundary of the AdS space towards the bulk interior.

Of course such a Vaidya-like metric is not a solution of the action (3.5) anymore: there must be some external matter action S_m sourcing the time variation of $M(v)$ and $Q(v)$. If we take this external contribution into account, the Einstein-BI equations of motion become (we restore the factors of G for a moment):

$$R_{\mu\nu}-\frac{1}{2}Rg_{\mu\nu}+\Lambda g_{\mu\nu}-2\beta^2 g_{\mu\nu}\left(1-\sqrt{1+F^2/2\beta^2}\right)-\frac{2F_{\mu\alpha}F_\nu{}^\alpha}{\sqrt{1+F^2/2\beta^2}} = -8\pi G T^{(m)}_{\mu\nu} \tag{3.18}$$

$$\nabla_\mu\left(\frac{F^{\mu\nu}}{\sqrt{1+F^2/2\beta^2}}\right) = -8\pi G J^\nu_{(m)}\,. \tag{3.19}$$

The Vaidya-BI-AdS metric above-mentioned is a solution to these equations provided the external sources satisfy

$$8\pi G T^{(m)}_{\mu\nu} = \frac{(d-1)z^{d-1}}{2l^{2d-2}}\left[\dot{M}(v)-2\left(\frac{z}{l^2}\right)^{d-2}{}_2F_1\left[\tfrac{d-2}{2d-2},\tfrac{1}{2};\tfrac{3d-4}{2d-2};-\tfrac{(d-1)(d-2)Q(v)^2}{2\beta^2(z/l^2)^{2-2d}}\right]Q(v)\dot{Q}(v)\right]\delta^v_\mu\delta^v_\nu \tag{3.20}$$

$$8\pi G J^\nu_{(m)} = \sqrt{\frac{(d-1)(d-2)}{2}}\frac{z^{d+1}}{l^{d+2}}\dot{Q}(v)\delta^\nu_z\,, \tag{3.21}$$

where the dot denotes ∂_v. We notice that there is no β dependence on $J^\nu_{(m)}$ above, and indeed this is exactly the same current found in [78] in the Vaidya-Reissner-Nordström-AdS case. $T^{(m)}_{\mu\nu}$, on the other hand, differs from the corresponding one in the Reissner-Nordström case due to the hypergeometric term (but naturally reduces to it in the $\beta\to\infty$ limit, since ${}_2F_1[a,b;c;0]=1$).

3.3 Holographic probes of thermalization

In this section we are going to study the thermalization process of a strongly coupled quantum field theory whose bulk gravity dual corresponds to the Einstein-Born-Infeld system presented in the previous section. Following [74], we use the dynamical Vaidya-BI-AdS metric discussed in Section 3.2.1 to holographically model the nonequilibrium process leading to thermalization of the boundary

theory after a rapid injection of energy. Namely (we set the AdS radius $l = 1$ hereafter), the metric is

$$ds^2 = \frac{1}{z^2}\left[-f(v,z)dv^2 - 2dvdz + \sum_{i=1}^{d-1} dx_i^2\right] , \tag{3.22}$$

where $f(v,z)$ is given by (3.14) with the mass and charge functions given by (see [94] for an interesting discussion on the corresponding bulk null energy condition)

$$M(v) = \frac{M}{2}\left(1 + \tanh\frac{v}{v_0}\right) \tag{3.23}$$

$$Q(v) = \frac{Q}{2}\left(1 + \tanh\frac{v}{v_0}\right) . \tag{3.24}$$

Clearly, for $v \to -\infty$ we have pure AdS ($M(v) = 0 = Q(v)$) and for $v \to \infty$ we have $M(v) = M$ and $Q(v) = Q$ which is the BI-AdS black brane (3.13). Indeed, equations (3.23)-(3.24) are just smooth versions (convenient for the numerical analysis) of the step functions $M(v) = M\theta(v)$ and $Q(v) = Q\theta(v)$, which represent a shock wave (a zero thickness shell of charged matter suddenly forming at $v = 0$). The constant v_0 represents a finite shell thickness and for $v_0 \to 0$ we go back to the step function.

The next step is to choose a set of observables to use as probes of thermalization. Since local observables in the boundary such as expectation values of the energy-momentum tensor are not sensitive to the thermalization process, one needs to consider extended non-local observables.[3] Here we shall focus on equal time two-point correlation functions and expectation values of rectangular Wilson loops, which have well known holographic descriptions in the bulk in terms of renormalized geodesic lengths and minimal area surfaces, respectively. A third observable that could be used is the entanglement entropy of boundary regions, which have a very similar description in terms of minimal volumes of codimension-two surfaces in the bulk. However, as the results of entanglement entropy lead essentially to the same conclusions, we will not show them here in order to avoid unnecessary repetitions.

3.3.1 Renormalized geodesic lengths and two-point functions

We start with the equal-time two-point correlation functions of local gauge invariant operators $\mathcal{O}(t,\mathbf{x})$ of conformal dimension Δ. The AdS/CFT correspondence provides a simple geometrical way to compute it in the bulk gravity dual when the operator $\mathcal{O}$ is "heavy", i.e., when $\Delta \gg 1$ [95]. Namely,

$$\langle \mathcal{O}(t,\mathbf{x})\mathcal{O}(t,\mathbf{x}')\rangle \approx e^{-\Delta\mathcal{L}} , \tag{3.25}$$

where $\mathcal{L}$ stands for the length of the bulk geodesic between the points $(t,\mathbf{x})$ and $(t,\mathbf{x}')$ located on the AdS boundary.[4] Actually, one should be careful when doing such an approximation because the geodesic length above is divergent due to the contribution of the AdS boundary (because the AdS metric itself diverges at the boundary $z = 0$). In order to extract a meaningful quantity we need to introduce a cutoff z_0. It turns out that the divergent part of $\mathcal{L}$ is universal and equals to $2\ln(2/z_0)$ [74]. Then, we define a (finite) renormalized geodesic length $\mathcal{L}_{ren} = \mathcal{L} - 2\ln(2/z_0)$, which will be related to the renormalized two-point function $\langle \mathcal{O}(t,\mathbf{x})\mathcal{O}(t,\mathbf{x}')\rangle_{ren}$ just as in equation (3.25).

We choose the coordinate axes for the boundary directions $(t,\mathbf{x})$ such that the spatial separation $\ell = |\mathbf{x}-\mathbf{x}'|$ between the points lies entirely over the x^1 direction, i.e., we consider space-like geodesics between the boundary points $(t, x^1 = -\ell/2, \ldots)$ and $(t, x'^1 = +\ell/2, \ldots)$, where the ellipsis denotes

[3] Holography provides a geometric intuition for why local operators are insensitive to details of the progress towards thermalization: being local, they are only sensitive to phenomena happening in their vicinity near the AdS boundary. Thus they are not aware of the details of phenomena occurring near the thermal scale. We need observables dual to AdS quantities that probe deeper into the bulk in order to see signals of thermalization.

[4] If there is more than one geodesic we should sum over them on the right-hand side.

the remaining coordinates $(x^2, \ldots, x^{d-1})$ which are the same for both points. Then, by symmetry the geodesics cannot depend on coordinates other than x^1, and we can use x^1 as the geodesic parameter (we call it simply x hereinafter). The solutions of the geodesic equations are then given by a pair of functions $v(x)$ and $z(x)$. The boundary conditions at the AdS boundary $z = z_0$ are

$$z(\pm\ell/2) = z_0, \qquad v(\pm\ell/2) = t \ . \tag{3.26}$$

The length functional between the referred points follows immediately from the line element (3.22) as being

$$L[v, z] = \int_{-\ell/2}^{\ell/2} dx \frac{\sqrt{1 - 2z'(x)v'(x) - f(v,z)v'(x)^2}}{z(x)} \ . \tag{3.27}$$

It clearly depends on the path taken from one point to the other. The geodesic corresponds to the functions $v(x)$ and $z(x)$ that minimize the length and can be found by standard methods. The geodesic length (which we will call $\mathcal{L}$) is just the value of the length functional L evaluated at the geodesic solution.

The variational problem simplifies by noticing that the integrand in (3.27) does not depend explicitly on x and, therefore, there is a conserved Hamiltonian $\mathcal{H}$ given by

$$\mathcal{H} = \frac{1}{z(x)\sqrt{1 - 2z'(x)v'(x) - f(v,z)v'(x)^2}} \ . \tag{3.28}$$

Using the conditions on the turning point of the geodesic,

$$z(0) = z_*, \qquad v(0) = v_*, \qquad z'(0) = 0, \qquad v'(0) = 0 \ , \tag{3.29}$$

arising from the fact that the geodesic must be symmetric with respect to $x = 0$, the conservation equation simplifies to

$$\sqrt{1 - 2z'(x)v'(x) - f(v,z)v'(x)^2} = \frac{z_*}{z(x)} \ . \tag{3.30}$$

The advantage of working with the boundary conditions (3.29) instead of the original ones (3.26) is that we can use the conservation equation above to write the geodesic length (3.27) as

$$\mathcal{L} = 2\int_0^{\ell/2} dx \frac{z_*}{z(x)^2} \ . \tag{3.31}$$

Hence, after solving the equations of motion and finding the geodesic functions $v(x)$ and $z(x)$ for a given pair of initial conditions (v_*, z_*) it is a trivial task to use the relations (3.26) to read the corresponding values of boundary separation ℓ and time t, as well as obtaining the corresponding renormalized geodesic length $\mathcal{L}_{ren} = \mathcal{L} - 2\ln(2/z_0)$ by means of expression (3.31).

The hard part is to find the geodesic, which means to solve the Euler-Lagrange equations for $z(x)$ and $v(x)$. With the help of the conservation equation (3.30) they can be written, respectively, as

$$2 - 2v'(x)^2 f(v,z) - 4v'(x)z'(x) - 2z(x)v''(x) + z(x)v'(x)^2\partial_z f(v,z) = 0 \tag{3.32a}$$

$$z(x)v''(x)f(v,z) + z(x)z''(x) + z(x)z'(x)v'(x)\partial_z f(v,z) + \frac{1}{2}z(x)v'(x)^2\partial_v f(v,z) = 0 \ . \tag{3.32b}$$

This is a set of coupled, highly nonlinear differential equations and for that reason it is quite hard to handle with analitical methods. However, for a given pair (v_*, z_*) it is possible to find a numerical solution subject to the boundary conditions (3.29). Indeed, by solving for sufficiently many pairs of initial conditions (v_*, z_*) (carefully chosen in order to give the same boundary separation ℓ and different times), we can track time after time the whole evolution of the geodesics in the Vaidya-BI-AdS spacetime. In particular, if we calculate the renormalized geodesic length of each of these solutions using (3.31) we will be able to see the full time evolution of $\mathcal{L}_{ren}$ towards thermalization. This will be done in Section 3.4, where we provide a detailed explanation of the numerical procedure as well as the choice of parameters and show our results.

3.3.2 Minimal area surfaces and Wilson loops

We now study a second class of thermalization probes, namely the expectation values of Wilson loop operators in the boundary field theory. The Wilson loop is a non-local gauge-invariant observable defined as the path-ordered integral of the gauge field over a closed path $\mathcal{C}$:

$$W(\mathcal{C}) = \frac{1}{N}\mathrm{Tr}\left(\mathcal{P}e^{\oint_{\mathcal{C}} A_\mu dx^\mu}\right) , \tag{3.33}$$

where N is the number of colors and A_μ is the non-abelian gauge field. Wilson loops contain useful information about the non-perturbative behavior of non-abelian gauge theories, such as whether they exhibit confinement or not. It is possible, in principle, to express all gauge-invariant functions of A_μ in terms of Wilson loops by appropriate choices of the path $\mathcal{C}$, but unfortunately they are in general hard to compute.

The AdS/CFT correspondence again provides an elegant way to compute the expectation value of Wilson loops of a strongly coupled gauge theory with a gravitational dual in terms of a geometrical quantity in the bulk [96]:

$$\langle W(\mathcal{C})\rangle \approx e^{-\frac{1}{\alpha'}\mathcal{A}(\Sigma_0)} , \tag{3.34}$$

where α' is the inverse string tension, Σ_0 denotes the minimal area bulk surface whose boundary is the original contour $\mathcal{C}$, and $\mathcal{A}(\Sigma_0)$ is the area of that surface. Σ_0 will be a solution of the bosonic part of the string action (the Nambu-Goto action), which is nothing but the area of the classical world-sheet with $\mathcal{C}$ as its boundary. Indeed, equation (3.34) has its origin in a saddle-point approximation of the string theory partition function around the classical solution, which is only valid when the dual gauge theory has strong coupling.

Now we proceed to compute the minimal area surfaces in the Vaydia-BI-AdS spacetime as described before just as we did for the geodesic lengths. We will focus on a spacelike rectangular Wilson loop on the boundary. The rectangle $\mathcal{C}$ can always be chosen to lie on the x^1-x^2 plane, centered at the origin, with sides ℓ on the x^1 direction and R on the x^2 direction. One also assumes translational invariance along x^2, such that the shape of the bulk surface depends only on x^1 and again we can use $x^1 \equiv x$ to parametrize the functions $v(x)$ and $z(x)$ that characterize the surface. The boundary conditions at the AdS boundary $z = z_0$ are again given by equations (3.26).

Using the Vaidya-BI-AdS metric (3.22), the Nambu-Goto action (or area functional divided by 2π) becomes

$$A_{NG}[v,z] = \frac{R}{2\pi}\int_{-\ell/2}^{\ell/2} dx \frac{\sqrt{1-2z'(x)v'(x)-f(v,z)v'(x)^2}}{z(x)^2} . \tag{3.35}$$

Notice that an obvious consequence of our assumption of translational invariance is that the length R factorizes. Since we are interested just in the ℓ dependence, we can study A_{NG}/R instead of A_{NG} itself and forget about R in what follows. As for the geodesics, the pair of functions $(v(x), z(x))$ that minimizes the Nambu-Goto action will be the minimal surface Σ_0. The on-shell value of the Nambu-Goto action (i.e., $A_{NG}[\Sigma_0]$), which we call $\mathcal{A}$, will be our object of interest.

The subsequent calculation is closely analogous to the geodesics case. There is again a conserved Hamiltonian associated to (3.35) and we can introduce the alternative boundary conditions on the turning point of the minimal surface, which are the same as equations (3.29), to find an expression similar to (3.30) for the conservation equation. Replacing this back into (3.35), the on-shell Nambu-Goto action becomes

$$\mathcal{A} = \frac{R}{\pi}\int_0^{\ell/2} dx \frac{z_*^2}{z(x)^4} , \tag{3.36}$$

which can be used to easily obtain the minimal area surface once we have solved the equations of motion and found the functions $v(x)$ and $z(x)$ for a given pair of initial conditions (v_*, z_*). The corresponding values of boundary separation ℓ and time t can be read from the original conditions (3.26) as well. Here again we have to face the problem that the area $\mathcal{A}$ diverges due to the contribution

near the AdS boundary, but we can regularize the divergent part using again a cutoff z_0 and subtract it from $\mathcal{A}$ to define the renormalized minimal area $\mathcal{A}_{ren} = \mathcal{A} - R/\pi z_0$ [74].

The functions $z(x)$ and $v(x)$ are found by solving the Euler-Lagrange equations coming from the action (3.35). The simplified equations of motion (after using the conservation equation) are, respectively

$$z(x)v'(x)^2\partial_z f(v,z) - 4v'(x)^2 f(v,z) - 2z(x)v''(x) - 8v'(x)z'(x) + 4 = 0 \tag{3.37a}$$

$$v'(x)z'(x)\partial_z f(v,z) + \frac{1}{2}v'(x)^2\partial_v f(v,z) + v''(x)f(v,z) + z''(x) = 0\ . \tag{3.37b}$$

As before, for a given pair (v_*, z_*) we can solve this set of equations numerically subject to the boundary conditions (3.26). Thus, for some chosen length ℓ of the Wilson loop, by iterating for enough pairs (v_*, z_*) we can track the whole time evolution of the minimal surfaces and, in particular, of their renormalized areas $\mathcal{A}_{ren}$ towards thermalization. This will be the aim of Section 3.4.

3.4 Numerical results

3.4.1 Renormalized geodesic lengths

In this section, we numerically solve the geodesic equations of motion (3.32) in order to find how the geodesic length evolves with time. Afterwards, we explore how the charge of the black hole and BI parameter affect the thermalization time. For the latter it will be convenient in the numerical calculations to use an inverse BI parameter $b = 1/\beta$ instead of the original β, such that the Maxwell limit is $b \to 0$ and increasing b accounts for increasingly nonlinear electrodynamics.

First of all, we fix the free parameters. We will take the shell thickness and AdS space UV cut-off to be $v_0 = 0.01$ and $z_0 = 0.01$, respectively. Since the effect of the number of spacetime dimensions and boundary separation on the thermalization probes has already been analyzed in previous works [74, 75, 78], we focus here in the case $d = 4$ (namely, AdS_5 space, which is dual to a 4−dimensional gauge theory) and a fixed boundary separation $\ell = 4$. The mass M of the final state black brane can be expressed in terms of the radius of its event horizon using the definition of r_h, i.e., the largest solution of $U(r_h) = 0$. Then, if we choose to fix the horizon at $r_h = 1$,[5] the mass is given by

$$M = 1 + \frac{1}{3b^2}\left(1 - \sqrt{1+3b^2Q^2}\right) + \frac{3}{2}Q^2\ {}_2F_1\left[\frac{1}{3}, \frac{1}{2}; \frac{4}{3}; -3b^2Q^2\right]\ , \tag{3.38}$$

which of course only holds provided that b and Q take values consistent with the existence of an event horizon. For a given b this means that Q is allowed to take values from $Q = 0$ to the extremal value (3.16), which now reads

$$Q_{ext}(b) = \sqrt{2+3b^2}\ . \tag{3.39}$$

As we pointed out in Section 3.2.1, for each b, considering values of charge $0 \leq Q \leq Q_{ext}(b)$ we can study all the range $0 \leq \mu/T \leq \infty$ in the dual gauge theory. It is instructive to illustrate this fact here by looking at the form of expression (3.17) in the present case (we choose the scale $\xi = 1$ for simplicity), namely,

$$\frac{\mu}{T} = \frac{3\sqrt{3}\pi b^2 Q\ {}_2F_1\left[\frac{1}{3}, \frac{1}{2}; \frac{4}{3}; -3b^2Q^2\right]}{2 + 6b^2 - 2\sqrt{1+3b^2Q^2}}\ . \tag{3.40}$$

A plot of this as a function of the charge for distinct values of b is shown in Figure **1**, showing that indeed all the range of μ/T is covered. We also notice that for small values of charge (up to ~ 0.5) the BI parameter has no effect on the chemical potential since all the curves agree, so we will concern only about charges above this value in what follows.

[5] This will be interesting to compare the thermalization for different values of Q and b, since the black hole will always form at the same location for all Q, b.

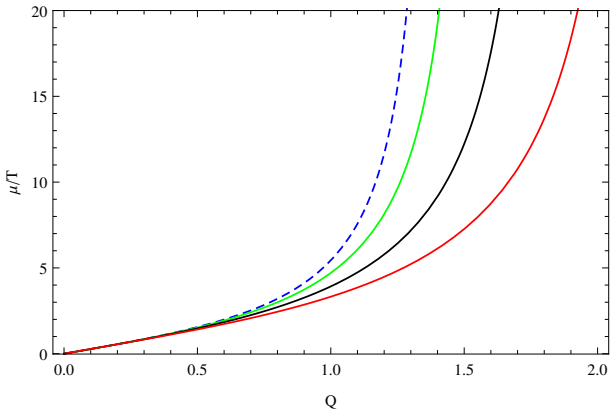

Figure 1: The chemical potential per temperature ratio in the $d = 4$ field theory as a function of the charge Q of the black hole for different values of the inverse BI parameter: $b = 0$ (dashed blue), $b = 0.4$ (green), $b = 0.7$ (black), $b = 1$ (red). The dashed curve represents the Maxwell limit case.

Now we proceed to investigate the effects of Q and b on the thermalization process. We choose the test values $b = 0, 0.4, 1$ and $Q = 0.5, \ldots, Q_{ext}(b)$ for the numerical analysis. The procedure is the following: for a given (b, Q) pair we solve the geodesic equations (3.32) subject to the boundary conditions (3.29) characterized by a pair of values (v_*, z_*). We do this recursively for various pairs of initial conditions and collect from these just those yielding a boundary separation $\ell = 4$.[6] Each of these collected solutions correspond to a different stage of the motion of the geodesics, as we may check by computing the corresponding boundary time t via equation (3.26). We then calculate the renormalized geodesic length $\mathcal{L}_{ren}$ of each of these collected solutions and construct a list of points $(t, \mathcal{L}_{ren}(t))$ which contains all the information about the time evolution of the renormalized geodesic length. Actually, it will be convenient to divide all the lengths by ℓ in order to obtain a dimensionless, $\ell-$independent quantity $\tilde{\mathcal{L}} = \frac{\mathcal{L}_{ren}}{\ell}$. In addition, we subtract from this the final (thermal) value just to force all thermalization curves to end at zero, so that the quantity to be plotted is $\tilde{\mathcal{L}} - \tilde{\mathcal{L}}_{\text{thermal}}$ versus t.

Before showing the thermalization curves, in Figure **2** we present an intuitive simple view of the effect of the BI parameter on the thermalization. It consists of a sequence of snapshots of the time evolution of geodesic profiles as well as the shell of charged dust described by the Vaidya-BI-AdS metric to form a black brane at $z_h = 1$ at late times, for different values of the inverse BI parameter b and fixed charge $Q = 1$. Each column, top to bottom, corresponds to the time evolution for a given value of b. It is found that at the early stages of the evolution, up to $t \sim 1$, the value of b has little effect on the dynamics. After that, b plays a crucial role in the evolution. We see that the bigger b is (i.e., columns to the right), the sooner the black hole is formed. This is clear from the bottom line of the picture, corresponding to boundary time $t = 1.82$, where the $b = 1$ black brane has just formed while the $b = 0.4$ one is about to form and the $b = 0$ one still needs some time to do so. This is a hint that the thermalization of the dual boundary field theory occurs sooner as b increases, what indeed will be confirmed in Figure **4**.

In Figures **3** and **4** we show the thermalization curves for the renormalized geodesic lengths with varying charge at fixed b and varying b at fixed charges, respectively. Instead of plotting point by point all the results obtained as described above, we find more instructive to fit those points using some polynomial function and plot the resulting curve. Details about the fits will be given below. We use dashed curves in all the plots hereinafter to highlight the Maxwell limiting case studied in [78]. The thermalized (final) state corresponding to the completely formed black brane is reached

[6] There is a small subtlety here. ℓ is determined numerically, via equation (3.26), after we have solved the equations using the modified boundary conditions (3.29), hence we must establish a criterion for what we mean by "$\ell = 4$". We adopt the convention of 0.0005 tolerance, meaning that "$\ell = 4$" here corresponds to $\ell \in (3.9995, 4.0005)$.

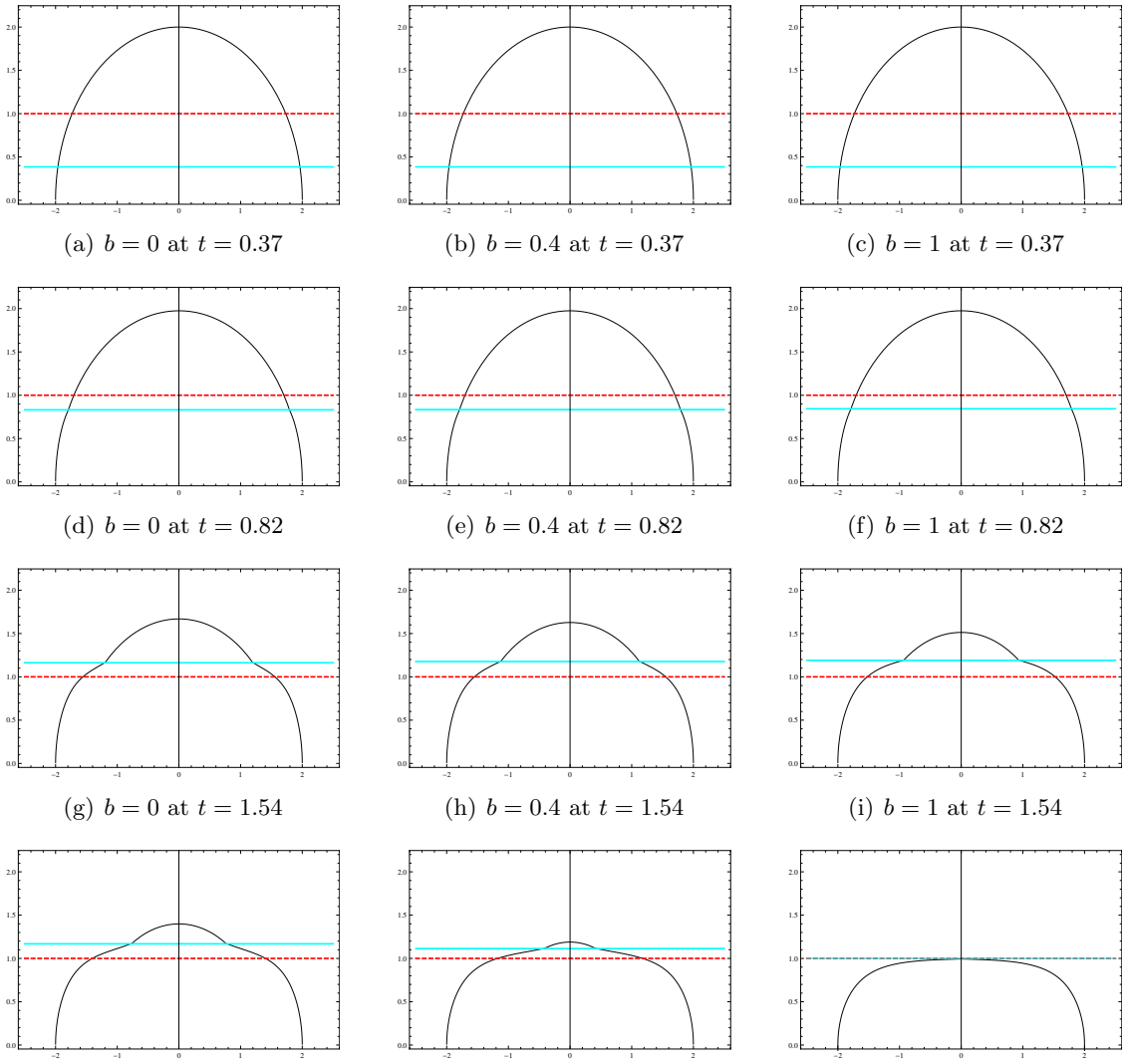

(a) $b = 0$ at $t = 0.37$ (b) $b = 0.4$ at $t = 0.37$ (c) $b = 1$ at $t = 0.37$

(d) $b = 0$ at $t = 0.82$ (e) $b = 0.4$ at $t = 0.82$ (f) $b = 1$ at $t = 0.82$

(g) $b = 0$ at $t = 1.54$ (h) $b = 0.4$ at $t = 1.54$ (i) $b = 1$ at $t = 1.54$

(j) $b = 0$ at $t = 1.82$ (k) $b = 0.4$ at $t = 1.82$ (l) $b = 1$ at $t = 1.82$

Figure 2: A sequence of snapshots of the time evolution of geodesic profiles and the shell of charged dust described by the Vaidya-BI-AdS metric to form a black brane at $z_h = 1$ at late times, for different values of the inverse BI parameter b and fixed charge $Q = 1$. In all cases the separation of the boundary points is $\ell = 4$. Each column, from top to bottom, indicates the time evolution for a given value of b. The cyan line indicates the position of the shell in each case, while the dashed red line is an imaginary line denoting the position of the (still to be formed) black brane horizon.

in each case when the curve touches the zero point of the vertical axis. The effect of the charge Q on the thermalization is clear from Figure **3**. As Q grows, the thermalization time increases, meaning that the dual field theory thermalizes later. This had already been pointed out in [78] for the case of Maxwell electrodynamics ($b = 0$), and now we show that the same holds for BI nonlinear electrodynamics. Since the charge corresponds to the chemical potential, this means that the smaller the chemical potential is, the faster is the pair production and the screening effect takes over in an easier way. This is compatible with lower dimensional models, where screening effects are known to prevail over confinement [97, 98]. The second, more interesting result, is the effect of the inverse BI parameter b shown in Figure **4**. As one can see, increasing b decreases the thermalization time, which means that the more nonlinear the bulk theory is, the sooner its dual field theory thermalizes. This confirms our intuition coming from the analysis of the geodesic profiles and shell motion in Figure **2**. Such a behavior is similar to the effect of the Gauss-Bonnet parameter on the thermalization reported in [99]. As we discuss in the conclusions, this seems to be a general feature of introducing extra derivatives in the bulk theory. The numerical values obtained for the thermalization times are summarized in Table 1.

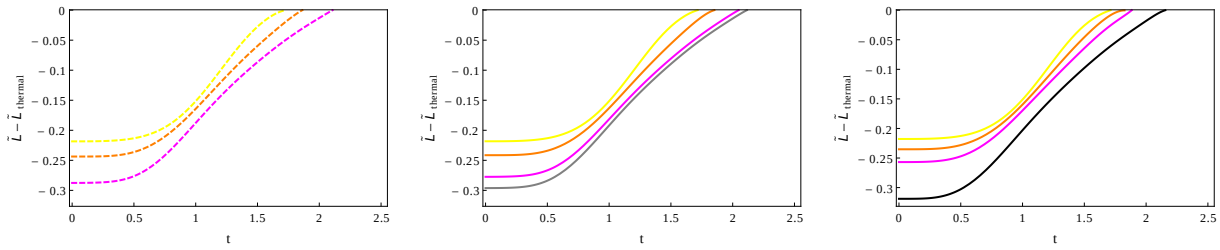

(a) $b = 0$ (b) $b = 0.4$ (c) $b = 1$

Figure 3: Thermalization curves of the renormalized geodesic lengths in the Vaidya-BI-AdS spacetime at fixed values of b for different charges Q, from $Q = 0.5$ to the corresponding extremal value $Q_{ext}(b) = \sqrt{2 + 3b^2}$. Figure (a) shows the Maxwell limiting case, with $Q = 0.5$ (yellow) in the top, $Q = 1$ (orange) in the middle and $Q = \sqrt{2}$ (magenta) in the bottom. In (b) and (c) we have the same values of charge together with the extremal values $Q = \sqrt{2.48}$ (gray) and $Q = \sqrt{5}$ (black), respectively. The spatial separation of the boundary points is $\ell = 4$ for all the cases.

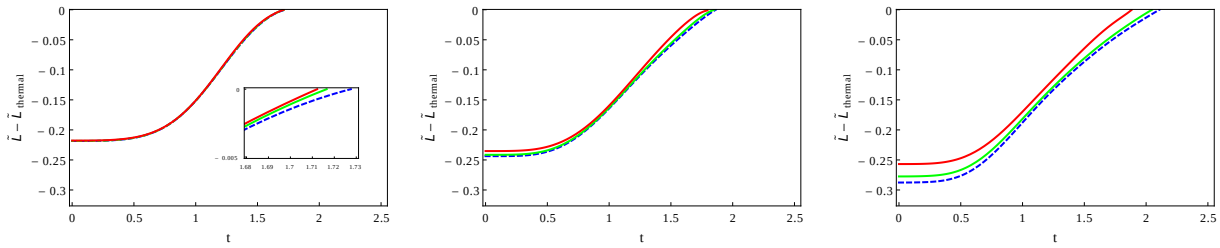

(a) $Q = 0.5$ (b) $Q = 1$ (c) $Q = \sqrt{2}$

Figure 4: Thermalization curves of the renormalized geodesic lengths in the Vaidya-BI-AdS spacetime at fixed charges Q for different inverse BI parameters b. Here $b = 0$ (dashed blue) is always the bottom curve, $b = 0.4$ (green) is the middle curve, and $b = 1$ (red) is the top one. The spatial separation of the boundary points is $\ell = 4$.

Having smooth fit functions for all the sets of numerical data we can use them to study the thermalization velocities $\frac{d}{dt}(\tilde{\mathcal{L}} - \tilde{\mathcal{L}}_{\text{thermal}})$ aiming for more details of the nonequilibrium process. These are plotted in Figure **5** (only for the cases $Q = 1$ fixed and $b = 0.4$ fixed, respectively, to avoid

	$b=0$	$b=0.4$	$b=1$
$Q=0.5$	1.728	1.717	1.712
$Q=1$	1.863	1.852	1.796
$Q=\sqrt{2}$	2.108	2.048	1.887
$Q=\sqrt{2.48}$	–	2.116	–
$Q=\sqrt{5}$	–	–	2.156

Table 1: Summary of the numerical values obtained for the thermalization times of the renormalized geodesic length curves shown in Figures **3** and **4**.

unnecessary repetitions). We notice from the velocity curves the existence of a phase transition point at the middle stage of the thermalization, which divides the process into an accelerating and a decelerating phase. Furthermore, we see that the phase transition point is shifted depending on the values of b and Q. Figure (a) shows that increasing the value of b causes a delay in the phase transition point, meaning that the accelerated phase lasts longer for the $b=1$ theory. This is to be contrasted with the fact that the $b=1$ theory is the first to thermalize, indicating that the dynamical process in this case consists of a slowly accelerating phase followed by a quick deceleration towards the equilibrium state. On the other hand, Figure (b) shows that the charge has the opposite effect, i.e., as Q increases the phase transition point arrives earlier. In other words, for large values of Q (or μ/T in the boundary field theory) the thermalization process consists of a quick accelerating phase followed by a slowly decelerating phase to the final state.

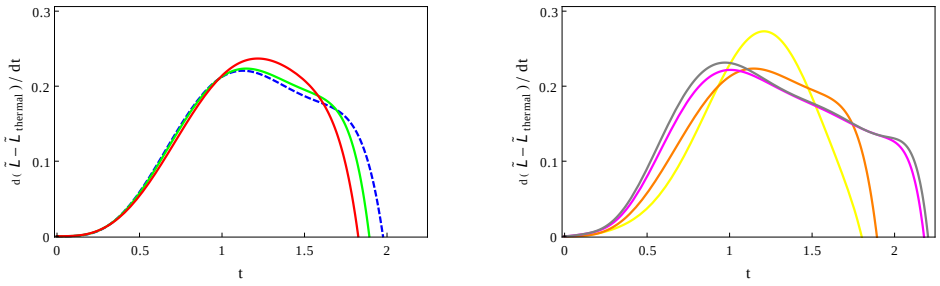

(a) $Q=1$ (b) $b=0.4$

Figure 5: Thermalization velocities of the renormalized geodesic lengths at both fixed charge and fixed b. The dashed blue, green, and red curves in (a) correspond respectively to $b=0, 0.4, 1$. The curves in (b) correspond to $Q=0.5$ (yellow), $Q=1$ (orange), $Q=\sqrt{2}$ (magenta) and $Q=\sqrt{2.48}$ (gray). The spatial separation of the boundary points is $\ell=4$.

It should be stressed that in this work, in contrast to the authors of [100], we find no evidence for a negative thermalization velocity at initial times. They argue that the velocity should be negative in the very beginning of the evolution corresponding to a"quantum"stage of the nonequilibrium process, which soon becomes"classical"once the velocity becomes positive. In our case (Figure **5**) all the thermalization velocities start from zero and increase monotonically until the phase transition point, indicating that nothing particularly odd seems to happen at the initial stages of the thermalization process. This is also clear from the comparison of the numerical results with the fitting functions presented in Figure **6**. The zoomed region shows that the numerical points sit all over a horizontal line for initial times (up to ~ 0.2) and therefore there is no reason for a non-vanishing slope at such stage. For that reason, we use for our fit functions degree 9 polynomials $f(t)=\sum_{n=0}^{9}\alpha_n t^n$ with the first powers of t (α_1,α_2) set to zero in order to ensure the strictly constant behavior $f(t)\sim\alpha_0$ up to $t\sim 0.2$. This allows us to make an accurate fit of the whole set of numerical points, which after all are the ones carrying the physical information.

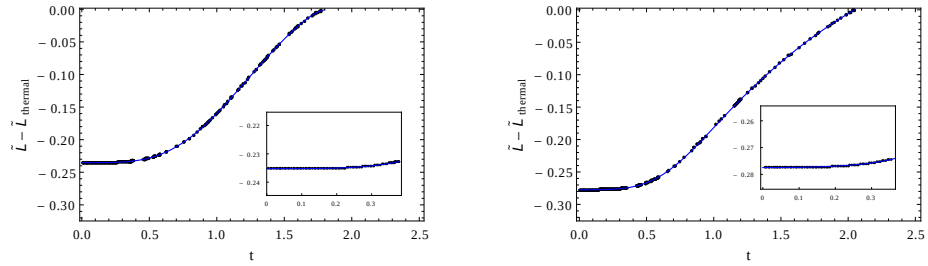

(a) $Q = 1, b = 1$ (b) $Q = \sqrt{2}, b = 0.4$

Figure 6: A comparison between the numerical results and the polynomial fits for the geodesic lengths. The inset emphasizes the constant behavior of the curve at initial times.

3.4.2 Renormalized minimal area surfaces

In this section, we numerically solve the equations of motion (3.37) for the minimal area surfaces in order to track their time evolution. The strategy will follow closely that of the renormalized geodesic lengths done in the previous subsection, so we will not repeat all the details on the numerical procedure as well as the fixing of free parameters since they are essentially identical.

Again we choose the test values $b = 0, 0.4, 1$ and $Q = 0.5, \ldots, Q_{ext}(b)$ for the numerical analysis. The procedure is the same as before, i.e., for a given (b, Q) pair we solve the geodesic equations (3.37) subject to the boundary conditions (3.29) characterized by a pair of values (v_*, z_*). We repeat this for various pairs of (v_*, z_*) and collect just those yielding a Wilson loop with side $\ell = 2$ (keep in mind that the other side R does not influence in our analysis).[7] Each of the collected solutions will correspond to a different stage of the time evolution determined by calculating the boundary time t via equation (3.26). Then we integrate each of the collected solutions using equation (3.36), subtract the universal divergent part to obtain $\mathcal{A}_{ren}$, and construct a list of points $(t, \tilde{\mathcal{A}} - \tilde{\mathcal{A}}_{\text{thermal}})$ to be plotted against t. Here $\tilde{\mathcal{A}} \equiv \mathcal{A}_{ren}/(R\ell\pi^{-1})$ is a dimensionless quantity independent of the dimensions of the boundary Wilson loop and $\tilde{\mathcal{A}}_{\text{thermal}}$ is the corresponding thermal value.

A sequence of snapshots of the time evolution of the minimal area surfaces as well as the shell of charged dust described by the Vaidya-BI-AdS metric is shown in Figure **7** for different values of the inverse BI parameter b and a fixed charge $Q = \sqrt{2}$. Each column, from top to bottom, follows the time evolution for a given value of b. Again we can see that up to $t \sim 1.0$ the value of b has little effect on the dynamics, while at the final stages of the evolution b plays a decisive role. This is clear from the bottom row at $t = 1.54$, where we see that the $b = 1$ black brane has already formed while the other two are about to form. That illustration suggests that increasing the value of b makes the black hole form earlier, which indeed will be confirmed below.

The thermalization curves for the renormalized minimal area surfaces are shown in Figures **8** and **9** for varying Q at fixed values of b and varying b at fixed charges, respectively. All the curves are polynomial fits of the numerical points (see below) and the zero point of the vertical axis corresponds to the final state of the process, i.e., the static Einstein-BI black brane fully formed. We immediately notice that all the effects are less evident than those displayed before for the geodesic lengths (the reason why we show the insets in Figure **9**) due to our choice of $\ell = 2$ as the characteristic scale in the boundary, in contrast to the $\ell = 4$ used for the geodesics. This just illustrates the argument made in the beginning that the holographic thermalization is a top-down process. Figure **8** shows that for a given b the effect of the charge Q is to delay the thermalization process as it is increased, that is to say, as the chemical potential in the dual field theory grows, the time needed to reach the thermal state also raises. This reinforces the conclusions drawn from the analysis of the renormalized

[7] Remember that ℓ is determined from the numerics, via equation (3.26), so we again use he same criterion of ± 0.0005 for what we mean by "$\ell = 2$".

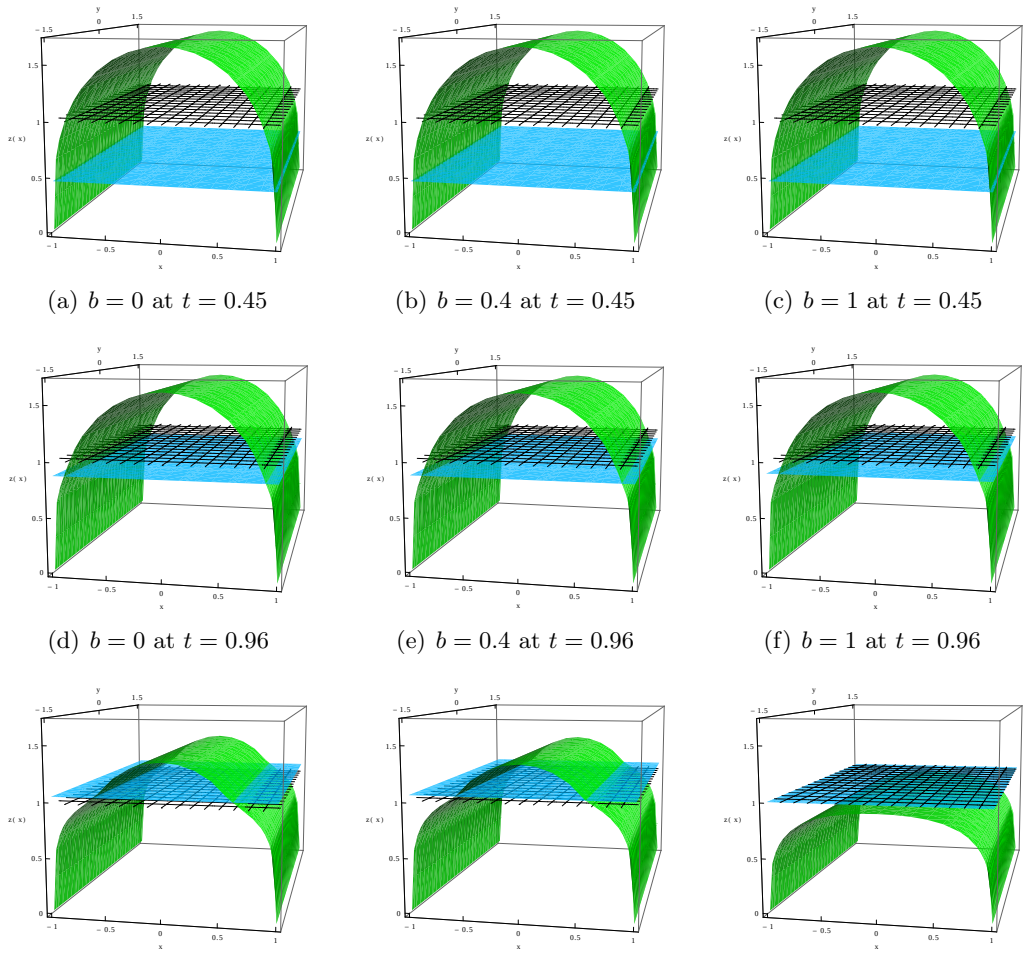

(a) $b = 0$ at $t = 0.45$ (b) $b = 0.4$ at $t = 0.45$ (c) $b = 1$ at $t = 0.45$

(d) $b = 0$ at $t = 0.96$ (e) $b = 0.4$ at $t = 0.96$ (f) $b = 1$ at $t = 0.96$

(g) $b = 0$ at $t = 1.54$ (h) $b = 0.4$ at $t = 1.54$ (i) $b = 1$ at $t = 1.54$

Figure 7: A sequence of snapshots of the time evolution of the minimal area surface and the shell of charged dust described by the Vaidya-BI-AdS metric for different values of the inverse BI parameter b and fixed charge $Q = \sqrt{2}$. In all cases the boundary Wilson loop has sides $\ell = 2$ in the x direction and $R = 3$ in the y direction. Each column, from top to bottom, indicates the time evolution for a given value of b. The cyan plane indicates the position of the shell in each case, while the gridded plane at $z = 1$ denotes the position of the (still to be formed at late times) black brane horizon.

geodesic lengths in the previous subsection. The effect of the inverse BI parameter b for fixed charges can be inferred from Figure **9**, namely, the larger b is, the shorter the thermalization time is. This implies that the boundary field theory is easier to thermalize in the nonlinear case, which is in perfect agreement with our results from the previous subsection. The numerical values obtained for the thermalization times are summarized in Table 2.

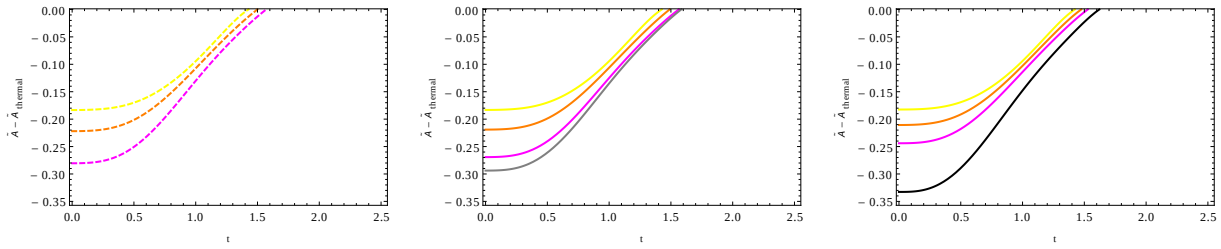

(a) $b = 0$ (b) $b = 0.4$ (c) $b = 1$

Figure 8: Thermalization curves of the renormalized minimal area surfaces in the Vaidya-BI-AdS spacetime at fixed values of b for different charges Q, from $Q = 0.5$ to the extremal charge $Q_{ext}(b) = \sqrt{2 + 3b^2}$. In (a) we show $Q = 0.5$ (yellow) in the top, $Q = 1$ (orange) in the middle, and $Q = \sqrt{2}$ (magenta) in the bottom. In (b) and (c) the same values appear together with the extremal values $Q = \sqrt{2.48}$ (gray) and $Q = \sqrt{5}$ (black), respectively. The relevant side of the boundary Wilson loop is $\ell = 2$.

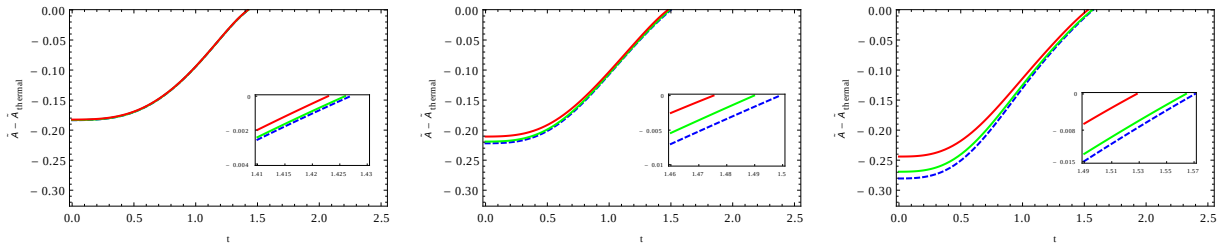

(a) $Q = 0.5$ (b) $Q = 1$ (c) $Q = \sqrt{2}$

Figure 9: Thermalization curves of the renormalized minimal area surfaces in the Vaidya-BI-AdS spacetime for different inverse BI parameters b at fixed values of charge. In each case we have $b = 0$ (dashed blue) in the bottom, $b = 0.4$ (green) in the middle, and $b = 1$ (red) in the top. The insets show details of the curves right before thermalization. The side of the boundary Wilson loop is $\ell = 2$.

Just as we did before, we also use the fit functions to study the thermalization velocities for the minimal area surfaces, $\frac{d}{dt}(\tilde{\mathcal{A}} - \tilde{\mathcal{A}}_{\text{thermal}})$, which are plotted in Figure **10** for the cases $Q = \sqrt{2}$ fixed and $b = 1$ fixed, respectively. The plots confirm the results obtained from the geodesics in what concerns the different stages of the dynamical process. Namely, there is always a phase transition instant at the middle stage of the evolution where the process changes from an accelerating phase to a decelerating phase. Such a phase transition point is reached later as we increase b for a fixed charge (see Figure (a)), or sooner as the charge Q is increased for a given b (see Figure (b)). In other words, the thermalization of expectation values of Wilson loops in the dual field theory consists in a slow (quick) accelerating phase followed by a quick (slow) decelerating phase towards the final state as the nonlinearity parameter b (the charge Q, or chemical potential μ/T) is increased.

Once more we point out that our velocity plots do not provide any evidence of a negative thermalization velocity at initial times, in contrast to [100]. This can also be seen from Figure **11**, where we show a comparison of the numerical results with the fitting functions. The zoomed region shows

	$b=0$	$b=0.4$	$b=1$
$Q=0.5$	1.427	1.426	1.423
$Q=1$	1.499	1.490	1.475
$Q=\sqrt{2}$	1.571	1.564	1.528
$Q=\sqrt{2.48}$	–	1.584	–
$Q=\sqrt{5}$	–	–	1.622

Table 2: Summary of the numerical values obtained for the thermalization times of the renormalized minimal area surfaces shown in Figures 8 and 9.

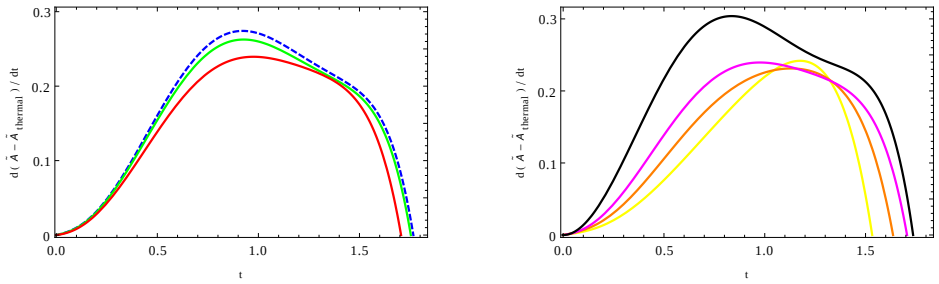

(a) $Q=\sqrt{2}$ (b) $b=1$

Figure 10: Thermalization velocities of the renormalized minimal area surfaces at both fixed charge and fixed b. The dashed blue, green, and red curves in (a) correspond respectively to $b=0, 0.4, 1$. The curves in (b) correspond to $Q=0.5$ (yellow), $Q=1$ (orange), $Q=\sqrt{2}$ (magenta), and $Q=\sqrt{5}$ (black). The side of the boundary Wilson loop is $\ell=2$.

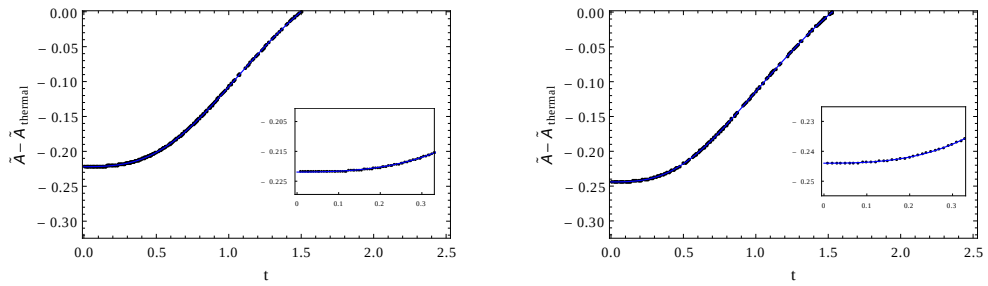

(a) $Q=1, b=0$ (b) $Q=\sqrt{2}, b=1$

Figure 11: A comparison between the numerical results and the polynomial fits for the minimal area surfaces. The inset emphasizes the constant behavior of the curve at initial times.

that at the initial times, up to $t \sim 0.1$, all the numerical points lie over a horizontal line and thus the curve must have vanishing slope in that region. We should mention that the fitting functions used here were degree 7 polynomials $f(t) = \sum_{n=0}^{7} \alpha_n t^n$ with the linear term (α_1) set to zero to ensure the strictly constant behavior $f(t) \sim \alpha_0$ up to $t \sim 0.1$ as required by the numerical data.

3.5 Discussion and conclusions

In this Chapter, the effect of the chemical potential and the inverse BI parameter on the thermalization time of the dual boundary field theory has been studied using the Vaidya-like toy model of a collapsing shell of charged dust. The bulk spacetime is dynamical, constructed to interpolate between a pure AdS space at initial times and a charged Einstein-Born-Infeld AdS black brane at late times. We use as thermalization probes the equal-time two-point functions and expectation values of Wilson loops, which have well defined dual gravity descriptions in terms of renormalized geodesic lengths and minimal area surfaces in the bulk. Another class of nonlocal observables, the entanglement entropy of boundary regions, which also have well known holographic descriptions in terms of minimal volumes of codimension-2 surfaces in the bulk, can also be used as a third thermalization probe. However, as the results are similar, we focus only on the first two since they are enough to capture all the relevant effects.

We conclude that as the charge (or, equivalently, the chemical potential) grows, the thermalization time is also increased. The inverse BI parameter, on the other hand, has the opposite effect, i.e., the larger the value of b turns, the shorter the thermalization time is. This is a new result, whose interpretation becomes clear if we think in terms of bulk physics: the larger the value of b is, the stronger the electromagnetic interaction in the bulk becomes, which implies that thermalization (thought of as the result of collisions between bulk particles) should be reached sooner.[8] At the initial stages of the thermalization we find that Q and b have little effect on the time evolution, becoming important only from the middle stage on. We arrive at the same results independently for both the renormalized geodesic lengths and minimal area surfaces. In each case they can be seen just by looking to a sequence of snapshots of the motion profiles of the geodesics and minimal surfaces as the time goes by or, alternatively, from the thermalization curves obtained from the full numerical analysis. The effect of the charge happens to be the same found in [78] using Einstein-Maxwell theory and [100], where Gauss-Bonnet curvature corrections were included. The outcome of introducing a nonvanishing b, on the other hand, is a new result. In particular, the effect is the same as that of the Gauss-Bonnet parameter reported in [100]. Since BI electrodynamics consists essentially of higher order derivatives of the gauge field, we suggest that this may be a general feature of introducing extra derivatives in the bulk, i.e., that boundary gauge theories whose gravity dual carry more than two derivatives tend to thermalize sooner than two-derivative theories after a sudden injection of energy. It would be interesting to explore this idea with other theories possessing this characteristic in order to have definite answers.

Moreover, by fitting the numerical data with smooth functions we were also able to study the thermalization velocities associated to each curve. Although this is not rigorous, it reveals some interesting features of the dynamical process of thermalization and how they are affected by Q and b. We notice the existence of a phase transition point at the middle stage of the thermalization, which divides the process into an accelerating and a decelerating phase. The phase transition point is shifted depending on the values of b and Q. Namely, as Q increases, the phase transition point arrives earlier. This indicates that for large values of chemical potential the thermalization process consists of a quick accelerating phase followed by a slowly decelerating phase to the final state. Increasing the value of b, oppositely, causes a delay in the phase transition point. This is to be contrasted with the fact that nonlinear theories thermalize first, indicating that the dynamical process for non-vanishing b consists of a slowly accelerating phase followed by a quick deceleration towards the equilibrium state.

[8] I am grateful to Fernando Brandt for pointing this out.

We also show from the velocity plots that the thermalization process is monotonic and the velocity is always positive at the initial stages, in contrast to the claim by the authors of [100] that there should be a negative thermalization velocity at the very beginning of the evolution.

Chapter 4

Holographic quenches towards a Lifshitz point

In this Chapter we present a different application of holography to describe the far-from-equilibrium dynamics of quantum systems (not completely disconnected to the thermalization problem studied in the previous Chapter, as we shall see). Namely, we shall now approach the problem of *quantum quenches*, which is a well known class of problems in statistical and condensed matter physics. The idea there is to study the response (the *quench dynamics*) of a quantum many-body system to a time-dependent coupling $\lambda(t)$ in the Hamiltonian, but a similar problem can in fact be setup for any quantum system. The interest on quantum quenches is motivated by recent experimental breakthroughs involving ultracold atoms, which have made possible for the very first time to monitor the full real-time evolution of quantum states in isolated quantum systems (see [101] for a review). In spite of such remarkable experimental advances, however, from a theoretical point of view the fundamental principles underlying the far-from-equilibrium dynamics of interacting quantum systems still remain elusive. Some relevant open questions are the following

- Does the theory always relax to an equilibrium state at late times?
- If so, is this state thermal in some sense? What are the necessary conditions for thermalization?
- How do the relevant degrees of freedom organize to make up such an equilibrium state at the end of the process?
- How do different observables (both local and nonlocal) evolve in time before equilibrating? Is there any signature of universal behavior in their time evolution?
- What happens if $\lambda(t)$ crosses a critical point λ_c, i.e., how is the dynamics during the breaking of a global symmetry?

We take here a modest step onto some of these questions using a holographic point of view. After briefly introducing the problem of quantum quenches and explaining why holography is a useful tool to approach it, we present our original contribution to the subject, namely a specific quench of a strongly coupled CFT that leads to a breaking of the relativistic scaling symmetry of the CFT towards a non-relativistic theory with Lifshitz-type scaling symmetry.

The results shown in this Chapter have been published as [102]

Holographic quenches towards a Lifshitz point,
G. Camilo, B. Cuadros-Melgar, and E. Abdalla, JHEP **02** (2016) 014

and the exposition below makes substantial use of the published text, including literal transcriptions.

4.1 Holographic quenches

Let us start with a precise statement of what we mean by a quantum quench. The typical setup consists in a Hamiltonian (for a quantum mechanical system) or a Lagrangian (for a quantum field theoretical system) containing a time-dependent parameter $\lambda(t)$ which asymptotes to constant values λ_{initial} and λ_{final} at early and late times by varying between them over a time scale δt (see Figure **1**). Here λ may be for instance an external electric/magnetic field, the temperature, some chemical doping parameter or, in the case of QFTs, any coupling appearing in the Lagrangian such as a mass parameter or an interaction strength. The fact that $\lambda(t)$ asymptotes to a constant at early times means that the system is prepared in some known stationary initial state (usually the ground state or a thermal state[1]), which is then excited during a time scale δt to yield a new final state that may or may not be stationary. Key questions are whether (and how) an equilibrium state is reached at the end of the process, if such a steady state is "thermal" in any sense, as well as what are the properties of physical quantities after the quench is over.

Figure 1: Typical quench profiles of interest: (a) and (b) correspond to turning on or off the value of a given coupling constant, respectively, while (c) and (d) correspond to a finite pulse.

Of particular interest from a theoretical point of view is the case of quenches near quantum critical points, since the response is likely to exhibit universal features that might be shared by many different physical systems. Nevertheless, the study of quench dynamics at strong coupling using standard field theory methods is usually hard and, in fact, progress in this direction has been limited mostly to 2-dimensional conformal field theories (CFTs) [103, 104, 105, 106] (see [107] for a review).

The holographic duality once again appears as a helpful tool to study quenches in strongly coupled quantum field theories. Indeed, it has been used by many authors to model quenches in strongly coupled CFTs with a gravity dual (see [108, 109, 110, 111, 112, 113, 114, 115, 116, 117, 118, 119, 120, 121] for an incomplete list of references). The reason for that is a trivial consequence of the GKPW prescription for AdS/CFT studied in Section 2.3, which we now recall. Namely, we have seen that when the bulk metric is the pure AdS spacetime (1.13) (i.e., with no extra fields turned on) the dual field theory is a CFT in its vacuum state. If bulk fields are turned on, on the other hand, we get a deformation of the CFT whose action is of the form

$$S = S_{\text{CFT}} + \int dt d^{d-1}x \; J(t,\mathbf{x})\mathcal{O}_\Delta(t,\mathbf{x}) \; , \tag{4.1}$$

where $\mathcal{O}_\Delta$ is an operator of scaling dimension Δ (let us assume it is a scalar, for simplicity). The operator $\mathcal{O}_\Delta$ is dual to a bulk field[2] $\phi(t,\mathbf{x},u)$ with mass $m^2L^2 = \Delta(\Delta-d)$ in the sense that, near the AdS boundary $u=0$, it has an asymptotic behavior of the form

$$\phi(t,\mathbf{x},u) = u^{d-\Delta}J(t,\mathbf{x}) + u^\Delta B(t,\mathbf{x}) + \cdots \; . \tag{4.2}$$

In other words, the boundary condition $J(t,\mathbf{x})$ for the bulk field at the AdS boundary is understood as the source for the CFT operator $\mathcal{O}_\Delta$. Now, according to the definition given above, a quench $\lambda(t)$ of an operator $\mathcal{O}_\Delta$ in a CFT corresponds by definition to an action of the form (4.1) with the

[1] This case is often referred to as a thermal quench.

[2] In this Chapter we use u to denote the standard "inverse radial coordinate" z in the AdS Poincaré system (1.13) in order to avoid confusion with the Lifshitz dynamical exponent, which is traditionally named z in the literature.

desired quench profile $\lambda(t)$ replacing the source $J(t,\mathbf{x})$, i.e., $J(t,\mathbf{x}) \equiv \lambda(t)$. The difference is that, while $J(t,\mathbf{x})$ was treated before as a fictitious current used to obtain the correlation functions of the theory, now $\lambda(t)$ is to be treated as a truly physical time-dependent coupling in terms of which we want to calculate the time evolution of physical observables. Hence, we can define the following new entry to the holographic dictionary,

Quench $\lambda(t)$ of an operator $\mathcal{O}_\Delta(t,\mathbf{x})$
$$\longleftrightarrow$$
Time-dependent boundary condition for the the bulk field $\phi(t,u)$ dual to $\mathcal{O}_\Delta(t,\mathbf{x})$ at the AdS boundary, namely $\phi(t,u) = u^{d-\Delta}\lambda(t) + \cdots$

The imposition of such a time-dependent boundary condition causes the whole bulk solution to be dynamical, including the metric, and may lead for instance to an AdS black hole formation (if the initial state is pure AdS) or black hole equilibration (if there is already an AdS black hole at the beginning).

4.2 Lifshitz holography

Whilst some effective theories in condensed matter have relativistic conformal symmetry, which is the situation where AdS/CFT is best understood, there are in turn many quantum critical points that are not conformally invariant, exhibiting instead a non-relativistic scaling (which we refer to as *Lifshitz scaling*) of the form

$$(t, x^i) \to (\lambda^z t, \lambda x^i) \ , \tag{4.3}$$

where the parameter z is called the dynamical critical exponent[3]. Examples include phase transitions with $z = 2$ and $z = 3$ at the onset of antiferromagnetism and ferromagnetism in certain fermion systems, respectively [122]. By following the original AdS/CFT logic of matching global symmetries of the gauge theory with isometries of the metric on the gravity side, the following Lifshitz spacetime was proposed in [123, 124] as a candidate background for the holographic dual of such a non-relativistic theory

$$ds^2 = -\frac{r^{2z}}{l^{2z}}dt^2 + \frac{r^2}{l^2}d\mathbf{x}^2 + \frac{l^2}{r^2}dr^2 \ , \tag{4.4}$$

where the scaling symmetry (4.3) is realized as an isometry when combined with $r \to \lambda^{-1} r$. Unlike the AdS spacetime, however, this is not a vacuum solution of the Einstein equations with a negative cosmological constant – some matter content is required to support the geometry. A number of bottom-up models have been suggested in the literature giving rise to this Lifshitz solution, such as Einstein-Proca, Einstein-Maxwell-Dilaton and Einstein-p-form actions [123, 124] (see [125] for a very general analysis of bottom-up models including hyperscaling violating theories), or even using the nonrelativistic gravity theory of Hořava-Lifshitz [126], but at the moment no well defined top-down construction of such a non-relativistic version of AdS/CFT duality is known from string theory and the problem of setting up holography for non-relativistic scenarios remains open.

4.2.1 Lifshitz as a deformation of AdS

An interesting step in this direction was taken in [127] (see also [128] for the finite temperature case, and [129] for related work in Schrödinger backgrounds), where it was shown that Lifshitz geometries with z close to unity, i.e., $z = 1 + \epsilon^2$ with $\epsilon \ll 1$, can be understood as a continuous deformation of AdS. This implies that no more than the standard AdS/CFT dictionary is required to set up holography for such a Lifshitz solution. In fact, they showed that this particular class of Lifshitz

[3]The lack of boost invariance induced by z should not sound surprising since in typical condensed matter systems there is a preferred frame set by the rest frame of the atomic lattice.

spacetime is the holographic dual of a nonrelativistic theory which is a specific deformation of the relativistic CFT corresponding to $z = 1$. Namely, it is the theory obtained by deforming the CFT with the time component of a vector primary operator $\mathcal{V}^a$ of conformal dimension $\Delta = d$,

$$S_{\rm Lif} = S_{\rm CFT} + \sqrt{2}\epsilon \int d^d x \mathcal{V}^t(x) \ . \tag{4.5}$$

Notice that ϵ appears here as a dimensionless small coupling constant, suggesting that conformal perturbation theory can be used to check calculations on the field theory side. After establishing the holographic dictionary for this new class of holographic theories using an Einstein-Proca model in the bulk, the authors have checked that Lifshitz invariance indeed holds at the quantum level (to order ϵ^2) and have provided a general field theoretical argument for the construction of such Lifshitz invariant models using the above recipe. Despite the operational convenience of working perturbatively in powers of ϵ, there is also a possibility of application of these results since a number of theoretical models with z close to one has appeared in condensed matter (see [130, 131, 132, 133, 134, 135]).

Static solutions with Lifshitz isometries can be constructed from several gravity models. Here we will focus on the simplest one, first presented in [124], involving gravity with a negative cosmological constant and a massive vector field[4],

$$S = \frac{1}{16\pi G_{d+1}} \int d^{d+1}x \ \sqrt{-g} \left[R + d(d-1) - \frac{1}{4} F^{\mu\nu} F_{\mu\nu} - \frac{1}{2} M^2 A_\mu A^\mu \right] \ . \tag{4.6}$$

The Einstein and Proca equations of motion are, respectively,

$$R_{\mu\nu} = -d \ g_{\mu\nu} + \frac{M^2}{2} A_\mu A_\nu + \frac{1}{2} F_\mu{}^\sigma F_{\nu\sigma} + \frac{1}{4(1-d)} F^{\rho\sigma} F_{\rho\sigma} g_{\mu\nu} \tag{4.7a}$$

$$\nabla_\mu F^{\mu\nu} = M^2 A^\nu \ . \tag{4.7b}$$

If we define

$$M^2 = \frac{z d (d-1)^2}{z^2 + z(d-2) + (d-1)^2} \qquad \text{and} \qquad l^2 = \frac{z(d-1)}{M^2} = \frac{z^2 + z(d-2) + (d-1)^2}{d(d-1)} \ , \tag{4.8}$$

the action (4.6) admits a Lifshitz solution given by

$$ds^2 = -\frac{r^{2z}}{l^{2z}} dt^2 + \frac{r^2}{l^2} d\mathbf{x}^2 + \frac{l^2}{r^2} dr^2 \tag{4.9a}$$

$$A = \sqrt{\frac{2(z-1)}{z}} \frac{r^z}{l^z} dt \ . \tag{4.9b}$$

The Lifshitz scaling is realized for arbitrary dynamical exponent z by the transformation $(t, x, r) \to (\lambda^z t, \lambda \mathbf{x}, \lambda^{-1} r)$. Clearly, when $z = 1$ this becomes the usual relativistic scaling transformation, the gauge field vanishes, and the solution above reduces to the well known AdS_{d+1} solution with unit curvature radius, $l_{AdS} \equiv l(z = 1) = 1$.

By the standard AdS/CFT dictionary, the presence of the massive vector field A_μ (viewed as a perturbation at the AdS critical point) in the bulk implies that the CFT dual to the action (4.6) contains in its spectrum a vector primary operator $\mathcal{V}^a$ of dimension Δ given by

$$\Delta = \frac{1}{2}\left[d + \sqrt{(d-2)^2 + 4M^2} \right] = \frac{d}{2} + \sqrt{\frac{(d-2)^2}{4} + \frac{z d (d-1)^2}{z^2 + z(d-2) + (d-1)^2}} \ . \tag{4.10}$$

[4]However, the conventions used here are slightly different from [124]. Namely, we follow [127] where the fields and coordinates are conveniently rescaled with respect to [124] by appropriate factors of l in order to set the cosmological constant term independent of z: $g_{\mu\nu} \to l^2 g_{\mu\nu}, A_\mu \to l A_\mu, x^\mu \to l x^\mu$, with the overall factor of l^{2d} absorbed into G_{d+1}. Then, by setting e.g. the AdS radius to unity this means that all dimensionful quantities are measured in units of $l_{\rm AdS}$.

The asymptotic expansion of the bulk vector field near $r = \infty$ is given in general by

$$A_t(t, x^i, r) = r^{\Delta-d+1} A_t^{(0)}(t, x^i) + \cdots + r^{-(\Delta-1)} A_t^{(d)}(t, x^i) + \cdots \ , \tag{4.11}$$

where the non-normalizable mode $A_t^{(0)}$ is interpreted as the source for the dual operator and $A_t^{(d)}$ is related to its expectation value. The theory also admits a Lifshitz critical point with $z > 1$ provided M^2 takes values in the range [127]

$$\frac{(d-1)^2(8-3d+4\sqrt{3d^2-6d+4})}{13d-16} < M^2 \leq \frac{d(d-1)^2}{3d-4} \ . \tag{4.12}$$

We will be interested in the case where the dynamical exponent z is very close to one, $z = 1 + \epsilon^2$, with $\epsilon \ll 1$. In this case the static solution (4.9) reads

$$ds^2 = -r^2\left[1 + 2\epsilon^2 \ln r + \frac{\epsilon^2}{1-d}\right]dt^2 + r^2\left[1 + \frac{\epsilon^2}{1-d}\right]d\mathbf{x}^2 + \left[1 - \frac{\epsilon^2}{1-d}\right]\frac{dr^2}{r^2} + \mathcal{O}(\epsilon^4) \tag{4.13a}$$

$$A = \sqrt{2}\epsilon r \ dt + \mathcal{O}(\epsilon^3) \ , \tag{4.13b}$$

with the corresponding mass being

$$M^2 = d - 1 + (d-2)\epsilon^2 + \mathcal{O}(\epsilon^4) \ . \tag{4.14}$$

This means that the dual operator $\mathcal{V}^t$ has dimension

$$\Delta = d + \frac{d-2}{d}\epsilon^2 + \mathcal{O}(\epsilon^4) \ . \tag{4.15}$$

The asymptotic expansion (4.11) in this case reduces to

$$A_t(t, x^i, r) = r\left(1 + \mathcal{O}(\epsilon^2)\right) A_t^{(0)}(t, x^i) + \cdots + r^{-(d-1)}\left(1 + \mathcal{O}(\epsilon^2)\right) A_t^{(d)}(t, x^i) + \cdots \ , \tag{4.16}$$

which perfectly matches the static solution (4.13) if we identify $A_t^{(0)} \equiv \sqrt{2}\epsilon + \mathcal{O}(\epsilon^3)$ and $A_t^{(d)} \equiv \mathcal{O}(\epsilon^3)$. In other words, the full static solution (4.13) matches precisely the right asymptotic solution required for the standard AdS/CFT interpretation of the bulk model as a deformed CFT[5]. Therefore, to order ϵ^2 the Lifshitz solution with $z = 1 + \epsilon^2$ has the holographic interpretation as a deformation of the corresponding CFT by a vector operator $\mathcal{V}^t$ of dimension $\Delta = d$ as anticipated in (4.5), namely

$$S_{\text{Lif}} = S_{\text{CFT}} + \sqrt{2}\epsilon \int d^d x \mathcal{V}^t(x) \ . \tag{4.17}$$

Before moving on to the study of holographic quenches in the next section we shall make some brief comments on the massive vector model (4.6) used to construct the Lifshitz spacetime. This is a bottom-up model that captures the desired Lifshitz scaling provided the mass of the vector field is in the range (4.12), but at the moment it is still unclear if a precise embedding in string theory exists. There are consistent Kaluza-Klein truncations of type IIB [136] and few other supergravities [137, 138, 139] that lead to massive vectors with M^2 in the required range, each corresponding to a specific value of z, but they all contain additional scalar fields coupled to the massive vector. Hence, a top-down construction of holographic duality involving theories with Lifshitz symmetry remains obscure. As mentioned above, the standard AdS/CFT dictionary does not directly apply to such models since the geometry is not asymptotically AdS, and in fact not even the field theory dual (if any) to the Lifshitz geometry is known for arbitrary z.

[5]It is important to notice that this does not happen for arbitrary z, since the asymptotic behavior $\sim r^{\Delta-d+1}$ of (4.11) (with Δ given in (4.10)) is completely different from the exact solution $\sim r^z$ shown in (4.9), unless $z = 1 + \epsilon^2$. This means that setting up holography for the Lifshitz solution with arbitrary z (if possible) will require more than just the standard AdS/CFT dictionary, which we shall not pursue here.

4.3 Holographic quenches and the breaking of relativistic scaling

We now turn to the main proposal of the present Chapter. The idea is to study holographic quenches of CFTs in the framework of [127] described above, as an attempt to model the dynamics following the breaking of the relativistic scaling symmetry of a CFT towards a nonrelativistic Lifshitz scaling of the type (4.3) with $z = 1 + \epsilon^2$ ($\epsilon \ll 1$). The operator to be quenched according to a prescribed time-dependent profile is the vector operator $\mathcal{V}^t$ mentioned above. Namely, we study a quantum quench of $\mathcal{V}^t$ in (4.17) according to some prescribed quench profile $j(t)$, i.e., we consider the action (4.17) with a time depending coupling[6] $j(t) \equiv \sqrt{2}\epsilon J(t)$ which smoothly interpolates between the values 0 (corresponding to a strongly coupled CFT) and $\sqrt{2}\epsilon$ (corresponding to the Lifshitz theory discussed above) as time evolves from $-\infty$ to $+\infty$,

$$S = S_{\text{CFT}} + \sqrt{2}\epsilon \int d^d x \; J(t)\mathcal{V}^t(t, \mathbf{x}) \; . \tag{4.18}$$

This may provide new insights into the nonequilibrium process of reaching a Lifshitz critical point, e.g., in condensed matter systems.

From the point of view of the dual gravitational description, all one needs to do is to consider the Einstein-Proca model (4.6) and solve the equations of motion in a time-dependent setting subject to quench-like boundary conditions at $r \to \infty$. Namely, the non-normalizable mode of the bulk vector field A_t must coincide with the desired quench profile $\sqrt{2}\epsilon J(t)$ (see details below). Notice that by turning on a non-normalizable mode proportional to ϵ the full bulk vector field will also be proportional to ϵ, and therefore working perturbatively in ϵ (which is the only situation where a holographic interpretation of the final state Lifshitz theory is clear) is equivalent to solving the Einstein-Proca equations (4.7) perturbatively in powers of A_μ. This is similar to the weak field collapse models studied in [69, 70].

We begin by specifying our ansatz for the metric and vector field, which we do for arbitrary exponent z before particularizing to the case of interest. As typical in dynamical problems (see e.g. [68]), it will be useful to work with the ingoing Eddington-Finkelstein (EF) coordinate system $(v, r, \mathbf{x})$, where v is related to the usual t coordinate appearing in (4.9) via $dv = dt + \frac{l^{z+1}}{r^{z+1}} dr$. Notice that at the asymptotic boundary $r = \infty$ both v and t coincide, thus, any function $J(v)$ appearing in the bulk solution is understood as $J(t)$ for an observer living on this boundary (in particular, this will be the case for our quench profile on the CFT side). The ansatz for the metric and the vector field is

$$ds^2 = 2h(v, r)dvdr - f(v, r)dv^2 + r^2 d\mathbf{x}^2 \tag{4.19a}$$

$$A(v, r) = a(v, r)dv + b(v, r)dr \; . \tag{4.19b}$$

It involves 4 unknown functions f, h, a, b of both (v, r), and clearly reduces to the static Lifshitz solution (4.9) written in EF coordinates if the functions assume the static forms

$$f_{\text{Lif}}(r) = \frac{r^{2z}}{l^{2z}} \; , \quad h_{\text{Lif}}(r) = \frac{r^{z-1}}{l^{z-1}} \; , \quad a_{\text{Lif}}(r) = \sqrt{\frac{2(z-1)}{z}} \frac{r^z}{l^z} \; , \quad b_{\text{Lif}}(r) = -\frac{l^{z+1}}{r^{z+1}} a_{\text{Lif}}(r) \; ,$$

and of course the particular case of pure AdS follows by taking $z = 1$.

The particularization to our case of interest ($z = 1 + \epsilon^2 + \cdots$) is done by formally expanding each

[6] For simplicity we normalize our quench profile with the factor of $\sqrt{2}\epsilon$, in such a way that when $J(v) \to 1$ we get the Lifshitz solution with $z = 1 + \epsilon^2$, equation (4.13).

function in the ansatz (4.19) as a power series in ϵ, i.e.,

$$f(v,r) = \sum_{n=0}^{\infty} f^{(n)}(v,r)\epsilon^n \tag{4.20a}$$

$$h(v,r) = \sum_{n=0}^{\infty} h^{(n)}(v,r)\epsilon^n \tag{4.20b}$$

$$a(v,r) = \sum_{n=0}^{\infty} a^{(n)}(v,r)\epsilon^n \tag{4.20c}$$

$$b(v,r) = \sum_{n=0}^{\infty} b^{(n)}(v,r)\epsilon^n \ , \tag{4.20d}$$

and then solving the equations of motion order by order in an ϵ expansion. We shall carry this expansion to leading non-trivial order for each function, which happens to be order ϵ^2 as we will see, but the extension to arbitrary order can be done in a similar way.

Besides the ansatz, in order to solve the equations of motion one still needs to specify two more sets of data, the boundary conditions and the initial conditions. We first discuss the latter. Our initial configuration on the field theory side corresponds simply to a strongly coupled CFT in the vacuum state (no deformation at all). In the bulk description this is represented by a pure AdS geometry and no gauge field, i.e.,

$$f(v \to -\infty, r) = r^2 \tag{4.21a}$$

$$h(v \to -\infty, r) = 1 \tag{4.21b}$$

$$a(v \to -\infty, r) = 0 \tag{4.21c}$$

$$b(v \to -\infty, r) = 0 \ . \tag{4.21d}$$

In particular, this set of conditions completely determines the zeroth order coefficients in the expansions (4.20) to be

$$f^{(0)}(v,r) = r^2, \qquad h^{(0)}(v,r) = 1, \qquad a^{(0)}(v,r) = 0, \qquad b^{(0)}(v,r) = 0 \ , \tag{4.22}$$

and demands that all the remaining $f^{(n)}, h^{(n)}, a^{(n)}, b^{(n)}$ $(n \neq 0)$ vanish for $v \to -\infty$.

Now we turn to the boundary conditions at $r \to \infty$. For the vector field, in order to simulate a quench in the boundary field theory with quench profile $j(t) = \sqrt{2}\epsilon J(t)$, according to the AdS/CFT dictionary we must turn on the non-normalizable mode for its time component $a(v,r)$ with exactly the same profile $j(v) = \sqrt{2}\epsilon J(v)$ (remember that the time coordinates v and t coincide at $r = \infty$). For the metric components we impose that the geometry is asymptotically Lifshitz[7]. Thus, to order ϵ^2, the boundary conditions read

$$f(v, r \to \infty) = r^2 \left(1 + 2\epsilon^2 J(v)^2 \ln r + \cdots\right) \tag{4.23a}$$

$$h(v, r \to \infty) = 1 + \epsilon^2 J(v)^2 \ln r + \cdots \tag{4.23b}$$

$$a(v, r \to \infty) = \sqrt{2}\epsilon J(v) r + \cdots \tag{4.23c}$$

$$b(v, r \to \infty) = 0 \ . \tag{4.23d}$$

[7]Actually there is an abuse of terminology here. Strictly speaking, the metric is not asymptotically Lifshitz (in the usual sense) during the whole dynamical process, since the Lifshitz exponent z in practice is evolving in time from $z = 1$ to $z = 1 + \epsilon^2$, and hence the Lifshitz scaling is not realized in the intermediate steps. In a way, we are modelling a continuous breaking of the relativistic scaling symmetry due to the injection of energy in the form of a quench. What one really wants to ensure with such a boundary condition is that asymptotic Lifshitz behavior in its strict sense is reached in the final state at $v \to +\infty$, when the quench profile has stabilized to a constant value ($J(v) \to 1$) and the metric exhibits the usual Lifshitz isometry as in equation (4.13).

At first sight the asymptotic Lifshitz behavior at the final state may sound conflicting with the pure AdS initial conditions (4.21), but it should be kept in mind that we are dealing here with the case of z very close to 1, for which we have shown that the Lifshitz spacetime can be understood as a deformation of AdS.

It should be stressed that the function $J(v)$ is known from the beginning as an input from the CFT side (it models the precise way in which energy is injected into the system, causing a dynamical breaking of the relativistic scaling). In fact, it is the only responsible for introducing dynamics in the bulk. Our main goal is to solve the equations of motion (4.7) for the unknown functions in the ansatz (4.19)-(4.20) as functionals of $J(v)$.

4.3.1 The solution to order ϵ^2

For simplicity we focus here on the case $d = 3$, namely a quantum quench of a CFT living in (2+1) dimensions, which is motivated by a variety of layered 2-dimensional systems in condensed matter, but a similar analysis should hold for any number d of dimensions with no additional complications. By carrying out the perturbative scheme introduced above and taking into account the initial conditions (4.21) and boundary conditions (4.23), the solution to order ϵ^2 for the vector field and the metric reads

$$A(v,r) = \epsilon \left[a^{(1)}(v,r)dv + b^{(1)}(v,r)dr \right] + \mathcal{O}(\epsilon^3) \tag{4.24a}$$

$$ds^2 = 2\left[1 + \epsilon^2 h^{(2)}(v,r)\right] dvdr - \left[r^2 + \epsilon^2 f^{(2)}(v,r)\right] dv^2 + r^2\left(dx_1^2 + dx_2^2\right) + \mathcal{O}(\epsilon^4)\ , \tag{4.24b}$$

with the functions $a^{(1)}, b^{(1)}, f^{(2)}, h^{(2)}$ given in terms of the quench profile $J(v)$ as

$$a^{(1)}(v,r) = \sqrt{2}r\left(J(v) + \frac{\dot{J}(v)}{r} + \frac{\ddot{J}(v)}{2r^2}\right) \tag{4.25a}$$

$$b^{(1)}(v,r) = -\frac{\sqrt{2}}{r}\left(J(v) + \frac{\dot{J}(v)}{2r}\right) \tag{4.25b}$$

$$f^{(2)}(v,r) = 2r^2\left(\ln r - \frac{1}{4}\right) J(v)^2 - 3rJ(v)\dot{J}(v) - \dot{J}(v)^2 - \frac{I(v)}{r} \tag{4.25c}$$

$$h^{(2)}(v,r) = J(v)^2 \ln r - \frac{J(v)\dot{J}(v)}{r} - \frac{\dot{J}(v)^2}{8r^2}\ . \tag{4.25d}$$

The coefficient $I(v)$ is defined as

$$I(v) = \frac{1}{2}\int_{-\infty}^{v} \ddot{J}(w)^2\, dw\ . \tag{4.26}$$

Unlike all the remaining coefficients, its value at instant v depends on the whole history of the function $\ddot{J}^2$ integrated up to this time, and for that reason this coefficient will play a decisive role in determining the end state of the process, as we shall see in the sequence.

We begin the discussion by checking the trivial limit $v \to -\infty$, where the function J and all its derivatives vanish due to our assumption that $J(v)$ asymptotes to zero. The coefficient $I(v)$ also trivially vanishes, and we are left with the static AdS solution with no gauge field, in agreement with our initial conditions (4.21).

Now let us analyze the final state at $v \to +\infty$. We have assumed that the quench profile $J(v)$ asymptotes to the constant value 1, so all coefficients involving derivatives of $J(v)$ will vanish except for $J(v)$ itself. In addition, the coefficient $I(v)$ approaches a constant positive value, namely

$$I_f = \frac{1}{2}\int_{-\infty}^{\infty} \ddot{J}(w)^2 dw > 0\ . \tag{4.27}$$

This means that the end state will correspond to an asymptotically Lifshitz black brane with $z = 1+\epsilon^2$, namely

$$ds_f^2 = 2\left(1+\epsilon^2 \ln r\right) dvdr - r^2\left(1+2\epsilon^2 \ln r - \epsilon^2 \frac{I_f}{r^3}\right) dv^2 + r^2\left(dx_1^2+dx_2^2\right) + \mathcal{O}(\epsilon^4)\ , \tag{4.28}$$

supported by a finite vector field configuration $A = \sqrt{2}\epsilon r(dv - \frac{1}{r^2}dr)$. The corresponding event horizon will be located at $r = r_h$ given by the largest solution of

$$1 + 2\epsilon^2 \ln r_h - \epsilon^2 \frac{I_f}{r_h^3} = 0\ . \tag{4.29}$$

The fact that $I_f > 0$ implies that it is impossible to reach a pure Lifshitz solution at the final state, since there will always occur a black hole formation. Exciting the non-normalizable mode of the vector field triggers a gravitational collapse in the bulk. From the boundary field theory point of view, this means that quenching the vector operator $\mathcal{V}^t$ in the CFT vacuum will always drive the system to a nonrelativistic Lifshitz theory *at finite temperature*. Another way to state this is that it is impossible to reach the vacuum state of the Lifshitz theory from the vacuum of a CFT as result of a (continuous) quench of the operator $\mathcal{V}^t$. This is our main result.

The Ricci scalar for the solution (4.24)-(4.25) is easily found by taking the trace of the Einstein equation (4.7a), namely

$$\begin{aligned} R &= -d(d+1) + \frac{M^2}{2} A_\mu A^\mu + \frac{3-d}{4(1-d)} F_{\mu\nu}F^{\mu\nu} \\ &= -12 - 2\epsilon^2\left[J(v)^2 + \frac{2J(v)\dot{J}(v)}{r} + \frac{J(v)\ddot{J}(v) + \frac{3}{4}\dot{J}(v)^2}{r^2} + \frac{\dot{J}(v)\ddot{J}(v)}{2r^3}\right] + O\left(\epsilon^4\right). \end{aligned} \tag{4.30}$$

A curvature singularity appears at $r = 0$ but, as discussed above (see also next section for two explicit examples), it is not naked since it is always covered by a horizon at $r_{\rm EH}(v) \sim \left(\epsilon^2 I(v)\right)^{1/3}$. This also sets the regime of validity for our perturbative solution, namely the range of values for the radial coordinate going from the boundary $r = \infty$ down to $r_h \sim \left(\epsilon^2 I_f\right)^{1/3}$. Together with $\epsilon \ll 1$ this ensures that none of the terms in the solution (4.24)-(4.25) spoil the assumption of weak field and, hence, the solution can be trusted.

4.3.2 Two quench profiles of interest

We now discuss two particular quench profiles of interest, which will be used for a detailed study of observables in the sequence.

The first one is a function which interpolates between the values 0 and 1 in a time scale δt, such as (see e.g. [75])

$$J(v) = \frac{1}{2}\left(1 + \tanh\frac{v}{\delta t}\right)\ . \tag{4.31}$$

This is the case we have been anticipating from the beginning, in which our solution describes a dynamical geometry evolving from pure AdS to a Lifshitz black hole with $z = 1+\epsilon^2$. For such a profile, the coefficient $I(v)$ (the only nontrivial coefficient in the solution (4.25)) can be analytically found as being

$$I(v) = \frac{2 + 5\tanh^3(v/\delta t) - 3\tanh^5(v/\delta t)}{30\delta t^3}\ . \tag{4.32}$$

In particular, its final value at $v \to +\infty$, which according to (4.28) is related to the mass parameter of the final state Lifshitz black hole, is

$$I_f = \frac{2}{15\delta t^3}\ . \tag{4.33}$$

The fact that it goes with $\sim 1/\delta t^3$ implies that one should be careful when using our perturbative solution for the case of a fast quench ($\delta t \to 0$). As we have mentioned before, the perturbative solution is only valid for values of r going from infinity up to $r \sim r_h$ (the event horizon of the final state black hole) given by $r_h \simeq \left(\epsilon^2 I_f\right)^{1/3} \simeq 0.5\epsilon^{2/3}/\delta t$. Therefore, for this choice of quench the perturbative solution can only be trusted deep inside the bulk provided $\epsilon \ll 1$ but also $\epsilon^{2/3}/\delta t \ll 2$ (or $r_h \ll 1$).

A second quench profile of interest, which is slightly different from the transition we have been considering, is a Gaussian function that starts and ends asymptotically at 0, i.e.,

$$J(v) = e^{-v^2/2\delta t^2} \ . \tag{4.34}$$

This means that the relativistic scaling of the CFT is broken by the quench at intermediate times but restored at the end state and it would be interesting to explore how this happens. In the bulk description such a choice corresponds to a dynamical spacetime starting at pure AdS, evolving in time in a nontrivial way, and ending up by forming an asymptotically AdS black hole. One must have in mind that the expression for the final state black hole in this case will again have the form (4.28), but now without the two $\ln r$ terms which are exclusive of Lifshitz black holes. The coefficient $I(v)$ then is

$$I(v) = \frac{1}{16\delta t^6}\left[3\sqrt{\pi}\delta t^3\left(1+\mathrm{erf}(v/\delta t)\right) + 2ve^{-v^2/\delta t^2}\left(\delta t^2 - 2v^2\right)\right] \ , \tag{4.35}$$

and the corresponding final value at $v \to +\infty$ reads

$$I_f = \frac{3\sqrt{\pi}}{8\delta t^3} \ . \tag{4.36}$$

This quantity will be related to the mass of the Schwarzschild-like AdS black hole formed at the end of the process. It again depends on the quenching time as $\sim 1/\delta t^3$, so the same comment made for the first quench concerning the regime of validity applies here and, in particular, one must be careful when applying our solution if we are interested in the fast quench limit. Namely, the location of the horizon now will be $r_h = (\epsilon^2 I_f)^{1/3} \simeq 0.9\epsilon^{2/3}/\delta t$, hence the perturbative solution is only reliable deep inside the bulk provided $\epsilon \ll 1$ as well as $\epsilon^{2/3}/\delta t \ll 1$ (or $r_h \ll 1$).

4.3.3 All-order structure of the perturbative solution

Although here we are only interested in keeping terms up to ϵ^2 in the perturbative expansion introduced in (4.20), nothing prevents us from proceeding to higher orders in ϵ [8]. For the sake of completeness, here we analyze the all-order structure of the Einstein-Proca equations of motion (4.7).

Since the vector field (which is turned on at order ϵ^1 by the boundary condition (4.23c)) backreacts quadratically on the Einstein equation, it is straightforward to see that the metric will only receive contributions at even powers of ϵ. As a consequence, the gauge field will contain only odd powers of ϵ. In summary, the final form of the perturbative solution will look schematically like

$$f(v,r) = r^2 + \sum_{n=1}^{\infty} \epsilon^{2n} f^{(2n)}(v,r) \tag{4.37a}$$

$$h(v,r) = 1 + \sum_{n=1}^{\infty} \epsilon^{2n} h^{(2n)}(v,r) \tag{4.37b}$$

$$a(v,r) = \sum_{n=0}^{\infty} \epsilon^{2n+1} a^{(2n+1)}(v,r) \tag{4.37c}$$

$$b(v,r) = \sum_{n=0}^{\infty} \epsilon^{2n+1} b^{(2n+1)}(v,r) \ . \tag{4.37d}$$

[8] Of course the boundary conditions (4.23) must be appropriately modified in these cases.

4.4 Holographic probes of thermalization

In this section we use the gravity solution previously obtained to study the nonequilibrium dynamics of observables with a known holographic description. Since the solution (4.24)-(4.25) fluctuates at intermediate times but always reaches a static thermal configuration after some time, as shown above, a clear notion of thermalization is ensured to happen in our model. Then, an interesting point would be to study the thermalization time of the field theory following the quench, and how this is affected at different scales. In Vaidya-like approaches to the problem of holographic thermalization (see e.g. [75]) the conclusion was that the UV (short distance) modes thermalize before IR (large distance) modes, the so called top-down thermalization. It would be useful to check if the same holds here, as well as the role played by the quenching rate δt.

4.4.1 Time evolution of the apparent and event horizons

We begin studying the time evolution of the apparent and event horizons. Although for a static black hole the two horizons necessarily coincide, this is not the case in a dynamical spacetime [140]. In fact, they can evolve in time in completely different ways, being coincident only when the equilibrium state is reached and the black hole is formed. In general, if a gravitational collapse process is sourced by a physically reasonable matter field, the apparent horizon should always lie inside the event horizon. In addition, the area of the event horizon is expected to grow monotonically during the entire process. Here we study these two features for our dynamical solution, since they provide nontrivial consistency checks of the solution.

The apparent horizon is defined as the outermost trapped surface, that is, the closed surface on which all outgoing null rays normal to it have zero expansion (i.e., they stop expanding outwards). It is a local concept in the sense that its existence can be inferred by an observer looking only at a small region of the spacetime. The notion of apparent horizon is not an invariant property of the spacetime, since its location or even its existence depends on how spacetime is foliated. This is in sharp contrast with the concept of event horizon, defined as the null surface inside of which light rays can never escape to null infinity. Notice that the existence of an event horizon is a fundamental causal property of the spacetime which does not depend on the choice of coordinates, since determining whether or not light is able to escape to null infinity requires the knowledge of the entire history of the spacetime.

We begin by calculating the event horizon for our solution. It is defined as the null surface $\mathcal{S}(v,r) \equiv r - r_{\rm EH}(v) = 0$, meaning that its normal vector $\partial_\mu \mathcal{S} = \partial_r - r'_{\rm EH}(v)\partial_v$ must be null, i.e., $g^{\mu\nu}\partial_\mu \mathcal{S}\partial_\nu \mathcal{S} = 0$. For a spacetime of the form (4.19) this results in the following differential equation for $r_{\rm EH}$:

$$\frac{dr_{\rm EH}}{dv} = \frac{f(v, r_{\rm EH})}{2h(v, r_{\rm EH})} \ . \tag{4.38}$$

In order to obtain the apparent horizon, we first need to introduce the tangent vectors $\xi^\mu_{\rm in/out}$ to the ingoing and outgoing radial null geodesics in the spacetime (4.19). They are given by

$$\xi^\mu_{\rm in} = -\partial_r \ , \qquad \xi^\mu_{\rm out} = \frac{1}{h(v,r)}\left[\frac{f(v,r)}{2h(v,r)}\partial_r + \partial_v\right] \ , \tag{4.39}$$

where the normalization was chosen such that $\xi^2_{\rm in} = \xi^2_{\rm out} = 0$ and $\xi_{\rm in}\cdot\xi_{\rm out} = -1$. Then the apparent horizon is located at the radius $r_{\rm AH}(v)$ where the expansion $\theta_{\rm out}(v,r)$ of a congruence of outward pointing null geodesics vanishes, namely

$$\theta_{\rm out} = \mathcal{L}_{\xi_{\rm out}} \ln\sqrt{-\gamma} = \xi^\mu_{\rm out}\partial_\mu \ln\sqrt{-\gamma} \quad \equiv 0 \quad \text{for } r = r_{\rm AH}(v) \ . \tag{4.40}$$

Here $\mathcal{L}_{\xi_{\rm out}}$ denotes the Lie derivative along $\xi_{\rm out}$ (which acts just as a directional derivative for a scalar function) and $\sqrt{-\gamma} = r^2$ is the area element on the codimension-2 surface $\gamma_{ij}dx^i dx^j = r^2(dx_1^2 + dx_2^2)$

which is orthogonal to this null congruence. It is straightforward to show from the formulas above that $\theta_{\text{out}} = \frac{f(v,r)}{rh(v,r)^2}$, so the apparent horizon is determined by the equation

$$f(v, r_{\text{AH}}) = 0 \ . \tag{4.41}$$

Expressions (4.38) and (4.41) with $f(v,r) = r^2 + \epsilon^2 f^{(2)}(v,r)$ completely determine the location of the event and apparent horizons for our solution (4.24)-(4.25) once the quench profile $J(v)$ is specified. In figure 2 we show a comparison of $r_{\text{EH}}(v)$ and $r_{\text{AH}}(v)$ during the whole time evolution for the two quench profiles of interest. In both cases one sees that the apparent horizon lies behind the event horizon during the whole collapse process, as expected. It also follows that the area of the event horizon, which is proportional to $r_{\text{EH}}(v)^2$, will grow monotonically in time (and similarly for the area of the apparent horizon). The two horizons reach the same static values at the end of the process, as expected, and this happens at roughly the same time of order $\sim \delta t$. Therefore we see that our solution trivially passes the two consistency checks.

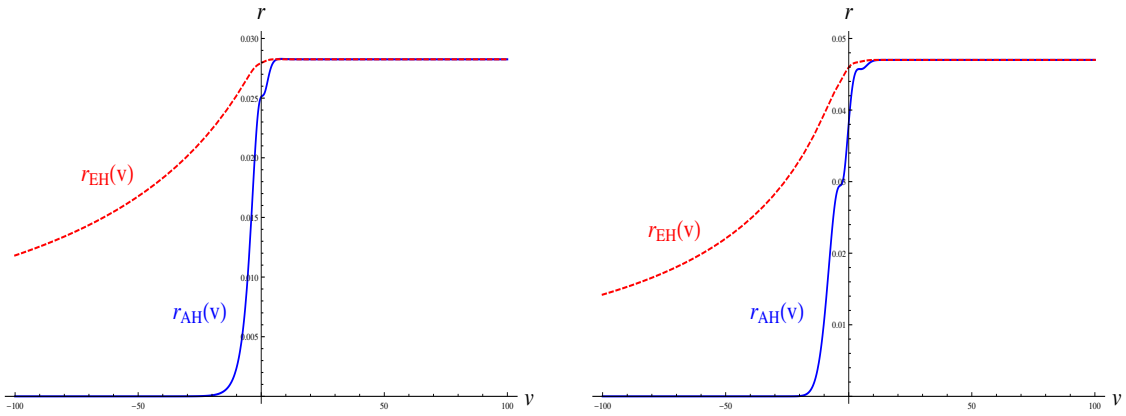

(a) Quench profile $J(v) = \frac{1}{2}\left(1 + \tanh \frac{v}{\delta t}\right)$ (b) Quench profile $J(v) = e^{-v^2/2\delta t^2}$

Figure 2: Evolution of the apparent horizon $r_{\text{AH}}(v)$ (blue) and the event horizon $r_{\text{EH}}(v)$ (red, dashed), as dictated by equations (4.41) and (4.38), respectively. For the plots we choose $\epsilon = 0.1$ and $\delta t = 4$. The relatively large value for δt was chosen for didatic purposes to make evident the non-trivial behavior of $r_{\text{AH}}(v)$. As the value of δt is decreased (faster quenches) $r_{\text{AH}}(v)$ approaches a step function.

4.4.2 Entanglement entropy

An interesting non-local observable in field theory with a well known dual gravity description is the entanglement entropy of a spatial subregion A. For any quantum field theory in a given state ρ (such as the vacuum state $|0\rangle\langle 0|$) the entanglement entropy of a spacetime region A with its complement B provides a notion of how much entanglement exists between the two regions. It is defined as

$$S_A = -\text{Tr}_A \left(\rho_A \ln \rho_A\right) \ , \tag{4.42}$$

i.e., as the von Neumann entropy associated with the reduced density matrix $\rho_A = \text{Tr}_B \rho$ obtained by tracing over the degrees of freedom in region B.

The $\text{AdS}_{d+1}/\text{CFT}_d$ correspondence provides a simple and elegant way to compute the entanglement entropy in a strongly coupled gauge theory with a gravitational dual in terms of a geometrical quantity in the bulk. This so called holographic entanglement entropy formula, first proposed by Ryu and Takayanagi [141] (see also [142] for the covariant version) is given by

$$S_A = \frac{1}{4G_N^{(d+1)}} \text{ext}_{\gamma_A} (\text{Area}(\gamma_A)) \ , \tag{4.43}$$

where $G_N^{(d+1)}$ is the Newton's constant in $d+1$ dimensions and γ_A is a codimension-2 surface in the bulk with its border $\partial\gamma_A$ coinciding with the border ∂A of the desired entangling region A of the CFT living in the AdS boundary. The symbol ext_{γ_A} denotes the extremal surface among all the γ_A's (in the sense of [142]). In the case where the entangling region A is chosen at a constant time slice (which will be our case), this condition reduces simply to finding the minimal area bulk surface with $\partial\gamma_A = \partial A$.

As one can see from the holographic formula above, the entanglement entropy clearly depends on both the size and shape of the entangling region. This means that it can capture physical properties at many different length scales, and hence using the entanglement entropy as a probe for the quench dynamics of the CFT may be helpful to understand the equilibration process at different scales.

Now we particularize to $d = 3$, which is our case of interest. For simplicity, we consider the simplest shape for the boundary entangling region A, namely a strip-like geometry in the (x^1, x^2) directions at a constant time slice. We take the strip to have infinite width (regulated by $\ell_\perp \to \infty$) in the x^2 direction and a finite width ℓ in the x^1 direction. Due to this infinite extension, the entangling region is translation invariant along x^2 and hence the bulk surface will depend only on $x^1 \equiv x$, which can be used to parametrize the functions $v(x)$ and $r(x)$ characterizing the surface.

The area functional for the class of bulk surfaces γ_A described above becomes

$$A[v,r] = \ell_\perp \int_{-\ell/2}^{\ell/2} dx\; r(x)\sqrt{r(x)^2 + 2h(v,r)r'(x)v'(x) - f(v,r)v'(x)^2}\;, \tag{4.44}$$

where $' = \frac{d}{dx}$. Notice that the infinite length $\ell_\perp$ of the x^2 direction factorizes and, since we are interested just in the ℓ dependence, we can study the density $A[v,r]/\ell_\perp$ instead of the area itself. The pair of functions $(v_{\min}(x), r_{\min}(x))$ minimizing this functional will be the minimal surface γ_A appearing in the Ryu-Takayanagi formula and, then, the holographic entanglement entropy will be $S_A = \mathcal{A}/4G_N$, where $\mathcal{A} \equiv A[v_{\min}, r_{\min}]$.

Expanding the metric coefficients f, h in powers of ϵ as dictated by the solution (4.25), and also the time and radial profiles[9] $v(x), r(x)$ of the minimal surface as

$$v = v_0 + \epsilon^2 v_2 + \mathcal{O}(\epsilon^4) \tag{4.45a}$$

$$r = r_0 + \epsilon^2 r_2 + \mathcal{O}(\epsilon^4)\;, \tag{4.45b}$$

it follows that the entanglement entropy can also be written as a power series in ϵ, i.e.,

$$S_A = S_A^{(0)} + \epsilon^2 S_A^{(2)} + \mathcal{O}(\epsilon^4)\;. \tag{4.46}$$

The zeroth order contribution is given by

$$S_A^{(0)} = \frac{\ell_\perp}{4G_N}\int_{-\ell/2}^{\ell/2} dx\; L(v_0, r_0) \tag{4.47}$$

where we have defined (the "Lagrangian" for minimal surfaces in the background AdS spacetime)

$$L(v_0, r_0) = r_0\sqrt{r_0^2 + 2r_0'v_0' - r_0^2 v_0'^2}\;. \tag{4.48}$$

The second order contribution is

$$\begin{aligned} S_A^{(2)} \;=\; & \frac{\ell_\perp}{4G_N}\int_{-\ell/2}^{\ell/2} dx\; \frac{r_0^2\left[2v_0'r_0'h^{(2)}(v_0,r_0) - v_0'^2 f^{(2)}(v_0,r_0)\right]}{2L(v_0,r_0)} \\ & + \frac{\ell_\perp}{4G_N}\int_{-\ell/2}^{\ell/2} dx\; \frac{r_0^2 v_0' r_2' + r_0^2(r_0' - r_0^2 v_0')v_2' + 2r_0\left[r_0'v_0' + r_0^2(1 - v_0'^2)\right]r_2}{L(v_0,r_0)}\;. \end{aligned} \tag{4.49}$$

[9] A comment on notation: we will omit from now on the subscript "min" to denote the minimal area surface, and also denote the ϵ^n terms in the ϵ expansion of the functions v and r as $v_n \equiv v^{(n)}, r_n \equiv r^{(n)}$ in order to keep the notation as clean as possible in the sequence.

Notice that it depends on both the zeroth order profiles (v_0, r_0) and second order profiles (v_2, r_2), meaning that in order to get $S_A^{(2)}$ one needs to calculate v_2, r_2 as well. As we shall see below, the integral in the second line contributes to the entanglement entropy only a term proportional to $r_2(\ell/2)$. Thus it is not necessary to solve for the full $r_2(x)$ (only near $x = \ell/2$, what is considerably easier).

To get v_0 and r_0 we need to solve the Euler-Lagrange equations arising from (4.47). This can be done with the help of two immediate conserved quantities, the "Hamiltonian" H and the "momentum" p_{v_0} arising from the fact that $L(v_0, r_0)$ does not depend explicitly on x and on $v_0(x)$, respectively, i.e.,

$$H(x) \equiv -\frac{r_0(x)^3}{\sqrt{r_0(x)^2 + 2r_0'(x)v_0'(x) - r_0(x)^2 v_0'(x)^2}} = -r_*^2 \tag{4.50a}$$

$$p_{v_0}(x) \equiv \frac{r_0(x)\left[r_0'(x) - r_0(x)^2 v_0'(x)\right]}{\sqrt{r_0(x)^2 + 2r_0'(x)v_0'(x) - r_0(x)^2 v_0'(x)^2}} = 0 \ . \tag{4.50b}$$

Above, we have introduced the modified boundary conditions for the minimal surface at $x = 0$, namely

$$v_0(0) = v_*, \qquad r_0(0) = r_*, \qquad r_0'(0) = v_0'(0) = 0 \ . \tag{4.51}$$

These follow from the fact that the surface stretching from the boundary to the bulk interior must be symmetric with respect to $x = 0$, therefore this must be a turning point. Of course these are not our original boundary conditions defined by the boundary time t and separation ℓ, but it will turn out to be convenient to work with these modified boundary conditions when integrating the equations of motion. At the end we can go back and express our solution in terms of t, ℓ instead of v_*, r_* using the relations

$$v_0(\pm\ell/2) = t, \qquad r_0\left(\pm\ell/2\right) = r_\infty \ . \tag{4.52}$$

Here, r_∞ is a cutoff for the AdS boundary introduced to regulate possible divergences arising due to the UV behavior of the metric.

Solving the two conservation equations (4.50) for $r_0'(x)$ and $v_0'(x)$ results in

$$v_0'(x) = \frac{r_0'(x)}{r_0(x)^2} \tag{4.53a}$$

$$r_0'(x) = r_0(x)^2\sqrt{\frac{r_0(x)^4}{r_*^4} - 1} \ . \tag{4.53b}$$

It is not possible to integrate these equations in terms of elementary functions due to the fourth power appearing inside the square root. However, an exact solution can be obtained in terms of special functions[10]. Taking into account the modified boundary conditions (4.51) the solution is given as an implicit function of x by

$$v_0(x) = v_* + \frac{1}{r_*} - \frac{1}{r_0(x)} \tag{4.54a}$$

$$x = \frac{\sqrt{\pi}\Gamma(3/4)}{r_*\Gamma(1/4)} - \frac{r_*^2}{3r_0(x)^3}\,{}_2F_1\left(\frac{1}{2}, \frac{3}{4}; \frac{7}{4}; \frac{r_*^4}{r_0(x)^4}\right) \tag{4.54b}$$

where $\Gamma(u)$ is the gamma function, ${}_2F_1(a, b; c; x)$ is the hypergeometric function, and the parameters v_*, r_* are related to the original t, ℓ boundary conditions via

$$t = v_* + \frac{1}{r_*}, \qquad \ell = \frac{2}{r_*}\frac{\sqrt{\pi}\Gamma(3/4)}{\Gamma(1/4)} = \frac{1.19814}{r_*} \ . \tag{4.55}$$

[10] Although, in order to get the entanglement entropy, it is not actually necessary to integrate these equations and find the explicit form of the functions v_0, r_0. Namely, one could simply change the integration variable from x to $r_0(x)$ inside the integral in (4.49) using (4.53) and never worry about the exact form of $r_0(x)$ itself. Anyway, we find it instructive to present the exact form (4.54).

The background contribution to the entanglement entropy, $S_A^{(0)}$, does not depend on t [11], so in order to study the time evolution one subtracts this constant value and study $\delta S_A(t) = S_A(t) - S_A^{(0)}$ instead of $S_A(t)$ itself. To order ϵ^2 this is given by equation (4.49). In the integral appearing in the first line we simply change the integration variable from x to $r_0(x)$ with the help of (4.53). In the second line, we first integrate the r_2' term by parts to get a total derivative and a term proportional to r_2; then use the equations of motion (4.53) to show that the coefficients multiplying r_2 and v_2' vanish; the only term remaining is the total derivative $\left(\sqrt{1-r_*^4/r_0^4}\, r_2\right)'$. This is trivially integrated to yield a surface term that can be simplified using the boundary condition (4.52), resulting simply in $2r_2(\ell/2)$. Therefore, the time evolution of the entanglement entropy finally becomes

$$\begin{aligned}\delta S_A(t) &= \epsilon^2 \frac{\ell_\perp}{4G_N}\int_{r_*}^{r_\infty} dr_0\, \frac{\sqrt{r_0^4-r_*^4}}{r_0^4}\left[2r_0^2 h^{(2)}(t-1/r_0,r_0) - f^{(2)}(t-1/r_0,r_0)\right] \\ &\quad +\epsilon^2 \frac{\ell_\perp}{2G_N} r_2(\ell/2) + \mathcal{O}(\epsilon^4)\ . \end{aligned} \tag{4.56}$$

Notice that the integrand in the first line is completely determined once the quench profile J is specified, since the metric coefficients $f^{(2)}$ and $h^{(2)}$ are known from (4.25). The constant r_* is related to the boundary separation ℓ via the analytic expression (4.55)[12]. As we shall see, the contribution of $r_2(\ell/2)$ in the second line will depend on time and therefore must be taken into account into the time evolution of $\delta S_A(t)$.

However, there are two immediate problems with the expression (4.56): the integral in the first line of (4.56) diverges due to the contribution near the boundary $r = r_\infty \to \infty$, as well as the $r_2(\ell/2)$ term diverges due to our boundary conditions, and we need a regularization procedure in order to get a finite result for the entanglement entropy. In practice this can be done by using the large r regulator r_∞ to identify the divergences. Namely, our goal will be to split the entanglement entropy into two contributions: a divergent one, regulated by r_∞, and a finite subleading one (which will be studied in detail), i.e.,

$$\delta S_A(t) = \delta S_{A_{\rm div}}(t) + \delta S_{A_{\rm finite}}(t). \tag{4.57}$$

An alternative way would be to use the renormalized version of the entanglement entropy introduced in [143], but we shall not pursue this here.

We first regulate the term $r_2(\ell/2)$. In order to find the radial profile correction $r_2(x)$ we need to solve the Euler-Lagrange equations for $r_2(x), v_2(x)$ appearing in the functional (4.49). They consist of a complicated set of coupled differential equations involving the order ϵ^2 metric coefficients $f^{(2)}, h^{(2)}$ (and their derivatives) as well as the order ϵ^0 profiles r_0, v_0 found before, which is hardly enlightening to show here. However, since we just need the value of r_2 at $x = \ell/2$ we can solve these equations only for x near $\ell/2$, in which case they simplify considerably. The order 0 radial profile appearing in (4.54) in this regime takes the simple power-law form

$$r_0(x) = \left(\frac{r_*^2}{3y}\right)^{1/3} + \cdots\ , \tag{4.58}$$

where $y \equiv \ell/2 - x \to 0$. By inserting this result in the aforementioned pair of equations and solving

[11] This follows simply from the background AdS spacetime being static, but it can also be seen explicitly from the fact the "Lagrangian" (4.48) does not depend on $v_0(x)$, which according to the solution (4.54)-(4.55) is the only place where t appears.

[12] Even without knowing the explicit solution (4.54) to the equations of motion we still could find the boundary separation ℓ by simply looking at equation (4.53b) as a differential equation for $x(r_0)$ instead of $r_0(x)$, then integrating from $x = 0$ to $x = \ell/2$ and using the boundary conditions $r_0(0) = r_*, r_0(\ell/2) = r_\infty \to \infty$ to get

$$\ell = 2\int_{r_*}^{\infty} \frac{dr}{r^2\sqrt{\frac{r^4}{r_*^4}-1}}\ .$$

perturbatively in y it is easy to find the profile $r_2(x)$ as being

$$\begin{aligned} r_2(x) &= \frac{1}{3}J(t)^2 \ln\left(\frac{3y}{r_*^2}\right)\left(\frac{r_*^2}{3y}\right)^{1/3} + \frac{1}{12}J(t)\dot{J}(t)\left(15+4\ln\frac{r_*^2}{3y}\right)+\cdots \\ &= -J(t)^2 r_0(x)\ln r_0(x) + J(t)\dot{J}(t)\ln r_0(x) + \frac{5}{4}J(t)\dot{J}(t)+\cdots \end{aligned} \tag{4.59}$$

for small y. The first two terms are clearly divergent for $x \to \ell/2$ ($y \to 0$), while the terms in the ellipsis all vanish in this limit. Using the same regulator r_∞ introduced before, i.e., $r_0(\ell/2) = r_\infty$, the value of r_2 at $x = \ell/2$ is then found to be

$$r_2(\ell/2) = -J(t)^2 r_\infty \ln r_\infty + J(t)\dot{J}(t)\ln r_\infty + \frac{5}{4}J(t)\dot{J}(t)\ . \tag{4.60}$$

Now we discuss the regularization of the integral term in (4.56). The divergent part comes from the leading behavior of the metric functions $f^{(2)}$ and $h^{(2)}$ near $r_0 \to \infty$. It follows from expressions (4.25) that the large r_0 behavior of the combination $2r_0^2 h^{(2)} - f^{(2)}$ appearing inside the integral is

$$2r_0^2 h^{(2)}(t-1/r_0, r_0) - f^{(2)}(t-1/r_0, r_0) = \frac{1}{2}r_0^2 J(t)^2 + \cdots\ .$$

Therefore, in order to identify the divergences one just needs to plug this result into the integrand and evaluate the integral with the UV regulator r_∞, namely

$$\begin{aligned} \delta S_{A_{\rm int,div}}(t) &= \epsilon^2 \frac{\ell_\perp}{4G_N}\int_{r_*}^{r_\infty} dr_0\ \frac{\sqrt{r_0^4 - r_*^4}}{r_0^4}\left[\frac{1}{2}r_0^2 J(t)^2\right] \\ &= \epsilon^2\frac{\ell_\perp}{4G_N}\left[\frac{1}{2}J(t)^2 r_\infty\right] + \epsilon^2\frac{\ell_\perp}{4G_N}\left[\frac{\sqrt{\pi}\Gamma(-1/4)}{16\Gamma(5/4)}r_* J(t)^2\right]\ . \end{aligned} \tag{4.61}$$

Therefore, the finite part of the entanglement entropy introduced in (4.57) follows simply from the general expression (4.56) by subtracting the divergent terms (all of them properly identified by the regulator r_∞ in equations (4.60),(4.61)). The final result, written explicitly in terms of the quench profile instead of the metric functions $f^{(2)}, h^{(2)}$, reads

$$\begin{aligned} \delta S_{A_{\rm finite}}(t) &= \epsilon^2\frac{\ell_\perp}{4G_N}\left\{\int_{r_*}^{\infty} dr \frac{\sqrt{r^4 - r_*^4}}{r^2}\left[\frac{J(t-1/r)^2 - J(t)^2}{2} + \frac{J(t-1/r)\dot{J}(t-1/r)}{r}\right.\right. \\ &\left.\left. + \frac{3\dot{J}(t-1/r)^2}{4r^2} + \frac{I(t-1/r)}{r^3}\right] + \frac{\sqrt{\pi}\Gamma(-1/4)}{16\Gamma(5/4)}r_* J(t)^2 + \frac{5}{2}J(t)\dot{J}(t)\right\}, \end{aligned} \tag{4.62}$$

where once again we stress that r_* is related to the boundary separation ℓ via (4.55)[13]. Notice that the integrand naturally vanishes at large r and hence the result of the integral is indeed finite.

In the following we will make a detailed study of this quantity for the two quench profiles of interest as a probe of the quench dynamics. In doing so, it will be convenient to ignore the prefactor of $\ell_\perp/4G_N$ by defining the entanglement entropy density (times $4G_N$) $\delta s_{A_{\rm finite}}(t) \equiv \frac{4G_N}{\ell_\perp}\delta S_{A_{\rm finite}}(t)$.

In Figure **3** we show the time evolution of the entanglement entropy for the tanh quench profile (4.31). For simplicity we fix the value $\epsilon = 0.1$, meaning that the final state Lifshitz theory will have the dynamical exponent $z = 1 + \epsilon^2 = 1.01$.

In part (a) the value of the boundary separation is fixed to be $\ell = 2$ so as to study the effect of the quenching time δt. We recall from the discussion above that the minimal surface penetrates inside

[13]Here we have used a trick in order to extract the finite contribution to the integral in (4.56): instead of calculating the full original integral and then subtracting the divergent piece $\epsilon^2\frac{\ell_\perp}{4G_N}[\frac{1}{2}J(t)^2 r_\infty]$ obtained in (4.61), we equivalently subtract the whole integral in (4.61) and add back separately the constant term coming from the lower limit. In this way, the UV divergence of the integral is cancelled directly in the integrand even before integrating (which is convenient for numerical integration) at the cost of adding back by hand the extra term.

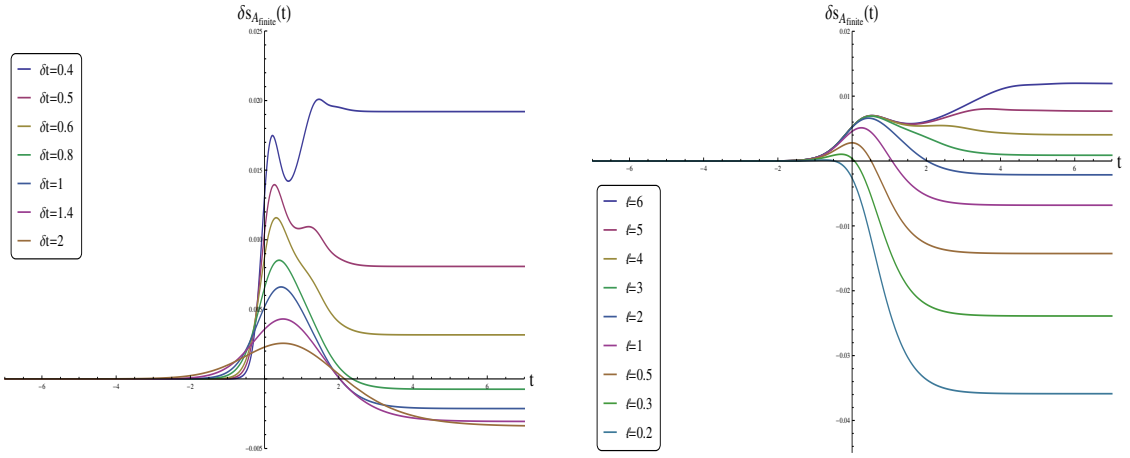

(a) $\ell = 2$ fixed and δt varying

(b) $\delta t = 1$ fixed and ℓ varying

Figure 3: Time evolution of $\delta s_{A_{\text{finite}}}(t) \equiv \frac{4G_N}{\ell_\perp}\delta S_{A_{\text{finite}}}(t)$ for the Tanh quench (4.31). In (a) the boundary separation $\ell = 2$ is fixed and we compare different quenching times δt. The curves go from $\delta t = 0.4$ (top) to 2 (bottom). For $\delta t \lesssim 0.35$ the perturbative solution is expected to break down (for our choice of $\epsilon = 0.1$), so we only show curves for δt above this value. In (b) the quenching time $\delta t = 1$ is fixed and we study the thermalization process at different length scales, from $\ell = 0.2$ (bottom) to $\ell = 6$ (top).

the bulk from $r = \infty$ up to $r_*(\ell)$ given by equation (4.55), which in the case of $\ell = 2$ corresponds to $r_* = 0.599$. This means that one can trust our solution to calculate the entropy with such a value of ℓ as long as the final state Lifshitz black brane forms at r_h sufficiently away from this value[14]. It follows from the definition of r_h that this constrains the quenching time to be $\delta t > 0.37$ (of course this constraint will change for a different ϵ), and for that reason we show in the plot a comparison of many curves with different values of δt only above this value. It can be seen from the plot that despite the quench $J(t)$ being a monotonically increasing function, the time evolution of the (finite part of) entanglement entropy is never monotonic and differs qualitatively depending on the quenching rate δt. Namely, fast enough quenches induce an oscillatory behavior at intermediate times before the thermal state is reached, while slower quenches do not. Increasing the value of δt we see that the equilibration curves become smoother, approaching the adiabatic regime studied in [110]. Remarkably, by comparing the equilibrium value of the entanglement entropy at the Lifshitz point with the initial background value we see that there may be an increase or decrease depending on the quenching time: slow quenches ($\delta t \gtrsim 0.8$) cause an entanglement loss in the process, while for quenches faster than these the amount of entanglement entropy is increased (the faster the quench is, the bigger the gap between the final and initial values becomes).

In part (b) we now fix the quenching time to be $\delta t = 1$ and analyze the thermalization curves for different boundary separations ℓ (i.e., at different energy scales in the boundary gauge theory). Note that with $\epsilon = 0.1$ and $\delta t = 1$ the horizon radius of the final state black hole is fixed at $r_h = 0.11$, so one can trust the calculation for all length scales up to $\ell \simeq 6$ (for which $r_* \sim 2r_h$). It is clear from the figure that the thermalization of the entanglement entropy is a top-down process, i.e., short-scale entanglement entropy equilibrates before its large-distance counterpart. From the dual gauge theory point of view, this result once again suggests that the dynamical breaking of the relativistic scaling symmetry to a Lifshitz symmetry happens faster at short distances (high energies). Another interesting aspect noted from the plot is that the dynamics (as told from the entanglement entropy) is qualitatively different at distinct length scales on the boundary. Namely, at very small distances ($\ell \sim 0.2$) the entropy decreases monotonically in the whole process towards its final value (which is considerably less than the initial one). At larger distances, on the other hand, the dynamics

[14]We will adopt here the convention of $r_* > 2r_h$ for what we mean by "sufficiently away". Thus, in the present case, for example, we demand $r_h \lesssim 0.3$.

becomes non-monotonic, the gap between the final and initial values is decreased, and the value of the entanglement entropy at the Lifshitz point can be even greater than the background one (for $\ell \gtrsim 3$).

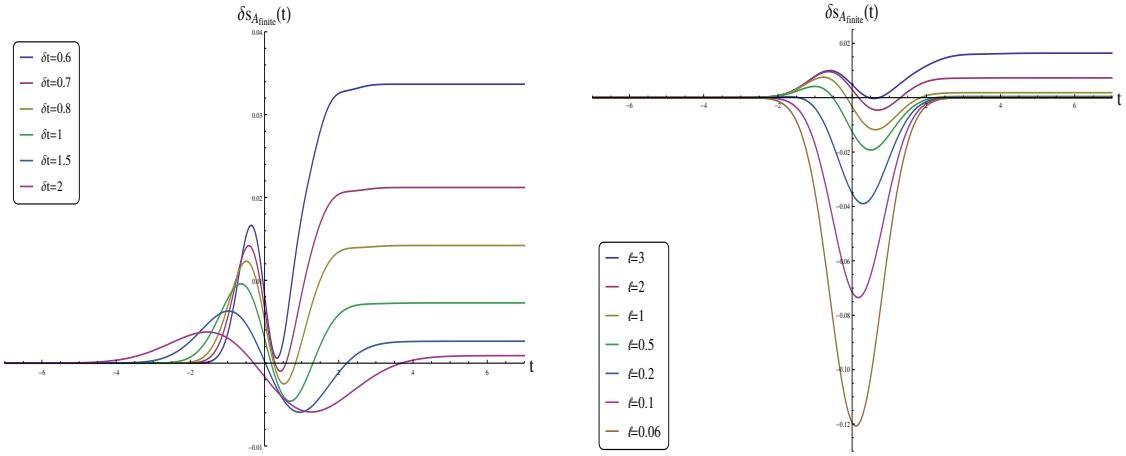

(a) $\ell = 2$ fixed and δt varying

(b) $\delta t = 1$ fixed and ℓ varying

Figure 4: Time evolution of $\delta s_{A_{\text{finite}}}(t) \equiv \frac{4G_N}{\ell_\perp}\delta S_{A_{\text{ren}}}(t)$ for the Gaussian quench (4.34). In (a) the boundary separation $\ell = 2$ is fixed and we compare different quenching times δt. The curves go from $\delta t = 0.6$ (top) to 2 (bottom). For $\delta t \lesssim 0.6$ the perturbative solution is expected to break down (for our choice of $\epsilon = 0.1$), so we only show curves for δt above this value. In (b) the quenching time $\delta t = 1$ is fixed and we study the thermalization process at different length scales, from $\ell = 0.06$ (bottom) to $\ell = 3$ (top).

In Figure **4** we make a similar analysis for the Gaussian quench profile (4.34). Again we use the value $\epsilon = 0.1$, but it should be kept in mind that now this does not correspond to the Lifshitz exponent since in the final state we have an asymptotically AdS black hole. In part (a) the value of the boundary separation is fixed ($\ell = 2$) and the quenching time δt is varied. The regime of validity of our solution now constrains $\delta t \gtrsim 0.6$, which is the reason why we show only curves with δt above this value. We notice from the plot that the time evolution is always non-monotonic, as in the case of Tanh profile analyzed above, but the form of the curves is slightly different. The breaking of the relativistic scaling at intermediate times and its subsequent restoration manifests here as an oscillatory behavior of the entanglement entropy before reaching the final value. An important difference with respect to the Tanh quench previously analyzed is that the final equilibrium value of the entropy is always bigger than the initial one, i.e., there is always an entanglement growth in the process regardless of the value of δt. The quenching time sets the gap between the final and initial values for the entanglement entropy, namely, the gap is larger for faster quenches.

In part (b) it is the quenching time that is fixed to $\delta t = 1$, and we analyze the thermalization curves at different values of ℓ. Note that by choosing $\epsilon = 0.1$ and $\delta t = 1$ the horizon radius of the final state black hole is now fixed at $r_h = (3\sqrt{\pi}\epsilon^2/8\delta t^3)^{1/3} = 0.19$, so one can trust the calculation for all length scales up to $\ell \simeq 3$ (for which $r_* = 0.40 > 2r_h$). We see from the figure the same top-down thermalization observed for the Tanh profile. It is also interesting to notice that at distance scales up to $\ell \simeq 0.5$ the gap between the final and initial values for the entanglement entropy is almost zero. As already discussed, this should not be a surprise since differences between the final state AdS black hole and the pure AdS initial state can only be seen if we probe deep inside the bulk (i.e., for minimal surfaces with large ℓ). In the case of the Tanh quench, where we had a Lishitz black brane in the final state, such a gap had no reason to be small due to the $\ln r$ term in the metric (4.28) which can be sensed even without penetrating deep into the bulk.

We close by noticing from Figures **3** and **4** that $\delta s_{A_{\text{finite}}}$ eventually becomes negative for different combinations of ℓ and δt. However, this is not a problem since it represents only the finite contribution to the entanglement entropy. The full entanglement entropy has an additional divergent contribution

(regulated by the cutoff r_∞) in such a way that it always increases.

4.5 Discussion and Conclusions

We have considered here the problem of holographic quenches leading to a breaking of the standard relativistic scaling symmetry towards a Lifshitz scaling with $z = 1 + \epsilon^2$ ($\epsilon \ll 1$). The quenching operator is (the time component of) a vector operator $\mathcal{V}_t$ with dimension $\Delta = d$, in which case the Lifshitz theory can be understood as a standard deformation of the CFT.

After introducing the perturbative setup in the bulk, we have found (to order ϵ^2) the gravity solution describing the quench dynamics and discussed its regime of validity. In particular, this regime excludes the case of infinitely fast quenches. The solution interpolates between AdS space at past infinity and an asymptotically Lifshitz black hole at future infinity. This means that the corresponding non-relativistic dual field theory appearing at the end state is always at finite temperature or, conversely, that it is impossible to reach the vacuum state of the Lifshitz theory from the CFT vacuum using the continuous quench mechanism proposed here. This is the main result of the present Chapter.

We have also probed the nonequilibrium dynamics following the breaking of the relativistic scaling using both local (the apparent and event horizons) and non-local (the entanglement entropy) observables. Both horizons were shown to be monotonically increasing functions of time, with the apparent horizon being inside the event horizon during the whole process, agreeing with what is expected for physically reasonable collapse processes. The time evolution of the entanglement entropy was studied at different length scales ℓ at the boundary and for different values of the quenching rate δt. Specifically, we have concluded that the equilibration is a top-down process, i.e., the symmetry breaking takes place faster for UV modes than for low energy modes. In addition, the curves are slightly different depending on the value of δt and the gap between the final and initial values is bigger for faster quenches.

The present results can be generalized in many ways, such as changing the number of dimensions (we used $d = 3$ for the boundary theory) or the quench profile. More interesting generalizations to pursue are the inclusion of a hyperscaling violation parameter or the study of quenches in the Schrödinger background (in this case reference [129] may be helpful), which we leave for a future work.

Chapter 5

Expanding plasmas from Anti de Sitter black holes

In the present Chapter we propose a new analytical approach to the nonequilibrium dynamics of CFT plasmas using holography. The underlying idea is quite simple, namely, instead of directly worrying about the real-time dynamics of the strongly coupled finite T plasma, we consider as a toy model a locally static plasma placed in background spacetime that expands itself. Of course such a simplification is likely to ignore quantitative aspects of the real-world dynamics but, on the other hand, the possibility of analytically approach dynamical aspects of a strongly coupled plasma may offer important physical insights that compensate part of this ignorance.

Specifically, we consider a 4-dimensional CFT plasma defined in a Friedmann-Lemaître-Robertson-Walker (FLRW) spacetime with scale factor $a(t)$ as a toy model for its nonequilibrium dynamics. More than that, we propose to describe this toy model from a dual gravitational point of view using the AdS/CFT correspondence. This recquires constructing a new slicing of AdS_5 black holes such that the conformal boundary of AdS takes the form of a 4-dimensional FLRW spacetime with scale factor $a(t)$ (instead of the standard flat spacetime). We show that this task becomes feasible (in fact, it becomes very simple) if one employs Eddington-Finkelstein coordinates to describe the bulk spacetime, and the results are applicable to a wide class of AdS black holes. The holographic dual picture of a CFT plasma on a FLRW background provides an interesting prototype to gain insight into the nonequilibrium dynamics of expanding plasmas, as illustrated by extracting the renormalized energy-momentum tensor of the dual plasma for three representative black holes of interest. In particular, by studying a charged AdS-Reissner-Nördstrom black hole we show that the dynamics experienced by a CFT plasma subject to a quench in the chemical potential (i.e., a time-dependent chemical potential) resembles a cosmological evolution with the scale factor being inversely related to the quench profile, i.e., $a(t) \sim \mu(t)^{-1}$.

The results shown in this Chapter have been published as [144]

Expanding plasmas from Anti de Sitter black holes,
G. Camilo, Eur. Phys. J. C **76** (2016) 682,

and the exposition below makes substantial use of the published text, including literal transcriptions.

5.1 Introduction

The Friedmann-Lemaître-Robertson-Walker (FLRW) metric corresponds to the most general spacetime exhibiting spatial homogeneity and isotropy. In 4 dimensions the metric can be written as

$$ds^2 = -dt^2 + a(t)^2 d\Omega_k^2 \ , \tag{5.1}$$

where $a(t)$ is called the scale factor and $d\Omega_k^2 = \frac{d\rho^2}{1-k\rho^2} + \rho^2(d\theta^2 + \sin^2\theta d\phi^2)$ is the 3-dimensional spatial metric of a constant curvature space. The spatial curvature k can be positive, negative, or zero, and without loss of generality we can set its possible values to be $k = +1, 0, -1$ corresponding to a unit sphere, Euclidean space, or unit hyperbolic space, respectively. The FLRW metric describes an expanding (contracting) spacetime provided that $a(t)$ is a monotonically increasing (decreasing) function. It is largely used in cosmology due to the observation that our universe is homogeneous and isotropic (with $k = 0$) in cosmological scales [145].

The FLRW spacetime also provides a good prototype to approach the nonequilibrium dynamics of an expanding system. It is well known, for instance, that even a locally static fluid flow characterized by the 4-velocity $u^\mu = (1, 0, 0, 0)$ in the FLRW metric has a nonvanishing expansion rate $\nabla_\mu u^\mu = 3H(t)$ ($H(t) \equiv \frac{\dot{a}(t)}{a(t)}$ is the so-called Hubble parameter) due to the dynamical nature of the geometry itself. In spite of the time dependence, the high degree of spatial symmetry of the metric may render certain problems technically feasible. An interesting example is [146], where an analytical solution to the general relativistic Boltzmann equation in FLRW has been found describing the dynamics of an expanding massless gas with constant cross section.

In the present Chapter we use an expanding FLRW spacetime as the background arena where we study a strongly coupled field theory plasma. In particular, we shall focus on a conformal field theory (CFT) with a holographic dual and resort to gauge/gravity duality methods in order to extract information about the expanding CFT plasma. An advantage of the holographic approach is that non-equilibrium quantities of the expanding plasma such as the entropy density can be naturally associated with the gravitational entropy of the apparent horizon on the gravity side [147]. The crucial step here involves setting the Anti de Sitter (AdS) conformal boundary to take a FLRW form instead of the commonly used static boundaries. This is in principle possible since the boundary metric belongs to a conformal class, and one can switch between members of this class by appropriate bulk diffeomorphisms.

Previous efforts in this direction have been made in [148] (see also [149, 150, 151]) using Fefferman-Graham coordinates, but were restricted basically to pure Einstein gravity in the bulk. We propose here a different foliation of AdS_5 black hole spacetimes using Eddington-Finkelstein-like coordinates such that the asymptotic boundary becomes the 4-dimensional FLRW spacetime. The holographic dual picture is, therefore, that of a thermalized CFT on an expanding background, even though the bulk solution is not truly dynamical. The procedure is simple and applies equally well to a variety of AdS black holes, supported by external fields or not, leading to the same results of [148] when applied to the AdS-Schwarzschild solution.

5.2 AdS black holes with a FLRW boundary

We begin with a generic asymptotically AdS_5 black hole written in the usual form

$$ds^2 = -f(r)dt^2 + f(r)^{-1}dr^2 + \Sigma(r)^2 d\Omega_k^2 \,, \tag{5.2}$$

where $d\Omega_k^2$ denotes the metric of the horizon, corresponding to a spherical, planar, or hyperbolic horizon for $k = +1, 0, -1$ respectively. The blackening factor $f(r)$ and the function $\Sigma(r)$ are left completely general with the only assumption that $f(r) \sim \frac{r^2}{L^2}$ and $\Sigma(r) \sim \frac{r}{L}$ for large r, as required in order to have AdS asymptotics with curvature radius L.[1] The event horizon r_h is defined by (the largest root of) $f(r_h) = 0$ and the corresponding Hawking temperature is $T = |f'(r_h)|/4\pi$. There may eventually be matter fields supporting the geometry, but for our purposes at this section they will play no role.

The first step involves going to the so-called ingoing Eddington-Finkelstein coordinates (v, r). This is done by trading the time coordinate t to a new coordinate v adapted to ingoing null geodesics,

[1] Of course the zero temperature cases of Poincaré and global AdS are also included in this class and, incidentally, will be included in our analysis. However, we shall ignore them since we are interested only in CFTs at finite T.

which is defined by $dv = dt + f(r)^{-1}dr$. The metric then reads

$$ds^2 = 2dvdr - f(r)dv^2 + \Sigma(r)^2 d\Omega_k^2 \ . \tag{5.3}$$

Notice that the large r behavior of the metric is $ds^2 \sim 2dvdr + \frac{r^2}{L^2}[-dv^2 + d\Omega_k^2]$, from where it is clear that the 4-dimensional conformal boundary at $r = \infty$ (where the dual CFT lives) is the Einstein static universe $\mathbb{R} \times \Sigma_k$ with metric[2]

$$ds_0^2 = g_{\mu\nu}^{(0)} dx^\mu dx^\nu = -dt^2 + d\Omega_k^2 \ . \tag{5.4}$$

When $k = 0$ this is just the 4-dimensional Minkowski spacetime, which is by far the most studied one in holographic applications since most field theories of physical interest live in flat spacetime. In spite of that, for the sake of completeness we shall keep the spatial curvature k arbitrary in the sequence.

Before proceeding it is instructive to recall a simple reason why the AdS conformal boundary indeed goes well with the intuitive notion of a boundary. This can be seen by calculating the time interval $\Delta v(r_0)$ spent by an outgoing light ray to travel radially from $r_0 > r_h$ to the boundary at $r = \infty$ and back to r_0. It follows immediately from the definition of outgoing null geodesics in (5.3), $2dr - f(r)dv = 0$, that

$$\Delta v(r_0) = 4 \int_{r_0}^{\infty} \frac{dr'}{f(r')} < \infty \ , \tag{5.5}$$

which is obviously finite since there are no poles in the denominator for $r_0 > r_h$ and the integrand vanishes at large r'.

In the following we shall introduce a different foliation of the black hole spacetime (5.3) in such a way that the corresponding conformal boundary takes the form of a FLRW spacetime, namely

$$ds_0^2 = g_{\mu\nu}^{(0)} dx^\mu dx^\nu = -dt^2 + a(t)^2 d\Omega_k^2 \ . \tag{5.6}$$

In order to achieve that one needs two further coordinate transformations. We first define a new time coordinate V with respect to which the old v is a "conformal time" with scale factor $a(V)$, i.e., $dv = \frac{dV}{a(V)}$, where $a(V)$ is assumed to be everywhere continuous and non-vanishing. Finally, we introduce a new radial coordinate R defined as $R = \frac{r}{a(V)}$. After plugging $dv = \frac{dV}{a}$ and $dr = a(V)dR + R\dot{a}(V)dV$ the metric (5.3) becomes

$$\begin{aligned} ds^2 &= 2\frac{dV}{a}(adR + R\dot{a}dV) - f(Ra)\frac{dV^2}{a^2} + \Sigma(Ra)^2 d\Omega_k^2 \\ &= 2dVdR - \left[\frac{f(Ra)}{a^2} - 2R\frac{\dot{a}}{a}\right] dV^2 + \Sigma(Ra)^2 d\Omega_k^2 \end{aligned} \tag{5.7}$$

This form is the one we are interested in this work. Note that the metric is still expressed in Eddington-Finkelstein-like coordinates (in the sense that V is still adapted to null geodesics), but now it carries an artificial time dependence reminiscent of the transformation from v to V. At large R we have $f(Ra) \sim \frac{(Ra)^2}{L^2}$ and $\Sigma(Ra) \sim \frac{Ra}{L}$ due to our assumption of AdS asymptotics, and, therefore,

$$ds^2 \sim 2dVdR + \frac{R^2}{L^2}[-dV^2 + a(V)^2 d\Omega_k^2] \ .$$

As a result, the new conformal boundary at $R = \infty$ has precisely the desired FLRW form (5.6) with spatial curvature k (the time coordinate is now called V). We shall refer to this as the *cosmological boundary* just to remind that this is not the same as the commonly used AdS boundary at $r = \infty$.

Actually we shall pause for a moment here to argue that the cosmological boundary introduced above is indeed also compatible with the notion of a boundary. This is done by asking the same question asked previously for the AdS boundary, namely whether the time interval $\Delta V(R_0)$ spent by

[2]The time coordinates v and t coincide at fixed-r surfaces.

an outgoing light ray to go radially from R_0 to ∞ and back to R_0 in the metric (5.7) is finite or not. The outgoing null geodesics in this case satisfy

$$\frac{dR}{dV} = \frac{1}{2}\left[\frac{f(Ra)}{a^2} - 2R\frac{\dot{a}}{a}\right] = \frac{1}{2}\left[\frac{R^2}{L^2} - 2R\frac{\dot{a}}{a} + \cdots\right] . \tag{5.8}$$

For simplicity we focus on the case of pure AdS space ($f(r) = \frac{r^2}{L^2}$), without loss of generality since this corresponds to the asymptotic structure of any AdS black hole. In this case the ellipsis in the previous expression is not present and it can be exactly integrated to yield

$$R(V) = \frac{R_0 a_0}{a(V)\left[1 - \frac{R_0 a_0}{2L^2}\int_{V_0}^{V}\frac{dV'}{a(V')}\right]} , \tag{5.9}$$

where we have introduced $R_0 \equiv R(V_0)$ and $a_0 \equiv a(V_0)$. The time V_∞ corresponding to reaching the cosmological boundary $R = \infty$ is implicitly defined by

$$\frac{R_0 a_0}{2L^2}\int_{V_0}^{V_\infty}\frac{dV'}{a(V')} = 1 . \tag{5.10}$$

A straightforward consequence of our assumption that the scale factor $a(V)$ is a continuous and everywhere non-vanishing function is that V_∞ must be finite (although an explicit expression for it cannot be obtained without specifying the form of the scale factor). As a result, the time interval $\Delta V(R_0) = 2(V_\infty - V_0)$ is guaranteed to be finite and, therefore, $R = \infty$ also provides a sensible notion of asymptotic boundary.

To summarize, we have introduced a different type of foliation for 5-dimensional AdS black hole spacetimes of the form (5.2) where the 4-dimensional slices asymptotically approach the FLRW metric. This is very similar to the work done in [148]. It should be stressed, however, that our procedure is astonishingly simpler and, in particular, our metric (5.7) applies equally well for any AdS black hole (characterized by the functions f, Σ and eventually matter fields[3]), as we shall illustrate in the sequence, while the method of [148] is hardly applicable beyond the simplest case of the AdS-Schwarzschild solution.

5.2.1 Entropy production

We begin our analysis by finding the location of the apparent horizon in our FLRW-foliated black hole metric (5.7). The apparent horizon is formally defined as the outermost trapped surface, i.e., the closed null hypersurface on which all radially outgoing null geodesics have vanishing expansion (see e.g. [140]). For a generic 5-dimensional metric of the form

$$ds^2 = 2dVdR - \alpha(V,R)dV^2 + \beta(V,R)^2 d\Omega_k^2$$

the expansion along outgoing null rays is given by $\theta_{\text{out}} \equiv \left(\partial_V + \frac{\alpha}{2}\partial_R\right)\ln\beta^3$ and the apparent horizon hence corresponds to the location $R_h(V)$ for which $\theta_{\text{out}} = 0$. For the case of interest (5.7), with $\alpha(V,R) = \frac{f(Ra)}{a^2} - 2R\frac{\dot{a}}{a}$ and $\beta(V,R) = \Sigma(Ra)$, the result is

$$\left[\partial_V\Sigma + \left(\frac{f(Ra)}{2a^2} - R\frac{\dot{a}}{a}\right)\partial_R\Sigma\right]\Bigg|_{R=R_h} = 0 . \tag{5.11}$$

However, since Σ only depends on (V,R) through the combination $Ra(V)$, one can write $\partial_V\Sigma(Ra) = R\dot{a}\Sigma'(Ra)$, $\partial_R\Sigma(Ra) = a\Sigma'(Ra)$ (here a prime denotes the derivative with respect to the argument Ra) and, therefore, the definition of R_h reduces to

$$f(R_h a)\Sigma'(R_h a) = 0 . \tag{5.12}$$

[3]Of course matter fields when present must be changed according to the same coordinate transformations above to take a different (V,R)-dependent configuration that supports the FLRW-foliated metric (5.7). This is the case, e.g., for the AdS-Reissner-Nordström charged black hole (see Section 5.3).

For most black hole solutions of interest, which have $\Sigma(r) = \frac{r}{L}$ (see next section), the equation above gives simply $f(R_h a) = 0$ or, equivalently, $R_h(V) = \frac{r_h}{a(V)}$, where the constant r_h denotes the black hole event horizon in the standard coordinate system (5.3) (i.e., $f(r_h) = 0$). Nevertheless, if $\Sigma(r)$ has subleading contributions in r of any kind such that $\Sigma'(r)$ is not constant, there may appear an additional horizon corresponding to $\Sigma'(R_h a) = 0$.

Having determined its location, we now follow [147] and associate the non-equilibrium entropy density s of the expanding plasma living at the cosmological boundary with the Bekenstein-Hawking entropy of the apparent horizon, namely

$$s = \frac{\Sigma(R_h a)^3}{4G_5} \ . \tag{5.13}$$

From this it follows that, if $R_h = \frac{r_h}{a}$ is the only apparent horizon, then clearly

$$\frac{ds}{dV} = 0 \ , \tag{5.14}$$

i.e., there is no entropy production by the plasma during the dynamical process. This matches the expectation from the hydrodynamics of conformally invariant fluids, for which there is no entropy production at all orders in the hydrodynamic expansion (see [152]). However, if the bulk solution admits another apparent horizon corresponding to the root of $\Sigma'(R_h a)$, then there may be a nonzero entropy production by the plasma since the combination $R_h a$ on which s depends will not necessarily be constant anymore. This is the case, for instance, for the $\mathcal{N} = 2^*$ plasma studied in [152].

Similarly, one can associate to the expanding plasma the local temperature

$$T(V) = \frac{T_H}{a(V)} \ , \tag{5.15}$$

where T_H is the temperature of the corresponding static plasma (i.e., the Hawking temperature of the black hole). As argued in [148], this follows from the fact that the FLRW metric (5.6) and the static boundary metric (5.4) are connected by a Weyl rescaling, i.e., $ds^2_{\text{FLRW}} = a(\eta)^2 ds_0^2$ where $\eta \equiv \int \frac{dt}{a}$ is the conformal time. As a result, the local temperature of the plasma in FLRW and the equilibrium temperature T_H of the static plasma must be linked by a rescaling. Since the Euclidean proper time period in FLRW scales as a according to the formula above, the temperature of the expanding plasma, being inversely related to the period, must scale as a^{-1} with respect to T_H. Another way to see that is to recall that our new slicing does not change the physical content of the bulk solution, i.e., we still have the same static AdS black hole in thermal equilibrium with its Hawking radiation at temperature T_H. The difference now is that we have a new notion of boundary ($R = \infty$) that expands in time according to the scale factor $a(V)$, and a comoving observer sitting in there will experience a temperature appropriately corrected by a that corresponds precisely to (5.15).

5.2.2 One-point functions

We now follow the spirit of [148] and, by assuming that *i)* the cosmological boundary is holographic; *ii)* the standard holographic renormalization procedure can be carried out in the same way in there as in the usual AdS boundary, we proceed to calculate the one-point functions for the dual CFT operators living in the cosmological boundary, i.e., for CFTs in FLRW spacetime.

The first step involved is to find the Fefferman-Graham (FG) expansion of the bulk metric (and eventually matter fields) near the cosmological boundary, since knowledge of the FG coefficients determines the CFT correlators via the holographic dictionary. Namely, we need to put the metric (5.7) in the FG form

$$ds^2 = \frac{L^2}{z^2}\left[dz^2 + g_{\mu\nu}(z,x)dx^\mu dx^\nu\right] \tag{5.16}$$

(here $z \sim L^2/R$ such that the cosmological boundary is, in these coordinates, at $z = 0$) and find the first few coefficients of the near boundary expansion of $g_{\mu\nu}$,

$$g_{\mu\nu}(z,x) \;=\; g^{(0)}_{\mu\nu}(x) + z^2 g^{(2)}_{\mu\nu}(x) + z^4\big(g^{(4)}_{\mu\nu}(x) + h^{(4)}_{\mu\nu}(x)\log z\big) + \cdots \;, \tag{5.17}$$

where the leading one, $g^{(0)}_{\mu\nu}(x)$, is the FLRW metric (5.6), and the subleading ones are determined by the bulk equations of motion. A practical way to achieve that is to write generic coordinate transformations from (V, R) to FG coordinates $(x^0 \equiv \tau, z)$, i.e., $V = V(\tau, z)$ and $R = R(\tau, z)$, and then get the transformation equations by comparing our metric (5.7) with (5.16). This leads to the following set of equations

$$\begin{aligned} 2\partial_z R\partial_z V - \alpha(\partial_z V)^2 &= \frac{L^2}{z^2} \\ \partial_z V\partial_\tau R + \partial_\tau V\partial_z R - \alpha\partial_z V\partial_\tau V &= 0 \;, \end{aligned} \tag{5.18}$$

which determine the precise form of the transformations, together with the FG metric components expressed in terms of V and R, which can be massaged to take the simple form

$$g_{\tau\tau} = -\frac{(\partial_\tau V)^2}{(\partial_z V)^2} \qquad g_{ij}dx^i dx^j = \frac{z^2}{L^2}\Sigma^2 d\Omega_k^2 \qquad g_{\tau i} = 0 \;. \tag{5.19}$$

The near-boundary solution to the transformation equations (5.18) can be easily obtained to any desired order with a power series ansatz of the form

$$V(\tau,z) = \sum_{n=0} V_n(\tau) z^n \qquad R(\tau,z) = \sum_{n=0} R_n(\tau) z^{n-1} \tag{5.20}$$

with $V_0(\tau) \equiv \tau$ (such that V and τ coincide at the boundary) and $R_0(\tau) \equiv L^2$ (such that $R = \frac{L^2}{z} + \cdots$). Once this solution is found, by plugging it back into (5.19) and expanding for small z yields the desired FG asymptotic expansion (5.17). One is then ready to obtain the corresponding one-point functions of the dual CFT living on the cosmological boundary using standard holographic renormalization.

So far the analysis has been quite general. We shall now illustrate the procedure by particularizing the functions $f(r), \Sigma(r)$ to a few black holes of physical interest.

5.3 Examples

5.3.1 AdS-Schwarzschild black hole

The AdS-Schwarzschild black hole is an exact static solution to pure Einstein gravity with a negative cosmological constant $\Lambda = -12/L^2$ in the bulk, namely

$$S = \frac{1}{16\pi G_5}\int d^5x\sqrt{-g}\left[R + \frac{12}{L^2}\right]. \tag{5.21}$$

The solution with horizon curvature k corresponds to a metric of the form (5.2) with $f(r)$ and $\Sigma(r)$ given by

$$f(r) = \frac{r^2}{L^2}\left(1 + \frac{kL^2}{r^2} - \frac{M}{r^4}\right) \qquad \Sigma(r) = \frac{r}{L} \;, \tag{5.22}$$

where the mass M is related to the event horizon radius r_h according to $M = r_h^4\left(1 + \frac{kL^2}{r_h^2}\right)$. Its corresponding Hawking temperature is readily found to be

$$T_H = \frac{kL^2 + 2r_h^2}{2\pi L^2 r_h} \;. \tag{5.23}$$

The explicit form of the foliation (5.7) for the AdS-Schwarzschild black hole reads

$$ds^2 = 2dVdR - \left[\frac{R^2}{L^2}\left(1+\frac{kL^2}{R^2a^2}-\frac{M}{R^4a^4}\right) - 2R\frac{\dot{a}}{a}\right]dV^2 + \frac{R^2a^2}{L^2}d\Omega_k^2 \ . \tag{5.24}$$

If the standard holographic dictionary extrapolates to the cosmological boundary $R=\infty$, this metric would be the holographic dual of a $\mathcal{N}=4$ SYM plasma in the FLRW metric (5.6) with spatial curvature k. As discussed in Section 5.2.1, one can associate to this nonequilibrium plasma the local temperature (5.15), namely

$$T(V) = \frac{kL^2+2r_h^2}{2\pi L^2 r_h a} \ . \tag{5.25}$$

In the following for the sake of simplicity we take $L=1$.

It is worth mentioning that the metric above in the planar case ($k=0$) has been previously used by the authors of [152] as the starting point to study the $\mathcal{N}=2^*$ plasma close to conformality in a FLRW spacetime.[4]

The transformation (5.20) from our (V,R) coordinates to the Fefferman-Graham system (τ,z) is given asymptotically by

$$\begin{aligned}
V(\tau,z) &= \tau - z + \frac{-2a\ddot{a}+\dot{a}^2+k}{12a^2}z^3 + \frac{a^2\dddot{a}+\dot{a}^3+\dot{a}\,(k-2a\ddot{a})}{24a^3}z^4 \\
&\quad + \frac{3\dot{a}^4 - 2a^{(4)}a^3 - 3\left(k^2+6M\right) + 2a\ddot{a}\left(5k-\dot{a}^2\right) + a^2\left(6\dddot{a}\,\dot{a}-8\ddot{a}^2\right)}{240a^4}z^5 + \cdots \\
R(\tau,z) &= \frac{1}{z} + \frac{\dot{a}}{a} - \frac{2a\ddot{a}-3\dot{a}^2+k}{4a^2}z + \frac{a^2\dddot{a}+4\dot{a}^3-\dot{a}\,(5a\ddot{a}+2k)}{6a^3}z^2 \\
&\quad + \frac{13\dot{a}^4 - a^3a^{(4)} - 11k\dot{a}^2 + a\ddot{a}\left(5k-21\dot{a}^2\right) + a^2\left(2\ddot{a}^2+7\dddot{a}\,\dot{a}\right) + 3M}{24a^4}z^3 + \cdots
\end{aligned} \tag{5.26}$$

with a and its derivatives now viewed as functions of τ. From (5.19) it then follows that the Fefferman-Graham expansion (5.17) of the metric in this case has the following non-null coefficients

$$\begin{aligned}
g^{(0)}_{\tau\tau} &= -1 \\
g^{(2)}_{\tau\tau} &= -\frac{\dot{a}^2-2a\ddot{a}+k}{2a^2} \\
g^{(4)}_{\tau\tau} &= -\frac{\dot{a}^4+4a^2\ddot{a}^2+2\dot{a}^2(k-2a\ddot{a})-4ka\ddot{a}+k^2-12M}{16a^4} \\
g^{(0)}_{ij}dx^idx^j &= a^2d\Omega_k^2 \\
g^{(2)}_{ij}dx^idx^j &= -\frac{\dot{a}^2+k}{2}d\Omega_k^2 \\
g^{(4)}_{ij}dx^idx^j &= \frac{2k\dot{a}^2+\dot{a}^4+k^2+4M}{16a^2}d\Omega_k^2 \ .
\end{aligned} \tag{5.27}$$

The holographic renormalization for pure Einstein gravity in the bulk has been done in [153], to which we refer the reader for details. The resulting expression for the renormalized energy-momentum tensor of the dual CFT living on the boundary with metric $g^{(0)}$ is generically given by

$$\langle T_{\mu\nu}\rangle = \frac{1}{4\pi G_5}\left\{g^{(4)}_{\mu\nu} - \frac{1}{2}g^{(2)\sigma}_{\mu}g^{(2)}_{\sigma\nu} + \frac{1}{4}\big(g^{(2)\sigma}_{\sigma}\big)g^{(2)}_{\mu\nu} - \frac{1}{8}\big[\big(g^{(2)\sigma}_{\sigma}\big)^2 - g^{(2)}_{\sigma\rho}g^{(2)\rho\sigma}\big]g^{(0)}_{\mu\nu}\right\} \ , \tag{5.28}$$

where indices are to be raised and lowered with the boundary metric $g^{(0)}$. In our case, with the FG coefficients (5.27), this yields the following energy density $\mathcal{E}\equiv\langle T_{\tau\tau}\rangle$ and pressure $\mathcal{P}\equiv\langle T^i_{\ i}\rangle$ (no

[4] We emphasize that, although not obvious, this is nothing but AdS-Schwarzschild expressed in unusual coordinates.

summation over i implied) for the $\mathcal{N}=4$ SYM plasma

$$\begin{aligned}\mathcal{E} &= \frac{3(\dot{a}^2+k)^2+12M}{64\pi G_5 a^4} \\ \mathcal{P} &= \frac{(\dot{a}^2+k)^2+4M-4a\ddot{a}(\dot{a}^2+k)}{64\pi G_5 a^4}\,,\end{aligned} \tag{5.29}$$

in perfect agreement with the results of [148]. These expressions can be cast entirely in 4-dimensional CFT language by expressing the mass parameter $M=r_h^4\left(1+\frac{kL^2}{r_h^2}\right)$ in terms of the local temperature T of the plasma using (5.25) and the 5-dimensional Newton constant G_5 in terms of the number of colors N_c via the standard $\mathrm{AdS}_5/\mathrm{CFT}_4$ relation $G_5=\frac{\pi L^3}{2N_c^2}$. For instance, in the $k=0$ case, with $M=(\pi aT)^4$ we obtain

$$\begin{aligned}\mathcal{E} &= \frac{3N_c^2T^4}{8}+\frac{3N_c^2}{32\pi^2}\frac{\dot{a}^4}{a^4} \\ \mathcal{P} &= \frac{\mathcal{E}}{3}-\frac{N_c^2}{8\pi^2}\frac{\ddot{a}\dot{a}^2}{a^3}\,.\end{aligned} \tag{5.30}$$

It interesting to note that when $a(V)\equiv 1$ (where $R=\infty$ becomes the usual AdS boundary $r=\infty$) we get the expected conformal plasma in $\mathbb{R}\times\Sigma_k$ with $\mathcal{E}=3\mathcal{P}$, while the presence of a non-constant scale factor breaks the conformal invariance leading to a conformal anomaly given by

$$\langle T^{\mu}_{\ \mu}\rangle = 3\mathcal{P}-\mathcal{E} = -\frac{3\ddot{a}(\dot{a}^2+k)}{16\pi G_5 a^3}\,. \tag{5.31}$$

The anomaly has a clearly geometric nature due exclusively to the nontrivial rate of cosmological expansion. For an expanding plasma ($\ddot{a}>0$) in flat space or in a sphere this quantity is strictly negative.

5.3.2 AdS-Gauss-Bonnet black hole

We start by reviewing the Einstein-Gauss-Bonnet action in 5 dimensions. It consists in one of the simplest generalizations of Einstein gravity built from higher derivative terms in the action that still yield second order equations of motion for the metric.[5] With the inclusion of a negative cosmological constant $\Lambda\equiv -12/L^2$, the action is

$$S = \frac{1}{16\pi G_5}\int d^5x\sqrt{-g}\Big[R+\frac{12}{L^2}+\frac{L^2}{2}\lambda_{\rm GB}(R_{abcd}R^{abcd}-4R_{ab}R^{ab}+R^2)\Big], \tag{5.32}$$

where $\lambda_{\rm GB}$ is the Gauss-Bonnet parameter. It is still unclear at the moment whether a higher curvature correction of the Gauss-Bonnet type (5.32) can be obtained from a top-down string theory construction: the leading α' corrections to the action of Type IIB supergravity, corresponding to finite 't Hooft coupling corrections to the dual $\mathcal{N}=4$ SYM theory, are known to take the form of more complicated higher curvature terms schematically of the form α'^3R^3 [155]. Nevertheless, the general belief is that it may provide qualitative information into properties shared by generic higher curvature terms, with the practical advantages of being tractable and having a number of exact solutions available in the literature.

The action (5.32) has been extensively studied in the context of holography. Interestingly, the presence of the extra Gauss-Bonnet coupling $\lambda_{\rm GB}$ in the bulk allows for a holographic dual CFT with

[5] In fact, the Einstein-Gauss-Bonnet action is just a very special case of the so-called *Lovelock gravity*, which is the most general metric theory of gravity giving rise to second order equations of motion (see [154] for a review).

two distinct central charges $c \neq b$ [156, 157].[6] Namely, the central charges, defined in the standard way via the conformal anomaly as

$$\langle T^{\mu}_{\ \mu} \rangle = \frac{1}{16\pi^2}(cW - bE) \ , \tag{5.33}$$

are related to $\lambda_{\rm GB}$ and the other gravitational parameters via [158]

$$\begin{aligned} c &= \frac{\pi L^3_{\rm AdS}}{8G_5}\sqrt{1-4\lambda_{\rm GB}} \\ b &= \frac{\pi L^3_{\rm AdS}}{8G_5}\left(-2+3\sqrt{1-4\lambda_{\rm GB}}\right) . \end{aligned} \tag{5.34}$$

The AdS radius appearing above depends on $\lambda_{\rm GB}$ (see below for details), while the quantities $W \equiv W_{\mu\nu\rho\sigma}W^{\mu\nu\rho\sigma}$ and $E \equiv \mathcal{R}_{\mu\nu\sigma\rho}\mathcal{R}^{\mu\nu\sigma\rho} - 4\mathcal{R}_{\mu\nu}\mathcal{R}^{\mu\nu} + \mathcal{R}^2$ are respectively the squared Weyl tensor and the Euler density associated with the 4-dimensional metric where the CFT lives. In the Einstein gravity limit $\lambda_{\rm GB} = 0$ the two central charges collapse to a single one $c = b \sim N_c^2$ and the $SU(N_c)$ $\mathcal{N} = 4$ SYM theory is recovered consistently.

The AdS-Gauss-Bonnet black hole with horizon curvature k is an exact static spherically symmetric solution to the equations of motion of (5.32), first obtained in [159]. The metric has the standard black hole form (5.3) with

$$\begin{aligned} f(r) &= k + \frac{r^2}{2L^2\lambda_{\rm GB}}\left[1 - \sqrt{1-4\lambda_{\rm GB}\left(1-\frac{ML^2}{r^4}\right)}\ \right] \\ \Sigma(r) &= \frac{r}{L} \ , \end{aligned} \tag{5.35}$$

where M is a parameter related to the black hole mass that can be conveniently expressed in terms of the event horizon location r_h as

$$M \equiv r_h^4\left(\frac{1}{L^2} + \frac{k}{r_h^2} + \lambda_{\rm GB}\frac{L^2k^2}{r_h^4}\right) \ .$$

The Hawking temperature associated to this solution reads

$$T_H = \frac{r_h(2r_h^2 + kL^2)}{2\pi L^2(r_h^2 + 2kL^2\lambda_{\rm GB})} \ . \tag{5.36}$$

It is worth noticing that the AdS-Gauss-Bonnet is an asymptotically AdS black hole, i.e., $f(r) \sim \frac{r^2}{L^2_{\rm AdS}}$ for large r. However, the AdS curvature radius is shifted from the usual L to an effective radius $L_{\rm AdS}$ due to the presence of $\lambda_{\rm GB}$, namely $L^2_{\rm AdS} \equiv \frac{L^2}{2}(1+\sqrt{1-4\lambda_{\rm GB}})$. In particular, when the standard choice of units $L = 1$ is made (which corresponds to making the cosmological constant $\Lambda = -12$) it should be kept in mind that the resulting AdS radius appearing in the metric is not unity.

Our FLRW foliation (5.7) of the AdS-Gauss-Bonnet black hole metric takes the form

$$ds^2 = 2dVdR + \frac{R^2a^2}{L^2_{\rm eff}}d\Omega_k^2 - \left\{\frac{k}{a^2} + \frac{R^2}{2L^2\lambda_{\rm GB}}\left[1-\sqrt{1-4\lambda_{\rm GB}\left(1-\frac{ML^2}{R^4a^4}\right)}\right] - 2R\frac{\dot{a}}{a}\right\}dV^2 \tag{5.37}$$

where the spatial coordinates were conveniently redefined by appropriate factors so as to make $\frac{d\Omega_k^2}{L^2} \to \frac{d\Omega_k^2}{L^2_{\rm AdS}}$ and, hence, have a canonically normalized FLRW boundary of the form (5.6). Just as in the

[6] We denote here the second central charge by b instead of the commonly used a in order to avoid confusion with the scale factor $a(V)$ appearing throughout the rest of the Chapter.

AdS-Schwarzschild case (see previous section), the holographic dual expanding CFT plasma living at $R=\infty$ can be associated the local temperature $T(V)=\frac{T_H}{a(V)}$.

From now on we shall take $L=1$ and treat the Gauss-Bonnet parameter as small, working always to linear order in $\lambda_{\rm GB}$ for simplicity (hence all the formulas containing $\lambda_{\rm GB}$ below are valid up to $\mathcal{O}(\lambda_{\rm GB}^2)$ corrections, although we choose not to unnecessarily repeat this symbol in each and every expression). The transformation from (V,R) to the Fefferman-Graham coordinates (τ,z) can be obtained precisely in the same way as before (the expressions are too cumbersome to be shown here, though), from where we get the following FG metric coefficients

$$\begin{aligned}
g^{(0)}_{\tau\tau} &= -1 \\
g^{(2)}_{\tau\tau} &= -\frac{1}{2a^2}(1-\lambda_{\rm GB})\left(-2a\ddot{a}+\dot{a}^2+k\right) \\
g^{(4)}_{\tau\tau} &= -\frac{1}{16a^4}\big[(1-2\lambda_{\rm GB})\big(4a\ddot{a}(a\ddot{a}-\dot{a}^2-k)+2k\dot{a}^2+\dot{a}^4+k^2\big)-12(1+\lambda_{\rm GB})M\big] \\
g^{(0)}_{ij}dx^idx^j &= a^2 d\Omega_k^2 \\
g^{(2)}_{ij}dx^idx^j &= -\frac{1}{2}(1-\lambda_{\rm GB})\left(\dot{a}^2+k\right)d\Omega_k^2 \\
g^{(4)}_{ij}dx^idx^j &= \frac{1}{16a^2}\big[(1-2\lambda_{\rm GB})(2k\dot{a}^2+\dot{a}^4+k^2)+4(1+\lambda_{\rm GB})M\big]d\Omega_k^2 \ .
\end{aligned} \tag{5.38}$$

The holographic renormalization of the Einstein-Gauss-Bonnet action (5.32) has been carried out in detail in [160, 161, 162] to linear order in $\lambda_{\rm GB}$ (see also [163] for arbitrary $\lambda_{\rm GB}$).[7] The final expression for the boundary energy-momentum tensor can be expressed in terms of the Fefferman-Graham coefficients as

$$\langle T_{\mu\nu}\rangle = \langle T_{\mu\nu}\rangle_{\rm Einstein} + \lambda_{\rm GB}\langle T_{\mu\nu}\rangle_{\rm GB} \ , \tag{5.39}$$

where the $\lambda_{\rm GB}=0$ contribution $\langle T_{\mu\nu}\rangle_{\rm Einstein}$ due to pure Einstein gravity is the same as in (5.28), while the first order Gauss-Bonnet correction $\langle T_{\mu\nu}\rangle_{\rm GB}$ reads

$$\begin{aligned}
\langle T_{\mu\nu}\rangle_{\rm GB} \;=\; & \frac{1}{16\pi G_5}\big[-4g^{(2)\sigma}_{\mu}g^{(2)}_{\nu\sigma}+7g^{(2)\sigma}_{\sigma}g^{(2)}_{\mu\nu}-6g^{(4)}_{\mu\nu}-g^{(2)}_{\sigma\rho}g^{(2)\sigma\rho}g^{(0)}_{\mu\nu}-2\big(g^{(2)\sigma}_{\sigma}\big)^2g^{(0)}_{\mu\nu} \\
& +6g^{(4)\sigma}_{\sigma}g^{(0)}_{\mu\nu}-3h^{(4)}_{\mu\nu}+3h^{(4)\sigma}_{\sigma}g^{(0)}_{\mu\nu}+\tfrac{13}{4}\mathcal{R}^{(0)}g^{(2)}_{\mu\nu}-2\mathcal{R}^{(0)}g^{(2)\sigma}_{\sigma}g^{(0)}_{\mu\nu} \\
& +\tfrac{29}{2}g^{(2)\sigma\rho}\mathcal{R}^{(0)}_{\mu\sigma\nu\rho}+4g^{(2)\sigma}_{\sigma}\mathcal{R}^{(0)}_{\mu\nu}-\tfrac{53}{4}g^{(2)\sigma}_{\nu}\mathcal{R}^{(0)}_{\mu\sigma}-\tfrac{53}{4}g^{(2)\sigma}_{\mu}\mathcal{R}^{(0)}_{\nu\sigma}+\tfrac{11}{4}g^{(2)\sigma\rho}\mathcal{R}^{(0)}_{\sigma\rho}g^{(0)}_{\mu\nu} \\
& +\tfrac{37}{4}\nabla^{(0)}_{\nu}\nabla^{(0)}_{\mu}g^{(2)\sigma}_{\sigma}-\tfrac{37}{4}\nabla^{(0)}_{\mu}\nabla^{(0)}_{\sigma}g^{(2)\sigma}_{\nu}-\tfrac{37}{4}\nabla^{(0)}_{\nu}\nabla^{(0)}_{\sigma}g^{(2)\sigma}_{\mu}+\tfrac{5}{4}g^{(0)}_{\mu\nu}\nabla^{(0)}_{\rho}\nabla^{(0)}_{\sigma}g^{(2)\sigma\rho} \\
& +\tfrac{37}{4}\Box^{(0)}g^{(2)}_{\mu\nu}-\tfrac{5}{4}g^{(0)}_{\mu\nu}\Box^{(0)}g^{(2)\sigma}_{\sigma}\big] \ .
\end{aligned} \tag{5.40}$$

In the above the covariant derivatives $\nabla^{(0)}$ as well as the curvatures $\mathcal{R}^{(0)}$ are to be calculated with the boundary metric $g^{(0)}_{\mu\nu}$. In our case, inserting the FG coefficients (5.38) and expanding to linear order in $\lambda_{\rm GB}$ results in the following energy density $\mathcal{E}\equiv\langle T_{\tau\tau}\rangle$ and pressure $\mathcal{P}\equiv\langle T^i{}_i\rangle$ of the dual CFT

$$\begin{aligned}
\mathcal{E} &= \frac{3(\dot{a}^2+k)^2+12M}{64\pi G_5 a^4}-\frac{3\big[15(k+\dot{a}^2)^2+4M-64a\ddot{a}(k+\dot{a}^2-a\ddot{a})\big]}{128\pi G_5 a^4}\lambda_{\rm GB} \\
\mathcal{P} &= \frac{(\dot{a}^2+k)^2+4M-4a\ddot{a}(k+\dot{a}^2)}{64\pi G_5 a^4}-\frac{15(k+\dot{a}^2)^2+4M-4a\ddot{a}[31(k+\dot{a}^2)-16a\ddot{a}]}{128\pi G_5 a^4}\lambda_{\rm GB} \ .
\end{aligned} \tag{5.41}$$

Notice, in particular, that there is a conformal anomaly given by

$$\langle T^\mu{}_\mu\rangle = 3\mathcal{P}-\mathcal{E} = -\Big(1-\frac{15}{2}\lambda_{\rm GB}\Big)\frac{3\ddot{a}(k+\dot{a}^2)}{16\pi G_5 a^3} \ , \tag{5.42}$$

[7] We follow here the same conventions of [162]. In particular, the Gauss-Bonnet parameter $\lambda_{\rm GB}$ used here differs from the α used in [160], namely $\alpha\equiv\frac{L^2}{2}\lambda_{\rm GB}$.

in agreement with the generic structure (5.33). Namely, the central charges c and b of (5.34) when linearized in $\lambda_{\rm GB}$ read $c = \frac{\pi}{8G_5}\big(1-\frac{7}{2}\lambda_{\rm GB}\big)$ and $b = \frac{\pi}{8G_5}\big(1-\frac{15}{2}\lambda_{\rm GB}\big)$, which together with the expressions $W = 0$ and $E = \frac{24\ddot{a}(k+\dot{a}^2)}{a^3}$ for the FLRW metric reduce the general expression (5.33) to (5.42).

The results above generalize the expressions (5.29) and (5.31) obtained in the previous section to linear order in the Gauss-Bonnet parameter. They are believed to share qualitative features with the corresponding result for the $\mathcal{N} = 4$ plasma including leading $1/\lambda$ corrections (here $\lambda = g^2_{\rm YM}N_c$ is the 't Hooft coupling). Once again one would like to emphasize that it follows naturally from our FLRW-like foliation (5.7) of generic AdS spacetimes as a simple application to the AdS-Gauss-Bonnet black hole.

5.3.3 AdS-Reissner-Nordström black hole

We now turn to the case of a charged black hole in order to introduce a chemical potential for the dual plasma. This is the case, for instance, for the quark-gluon plasma of QCD which has a nonvanishing barion chemical potential. It is also interesting to illustrate how our procedure works when matter fields are present. The simplest bulk action includes a $U(1)$ gauge field minimally coupled to the Einstein-Hilbert action with a negative cosmological constant, namely

$$S = \frac{1}{16\pi G_5}\int d^5x\sqrt{-g}\left[R + \frac{12}{L^2} - \frac{1}{4}F_{ab}F^{ab}\right] . \tag{5.43}$$

An exact solution to the resulting Einstein and Maxwell equations is the AdS-Reissner-Nordström (AdSRN) black hole, a charged black hole whose metric can be cast in the standard black hole form (5.2) with $f(r)$ and $\Sigma(r)$ given by (for simplicity we consider only the planar horizon case $k = 0$)

$$f(r) = \frac{r^2}{L^2}\left(1 - \frac{M}{r^4} + \frac{Q^2}{r^6}\right) \qquad \Sigma(r) = \frac{r}{L} , \tag{5.44}$$

in addition to the nontrivial gauge field configuration

$$A_a dx^a = \mu\left(1 - \frac{r_h^2}{r^2}\right)dt . \tag{5.45}$$

In the above we have conveniently expressed the solution in terms of four parameters, the mass M, charge Q, chemical potential μ and horizon radius r_h (satisfying $f(r_h) = 0$), but only two of them are independent parameters. For instance, M and Q can be eliminated in favor of μ and r_h as

$$M = r_h^4 + \frac{Q^2}{r_h^2} , \qquad Q^2 = \frac{L^2\mu^2 r_h^4}{3} .$$

The corresponding Hawking temperature is

$$T_H = \frac{r_h}{\pi L^2}\left(1 - \frac{L^2\mu^2}{6r_h^2}\right) . \tag{5.46}$$

The AdSRN solution is believed to be holographically dual to a CFT plasma at temperature T_H and chemical potential μ living at the AdS boundary $r = \infty$. Notice that there is a critical value for the chemical potential $\mu_c = \sqrt{6}r_h/L$ (correspondingly $Q_c = \sqrt{2}r_h^3$) where the temperature vanishes and the solution becomes extremal.

The explicit form of the foliation (5.7) for the AdSRN black hole, including the corresponding

(V,R)-dependent gauge field configuration needed to support the metric[8], takes the following form

$$\begin{aligned} ds^2 &= 2dVdR - \left[\frac{R^2}{L^2}\Big(1-\frac{M}{R^4a^4}+\frac{Q^2}{R^6a^6}\Big) - 2R\frac{\dot{a}}{a}\right]dV^2 + \frac{R^2a^2}{L^2}d\mathbf{x}^2 \\ A_a dx^a &= \mu\left(1-\frac{r_h^2}{R^2a^2}\right)\left(\frac{1}{a}-\frac{L^2\dot{a}/Ra^2}{1-\frac{M}{R^4a^4}+\frac{Q^2}{R^6a^6}}\right)dV - \mu\left(1-\frac{r_h^2}{R^2a^2}\right)\frac{L^2/R^2a}{1-\frac{M}{R^4a^4}+\frac{Q^2}{R^6a^6}}dR, \end{aligned} \tag{5.47}$$

where we have used $d\mathbf{x}^2$ to denote the spatial part $d\Omega^2_{k=0}$. As before, the local temperature $T(V)$ of the holographic dual nonequilibrium plasma is given by (5.15).

It is interesting to notice that at the cosmological boundary $R=\infty$ what remains of the gauge field above is

$$A_\nu dx^\nu\big|_{\text{bdry}} = \frac{\mu}{a}dV\ , \tag{5.48}$$

showing that the CFT plasma living in there has a time-dependent chemical potential $\tilde{\mu}(V)\equiv\frac{\mu}{a(V)}$. Interestingly, by reversing the logic, one learns the important lesson that a CFT plasma subject to a time-dependent chemical potential $\tilde{\mu}(V)$ (what is sometimes referred to as a *quench* in the chemical potential) experiences a non-equilibrium dynamics equivalent to a cosmological evolution with the scale factor being inversely related to the "quench profile", i.e., $a(V)\sim 1/\tilde{\mu}(V)$.

The AdSRN metric (5.47) parametrized by (M,Q) differs from the AdS-Schwarzschild solution (5.24) only due to the presence of the charge Q, which comes with a subleading $1/R$ dependence and, thus, is expected to play a significant role only sufficiently deep inside the bulk spacetime. This suggests that the first terms in the Fefferman-Graham expansion of AdSRN near the cosmological boundary at $R=\infty$ should not differ from those obtained before. In fact, one can check explicitly that the transformation from (V,R) to FG coordinates (τ,z) takes exactly the same form as in (5.26) (with Q only beginning to affect at $\mathcal{O}(z^7)$ in $V(\tau,z)$ and $\mathcal{O}(z^5)$ in $R(\tau,z)$) and, consequently, that the first few FG metric coefficients are the same as in (5.27) (with Q only beginning its influence at $\mathcal{O}(z^6)$ in both $g_{\tau\tau}$ and g_{ij}).[9] The gauge field appearing in (5.47), on the other hand, has a nontrivial FG expansion that is readily found to be

$$A_a dx^a = \mu\left[\frac{1}{a}-\frac{a\ddot{a}-2\dot{a}^2+2r_h^2}{2a^3}z^2+\cdots\right]d\tau - \mu\left[\frac{\dot{a}}{a^2}z+\frac{\dot{a}\left(\dot{a}^2-2r_h^2\right)}{2a^4}z^3+\cdots\right]dz\ . \tag{5.49}$$

The holographic renormalization for the Einstein-Maxwell system can be found, e.g., in [164]. The expressions for the renormalized stress tensor and $U(1)$ conserved current of the dual CFT are generically given in terms of the FG coefficients as[10]

$$\begin{aligned} \langle T_{\mu\nu}\rangle &= \frac{1}{4\pi G_5}\left\{g^{(4)}_{\mu\nu}-\frac{1}{2}g^{(2)\sigma}_{\ \ \mu}g^{(2)}_{\sigma\nu}+\frac{1}{4}\big(g^{(2)\sigma}_{\ \ \sigma}\big)g^{(2)}_{\mu\nu}-\frac{1}{8}\big[\big(g^{(2)\sigma}_{\ \ \sigma}\big)^2g^{(2)}_{\sigma\rho}g^{(2)\rho\sigma}\big]g^{(0)}_{\mu\nu}+\frac{1}{48}\big(F^{(0)}_{\sigma\rho}F^{(0)\sigma\rho}\big)g^{(0)}_{\mu\nu}\right\} \\ \langle J^\mu\rangle &= \frac{1}{8\pi G_5}\big(A^{(2)}_\nu+B^{(2)}_\nu\big)g^{(0)\nu\mu}\ , \end{aligned} \tag{5.50}$$

[8] Namely, a gauge field configuration originally of the form $A_a dx^a=\phi(r)dt$ (such as (5.45)) after the sequence of coordinate transformations $dt=dv-f(r)^{-1}dr$, $dv=a(V)^{-1}dV$ and finally $r=Ra(V)$ becomes

$$A_a dx^a = \phi(Ra)\left[\left(\frac{1}{a}-\frac{R\dot{a}}{f(Ra)}\right)dV-\frac{a}{f(Ra)}dR\right].$$

[9] Of course we may want to parametrize the AdSRN metric using not (M,Q) but instead (r_h,Q), for instance. In this case the FG coefficients are still going to be given by the AdS-Schwarzschild expressions (5.27) with M now expressed in terms of (r_h,Q) as $M=r_h^4+\frac{Q^2}{r_h^2}$ (and obviously the statement about Q only starting to affect the expansion at higher orders must be forgotten).

[10] Up to scheme dependent terms that do not contribute to the conformal anomaly and can be removed by additional counterterms (see [164] for details).

where $A_\nu^{(2)}$ and $B_\nu^{(2)}$ are the second order coefficients appearing in the FG expansion of the bulk gauge field, i.e.,

$$A_\nu(z,x) = A_\nu^{(0)}(x) + z^2\big[A_\nu^{(2)}(x) + B_\nu^{(2)}(x)\log z^2\big] + \cdots \ .$$

Note that the expression for $\langle T_{\mu\nu}\rangle$ is almost the same as the one for pure Einstein gravity in the bulk, (5.28), the exception being the extra contribution due to the gauge field in the last term. Inserting our FG expansion constructed above gives the following result for the energy density, pressure, and charge density $\mathcal{Q} \equiv \langle J^\tau \rangle$ of a $U(1)$-charged plasma in a FLRW spacetime

$$\begin{aligned}
\mathcal{E} &= \frac{3\dot{a}^4 + 12r_h^2(r_h^2 + \frac{1}{3}\mu^2)}{64\pi G_5 a^4} \\
\mathcal{P} &= \frac{\dot{a}^4 + 4r_h^2(r_h^2 + \frac{1}{3}\mu^2) - 4a\ddot{a}\dot{a}^2}{64\pi G_5 a^4} \\
\mathcal{Q} &= \frac{\mu\big(2r_h^2 + 2\dot{a}^2 + a\ddot{a}\big)}{16\pi G_5 a^3} \ .
\end{aligned} \tag{5.51}$$

Once again this can be put entirely in 4d CFT language using $G_5 = \frac{\pi}{2N_c^2}$, eliminating r_h in favor of the local temperature $T(V)$ as $r_h = \frac{1}{2}\pi a T\big(1 + \sqrt{1 + 2\mu^2/3\pi^2T^2}\big)$ and, finally, writing $\mu = \tilde{\mu}a$, since the chemical potential associated to the expanding plasma is the time-dependent one $\tilde{\mu} = \frac{\mu}{a}$ instead of μ, as discussed above. The resulting expressions are lengthy and no more instructive than (5.51), so we do not show them explicitly here. We just point out, as a sanity check, that for $\mu = 0$ the result (5.30) is sucessfully recovered.

The conformal anomaly in this case is the same as in (5.31), i.e., there is no contribution from the chemical potential to the anomaly. The $U(1)$ gauge field usually contributes a term proportional to $\big(F_{\mu\nu}^{(0)}\big)^2$ (see [164]), but for our solution this is zero since at the boundary we only have $A_\nu^{(0)}dx^\nu = \frac{\mu}{a}d\tau$ (hence $F_{\mu\nu}^{(0)} = 0$). It is straightforward to check from (5.51) that

$$\begin{aligned}
\nabla_\mu\langle T^{\mu\nu}\rangle &= 0 \\
\nabla_\mu\langle J^\mu\rangle &= \frac{\mu}{2a^3}\left(-3\dot{a}\ddot{a} + a\dddot{a}\right) \ ,
\end{aligned} \tag{5.52}$$

i.e., the CFT energy-momentum tensor is conserved while the $U(1)$ current is not. This is a direct consequence of the dynamical chemical potential experienced by the plasma and should not come as a surprise.

5.4 Discussion and conclusions

We have introduced a new slicing of AdS black holes such that a non-standard notion of conformal boundary with a FLRW metric can be defined. The construction is based on the use of Eddington-Finkelstein coordinates instead of early approaches involving Fefferman-Graham coordinates, a fact that makes the task tremendously simpler and applicable to a large class of AdS black holes including eventual supporting matter fields. It also provides a good perspective into the numerical study of expanding plasmas in holography using the characteristic formulation of the Einstein equations in AdS [165], for which the use of EF coordinates is determinant. A Fefferman-Graham expansion near the new "cosmological" boundary can be easily constructed to any desired order for the FLRW-foliated metric, which leads to the renormalized stress tensor of the dual expanding CFT plasma upon the assumption that the standard holographic renormalization procedure is still applicable. In particular, the results of [148] are consistently recovered as a simple application to the AdS-Schwarzschild solution and then generalized to include a second central charge (using the AdS-Gauss-Bonnet black hole) or a nonvanishing chemical potential (using the AdS-Reissner-Nordström solution) for the dual CFT plasma.

The new dynamical foliation elucidates the procedure carried out in [152] by clarifying the assumptions involved and the background solution on which the perturbative study of the expanding $\mathcal{N} = 2^*$ plasma close to conformality relies. It also provides, as a by-product of the application to the AdS-Reissner-Nordström solution, the interesting lesson that the nonequilibrium dynamics of a CFT plasma subject to a quench $\tilde{\mu}(t)$ in the chemical potential resembles a cosmological evolution with the scale factor $a(t)$ being inversely related to the quench profile, $a(t) \sim \tilde{\mu}(t)^{-1}$. A similar conclusion can be drawn for a wider class of quenches of CFTs by applying our slicing to the corresponding dual static hairy black hole solution, since the (time-independent) non-normalizable mode associated with static matter field configurations naturally acquires time dependence in the new (V, R) coordinates.

The proposal also gives a novel tool to analytically explore properties of expanding plasmas that have not yet been explored. This involves, for instance, a study of the time evolution of nonlocal observables with a known holographic dual gravity description, such as higher-point correlators, Wilson loops and the entanglement entropy of spatial subsystems, which we choose to postpone for the future.

Chapter 6

Closing remarks

The primary concern of this thesis has been to apply the computational tools provided by the holographic duality to learn about strongly coupled quantum field theories in out-of-equilibrium situations. Some effort has been made in Chapters **1** and **2** to introduce in a didatic yet concise way all the necessary ingredients (including Anti de Sitter spacetimes, conformal field theories, non-Abelian gauge theories, and string theory) as well as the holographic duality itself (starting from the original Maldacena's AdS/CFT correspondence and, then, generalizing it for less symmetric setups motivated by QCD and condensed matter phenomenology). Accordingly, we have illustrated the usefulness of the holographic approach by studying different QFT problems having explicit time dependence by mapping them to a dual gravitational problem involving dynamical spacetimes. This resulted in three independent original contributions which we now summarize.

In Chapter **3** we dealt with the problem of holographic thermalization of a CFT plasma with a non-vanishing chemical potential. Using the simplest possible model for the gravitational collapse in the bulk – a Vaidya model describing the spherical collapse of a thin-shell of null matter – we have analyzed the effect of α'-like corrections of the Born-Infeld type in the bulk action to the thermalization time of the dual plasma. By probing the thermalization process using non-local observables (equal-time two-point functions and expectation values of Wilson loops) we have shown that the Born-Infeld nonlinear corrections have the effect of decreasing the thermalization time, which agrees with other classes of α'-like corrections obtained in the literature and seems to be a general feature of stringy corrections.

In Chapter **4** we have analyzed a different time-dependent problem, namely that of the response of a system to a coupling that changes in time during a certain finite interval (a quench). More specifically, we have studied a class of quenches that break the relativistic invariance of a zero-temperature CFT towards a non-relativistic scaling symmetry of Lifshitz type with dynamical exponent z very close to unity. The idea is that this provides a very simple model for the breaking of a global spacetime symmetry and, by probing the non-equilibrium dynamics during this controllable process, we might shed light into the dynamics of symmetry breaking in more general setups. We showed by an explicit analytic argument that the non-relativistic field theory obtained at the end is inevitably at finite temperature regardless of the form of the quench protocol $J(v)$. We also studied the time evolution of local and non-local observables following the quench, from where it becomes clear, for instance, that the symmetry breaking process happens from short to large distances, i.e., it is a top-down process.

Finally, in Chapter **5** we have introduced a new slicing of static Anti de Sitter black holes constructed in such a way that the conformal boundary of AdS becomes a Friedmann-Lemaître-Robertson-Walker (FLRW) spacetime. The construction is very simple due to the use of Eddington-Finkelstein coordinates and is applicable to any static AdS black hole, either supported by matter fields or not. The holographic dual picture of a CFT living on a FLRW background constitutes a useful prototype to analytically study the dynamics of CFT plasmas away from equilibrium such as, for instance, expanding plasmas. To illustrate the advantage of the method, we first reobtained

(by applying the slicing to the AdS_5-Schwarzschild solution) in a straightforward way known analytical expressions for the time evolution of the stress-tensor of a $\mathcal{N} = 4$ super Yang-Mills plasma in FLRW spacetime. Later we generalized these expressions to include finite coupling corrections (of the Gauss-Bonnet type) and a chemical potential for the SYM plasma, respectively. In the latter case, as a by-product of the process, we showed that the nonequilibrium dynamics experienced by a charged plasma following a quench $\mu(t)$ in the chemical potential resembles a cosmological evolution with the scale factor being inversely related to the quench profile, i.e., $a(t) \sim \mu(t)^{-1}$.

Outlook for the future

To summarize, there are still many interesting open questions left to explore. Time-dependent configurations in the gauge/gravity duality only started to receive a significant amount of attention over the last few years. As a matter of fact, even though they provide an outstanding meeting point of fundamental problems in general relativity and non-equilibrium quantum phenomena, there is much yet to be uncovered in the near future.

First and foremost, further holographic models for quenches and the thermalization of interesting physical systems (specially for QCD and condensed matter phenomenology) are certainly in order for the sequence. Another interesting possible direction to be explored is to analyze further consequences of the above-mentioned FLRW-like foliation of AdS spacetimes discussed in Chapter **5**. A comparison with the plethora of numerical results currently available in the literature for holographic thermalization should be done in order to clarify the possible (dis)advantages of this analytic toy model, as well as the calculation of non-local observables of the expanding plasma such as the entanglement entropy of spacelike subregions. In addition, as already commented in the partial conclusion of that Chapter, another aspect to be explored is the intriguing relation between quantum quenches and cosmological evolution. On the one hand, we have seen that when the slicing procedure is applied to static AdS black holes that are supported by any sort of matter field (hairy black holes), the resulting FLRW-like slicing naturally incorporates a time-dependent boundary condition – a quench! – for the bulk fields at the FLRW boundary. Hence, it would be interesting to clarify what can be learned from this relation. On the other hand, there is also the obvious question of what would this holographic approach to expanding plasmas mean from a cosmologist's point of view.

Bibliography

[1] J. M. Maldacena, *The Large N limit of superconformal field theories and supergravity*, *Int. J. Theor. Phys.* **38** (1999) 1113–1133, [hep-th/9711200].

[2] E. Witten, *Anti-de Sitter space and holography*, *Adv. Theor. Math. Phys.* **2** (1998) 253–291, [hep-th/9802150].

[3] S. S. Gubser, I. R. Klebanov and A. M. Polyakov, *Gauge theory correlators from noncritical string theory*, *Phys. Lett.* **B428** (1998) 105–114, [hep-th/9802109].

[4] S. R. Coleman, *The Quantum Sine-Gordon Equation as the Massive Thirring Model*, *Phys. Rev.* **D11** (1975) 2088.

[5] J. Polchinski, *Dualities of Fields and Strings*, 1412.5704.

[6] G. 't Hooft, *Dimensional reduction in quantum gravity*, in *Salamfest 1993:0284-296*, pp. 0284–296, 1993. gr-qc/9310026.

[7] L. Susskind, *The World as a hologram*, *J. Math. Phys.* **36** (1995) 6377–6396, [hep-th/9409089].

[8] S. Weinberg, *Gravitation and Cosmology: principles and applications of the general theory of relativity.*

[9] S. M. Carroll, *Spacetime and geometry: An introduction to general relativity.*

[10] M. E. Peskin and D. V. Schroeder, *Introduction to quantum field theory.*

[11] M. Maggiore, *A Modern Introduction to Quantum Field Theory.*

[12] R. Wald, *General Relativity.*

[13] S. J. Avis, C. J. Isham and D. Storey, *Quantum Field Theory in anti-De Sitter Space-Time*, *Phys. Rev.* **D18** (1978) 3565.

[14] M. Ammon and J. Erdmenger, *Gauge/gravity duality: Foundations and Applications.*

[15] M. Natsuume, *AdS/CFT Duality User Guide*, *Lect. Notes Phys.* **903** (2015) pp.1–294, [1409.3575].

[16] S. W. Hawking and G. F. R. Ellis, *The Large Scale Structure of Spacetime.*

[17] J. I. Kapusta and C. Gale, *Finite-temperature field theory: Principles and applications.*

[18] P. di Francesco, P. Mathieu and D. Senechal, *Conformal field theories.*

[19] E. Abdalla, M. C. B. Abdalla and K. C. Rothe, *Non-perturbative methods in 2 dimensional quantum field theory.*

[20] J. Polchinski, *String Theory, vol. I: An introduction to the bosonic string.*

[21] D. Simmons-Duffin, *TASI Lectures on the Conformal Bootstrap*, 1602.07982.

[22] H. Nastase, *Introduction to the AdS/CFT correspondence.*

[23] L. Brink, J. H. Schwarz and J. Scherk, *Supersymmetric Yang-Mills Theories*, *Nucl. Phys.* **B121** (1977) 77.

[24] M. F. Sohnius, *Introducing Supersymmetry*, *Phys. Rept.* **128** (1985) 39–204.

[25] B. Lucini and M. Panero, *SU(N) gauge theories at large N*, *Phys. Rept.* **526** (2013) 93–163, [1210.4997].

[26] G. 't Hooft, *A Planar Diagram Theory for Strong Interactions*, *Nucl. Phys.* **B72** (1974) 461.

[27] A. V. Ramallo, *Introduction to the AdS/CFT correspondence*, *Springer Proc. Phys.* **161** (2015) 411–474, [1310.4319].

[28] J. Polchinski, *String Theory, vol. II: Superstring theory and beyond.*

[29] E. Witten, *String theory dynamics in various dimensions*, *Nucl. Phys.* **B443** (1995) 85–126, [hep-th/9503124].

[30] J. Polchinski, *Dirichlet Branes and Ramond-Ramond charges*, *Phys. Rev. Lett.* **75** (1995) 4724–4727, [hep-th/9510017].

[31] J. M. Bardeen, B. Carter and S. W. Hawking, *The four laws of black hole mechanics*, *Communications in Mathematical Physics* **31** (1973) 161–170.

[32] J. D. Bekenstein, *Black holes and entropy*, *Phys. Rev. D* **7** (Apr, 1973) 2333–2346.

[33] S. W. Hawking, *Particle creation by black holes*, *Communications in Mathematical Physics* **43** (1975) 199–220.

[34] L. P. Kadanoff, *Scaling laws for Ising models near T(c)*, *Physics* **2** (1966) 263–272.

[35] K. G. Wilson, *The renormalization group: Critical phenomena and the kondo problem*, *Rev. Mod. Phys.* **47** (Oct, 1975) 773–840.

[36] J. L. Cardy, *Scaling and renormalization in statistical physics.* 1996.

[37] A. Adams, L. D. Carr, T. Schäfer, P. Steinberg and J. E. Thomas, *Strongly Correlated Quantum Fluids: Ultracold Quantum Gases, Quantum Chromodynamic Plasmas, and Holographic Duality*, *New J. Phys.* **14** (2012) 115009, [1205.5180].

[38] J. Zaanen, Y.-W. Sun, Y. Liu and K. Schalm, *Holographic Duality in Condensed Matter Physics.* Cambridge Univ. Press, 2015.

[39] J. Casalderrey-Solana, H. Liu, D. Mateos, K. Rajagopal and U. A. Wiedemann, *Gauge/String Duality, Hot QCD and Heavy Ion Collisions*, 1101.0618.

[40] G. T. Horowitz and A. Strominger, *Black strings and P-branes*, *Nucl. Phys.* **B360** (1991) 197–209.

[41] S. de Haro, D. R. Mayerson and J. Butterfield, *Conceptual Aspects of Gauge/Gravity Duality*, 1509.09231.

[42] P. Breitenlohner and D. Z. Freedman, *Positive Energy in anti-De Sitter Backgrounds and Gauged Extended Supergravity*, *Phys. Lett.* **B115** (1982) 197–201.

[43] G. T. Horowitz, *Introduction to Holographic Superconductors*, *Lect. Notes Phys.* **828** (2011) 313–347, [1002.1722].

[44] I. R. Klebanov and E. Witten, *AdS / CFT correspondence and symmetry breaking*, *Nucl. Phys.* **B556** (1999) 89–114, [hep-th/9905104].

[45] S. de Haro, S. N. Solodukhin and K. Skenderis, *Holographic reconstruction of space-time and renormalization in the AdS / CFT correspondence*, *Commun. Math. Phys.* **217** (2001) 595–622, [hep-th/0002230].

[46] K. Skenderis, *Lecture notes on holographic renormalization*, *Class. Quant. Grav.* **19** (2002) 5849–5876, [hep-th/0209067].

[47] J. de Boer, E. P. Verlinde and H. L. Verlinde, *On the holographic renormalization group*, *JHEP* **08** (2000) 003, [hep-th/9912012].

[48] E. Witten, *Anti-de Sitter space, thermal phase transition, and confinement in gauge theories*, *Adv. Theor. Math. Phys.* **2** (1998) 505–532, [hep-th/9803131].

[49] S. A. Hartnoll, C. P. Herzog and G. T. Horowitz, *Holographic Superconductors*, *JHEP* **12** (2008) 015, [0810.1563].

[50] U. Gursoy, E. Kiritsis, L. Mazzanti, G. Michalogiorgakis and F. Nitti, *Improved Holographic QCD*, *Lect. Notes Phys.* **828** (2011) 79–146, [1006.5461].

[51] O. DeWolfe, S. S. Gubser and C. Rosen, *A holographic critical point*, *Phys. Rev.* **D83** (2011) 086005, [1012.1864].

[52] R. Rougemont, A. Ficnar, S. Finazzo and J. Noronha, *Energy loss, equilibration, and thermodynamics of a baryon rich strongly coupled quark-gluon plasma*, *JHEP* **04** (2016) 102, [1507.06556].

[53] T. Sakai and S. Sugimoto, *Low energy hadron physics in holographic QCD*, *Prog. Theor. Phys.* **113** (2005) 843–882, [hep-th/0412141].

[54] A. Karch and E. Katz, *Adding flavor to AdS / CFT*, *JHEP* **06** (2002) 043, [hep-th/0205236].

[55] I. R. Klebanov and M. J. Strassler, *Supergravity and a confining gauge theory: Duality cascades and chi SB resolution of naked singularities*, *JHEP* **08** (2000) 052, [hep-th/0007191].

[56] O. Aharony, *The NonAdS / nonCFT correspondence, or three different paths to QCD*, in *Progress in string, field and particle theory: Proceedings, NATO Advanced Study Institute, EC Summer School, Cargese, France, June 25-July 11, 2002*, pp. 3–24, 2002. hep-th/0212193.

[57] G. Camilo, B. Cuadros-Melgar and E. Abdalla, *Holographic thermalization with a chemical potential from Born-Infeld electrodynamics*, *JHEP* **02** (2015) 103, [1412.3878].

[58] M. Gyulassy and L. McLerran, *New forms of QCD matter discovered at RHIC*, *Nucl. Phys.* **A750** (2005) 30–63, [nucl-th/0405013].

[59] B. Muller, J. Schukraft and B. Wyslouch, *First Results from Pb+Pb collisions at the LHC*, *Ann. Rev. Nucl. Part. Sci.* **62** (2012) 361–386, [1202.3233].

[60] E. V. Shuryak, *The QCD vacuum, hadrons and the superdense matter*, *World Sci. Lect. Notes Phys.* **71** (2004) 1–618.

[61] E. Shuryak, *Why does the quark gluon plasma at RHIC behave as a nearly ideal fluid?*, *Prog. Part. Nucl. Phys.* **53** (2004) 273–303, [hep-ph/0312227].

[62] G. Policastro, D. T. Son and A. O. Starinets, *The Shear viscosity of strongly coupled N=4 supersymmetric Yang-Mills plasma*, *Phys. Rev. Lett.* **87** (2001) 081601, [hep-th/0104066].

[63] D. T. Son and A. O. Starinets, *Viscosity, Black Holes, and Quantum Field Theory*, *Ann. Rev. Nucl. Part. Sci.* **57** (2007) 95–118, [0704.0240].

[64] U. W. Heinz, *The Quark gluon plasma at RHIC*, *Nucl. Phys.* **A721** (2003) 30–39, [nucl-th/0212004].

[65] U. H. Danielsson, E. Keski-Vakkuri and M. Kruczenski, *Black hole formation in AdS and thermalization on the boundary*, *JHEP* **02** (2000) 039, [hep-th/9912209].

[66] R. A. Janik, *Viscous plasma evolution from gravity using AdS/CFT*, *Phys. Rev. Lett.* **98** (2007) 022302, [hep-th/0610144].

[67] R. A. Janik and R. B. Peschanski, *Gauge/gravity duality and thermalization of a boost-invariant perfect fluid*, *Phys. Rev.* **D74** (2006) 046007, [hep-th/0606149].

[68] P. M. Chesler and L. G. Yaffe, *Boost invariant flow, black hole formation, and far-from-equilibrium dynamics in N = 4 supersymmetric Yang-Mills theory*, *Phys. Rev.* **D82** (2010) 026006, [0906.4426].

[69] S. Bhattacharyya and S. Minwalla, *Weak Field Black Hole Formation in Asymptotically AdS Spacetimes*, *JHEP* **09** (2009) 034, [0904.0464].

[70] E. Caceres, A. Kundu, J. F. Pedraza and D.-L. Yang, *Weak Field Collapse in AdS: Introducing a Charge Density*, *JHEP* **06** (2015) 111, [1411.1744].

[71] D. Garfinkle and L. A. Pando Zayas, *Rapid Thermalization in Field Theory from Gravitational Collapse*, *Phys. Rev.* **D84** (2011) 066006, [1106.2339].

[72] D. Garfinkle, L. A. Pando Zayas and D. Reichmann, *On Field Theory Thermalization from Gravitational Collapse*, *JHEP* **02** (2012) 119, [1110.5823].

[73] S. Lin and E. Shuryak, *Toward the AdS/CFT Gravity Dual for High Energy Collisions. 3. Gravitationally Collapsing Shell and Quasiequilibrium*, *Phys. Rev.* **D78** (2008) 125018, [0808.0910].

[74] V. Balasubramanian, A. Bernamonti, J. de Boer, N. Copland, B. Craps, E. Keski-Vakkuri et al., *Thermalization of Strongly Coupled Field Theories*, *Phys. Rev. Lett.* **106** (2011) 191601, [1012.4753].

[75] V. Balasubramanian, A. Bernamonti, J. de Boer, N. Copland, B. Craps, E. Keski-Vakkuri et al., *Holographic Thermalization*, *Phys. Rev.* **D84** (2011) 026010, [1103.2683].

[76] M. Blau, *Lecture Notes on General Relativity*.

[77] R. Baier, A. H. Mueller, D. Schiff and D. T. Son, *'Bottom up' thermalization in heavy ion collisions*, *Phys. Lett.* **B502** (2001) 51–58, [hep-ph/0009237].

[78] D. Galante and M. Schvellinger, *Thermalization with a chemical potential from AdS spaces*, *JHEP* **07** (2012) 096, [1205.1548].

[79] E. Caceres and A. Kundu, *Holographic Thermalization with Chemical Potential*, *JHEP* **09** (2012) 055, [1205.2354].

[80] M. Born and L. Infeld, *Foundations of the new field theory*, *Proc. Roy. Soc. Lond.* **A144** (1934) 425–451.

[81] S. Banerjee, *A Note on Charged Black Holes in AdS space and the Dual Gauge Theories*, *Phys. Rev.* **D82** (2010) 106008, [1009.1780].

[82] F. Nogueira and J. B. Stang, *Density versus chemical potential in holographic field theories*, *Phys. Rev.* **D86** (2012) 026001, [1111.2806].

[83] R.-G. Cai and Y.-W. Sun, *Shear Viscosity from AdS Born-Infeld Black Holes*, *JHEP* **09** (2008) 115, [0807.2377].

[84] H. S. Tan, *First order Born-Infeld Hydrodynamics via Gauge/Gravity Duality*, *JHEP* **04** (2009) 131, [0903.3424].

[85] Z. Zhao, Q. Pan, S. Chen and J. Jing, *Notes on holographic superconductor models with the nonlinear electrodynamics*, *Nucl. Phys.* **B871** (2013) 98–110, [1212.6693].

[86] W. Yao and J. Jing, *Holographic entanglement entropy in insulator/superconductor transition with Born-Infeld electrodynamics*, *JHEP* **05** (2014) 058, [1401.6505].

[87] W. Yao and J. Jing, *Holographic entanglement entropy in metal/superconductor phase transition with Born-Infeld electrodynamics*, *Nucl. Phys.* **B889** (2014) 109–119, [1408.1171].

[88] W. Yao and J. Jing, *Analytical study on holographic superconductors for Born-Infeld electrodynamics in Gauss-Bonnet gravity with backreactions*, *JHEP* **05** (2013) 101, [1306.0064].

[89] Q. Pan, J. Jing and B. Wang, *Holographic superconductor models with the Maxwell field strength corrections*, *Phys. Rev.* **D84** (2011) 126020, [1111.0714].

[90] Y. Liu and B. Wang, *Perturbations around the AdS Born-Infeld black holes*, *Phys. Rev.* **D85** (2012) 046011, [1111.6729].

[91] T. K. Dey, *Born-Infeld black holes in the presence of a cosmological constant*, *Phys. Lett.* **B595** (2004) 484–490, [hep-th/0406169].

[92] R.-G. Cai, D.-W. Pang and A. Wang, *Born-Infeld black holes in (A)dS spaces*, *Phys. Rev.* **D70** (2004) 124034, [hep-th/0410158].

[93] A. Chamblin, R. Emparan, C. V. Johnson and R. C. Myers, *Charged AdS black holes and catastrophic holography*, *Phys. Rev.* **D60** (1999) 064018, [hep-th/9902170].

[94] E. Caceres, A. Kundu, J. F. Pedraza and W. Tangarife, *Strong Subadditivity, Null Energy Condition and Charged Black Holes*, *JHEP* **01** (2014) 084, [1304.3398].

[95] V. Balasubramanian and S. F. Ross, *Holographic particle detection*, *Phys. Rev.* **D61** (2000) 044007, [hep-th/9906226].

[96] J. M. Maldacena, *Wilson loops in large N field theories*, *Phys. Rev. Lett.* **80** (1998) 4859–4862, [hep-th/9803002].

[97] E. Abdalla, R. Mohayaee and A. Zadra, *Screening in two-dimensional QCD*, *Int. J. Mod. Phys.* **A12** (1997) 4539–4558, [hep-th/9604063].

[98] E. Abdalla and R. Banerjee, *Screening in three-dimensional QED*, *Phys. Rev. Lett.* **80** (1998) 238–240, [hep-th/9704176].

[99] X. Zeng and W. Liu, *Holographic thermalization in Gauss-Bonnet gravity*, *Phys. Lett.* **B726** (2013) 481–487, [1305.4841].

[100] X.-X. Zeng, X.-M. Liu and W.-B. Liu, *Holographic thermalization with a chemical potential in Gauss-Bonnet gravity*, *JHEP* **03** (2014) 031, [1311.0718].

[101] A. Polkovnikov, K. Sengupta, A. Silva and M. Vengalattore, *Nonequilibrium dynamics of closed interacting quantum systems*, *Rev. Mod. Phys.* **83** (2011) 863, [1007.5331].

[102] G. Camilo, B. Cuadros-Melgar and E. Abdalla, *Holographic quenches towards a Lifshitz point*, *JHEP* **02** (2016) 014, [1511.08843].

[103] P. Calabrese and J. L. Cardy, *Evolution of entanglement entropy in one-dimensional systems*, *J. Stat. Mech.* **0504** (2005) P04010, [cond-mat/0503393].

[104] P. Calabrese and J. L. Cardy, *Time-dependence of correlation functions following a quantum quench*, *Phys. Rev. Lett.* **96** (2006) 136801, [cond-mat/0601225].

[105] C. de Grandi, V. Gritsev and A. Polkovnikov, *Quench dynamics near a quantum critical point*, *Phys. Rev. B* **81** (2010) 012303, [0909.5181].

[106] P. Calabrese and J. Cardy, *Quantum Quenches in Extended Systems*, *J. Stat. Mech.* **0706** (2007) P06008, [0704.1880].

[107] J. Dziarmaga, *Dynamics of a quantum phase transition and relaxation to a steady state*, *Advances in Physics* **59** (2010) 1063–1189, [0912.4034].

[108] T. Albash and C. V. Johnson, *Evolution of Holographic Entanglement Entropy after Thermal and Electromagnetic Quenches*, *New J. Phys.* **13** (2011) 045017, [1008.3027].

[109] J. Aparicio and E. Lopez, *Evolution of Two-Point Functions from Holography*, *JHEP* **12** (2011) 082, [1109.3571].

[110] P. Basu and S. R. Das, *Quantum Quench across a Holographic Critical Point*, *JHEP* **01** (2012) 103, [1109.3909].

[111] P. Basu, D. Das, S. R. Das and T. Nishioka, *Quantum Quench Across a Zero Temperature Holographic Superfluid Transition*, *JHEP* **03** (2013) 146, [1211.7076].

[112] A. Buchel, L. Lehner and R. C. Myers, *Thermal quenches in N=2* plasmas*, *JHEP* **08** (2012) 049, [1206.6785].

[113] H. Liu and S. J. Suh, *Entanglement growth during thermalization in holographic systems*, *Phys. Rev.* **D89** (2014) 066012, [1311.1200].

[114] N. Callebaut, B. Craps, F. Galli, D. C. Thompson, J. Vanhoof, J. Zaanen et al., *Holographic Quenches and Fermionic Spectral Functions*, *JHEP* **10** (2014) 172, [1407.5975].

[115] M. Rangamani, M. Rozali and A. Wong, *Driven Holographic CFTs*, *JHEP* **04** (2015) 093, [1502.05726].

[116] V. Keranen, E. Keski-Vakkuri and L. Thorlacius, *Thermalization and entanglement following a non-relativistic holographic quench*, *Phys. Rev.* **D85** (2012) 026005, [1110.5035].

[117] J. Sonner, A. del Campo and W. H. Zurek, *Universal far-from-equilibrium Dynamics of a Holographic Superconductor*, 1406.2329.

[118] S. R. Das, D. A. Galante and R. C. Myers, *Universal scaling in fast quantum quenches in conformal field theories*, *Phys. Rev. Lett.* **112** (2014) 171601, [1401.0560].

[119] S. R. Das, D. A. Galante and R. C. Myers, *Universality in fast quantum quenches*, *JHEP* **02** (2015) 167, [1411.7710].

[120] A. Buchel, R. C. Myers and A. van Niekerk, *Nonlocal probes of thermalization in holographic quenches with spectral methods*, *JHEP* **02** (2015) 017, [1410.6201].

[121] H. Liu and S. J. Suh, *Entanglement Tsunami: Universal Scaling in Holographic Thermalization*, *Phys. Rev. Lett.* **112** (2014) 011601, [1305.7244].

[122] S. A. Hartnoll, *Lectures on holographic methods for condensed matter physics*, *Class. Quant. Grav.* **26** (2009) 224002, [0903.3246].

[123] S. Kachru, X. Liu and M. Mulligan, *Gravity duals of Lifshitz-like fixed points*, *Phys. Rev.* **D78** (2008) 106005, [0808.1725].

[124] M. Taylor, *Non-relativistic holography*, 0812.0530.

[125] W. Chemissany and I. Papadimitriou, *Lifshitz holography: The whole shebang*, *JHEP* **01** (2015) 052, [1408.0795].

[126] T. Griffin, P. Hořava and C. M. Melby-Thompson, *Lifshitz Gravity for Lifshitz Holography*, *Phys. Rev. Lett.* **110** (2013) 081602, [1211.4872].

[127] Y. Korovin, K. Skenderis and M. Taylor, *Lifshitz as a deformation of Anti-de Sitter*, *JHEP* **08** (2013) 026, [1304.7776].

[128] Y. Korovin, K. Skenderis and M. Taylor, *Lifshitz from AdS at finite temperature and top down models*, *JHEP* **11** (2013) 127, [1306.3344].

[129] M. Guica, K. Skenderis, M. Taylor and B. C. van Rees, *Holography for Schrodinger backgrounds*, *JHEP* **02** (2011) 056, [1008.1991].

[130] D. Boyanovsky and J. L. Cardy, *Critical behavior of m-component magnets with correlated impurities*, *Phys. Rev. B* **26** (1982) 154–170.

[131] A. W. W. Ludwig, M. P. A. Fisher, R. Shankar and G. Grinstein, *Integer quantum Hall transition: An alternative approach and exact results*, *Phys. Rev. B* **50** (1994) 7526–7552.

[132] J. Ye and S. Sachdev, *Coulomb Interactions at Quantum Hall Critical Points of Systems in a Periodic Potential*, *Physical Review Letters* **80** (1998) 5409–5412, [cond-mat/9712161].

[133] I. F. Herbut, *Interactions and phase transitions on graphene's honeycomb lattice*, *Phys. Rev. Lett.* **97** (2006) 146401, [cond-mat/0606195].

[134] D. T. Son, *Quantum critical point in graphene approached in the limit of infinitely strong Coulomb interaction*, cond-mat/0701501.

[135] I. F. Herbut, *Critical exponents at the superconductor-insulator transition in dirty-boson systems*, *Phys. Rev. B* **61** (2000) 14723, [cond-mat/0001040].

[136] J. Maldacena, D. Martelli and Y. Tachikawa, *Comments on string theory backgrounds with non-relativistic conformal symmetry*, *JHEP* **10** (2008) 072, [0807.1100].

[137] S. Deger, A. Kaya, E. Sezgin and P. Sundell, *Spectrum of D = 6, N=4b supergravity on AdS in three-dimensions x S**3*, *Nucl. Phys.* **B536** (1998) 110–140, [hep-th/9804166].

[138] B. Biran, A. Casher, F. Englert, M. Rooman and P. Spindel, *The Fluctuating Seven Sphere in Eleven-dimensional Supergravity*, *Phys. Lett.* **B134** (1984) 179.

[139] H. J. Kim, L. J. Romans and P. van Nieuwenhuizen, *The Mass Spectrum of Chiral N=2 D=10 Supergravity on S**5*, *Phys. Rev.* **D32** (1985) 389.

[140] I. Booth, *Black hole boundaries*, *Can. J. Phys.* **83** (2005) 1073–1099, [gr-qc/0508107].

[141] S. Ryu and T. Takayanagi, *Holographic derivation of entanglement entropy from AdS/CFT*, *Phys. Rev. Lett.* **96** (2006) 181602, [hep-th/0603001].

[142] V. E. Hubeny, M. Rangamani and T. Takayanagi, *A Covariant holographic entanglement entropy proposal*, *JHEP* **07** (2007) 062, [0705.0016].

[143] H. Liu and M. Mezei, *A Refinement of entanglement entropy and the number of degrees of freedom*, *JHEP* **04** (2013) 162, [1202.2070].

[144] G. Camilo, *Expanding plasmas from Anti de Sitter black holes*, *The European Physical Journal C* **76** (2016) 682, [1609.07116].

[145] S. Dodelson, *Modern Cosmology*. Academic Press, Amsterdam, 2003.

[146] D. Bazow, G. S. Denicol, U. Heinz, M. Martinez and J. Noronha, *Analytic solution of the Boltzmann equation in an expanding system*, *Phys. Rev. Lett.* **116** (2016) 022301, [1507.07834].

[147] P. Figueras, V. E. Hubeny, M. Rangamani and S. F. Ross, *Dynamical black holes and expanding plasmas*, *JHEP* **04** (2009) 137, [0902.4696].

[148] P. S. Apostolopoulos, G. Siopsis and N. Tetradis, *Cosmology from an AdS Schwarzschild black hole via holography*, *Phys. Rev. Lett.* **102** (2009) 151301, [0809.3505].

[149] N. Lamprou, S. Nonis and N. Tetradis, *The BTZ black hole with a time-dependent boundary*, *Class. Quant. Grav.* **29** (2012) 025002, [1106.1533].

[150] N. Tetradis, *The Temperature and entropy of CFT on time-dependent backgrounds*, *JHEP* **03** (2010) 040, [0905.2763].

[151] S. Nojiri, S. D. Odintsov and S. Ogushi, *Friedmann-Robertson-Walker brane cosmological equations from the five-dimensional bulk (A)dS black hole*, *Int. J. Mod. Phys.* **A17** (2002) 4809–4870, [hep-th/0205187].

[152] A. Buchel, M. P. Heller and J. Noronha, *Entropy Production, Hydrodynamics, and Resurgence in the Primordial Quark-Gluon Plasma from Holography*, *Phys. Rev.* **D94** (2016) 106011, [1603.05344].

[153] S. de Haro, S. N. Solodukhin and K. Skenderis, *Holographic reconstruction of space-time and renormalization in the AdS / CFT correspondence*, *Commun. Math. Phys.* **217** (2001) 595–622, [hep-th/0002230].

[154] T. Padmanabhan and D. Kothawala, *Lanczos-Lovelock models of gravity*, *Phys. Rept.* **531** (2013) 115–171, [1302.2151].

[155] M. T. Grisaru and D. Zanon, *σ Model Superstring Corrections to the Einstein-hilbert Action*, *Phys. Lett.* **B177** (1986) 347–351.

[156] S. Nojiri and S. D. Odintsov, *On the conformal anomaly from higher derivative gravity in AdS / CFT correspondence*, *Int. J. Mod. Phys.* **A15** (2000) 413–428, [hep-th/9903033].

[157] M. Blau, K. S. Narain and E. Gava, *On subleading contributions to the AdS / CFT trace anomaly*, *JHEP* **09** (1999) 018, [hep-th/9904179].

[158] J. de Boer, M. Kulaxizi and A. Parnachev, *Holographic Entanglement Entropy in Lovelock Gravities*, *JHEP* **07** (2011) 109, [1101.5781].

[159] R.-G. Cai, *Gauss-Bonnet black holes in AdS spaces*, *Phys. Rev.* **D65** (2002) 084014, [hep-th/0109133].

[160] J. T. Liu and W. A. Sabra, *Hamilton-Jacobi Counterterms for Einstein-Gauss-Bonnet Gravity*, *Class. Quant. Grav.* **27** (2010) 175014, [0807.1256].

[161] D. Astefanesei, N. Banerjee and S. Dutta, *(Un)attractor black holes in higher derivative AdS gravity*, *JHEP* **11** (2008) 070, [0806.1334].

[162] V. Jahnke, A. S. Misobuchi and D. Trancanelli, *Holographic renormalization and anisotropic black branes in higher curvature gravity*, *JHEP* **01** (2015) 122, [1411.5964].

[163] Y. Brihaye and E. Radu, *Black objects in the Einstein-Gauss-Bonnet theory with negative cosmological constant and the boundary counterterm method*, *JHEP* **09** (2008) 006, [0806.1396].

[164] B. Sahoo and H.-U. Yee, *Electrified plasma in AdS/CFT correspondence*, *JHEP* **11** (2010) 095, [1004.3541].

[165] P. M. Chesler and L. G. Yaffe, *Numerical solution of gravitational dynamics in asymptotically anti-de Sitter spacetimes*, *JHEP* **07** (2014) 086, [1309.1439].